UNIVERSITY OF CALIFORNIA
SANTA CRUZ

TOTAL SYNTHESIS AND NMR-BASED MECHANISTIC ELUCIDATION OF NON-ENZYMATIC NATURAL PRODUCTS

A dissertation submitted in partial satisfaction of the requirements for the degree of

DOCTOR OF PHILOSOPHY

in

CHEMISTRY

by

Victor J. Aniebok

March 2022

The Dissertation of Victor J Aniebok is approved:

_____
Professor John B. MacMillan, advisor

_____
Professor Theodore Holman, chair

_____
Professor Bakthan Singaram

_____
Peter Biehl
Vice Provost and Dean of Graduate Studies

TABLE OF CONTENTS

List of Figures vi
List of Schemes ix
List of Tables xi
List of Abbreviations xii
Abstract xiv
Acknowledgements xv
Dedication xix
Chapter One: Introduction to Non-Enzymatic Chemistry i
1.2 Brief Overview of Natural Product Biosynthesis 4
1.2.1 Polyketides 5
1.2.2 Terpenoids 7
1.2.3 Non-Ribosomal Peptides 8
1.2.4 Alkaloids 9
1.3 Non-Enzymatic Chemistry in the Context of the Origins of Life 9
1.3.1 Non-Enzymatic Amino Acid Synthesis 10
1.3.2 Asymmetry in Abiotic Amino Acids i1
1.3.3 Non-Enzymatic Synthesis of Sugars i3
1.3.4 Non-Enzymatic Glycolysis i4
1.4 Modern Non-Enzymatic Chemistry i5
1.4.1 Dibohemamines i6
1.4.2 Ammosamides i9
1.4.3 Discoipyrroles 22
1.5 Conclusion 26
1.6 Chapter 1 References 26
Chapter Two: Synthesis of oxazinin A and Similar Analogs 33

2.1 Abstract....34
2.2 Introduction to Tuberculosis....34
2.2.1 Mode of Infection....35
2.2.2 *Mtb* as a Difficult to Treat Organism....36
2.2.3 Current Tuberculosis Treatment....37
2.2.3.1 First Line Drugs....38
2.2.3.2 Second and Higher Order Line Drugs....41
2.2.4 Resistance....45
2.3 Oxazinin A....46
2.3.1 Synthesis of oxazinin A Foreword....48
2.3.2 Original Schemes....48
2.3.3 Final Schemes....56
2.4 Conclusion....65
2.5 Experimental Procedures....65
2.6 References....105
2.7 Spectra and Data....109
Chapter Three: Synthesis and Mechanism Elucidation of the pyonitrins and the aerupyrroles....141
3.1 Abstract....143
3.2 Introduction....143
3.3 Introduction to the pyonitrins....145
3.4 Synthesis of the pyonitrins....147
3.5 Synthesis of pyonitrin/discoipyrrole chimeras....156
3.6 Conclusion....160
3.7 Experimental Procedures....161
3.8 Chapter Three References....191
3.9 Spectra and Data....194
Chapter Four: NMR Study of oxazinin A....246
4.1 Introduction....247
4.2 Synthesis of Methyl-Capped Aldehyde....248
4.3 ^{1}H-^{15}N NMR Study of oxazinin A Formation....251

4.4 Conclusion 262
4.5 Experimental Procedures 263
4.6 References 277
4.7 Spectra and Data 279
BIBLIOGRAPHY 286

LIST OF FIGURES

Chapter One

Figure 1.1 Types of natural products and examples of each……..5

Figure 1.2 Hopene formation via squalene cyclization……8

Figure 1.3 Conversion of G3P and DHAP to F16BP in ice……...15

Figure 1.4 Structures of dibohemamines A, B, and C……...17

Figure 1.5 Mechanism of dibohemamine formation……...18

Figure 1.6 Ammosamides A, B, C, and E……20

Figure 1.7 Ammosamides F – K……20

Figure 1.8 Discoipyrrole A formation……22

Figure 1.9 ^{15}N NMR Scale……..24

Figure 1.10 Reaction timeline for discoipyrrole A formation……25

Chapter Two

Figure 2.1 TB Infection and Equilibrium……...36

Figure 2.2 First Line TB Drugs……..38

Figure 2.3 Second Line and Higher Order TB Drugs……44

Figure 2.4 Proposed Biosynthesis of oxazinin A……47

Figure 2.5 Model Dimerization Reaction Condidtions……53

Figure 2.6 NMR Monitoring of Model oxazinin A System for 126 Hours……54

Figure 2.7 Mass Spectrometry Showing Formation of Intermediate Monomer and Dimer……..55

Figure 2.8 Crystal Structure of Compound 2.32 (Enantiomers)……...62

Figure 2.9 Key NMR Comparisons Across oxazinin A Analogs and the Isolated Natural Product……..65

Chapter Three

Figure 3.1 The pyonitrins and the metabolites they are derived from……146

Figure 3.2 Retrosynthesis of the pyonitrins……...148

Figure 3.3 NMR study of ^{15}N aminopyonitrin and aeruginaldehyde. (a) Formation of pyonitrin A along with the intermediates. (b) Representative time points from ^{1}H–^{15}N HMBC experiments……153

Figure 3.4 Real time investigation of imine 3.27 formation by comparison of ^{1}H NMR of starting materials 3.26, 3.7 and intermediate 3.28……155

Figure 3.5 Non-enzymatic reaction to form discoipyrrole A and discoipyrrole/pyonitrin hybrid……157

Chapter Four

Figure 4.1 NMR Study of the pyonitrins……247

Figure 4.2 NMR Study of the discoipyrroles……..247

Figure 4.3 Original (top) and Alternative (bottom) Non-Enzymatic ^{15}N NMR Study of oxazinin A Formation……248

Figure 4.4 ^{1}H-^{15}N HMBC of Anthranilic Acid……252

Figure 4.5 ^{1}H-^{15}N HMBC at 0.5 hours……253

Figure 4.6 ^{1}H-^{15}N HMBC at 1.5 hours……253

Figure 4.7 ^{1}H-^{15}N HMBC at 9.5 hours……254

Figure 4.8 ^{1}H-^{15}N HMBC at 47.5 hours……..254

Figure 4.9 Chemical Shift Comparison of 4.20 in DMSO-d_6 and Methanol-d_4……...256

Figure 4.10 Imine Mimic NMR Study…….259

Figure 4.11 Proposed Pathway of 4.20 Formation……..262

LIST OF SCHEMES

Chapter 2

Scheme 1 General Synthetic Route to oxazinin A……49

Scheme 2 First Synthetic Route to oxazinin A……50

Scheme 3 Formylation of 2.7……50

Scheme 4 Second Synthetic Scheme for oxazinin A……52

Scheme 5 Third Synthetic Scheme for oxazinin A……56

Scheme 6 Synthetic Route to Common Intermediate 23……..57

Scheme 7 Route to Non-Hydroxylation EZ Stereoisomeric oxazinin A 2.28……59

Scheme 8 Route from 2.23 to Brominated oxazinin A Analog 2.32……61

Scheme 9 Final Route to oxazinin A (2.1)……...63

Chapter 3

Scheme 1 Synthesis of aeruginaldehyde……..149

Scheme 2 Synthesis of the aminopyrrolnitrins……..150

Scheme 3 Synthesis of chloroaeruginaldehyde……158

Scheme 4 Synthesis of Oxidized 4-Methoxy sattabacin……159

Scheme 5 Synthesis of aerupyrroles……..160

Chapter 4

Scheme 1 Synthesis of Intermediate 4.15……249

Scheme 2 Synthesis of Methyl-Capped Prenylated Polyketide (4.18) from Intermediate 4.15……251

LIST OF TABLES

Chapter 2

Table 1 Formylation Conditions of 2.7……..51

Chapter 3

Table 1 NMR Data Comparison of Synthesized pyonitrin A and literature values……...151

LIST OF ABBREVIATIONS

A Alanine

ACN Acetonitrile

CD Circular Dichroism

$CDCl_3$ Deuterated Chloroform

CPL Circularly Polarized Light

DBU 1,8-Diazabicyclo[5.4.0]undec-7-ene

DCM Dichloromethane or Methylene Chloride

DIBAL-H Diisobutyl aluminum hydride

DMAP N,N-Dimethyl amino pyridine

DMF Dimethylformamide

DMSO Dimethyl Sulfoxide

DNA Deoxyribonucleic Acid

ee Enantiomeric Excess

HMBC Heteronuclear Multiple Bond Correlation

HMTA Hexamethylenetetramine

HSQC Heteronuclear Single Quantum Coherence

HPLC High Performance Liquid Chromatography

KOH Potassium Hydroxide

LCMS Liquid Chromatography Mass Spectrometry

***m*CPBA** *meta* chloroperoxybenzoic acid

MeOD Deuterated Methanol or Methanol-d_4

Mtb Mycobacterium Tuberculosis

nBuLi n-butyl lithium

NIS N-iodosuccinimide

NMR Nuclear Magnetic Resonance

NP Natural Product

NRP Non-Ribosomal Peptide

NRPS Non-Ribosomal Peptide Synthase

NSCLC Non-Small Cell Lung Cancer Cell Line

PEG Polyethylene Glycol

PKS Polyketide Synthase

RNA Ribonucleic Acid

TBAF Tetra butyl ammonium Fluoride

TBS Tertbutyl dimethyl silane

THF Tetrahydrofuran

TFAA Trifluoroacetic anhydride

UV Ultraviolet

Abstract

Total Synthesis and NMR-Based Mechanistic Elucidation of Non-Enzymatic Natural Products

By

Victor J. Aniebok

Natural products have been a source of inspiration for modern medicine, novel chemistries, and understanding the ecological systems with which organisms inhabit. Natural products are traditionally biosynthesized via enzymes and other chemistry catalyzing proteins. But within that framework there exists natural products that contain one or more non-enzymatic steps in their biosynthesis. In the context of this thesis, we have synthesized two natural products that contain one or more non-enzymatic steps in their biosynthesis: oxazinin A and the pyonitrins. To further elucidate these rare biosynthetic mechanisms, we have utilized ^{1}H-^{15}N NMR with isotopically labeled substrates to study the formation of these natural products and gain further insight into how these molecules form. This information allows us to not only see trends in terms of what kinds of natural products may form non-enzymatically but to exploit that non-enzymatic chemistry to get to natural products and natural product analogs in higher yields and faster times than traditional isolation. Furthermore, these natural products can be combined to form novel unnatural products that are not found in nature but may have ameliorated or altered bioactivity.

Acknowledgements

To start, I wanted to say thank you to Professor John B. MacMillan. None of this would be possible without the faith and trust you have placed in me. Our time together has had its ups and downs, but I honestly believe I have become a better scientist and human under your tutelage. My amino acid drawing skills have improved significantly as well. The support has been immense, the instruction helpful, and the check ins/evaluations timely. Thank you sincerely and hopefully I can pay it back/forward at some point, preferably over a fancy steak dinner.

I also wanted to say thank you to my committee, Bakthan and Ted. Bakthan, we have spent many a Saturday and Sunday chatting about everything under the sun and eating enough biryani to feed a small southern city. You always said that the hard work will pay off, and I kept those words with me whenever things got tough. Ted, the amount of time we spent on the farm weeding and aggressively hunting gophers is something I will always cherish. You honestly have an incredible knack for giving timely advice and helping me find my proverbial north star. Grad school was tough, but much more bearable with you there kicking me in the rear (with a smile no less) from time to time.

Duy, we came into grad school together and have spent more time together than I care to admit, but I wouldn't have it any other way. You're a selfless

warrior who always takes care of everyone (and you always have snacks for me to steal) and I'm sure all that goodwill will come back to you. I'm excited to see where life takes you. See you on the other side. David, you're like the little brother I never had. We fight, have meaningful conversations, get into trouble whatever we can, and laugh it off at the end of the day. The journey has been incredible, and I love seeing you thrive in LA. As I look back on our time here, I reflect on your words when you first join the lab: "Build your mass; everything else will follow". Hopefully my gravity is a little stronger now. Anam, we most definitely started our friendship out on the wrong foot, but the more I think about it, that's the only way it could have started/I'm glad it did. You've been a source of strength for me when things (inevitably) get rough, and I tilt (which happens a lot). Seeing you persevere and stay the course always brings me back and reminds me why I do this. You have a great heart and as much as I give you shit for your crunchy exterior, I hope your heart stays the same. Jocelyn, we've had so many burger and trash rom com nights I have lost count. You embodied (I bet you still do) what it meant to work, stay focused, and take care of business. Don't watch season 2 of Bridgerton without me. Kate, thanks for always being there when I needed to forget about things. I know I can be a lot sometimes (honestly most of the time), but you always put up with me and went along with whatever I wanted to do. Thanks for that and I hope you'll be writing one of these soon. Leah, we have the most interesting friendship ever. We both understand when the other doesn't want to talk or hang out but still randomly

check in with each other because we care. I hope that dying cat part of you never changes. Rebecca, you have the most memorable quotes that make me laugh my ass off. Your humor never gets old. The most unintentional funniest person in the lab. Aswad and Scott, thanks for being great friends and helping me keep my head on straight. Whenever I get distracted, I always remember TCoB. Sahar, you have one of the kindest souls I have ever encountered (sorry Rahul). As life takes swings at you, keep your chin up. Good things will come. Riley, you've started grad school off better than I have ever seen someone start. Your star is bright. Hopefully grad school remains fun for you, and you get to enjoy your time here and when it's your time to go, it'll be with a smile.

Rahul, this thesis wouldn't be possible without you. You're quite possibly the best chemist I have ever encountered, and I'm inspired by how much joy you find in doing chemistry. Even when reactions fail or a something goes wrong you still have a smile. You always say, "Do something small to make yourself feel good and get a positive result", and those words have imprinted on my soul. Chemistry is a game of inches, and every day and moment have a profound impact on your week/month/year. I like to think life is similar so whenever I find myself at an impasse, I reflect on those words. I am forever indebted to your mentorship, aid, and friendship. Thank you, my friend.

To all the friends, cohort mates (David Ricci, Ariel, Jenny, Pam, Patrick, Greg, Dorothy, and Dan), and mentors that I have made along the way, I also want to say thank you. For putting up with me and helping me grow as a person and friend. I will honestly miss all of you, and I hope to see you all on the other side soon.

Lastly, I would like to thank my family. It's been a whirlwind, but you all have been there through it all. The amount of support you all have given me has been wild: Yelling "put Victor in!" at every football game when I was (deservedly) riding the bench in middle school until the other parents got angry. Whenever I used to run the 400, you guys would run alongside the track with me (much to the chagrin of the staff) for the last 100 meters until I finished (and subsequently tossed my lunch). You always reminded me to treat every day like it was the 400: keep a strong pace and give it your all the last 100 meters. If you can move afterwards, you didn't run hard enough. I hated that growing up but appreciate it so much more now. Bronte, you've been my foundation from the moment I wanted to quit quals until now and I'm so grateful that you decided to be on this journey with me. My life has gone from grayscale to color with you in it and I just want you to know that. You inspire me, love me harder than I thought I could be loved, and keep me on track when I would much rather watch anime until I fall asleep.

Thank you all, and I love you dearly.

This thesis is dedicated to my family (Jackie, Tina, Mommy, Jalyn, Josiah, the Mowarins, and the Harrisons). This thesis is also dedicated to Essien James Aniebok, Maggie Ukpong, Jevante Wallace, David Waters Sr., Nick Williams, and to all of those who didn't live to see this or have the chance to see the possibilities in front of them.

Chapter One: Introduction to Non-Enzymatic Chemistry

1.1 Introduction

Small molecules are an integral part of nature. They are crucial for the survival of their producing organism and aid in their fitness. As such, these molecules are ubiquitous in nature. Small molecules that originate from organisms take many forms and can typically be classified as either primary or secondary metabolites. Primary metabolites refer to the molecules that are necessary for survival of the organism. They are necessary for basic, physiological functions such as growth, development, and reproduction. Without these compounds, the organisms would not be able to perform basic metabolic functions and could not survive. Simple molecules such as glucose, many amino acids, and cholesterol function as primary metabolites.[1,2]

Secondary metabolites have a more nuanced raison d'être. They are responsible for the fitness of the organism. They are not necessary for basic metabolic activity, but are needed for the organism to survive better in its environment. Natural products fall into this category of small molecules. Penicillin, one of the most famous natural products and antibacterials, was isolated from *Penicillium* molds by Sir Alexander Fleming.[3] These organisms produce penicillin to better survive in environments where bacteria also inhabited. As a result, natural products occupy a unique chemical space in nature that offer opportunities for discovering and exploiting novel and beneficial chemistries for the world.

Natural products have traditionally occupied a large amount of chemical space in the medicinal world. Starting from traditional herbal medicines and spearheaded by penicillin, natural products have been an integral part of medicine and the treatment of various ailments.[3] For example, commonly known drugs such as lovastatin (isolated from *Aspergillus sp* and used as a cholesterol-lowering agent), paclitaxel (isolated from the bark of a yew tree and acts as an anti-cancer treatment and commonly known as taxol), and vancomycin (isolated from *Amycolatopsis orientalis* and a last line antibacterial defense) have been heavily utilized in modern medicine and continue to serve as a source of inspiration for many natural product chemists. In addition, Newman and Cragg reported from 1981-2014 approximately 50% of all newly approved drugs were natural products, natural product derivatives/mimics, or synthetic drugs with a natural product pharmacophore.[4] This demonstrates that natural products are interesting molecules that also have value in medicine and related areas.

As widespread as natural products have been in chemistry and medicine, there are still many frontiers within the field for discovery of novel molecules of interest. Research done by *Pye et al* demonstrated that 76.8% of the known published marine natural product chemical space is occupied by molecules that contain structural similarities. This implies that 24.2% of the remaining published natural products occupy distinct chemical space, as well as the implication that traditional methods of obtaining natural products are yielding

similar natural products.[5] Traditionally, microbial natural products are grown in the laboratory and (typically) the organic soluble molecules are extracted, purified, and isolated. Ideally, improvements in isolation and growth techniques can lead to more novel natural products.

1.2 Brief Overview of Natural Product Biosynthesis

Natural products are produced via the Francis Crick coined central dogma of biology: DNA is transcribed into RNA and the RNA is translated from that DNA template into proteins that go on to perform particular functions for the organism. One of the functions of these proteins is the construction of natural products that improve the organism's fitness in its endemic environment. As a result, the manufacturer's instructions for the development of these proteins, and by virtue, the natural products are encoded in the DNA or the genes of that organism.

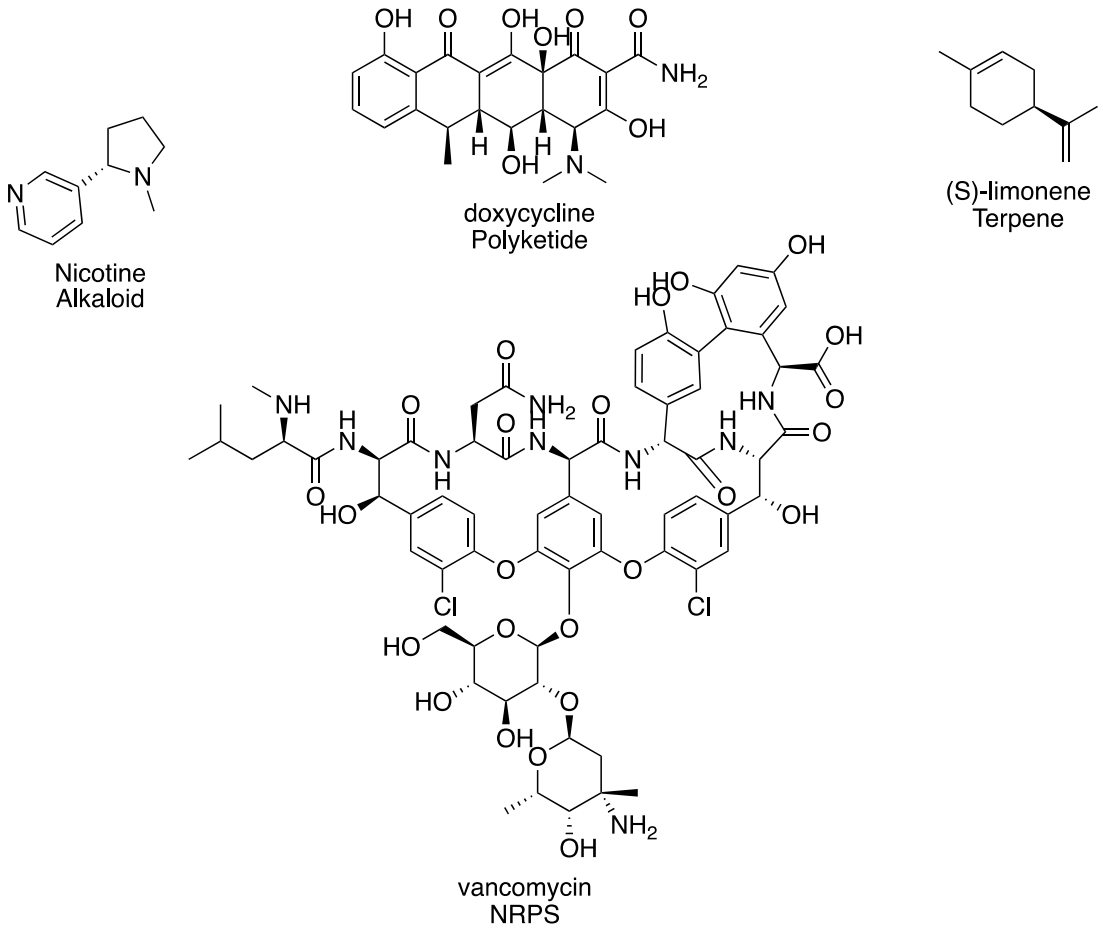

Figure 1. Types of natural products and examples of each.

There are many different types and classes of natural products. The majority of secondary natural products, especially marine natural products, fall into one of these main classes: 1) polyketides and fatty acids 2) terpenoids and steroids 3) nonribosomal peptides 4) alkaloids (Figure 1). These natural product classes each have their own, specific, enzymatic machinery that is utilized to construct the natural products that make up their ranks.[6]

1.2.1 Polyketides

Polyketides are natural products that are formed from the condensation of acetate or malonate starter units via decarboxylation by enzymatic machinery. These units can be further modified via oxidizations, eliminations, reductions, and other analogous chemistry/tailoring enzymes. The enzymes that piece together polyketides are a direct result of the genes that encode for each protein. The genes responsible for natural product formation tend to be clustered together. With the advent of bioinformatics and annotation of gene clusters and their encoded proteins, a certain level of prediction can be made regarding the products of certain gene clusters. Ultimately, polyketide structure can sometimes be predicted based on the clustered genes that make up the enzymatic machinery.

The enzymatic machinery (synthases) of polyketides falls into three categories: Type I, Type II, and Type III. Type I polyketide synthases (PKSs) are multifunctional enzymes where each domain performs a particular catalytic function (elongation of chains via acetyl or malonyl units, transfer of chains from one module to another via acyl carrier proteins, and chemical modification of existing chains) within a module. Type I PKSs are conventionally non-iterative, with sequential action performed on the growing chain at each domain within a module until the molecule is constructed.[7] Since Type I PKSs are non-iterative in nature, there tend to be more modules needed in the construction of natural products that arise from these synthases. Type I PKSs are responsible for the

production of macrolides: large macrocyclic lactones that sometimes contain sugar moieties attached to hydroxyl groups.

Like Type I PKSs, Type II PKSs are also multi enzymatic complexes with domains for piecing together natural products. The difference lies in the iterative nature of the synthase. Type II PKSs are iterative, with the same module performing chemistry on the substrate until the molecule is completed. Natural products produced by Type II PKSs are characterized by being highly cyclic and typically aromatic, usually polyphenolic by nature. Doxorubicin, a potent chemotherapy drug, and the tetracyclines, broad spectrum antibiotics, are structurally indicative of Type II PKS constructed natural products.[8]

Type III PKSs (also known as chalcone synthase-like PKSs) contain the simplest structure: they do not contain acyl carrier proteins and are composed of a homodimeric ketosynthase domain. Similar to Type II PKSs and their simple architecture, Type III PKSs iteratively act on their substrate until a natural product is completed. Natural products that result from Type III PKSs are typically mono- or bicyclic aromatic compounds such as flavolin.[9]

1.2.2 Terpenoids

Terpenes are a large group of natural products that are produced primarily in plants and fungi. They are made up of 5 carbon subgroups known as isoprenes that are joined together to give long-chain 5 carbon connections. An enzyme known as terpene cyclase holds these long chain carbon networks

in particular configurations so they can react via carbocation-mediated cyclizations and rearrangements. An example of which is the formation of hopene from squalene (Figure 2).

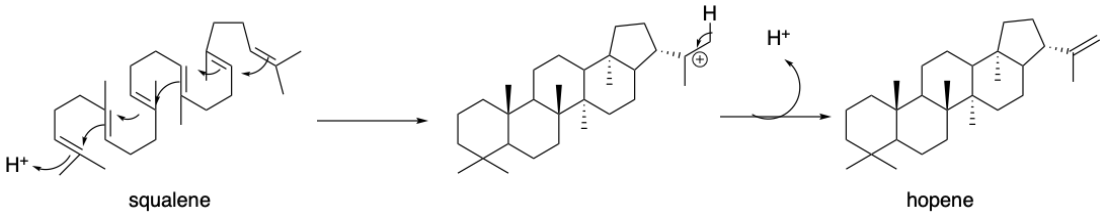

Figure 2. Hopene formation via squalene cyclization.

These newly formed molecules can be oxidized, or react with sugars, fatty acids, or other moieties to give complex structures.[10] Depending on the number of isoprene units joined together (10-monoterpene; 15-sesquiterpene; 20-diterpene) and various modifications, such as biosynthetic prenylations and alkylations, a vast number of potential terpenes can be made from simple starter units and basic chemistry.

1.2.3 Non-Ribosomal Peptides

Non-ribosomal peptides (NRPs) are a diverse set of natural products with an equally diverse set of properties. From actinomycin (an anticancer agent), the indigoidine (pigments), to pyoverdines (siderophores), NRPs are found in many systems and utilized in many industries. NRPs originate from non-ribosomal peptide synthases (NRPSs). Since these secondary metabolites do not require ribosomes in their biosynthesis, they are distinct from

conventional peptides and amino acids. Similar to PKSs, NRPSs are modular in nature with each domain within the module catalyzing additions to the molecule.[11]

1.2.4 alkaloids

Alkaloids represent a group of natural products that are related by having nitrogen in a heterocyclic ring. They vary from amino acids in that they are not ribosomally produced. They are most commonly produced by plants but they are also produced by fungi and bacteria as well. One of the most common alkaloids is the pain-relieving opioid morphine. Alkaloid biosynthesis is complex and typically begins with amino acids, followed by enzymatic decarboxylation to form an amine which undergoes further enzymatic reactions to construct the natural product. As many different starter units can be utilized, the diversity of the class of natural products is large and leads to compounds with interesting and diverse biological activities.

1.3 Non-enzymatic chemistry in the Context of the Origins of Life

The central dogma states that DNA contains the template for RNA and, thus, protein synthesis. These proteins/enzymes are then responsible for constructing the natural products that aid in an organism’s fitness in its environment. There exists, however, within the realm of traditional enzymatic natural product synthesis, cases in which intermediates, shunt products, or

even completed natural products in traditional natural product biosynthesis can react abiotically to form new bonds. This “non-enzymatic” chemistry can lead to new and diverse scaffolds with particularly interesting bioactivity. These products have been shown to not only lead to new scaffolds but also play important roles in metabolism and fitness.

Non-enzymatic chemistry is not a novel idea. It is something that has long existed in the realm of biochemistry, but never properly studied or properly classified in the natural products space. Examples of non-enzymatic chemistry can be seen throughout biology and chemistry and with importance to the producing organism. Natural amino acids and sugars are have assymmetry. When an abiotic reaction is performed in the lab without a chiral catalyst or handle, the result is typically a racemic mixture. In a prebiotic world without well-developed enzymes or machinery, asymmetric molecules were not only formed, but nature somehow developed a preference for a particular enantiomer. Events that could form chiral amino acids and important proteins have been extensively studied in the field of the origins of life.[12] A few examples of scenarios that could occur on a molecular basis are shown below.

1.3.1 Non-Enzymatic Amino Acid Synthesis

Chemistry is predicated on the notion that molecules collide and those intermolecular collisions/interactions predicate the formation and cleavage of bonds to get new molecules. These new molecules can then do the same thing

to get even more complex compounds. In the confines of space, small carbon, nitrogen, and oxygen based molecules in gaseous mixtures can condense onto interstellar dust grains to form interstellar ices.[13] It is believed that UV light and other radiation in space can cause chemical reactions between those carbon, nitrogen, and oxygen molecules.[14] These reactions were simulated in order to study the origin of interstellar small molecules that could have a hand in the beginnings of life terrestrially. To perform the simulation, gases (H_2O, NH_3, CO, CO_2, and CH_3OH) found to exist in space via infrared spectroscopy (IR) were condensed onto a surface and hit with various forms of radiation in order to stimulate chemical reactions at interstellar conditions (10-80K and under vacuum), and the results subsequently measured by Gas Chromatography Mass Spectrometry (GCMS).[15–17] Two teams simultaneously performed the interstellar ice reactions and both obtained amino acids as products, with one team obtaining glycine, serine, and alanine, while the other identifying 16 amino acids, six of which were amino acids found in proteins (alanine, glycine, serine, valine, proline, and aspartic acid).[18,19] Not only can fundamental sources of life and carbon be found in space, but they can also react with one another to form the foundational source of proteins important for life: amino acid derivatives. Most importantly, the only prerequisite for these reactions to occur is a surface to react on and irradiation from an external source.

1.3.2 Asymmetry in Abiotic Amino Acids

Circularly polarized light (CPL) is an electromagnetic wave that is composed of two perpendicular vectors that are of the same magnitude but offset by 90 degrees. As a result, CPL has inherent handed-ness, since the direction of rotation makes it either right-handed or left-handed. Using an analytical technique known as circular dichroism (CD), the right or left handed-ness of molecules can be studied.[20] CD measurements demonstrate the interaction of a molecule with the handed-ness of the CPL. If a molecule has a preference to absorb right or left CPL, the molecule's asymmetry can be inferred. If no absorption is observed and the molecule has no right or left CPL preference, the molecule is deemed a racemic mixture or achiral. CPL was utilized to photolyze samples and study desymmetrization in amino acids.[12] If one enantiomer in a mixture was photolyzed at a faster rate than the other, there was a clear case for an enantiomeric preference. Using Photoelectric CD (a method that photolyzes based on differential absorption of right or left circularly polarized light), gas phase alpha-alanine was irradiated with CPL to give gaseous alanine cations. The resulting alpha-alanine cations had an enantiomeric excess (ee) of 4%.[21] This result is particularly interesting in the context of space. It demonstrates that in the gaseous, crystalline dust vacuum that is the cosmos, natural CPL in space (potentially from the refraction of linear light with interstellar reflection nebulae), can cause an asymmetric preference within amino acids.

Meteorites have been studied extensively throughout history. They are a constant source of inspiration for scientists and give clues about the founding of the universe as well as the possibility of organic life outside of earth. In the context of the astrophysical basis for asymmetry, amino acids within meteorites have been explored. In 1969, the Murchison meteorite fell to earth and started a search for any interesting organic material within the meteorite, and, by proxy, outer space. Initially, seven amino acids were discovered via GCMS within the meteorite: glycine, alanine, valine, glutamic acid, proline, 2-methylalanine, and sarcosine.[22] Not only were these amino acids found within the meteorite, they were also found as racemic mixtures, demonstrating their extraterrestrial nature. More amino acids were discovered within the meteorite in 1971 and in the 1980s. In particular, iso-valine. Iso-valine is of particular interest since it lacks an alpha proton with which to racemize an enantiomerically pure sample. Alpha methyl amino acids were shown to be an important clue into the desymmetrization of these amino acids. Around this time, the alpha methyl amino acids in the Murchison and Murray meteorites were shown to have small percent enantiomeric excess (% ee) (ranging from 2.8-9.2% (±0.3-1.3%) and 1.0-6.0% (±0.3-0.7%) respectively. Furthermore, there was an even greater enantiomeric excess for the alpha methyl amino acids.[23–25] Since racemization is more difficult with alpha methyl amino acids, any desymmetrization that was present prior would be more readily maintained within the meteorite sample. It seems as if the desymmetrization could be caused by CPL in space and that

small level of stereo enrichment could be the basis for a preference of particular enantiomers from meteorites or other space debris in early, abiotic earth.

1.3.3 Non-Enzymatic Synthesis of Sugars

Sugars, like amino acids, also have an asymmetric preference in nature. They typically are derived from D-glyceraldehyde. In a similar vein to the amino acid story, the Murchison and Murray meteorites were studied by Cooper and Rios and sugars and acids of various carbon lengths were found.[26] Interestingly, of the sugar species found within the meteorite, only the acids such as threonic (2S, 3R) and erythronic acid (SR, 3R) were found as asymmetric. In addition, they were found to have all have an excess of the D-glyceraldehyde derived enantiomer. The alcoholic sugars were all found as racemic/achiral mixtures.

In order to simulate cosmic conditions in the formation of simple biological sugars, the interstellar ice method was utilized. The reaction was performed with a mixture of H_2O:CH_3OH:NH_3 (10:3.5:1) (to emulate space conditions) at low temperature (78K) and pressure (10^{-7} mbar). The condensed gases were irradiated and ribose was synthesized via the formose reaction, demonstrating an abiotic way to produce the biological building block.[27] More recently and using a simpler mixture, H2O:CH3OH (2:1) was irradiated to give 2-deoxyribose, a DNA precursor, and other deoxysugars.[28]

1.3.4 Non-Enzymatic Glycolysis

Metabolism is a complex balance of anabolism and catabolism that requires both for the support of life. Studies by *Messler et al*. were performed to demonstrate a non-enzymatic basis for metabolic processes. In particular, gluconeogenesis was studied.[29] Previous work had shown that glycolysis, the pentose phosphate pathway, and other metabolic pathways could be modeled non-enzymatically with gluconeogenesis being an important pathway in both of those processes.[30,31] Gluconeogenesis is responsible for the production of hexose-phosphates, which are used in both glycolysis and the pentose phosphate pathway. The C-C bonds cleaved by glycolysis are reformed in gluconeogenesis. One reaction of note is the formation of fructose 1,6-bisphosphate (F16BP) from dihydroxyacetone phosphate (DHAP) and D-glyceraldehyde 3-phosphate (G3P) (Figure 3).[29]

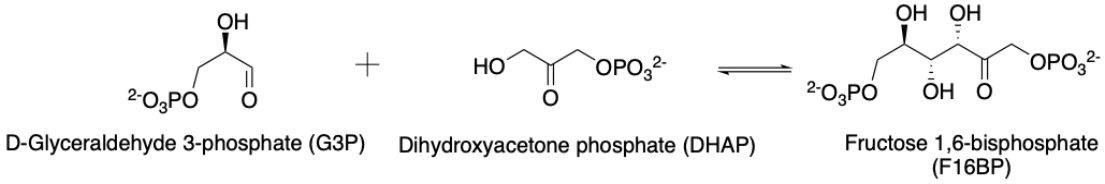

Figure 3. Conversion of G3P and DHAP to F16BP in ice.

Messler modeled the Aldol condensation of DHAP and G3P. At room and higher temperatures, the reactants convert readily into pyruvate, but at -20°C, the reactants convert into F16BP. Furthermore, the addition of lysine and glycine accelerate the rate of conversion into F16BP. The aforementioned examples demonstrate how non-enzymatic chemistry could play a crucial role

in the development of early life as we know it as well as set the foundation for modern enzymes and metabolic pathways.

1.4 Modern Non-Enzymatic Chemistry

The non-enzymatic chemistry that made up the abiotic world and set the foundation for modern proteins, enzymes, and other biologically imperative macromolecules remains important for the fitness of various organisms today as well as give us the ability to craft new molecules with interesting biological activity and inhabit new chemical spaces. A few examples indicative of the importance of current non-enzymatic chemistry for organisms are shown and discussed below.

1.4.1 Dibohemaines

The bohemamines are bacterial alkaloids, originally isolated from *Actinosporangium* and elucidated by *Doyle et al.,* that contain a pyrrolizidine core.[32] While many molecules in the pyrrolizidine class of alkaloids were known to have genotoxic and mutagenic properties as well as liver toxicity, the bohemamines did not show any promising antibacterial, antifungal, or antitumor behavior.[33] In 2016, three bohemamine dimers (dibohemamines) were isolated by the MacMillan lab, with all three dimers having the same motif: two bohemamine monomers pieced together by a methylene bridge (Figure 4).[34]

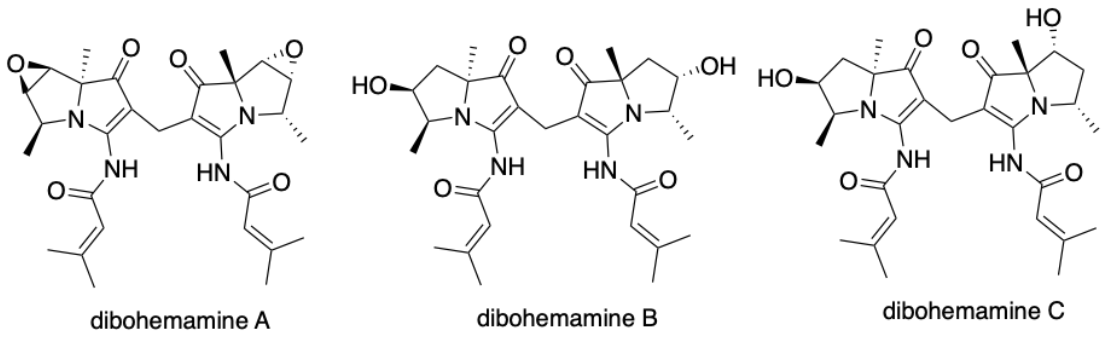

Figure 4. Structures of dibohemamines A, B, and C.

Since the bridging methylene group had no origins from the monomeric units, it was implied that the carbon addition was from an external source. Most notably, formaldehyde represents one of the reactive and common single carbon sources in nature. Performing the potential non-enzymatic reaction of bohemamine with 37% formaldehyde in THF gave the bohemamine dimer as well as a key intermediate where the aldehyde is added to the alpha position of the pyrrolizidine ketone of the bohemamine monomer but is not dimerized. It was believed that the monomeric aldehyde addition was the first step in dimerization. Once the primary alcohol is formed from the addition to one monomer, the alcohol is protonated (the media the strain is grown in is mildly acidic), the alcohol leaves as H_2O, and the second monomer then reacts at the carbocationic site via S_N1 to give the dimer (Figure 5). Unreacted intermediate was taken and pushed forward to the dimer by adding in 0.5% formic acid. The resulting products only contained formic acid and dibohemamine, demonstrating that the reaction is irreversible.

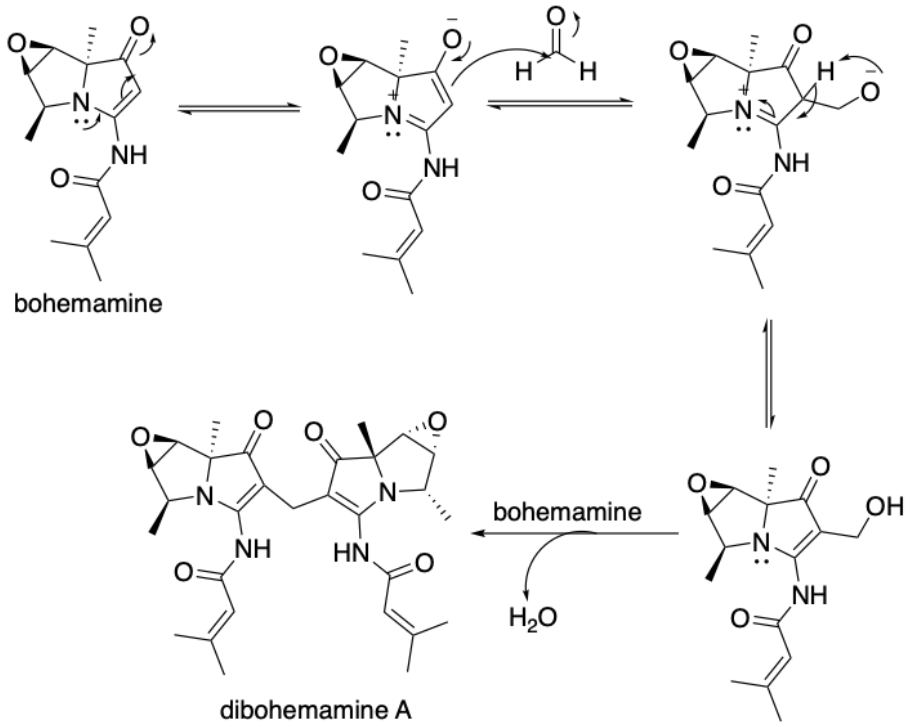

Figure 5. Mechanism of dibohemamine formation.

In the context of the producing organism, formaldehyde is generally toxic. It is a DNA damaging agent that crosslinks DNA and causes irreparable damage to various species. For something as toxic and dangerous as formaldehyde to an organism, it is necessary to have a means to detoxify and remove the potential source of danger for the producing organism. As a result, the bohemamines could be a source of detoxification for the producing organism. Also, the dimers could potentially be a byproduct of the non-enzymatic detoxification process for the organism rather than something intrinsically necessary for its survival or fitness.

In addition to the interesting dimerization chemistry, the dibohemamines, B and C in particular, had anticancer activity. When tested against Non-Small

Cell Lung Cancer Cell Lines (NSCLC cell lines), dibohemamines B and C exhibited 0.140 and 0.145 uM activity against the A549 NSCLC cell line.[34] The positive NSCLC assay results as well as the simplicity of the dimerization reaction inspired the group to create a suite of analogs to try and replicate or improve the bioactivity seen by dibohemamines B and C**.** The analogs could be made by modifying the aldehyde responsible for the methylene bridge. The analogs did not perform better than dibohemamines B and C but demonstrate the overall idea that non-enzymatic chemistry endemic to an organism can be utilized to further explore and improve upon the natural chemical space.

1.4.2 Ammosamides

The ammosamides are chlorinated alkaloids of a pyrroloquinoline family of natural products that contain multiple heteroatoms such as nitrogen, oxygen, and sulfur (ammosamide A). Ammosamides A and B were isolated from *streptomyces* strain CNR-698 in the Bahamas by the Fenical group. Ammosamides A and B were found to have anticancer activity when tested against colon sarcoma cancer cell line HCT-116 via selective targeting of myosin, a protein crucial for cellular motility.[35] In addition, it was demonstrated that ammosamide B was also shown to inhibit quinone reductase-2, through the inhibition of quinoline conversion into more reactive species.[36] In another ammosade-based study of *Streptomyces variabilis*, Pan et al. were able to

isolate ammosamide E, an analog with an fascinating endocyclic amidine moiety (Figure 6).

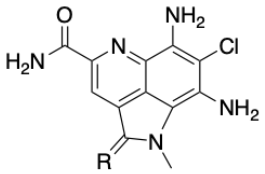

R = S = ammonsamide A R = O = ammonsamide B R = H = ammonsamide C R = NH = ammonsamide E

Figure 6. Ammosamides A, B, C, and E.

Hoping to induce the production of more ammosamide E, tryptophan, a common amine precursor, was fed into the media. The result was ammosamide F, which is based on the incorporation of anthranilic acid, a common tryptophan catabolite, into the endocyclic amidine. This led the group to introduce other amines into the media to induce the production of various other ammosamide derivatives (Figure 7).

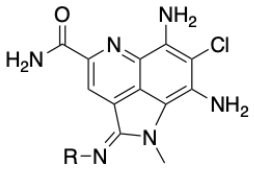

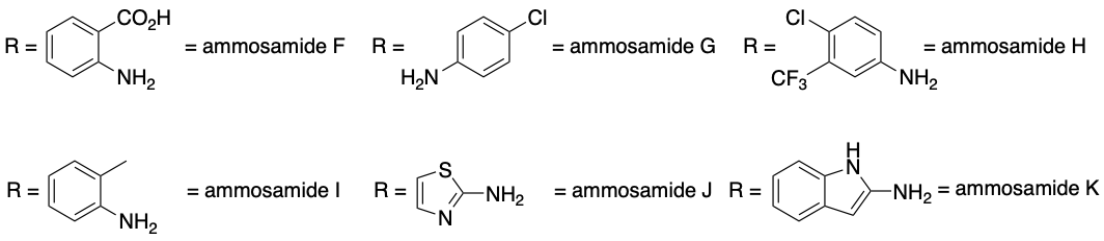

Figure 7. Ammosamides F - K.

The introduction of the various amines ammosamide skeleton was serendipitous and important to study. The group attempted to directly convert

the thioamide of ammosamide A to the amidine seen in the derivatives via late stage amidation but chemical conversion was poor, showing the difficulty in semi-synthetic methods. Two studies were performed to determine the formation of the ammosamide analogues: the first was the removal of the bacterial cells from a 4-day growth of *Streptomyces variabilis*, followed by incubation with 4-choloraniline. If the addition of the amines to the media was enzymatically-based, there would be no reaction with the 4-chloroaniline once the bacterial cells were removed from the media as the enzymatic machinery for the bacteria would be in the cell. The derivative was cleanly formed following addition of 4-choloraniline, illustrating that the incorporation of the amines in the ammosamide core was of a non-enzymatic origin. In particular, it was believed the addition occurred with ammosamide C, a reactive imine that was detected in the media. This was probed by reacting synthetic prepared ammosamide C with 4-chloroaniline in growth media for 24 hours. This reaction also yielded the 4-chloroaniline derivative cleanly with the only impurities being unreacted ammosamide C and ammosamide B (presumably through addition of water followed by oxidation in air). The ammosamides and the introduction of various amines via the non-enzymatic reaction with an imine intermediate further demonstrate the power of exploring and, ultimately, utilizing non-enzymatic chemistry found in natural product biosynthesis whenever possible.

1.4.3 Discoipyrroles

The discoipyrroles are alkaloid natural products isolated from the bacteria *Bacillus hunanensis* that were found to have NSCLC cell line activity via the disruption of the discoidin domain receptor 2 (DDR2) signaling pathway (crucial in cell motility). The discoipyrroles were linked to the inhibition of the DDR2 pathway via an intricate assay (FUSION) that associates molecular targets with biologically active natural products through the use of SiRNAs.[37] The utilization of various SiRNAs with a particular cell line of interest gives a unique genotypic signature. If the natural products/compounds tested give the same genotypic signature, it is believed to follow the same pathway in its effects against the cell line. As a result, the discoipyrroles were linked to the DDR2 pathway via FUSION. The discoipyrroles have a distinctive pyrrole-like core with a beta ketone with the sole stereocenter being the isopropyl group at the alpha position of the pyrrole nitrogen. The discoipyrroles originate from precursor molecules hydroxysattabacin, 4-hydroxybenzaldehyde, and an amine (anthranilic acid for discoipyrrole A) (Figure 8).

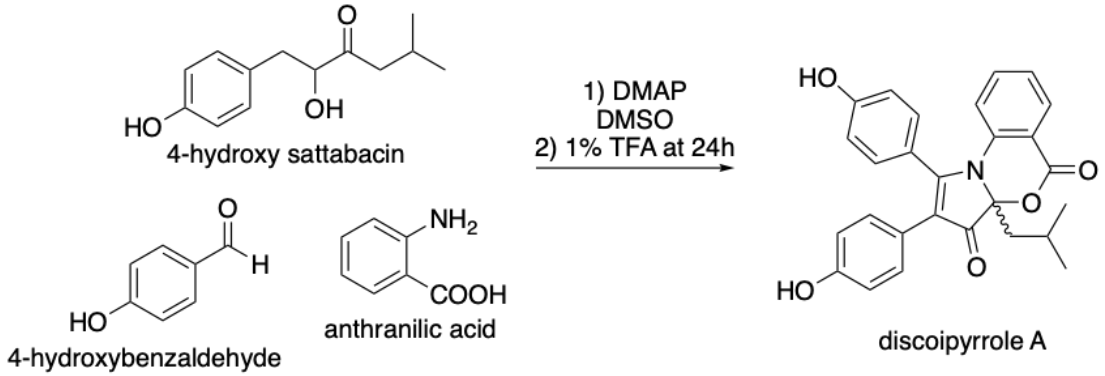

Figure 8. Discoipyrrole A formation.

The discoipyrroles were isolated as racemic mixtures, which implied the formation of the discoipyrroles contains one or more non-enzymatic steps in their biosynthesis. This non-enzymatic basis was further exemplified by feeding studies where hydroxysattabacin, 4-hydroxybenzaldehyde, and anthranilic acid were fed to cell-free “spent” media, or media without metals or cofactors that could help enzymes catalyze reactions. In addition, the media used was from a different strain of *bacillus*, one that did not produce discoipyrrole A. The result of the feeding study was that discoipyrrole A was still formed, demonstrating the non-enzymatic reaction that formed the discoipyrroles.

The non-enzymatic formation of discoipyrrole formation was studied by Colosimo et al.[38] This was done via the utilization of isotopically-labeled substrates (^{13}C, ^{15}N, ^{18}O) and Nuclear Magnetic Resonance (NMR). In particular, ^{15}N NMR was utilized since NMR is a particularly sensitive method of analysis and the ^{1}H-^{15}N correlations would give accurate data on the identity of transient nitrogen species. As the molecules react and change, the ^{15}N spectra changes accordingly, giving a relative time lapse of the formation of the discoipyrroles from the precursor molecules. The ^{15}N NMR scale shown below illustrates the dynamic range of various nitrogen species.

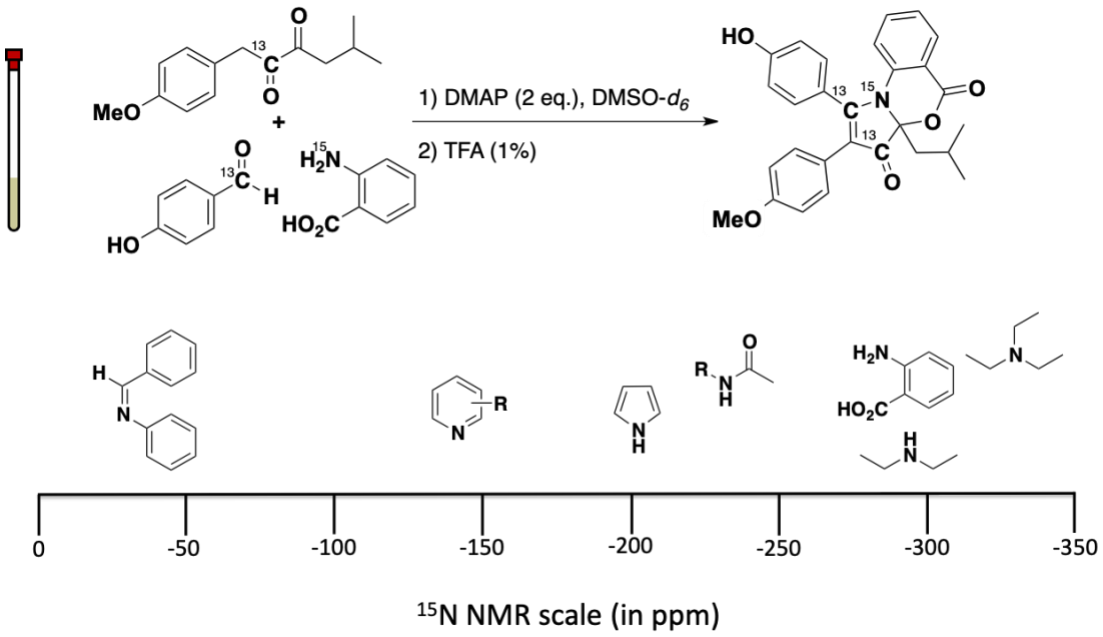

Figure 9. ^{15}N NMR Scale.

Of the three precursor molecules, ^{15}N labeled anthranilic acid was utilized as well as [1-^{13}C] para-hydroxybenzaldehyde for the NMR studies. The materials were placed in an NMR tube with DMAP and in DMSO and monitored with ^{1}H-^{15}N HMBC every 30 minutes for 36 hours (Figure 10).

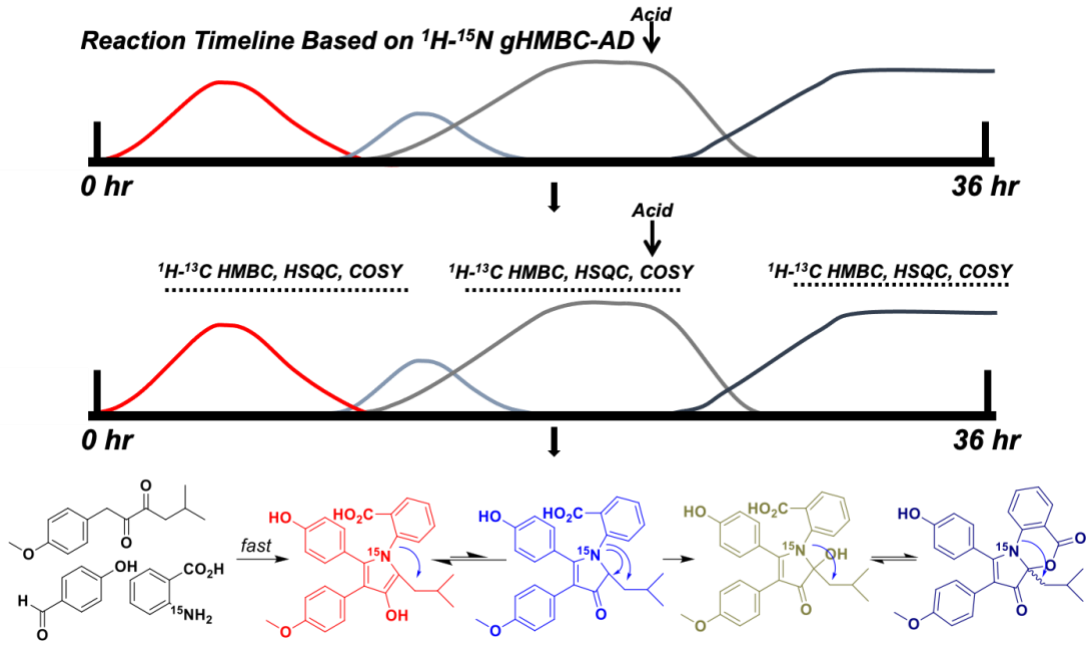

Figure 10. Reaction timeline for discoipyrrole A formation.

The ^{1}H-^{15}N correlations showed the appearance and disappearance of multiple intermediates over time, beginning from the signals of ^{15}N-labeled anthranilic acid. At around the 24 hour point, a free acid intermediate of discoipyrrole A was formed but there was no intramolecular esterification with the hydroxyl group beta to the pyrrole nitrogen. The reaction was run again, and, In order to promote the esterification, 1% TFA was added to the NMR tube at 24 hours. This provided the jolt the reaction needed, and discoipyrrole A was obtained. The non-enzymatic reaction in the NMR tube was run again, but different 2D NMR experiments were run this time, focusing on the the [1-^{13}C] of the para-hydroxybenzaldehyde in order to better ascertain the identity of the intermediates. The discoipyrroles demonstrate how to accurately study non-

enzymatic reactions and probe their mechanisms of formation with precision and reproducibility.

1.5 Conclusion

As shown above, non-enzymatic reactions play an important role not only in the production of secondary metabolites in various organisms, but also in the prebiotic reactions that helped define chemistry and life as we know it today. These reactions, while hard to find and even harder to study, provide a basis for which future chemistry can be modeled as well as handles for which to develop new molecules and explore further chemical space. These non-enzymatic reactions and examples thereof form the foundation for which the work that follows is closely modeled after.

1.6 Chapter 1 References

(1) Sapkota, A. Primary vs Secondary Metabolites- Definition, 12 Differences, Examples https://microbenotes.com/primary-vs-secondary-metabolites/ (accessed 2022 -02 -11).

(2) Metabolites https://byjus.com/biology/metabolites/ (accessed 2022 -02 -11).

(3) Gaynes, R. The Discovery of Penicillin—New Insights After More Than 75 Years of Clinical Use. *Emerging Infectious Diseases*. 2017, pp 849–853. https://doi.org/10.3201/eid2305.161556.

(4) Newman, D. J.; Cragg, G. M. Natural Products as Sources of New Drugs from 1981 to 2014. *J. Nat. Prod.* **2016**, *79* (3), 629–661.

(5) Pye, C. R.; Bertin, M. J.; Lokey, R. S.; Gerwick, W. H.; Linington, R. G. Retrospective Analysis of Natural Products Provides Insights for Future Discovery Trends. *Proc. Natl. Acad. Sci. U. S. A.* **2017**, *114* (22), 5601–5606.

(6) The Classes of Natural Product and Their Isolation. *Tutorial Chemistry Texts*. 2003, pp 1–34. https://doi.org/10.1039/9781847551535-00001.

(7) Miyanaga, A. Structure and Function of Polyketide Biosynthetic Enzymes: Various Strategies for Production of Structurally Diverse Polyketides. *Biosci. Biotechnol. Biochem.* **2017**, *81* (12), 2227–2236.

(8) Hertweck, C.; Luzhetskyy, A.; Rebets, Y.; Bechthold, A. Type II Polyketide Synthases: Gaining a Deeper Insight into Enzymatic Teamwork. *Nat. Prod. Rep.* **2007**, *24* (1), 162–190.

(9) Shen, B. Polyketide Biosynthesis beyond the Type I, II and III Polyketide Synthase Paradigms. *Curr. Opin. Chem. Biol.* **2003**, *7* (2), 285–295.

(10) Helfrich, E. J. N.; Lin, G.-M.; Voigt, C. A.; Clardy, J. Bacterial Terpene Biosynthesis: Challenges and Opportunities for Pathway Engineering. *Beilstein J. Org. Chem.* **2019**, *15*, 2889–2906.

(11) Martínez-Núñez, M. A.; López y López, V. E. Nonribosomal Peptides Synthetases and Their Applications in Industry. *Sustainable Chemical Processes*. 2016. https://doi.org/10.1186/s40508-016-0057-6.

(12) Garcia, A. D.; Meinert, C.; Sugahara, H.; Jones, N. C.; Hoffmann, S. V.; Meierhenrich, U. J. The Astrophysical Formation of Asymmetric Molecules and the Emergence of a Chiral Bias. *Life* **2019**, *9* (1). https://doi.org/10.3390/life9010029.

(13) Gargaud, M.; Irvine, W. M.; Amils, R.; Quintanilla, J. C.; Cleaves, H. J.; Pinti, D.; Rouan, D.; Spohn, T.; Tirard, S.; Viso, M. *Encyclopedia of Astrobiology*; Springer, 2015.

(14) Amils, R.; Quintanilla, J. C.; Cleaves, H. J.; Irvine, W. M.; Pinti, D.; Viso, M. *Encyclopedia of Astrobiology*; Springer, 2011.

(15) Website https://arxiv.org/abs/1902.04575.

(16) [No title] https://cs.uwaterloo.ca/~cdimarco/pdf/cogsci600/7_Greenberg.pdf (accessed 2022 -01 -01).

(17) [No title] https://iopscience.iop.org/article/10.1086/381182/pdf (accessed 2022 -01 -01).

(18) Bernstein, M. P.; Dworkin, J. P.; Sandford, S. A.; Cooper, G. W.; Allamandola, L. J. Racemic Amino Acids from the Ultraviolet Photolysis of Interstellar Ice Analogues. *Nature* **2002**, *416* (6879), 401–403.

(19) Muñoz Caro, G. M.; Meierhenrich, U. J.; Schutte, W. A.; Barbier, B.; Arcones Segovia, A.; Rosenbauer, H.; Thiemann, W. H.-P.; Brack, A.; Greenberg, J. M. Amino Acids from Ultraviolet Irradiation of Interstellar Ice Analogues. *Nature* **2002**, *416* (6879), 403–406.

(20) Barron, L. D. True and False Chirality and Absolute Asymmetric Synthesis. *Journal of the American Chemical Society*. 1986, pp 5539–5542. https://doi.org/10.1021/ja00278a029.

(21) Tia, M.; Cunha de Miranda, B.; Daly, S.; Gaie-Levrel, F.; Garcia, G. A.; Nahon, L.; Powis, I. VUV Photodynamics and Chiral Asymmetry in the Photoionization of Gas Phase Alanine Enantiomers. *J. Phys. Chem. A* **2014**, *118* (15), 2765–2779.

(22) Kvenvolden, K.; Lawless, J.; Pering, K.; Peterson, E.; Flores, J.; Ponnamperuma, C.; Kaplan, I. R.; Moore, C. Evidence for Extraterrestrial Amino-Acids and Hydrocarbons in the Murchison Meteorite. *Nature* **1970**, *228* (5275), 923–926.

(23) Cronin, J. R.; Pizzarello, S. Enantiomeric Excesses in Meteoritic Amino Acids. *Science* **1997**, *275* (5302), 951–955.

(24) Cronin, J. R.; Pizzarello, S. Amino Acid Enantiomer Excesses in Meteorites: Origin and Significance. *Advances in Space Research*. 1999, pp 293–299. https://doi.org/10.1016/s0273-1177(99)00050-2.

(25) Pizzarello, S.; Cronin, J. R. Non-Racemic Amino Acids in the Murray and Murchison Meteorites. *Geochim. Cosmochim. Acta* **2000**, *64* (2), 329–338.

(26) Cooper, G.; Rios, A. C. Enantiomer Excesses of Rare and Common Sugar Derivatives in Carbonaceous Meteorites. *Proc. Natl. Acad. Sci. U. S. A.* **2016**, *113* (24), E3322–E3331.

(27) Meinert, C.; Myrgorodska, I.; de Marcellus, P.; Buhse, T.; Nahon, L.; Hoffmann, S. V.; d'Hendecourt, L. L. S.; Meierhenrich, U. J. Ribose and Related Sugars from Ultraviolet Irradiation of Interstellar Ice Analogs. *Science* **2016**, *352* (6282), 208–212.

(28) Nuevo, M.; Cooper, G.; Sandford, S. A. Deoxyribose and Deoxysugar Derivatives from Photoprocessed Astrophysical Ice Analogues and Comparison to Meteorites. *Nat. Commun.* **2018**, *9* (1), 5276.

(29) Messner, C. B.; Driscoll, P. C.; Piedrafita, G.; De Volder, M. F. L.; Ralser, M. Nonenzymatic Gluconeogenesis-like Formation of Fructose 1,6-Bisphosphate in Ice. *Proc. Natl. Acad. Sci. U. S. A.* **2017**, *114* (28), 7403–7407.

(30) Keller, M. A.; Turchyn, A. V.; Ralser, M. Non-enzymatic Glycolysis and Pentose Phosphate Pathway-like Reactions in a Plausible A Rchean Ocean. *Molecular Systems Biology*. 2014, p 725. https://doi.org/10.1002/msb.20145228.

(31) Keller, M. A.; Zylstra, A.; Castro, C.; Turchyn, A. V.; Griffin, J. L.; Ralser, M. Conditional Iron and pH-Dependent Activity of a Non-Enzymatic Glycolysis and Pentose Phosphate Pathway. *Science Advances*. 2016. https://doi.org/10.1126/sciadv.1501235.

(32) Doyle, T. W.; Nettleton, D. E.; Balitz, D. M.; Moseley, J. E.; Grulich, R. E.; Mccabe, T.; Clardy, J. ChemInform Abstract: ISOLATION AND STRUCTURE OF BOHEMAMINE (1Aβ,2α,6Aβ,6Bβ)-3-METHYL-N-(1A,6,6A,6B-TETRAHYDRO-2,6A-DI# METHYL-6-OXO-2H-

OXIRENO(A)PYRROLIZIN-4-YL)-2-BUTENAMIDE. *Chemischer Informationsdienst*. 1980. https://doi.org/10.1002/chin.198029340.

(33) Riddelliine N-Oxide Is a Phytochemical and Mammalian Metabolite with Genotoxic Activity That Is Comparable to the Parent Pyrrolizidine Alkaloid Riddelliine. *Toxicol. Lett.* **2003**, *145* (3), 239–247.

(34) Fu, P.; Legako, A.; La, S.; MacMillan, J. B. Discovery, Characterization, and Analogue Synthesis of Bohemamine Dimers Generated by Non-Enzymatic Biosynthesis. *Chemistry - A European Journal*. 2016, pp 3491–3495. https://doi.org/10.1002/chem.201600024.

(35) Hughes, C. C.; MacMillan, J. B.; Gaudêncio, S. P.; Jensen, P. R.; Fenical, W. The Ammosamides: Structures of Cell Cycle Modulators from a Marine-Derived Streptomyces Species. *Angew. Chem. Int. Ed Engl.* **2009**, *48* (4), 725–727.

(36) Reddy, P. V. N.; Jensen, K. C.; Mesecar, A. D.; Fanwick, P. E.; Cushman, M. Design, Synthesis, and Biological Evaluation of Potent Quinoline and Pyrroloquinoline Ammosamide Analogues as Inhibitors of Quinone Reductase 2. *J. Med. Chem.* **2012**, *55* (1), 367–377.

(37) Hu, Y.; Potts, M. B.; Colosimo, D.; Herrera-Herrera, M. L.; Legako, A. G.; Yousufuddin, M.; White, M. A.; MacMillan, J. B. ChemInform Abstract: Discoipyrroles A-D: Isolation, Structure Determination, and Synthesis of Potent Migration Inhibitors from Bacillus Hunanensis. *ChemInform*. 2014, p no – no. https://doi.org/10.1002/chin.201408219.

(38) Colosimo, D. A.; MacMillan, J. B. Detailed Mechanistic Study of the Non-Enzymatic Formation of the Discoipyrrole Family of Natural Products. *J. Am. Chem. Soc.* **2016**, *138* (7), 2383–2388.

Chapter Two: Synthesis of oxazinin A and Similar Analogs

2.1 Abstract

Tuberculosis affects millions of people a year and is incredibly difficult to treat. Due to this, many drugs are utilized to combat the disease and ease the suffering of those affected. Due to rising resistance, it is necessary to have novel drugs that can effectively target drug resistant *Mycobacterium tuberculosis* (*Mtb*). Oxazinin A, a pseudo dimeric natural product isolated from a marine-derived fungus was shown to have low μM activity against *Mtb*. I describe the total synthesis of oxazinin A, study of the non-enzymatic formation, and analog generation processes that ultimately led to the total synthesis of this complex natural product.

2.2 Introduction to Tuberculosis

Tuberculosis is a devastating disease that affects over 10 million people a year.[1] Furthermore, approximately 1.5 million of those 10 million died from tuberculosis and tuberculosis-adjacent illnesses. The disease is caused by the gram-positive bacteria *Mycobacterium tuberculosis* (*Mtb*) and spreads through the air. Those infected can have mild symptoms such as a cough, fever, chills, or night sweats for many months: all things symptomatic of many illnesses such as the flu or even COVID-19. Individuals who are immuno-compromised due to other illnesses such as HIV have a much higher chance of being infected with and dying with tuberculosis (a factor of over 18 times). In fact, without

adequate treatment, 45% of all HIV negative people and all individuals who are HIV positive will die from the disease. This is represented by the fact that over 95% of all tuberculosis deaths and infections occur within developing countries.[1]

2.2.1 Mode of Infection

When infected with tuberculosis, *Mtb* infects the macrophages (specialized cells that help with the elimination of foreign organisms within the body) of their infected host.[2] Typically, when presented with a foreign organism, macrophages induce phagocytosis of the organism, and followed promptly by fusion with lysosomes, organelles that contain digestive enzymes. Once fusion is complete, the area with the bacteria present is acidified in order to eliminate the bacteria. When *Mtb* infects a macrophage, however, it interferes with the macrophage's ability to mature and, ultimately, acidify the lysosomes. Without the acidification ability, the bacteria can develop and spread more effectively. This ability to escape lysosomal elimination is one of the driving forces behind tuberculosis infection and pathogenicity. As the bacteria spreads to other organs and parts of the body, the cell-mediated immune response begins and the bacterial replication is thus controlled. As a result, a tenuous equilibrium between the innate immune response and bacterial replication is established: if the bacteria replicates too quickly and begins to be found in higher titers, the immune system will react; If the immune system is weakened and cannot field

a proper immune response, the bacterial concentration will increase exponentially. When the bacteria concentration is lower and in equilibrium with the innate immune response, it is referred to as latent *Mtb***.** Conversely, when the immune system is weakened and the bacteria is spreading rapidly, it is referred to as active *Mtb* (Figure 1).[3] When infected, a person who carries *Mtb* can be latent for many years before reactivation occurs, making tuberculosis much more difficult to treat than other common bacterial infections.

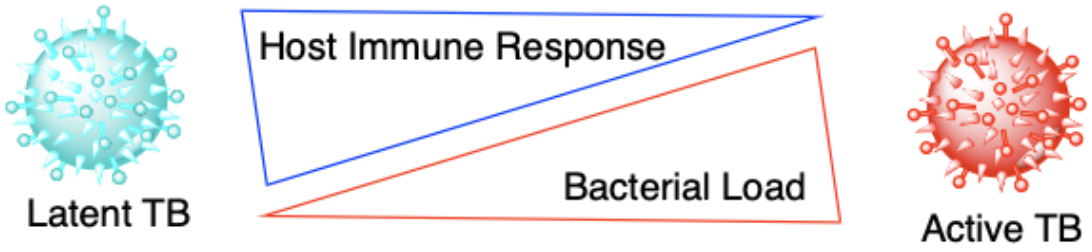

Figure 1. TB Infection and Equilibrium.

2.2.2 *Mtb* as a Difficult to Treat Organism

Mycobacterium tuberculosis is a gram positive bacteria that has a peculiar structure that makes it difficult to treat. Most gram positive bacteria are composed of a large peptidoglycan layer and a plasma membrane. Gram negative bacteria are composed of an outer lipid membrane, a much thinner peptidoglycan layer, and another outer membrane layer composed of lipopolysaccharides. As a result of the conflicting cell wall properties, treatments and therapeutics for gram positive and gram negative bacteria are typically different.

Interestingly, *Mycobacterium tuberculosis* has a hybrid cell wall structure with gram positive and gram negative bacterial characteristics. The main components of the *Mtb* cell wall (from the outside of the cell inwards) are the outer lipid layer, mycolic acid layer, arabinogalactan layer, and the peptidoglycan layer.[4,5] The peptidoglycan layer of *Mtb* is as thick as the peptidoglycan layer of gram positive bacteria, while the outer membrane (composed of the arabinogalactan and mycolic acid layers) resembles that of a gram negative bacteria. The outer layer is incredibly waxy. The mycolic acids are long chain (C60-C90) fatty acids, and the outer layer is composed of non-covalently attached (glyco)lipids and lipoglycans. When in combination with the peptidoglycan layer and the inner membrane, *Mtb* becomes incredibly difficult to treat due to the low permeability of compounds across the cell wall, and is a major part of its virulence factor.

2.2.3 Current Tuberculosis Treatment

Treatment for latent and active tuberculosis vary since an individual who carries latent tuberculosis is not contagious, contrary to the highly contagious active version of the disease. As mentioned above, latent TB becomes active when the host's immune system is weakened or compromised in any way. The goal in latent TB treatment is a preventative one rather than one to eliminate the bacteria. By keeping the immune system healthy and intact, the equilibrium between host immune response and bacterial load remains stable, and the

bacteria will remain in its latent stage, but not necessarily eliminating the bacteria. The infected individual will still carry the bacteria but may not fall ill or show symptoms. The current treatment for latent TB is a daily dose of isoniazid, an antibacterial and first line drug for 6 to 9 months. The treatment for active TB is isoniazid in conjunction with three other drugs such as rifampin, pyrazinamide, and ethambutol over a course of 6 to 12 months.[6]

2.2.3.1 First Line Drugs

The first line drugs are the initial treatment of choice for *Mtb* infection. Mentioned previously, the complex *Mtb* cell wall, and the lack of permeability of compounds across it, makes it difficult for the bacteria to be properly targeted. These drugs all have activity towards the bacteria and are extremely effective. They are isoniazid, rifampin, pyrazinamide, and ethambutol (Figure 2).

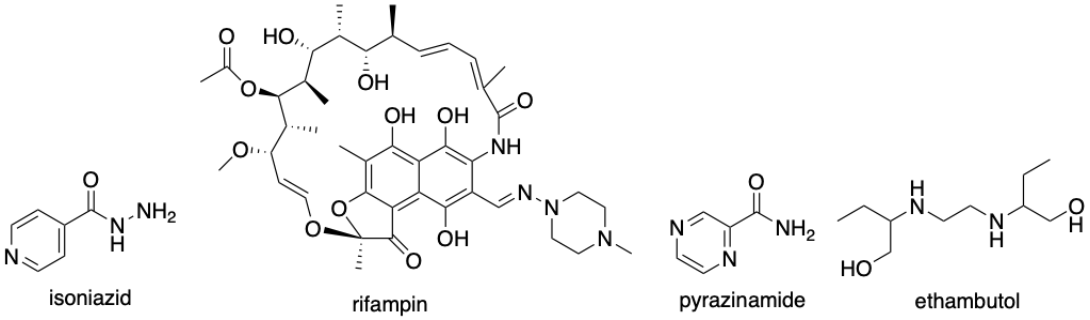

Figure 2. First Line TB Drugs.

Isoniazid, chemically known as isonicotinic acid hydrazide, was originally a synthetic drug and began to be used for TB treatment in 1952.[7] Isoniazid was shown to specifically target *Mtb* and *M. bovis* in the 0.02 - 0.2

μg/mL range.[8] In addition, isoniazid is a relatively simple synthetic drug (with no stereocenters or incredibly complex/susceptible functional groups), so mass production and manufacturing was more simple compared to drugs that are more complex and difficult to obtain synthetically. Its good activity and simple synthesis made isoniazid a particularly great drug for the treatment of TB (which recently has become more of a neglected disease since it affects the less developed parts of the world). Isoniazid's activity stems from its ability to diffuse effectively across the cell wall of *Mtb* and inhibit the synthesis of the mycolic acids in the cell wall, which are crucial to the virulence of the bacteria. The mycolic acid layers in *Mtb* are relatively conserved to *Mycobacteria* and, thus, represent one of the more promising targets for tuberculosis treatment.

Rifampin, or rifampicin, is a natural product derivative of rifamycin B that was originally isolated from *Norcardia mediterranei* at the Dow-Lepetit Research Laboratories in Milan, Italy in 1957. After isolation of rifamycin B, it was shown that activation of rifamycin B via introduction to aqueous environments caused multiple chemical transformations into the active rifamycin SV. Rifamycin SV was found to be particularly active against *Mtb* and moderately active against some gram negative bacteria.[9] Rifamycin SV was then synthetically modified in order to improve its potency and pharmacokinetic properties. Rifampin was the least toxic and most potent analog of rifamycin SV after the chemical modifications. Rifampin's mechanism of action is that it specifically binds to RNA polymerase, the enzyme responsible for DNA

transcription, at very low concentrations (0.01µg/mL at 50% effective dose).[10] Although RNA polymerase is conserved in mammalians cells as well as bacterial cells, the mammalians cells are not affected as much (mammalian cells were not affected even at 10,000 fold concentrations of rifampin), making it another crucial drug for TB treatment.

Ethambutol was discovered in 1961 by Lederle Laboratories of American Cynamid and, when tested against *Mtb* in animals, was shown to be incredibly stereospecific. The *dextro*-(S,S) form was shown to have 12 times more activity against TB than the *meso* form, while the *levo*-(R,R) form was completely inactive.[11] Interestingly, ethambutol is rapidly taken by both the inactive and active forms of *Mtb,* though only the active form was affected by the drug. Ethambutol's works by binding to proteins necessary in the construction of the arabinogalactan layer of *Mtb*. This explains earlier results that only active TB (rapidly multiplying and constructing defense mechanisms) was targeted and inactive TB was unaffected. Ethambutol's mechanism of action was demonstrated by mutating the proteins that bind to ethambutol and finding that activity diminished upon modification of those proteins.

Pyrazinamide is the last of the first line TB drugs and is one of the oldest. First formulated in the mid 1900s, it was initially discovered that nicotinamides prolonged the lifespans of *Mtb* infected guinea pigs.[11] This discovery led to the design of pyrazinamide by Lederle Laboratories of American Cynamid. In mice testing, pyrazinamide was the most active nicotinamide analog. During the in

vitro testing, pyrazinamide showed no activity unless incubated in acidic pH first. Further studies showed that pyrazinamide is a prodrug and gets metabolized into its active form after passive diffusion into *Mtb*. Unfortunately, pyrazinamide is only bacteriostatic and not bactericidal. Its exact mechanism of action is still currently unknown, but some have suggested the active component of pyrazinamide builds up within the bacteria, halting growth rather than killing the bacteria, though nothing has been proven yet.

2.2.3.2 Second and Higher Order Line Drugs

New drugs with structural variation are needed in the fight to treat TB. Chemical novelty has been of more importance with the increase of antibacterial, and, in particular, *Mtb* resistance. After the first line TB drugs, these second and third generation of drugs come from new chemical classes and have shown activity even against resistant *Mtb* strains (Figure 3).

The fluoroquinolones are a class of anti-TB molecules that are noted by their fused aromatic/quinone system with a fluorine present on the aromatic ring meta to the quinone ketone. Their use began with the discovery of nalidixic acid in 1967 for the treatment of gram negative bacteria in urinary tract infections.[12] This started a wave of synthesizing drugs that had similar structural motifs to nalidixic acid. The introduction of fluorine into the molecule increased the potency of these molecules. Furthermore, the addition of various functional groups was also crucial in increasing the antibacterial properties of

this class of molecules. The result of which was the synthetic production of thousands of fluoroquinolones such as levofloxacin and moxifloxacin. While these antibiotics worked incredibly well, bacterial resistance rose rapidly with the increasing use of the fluoroquinolones. [13] *In vitro* studies at the time demonstrated that resistant colonies were isolated at a much higher rate (10^{-7}) at traditional serum concentrations of 2 μg/mL.[14] The fluoroquinolones bactericidal activity is a result of their inhibition of bacterial DNA synthesis. They bind to the enzyme-DNA complex and disrupt the process. After DNA gyrase and topoisomerase create DNA strand breaks in preparation for replication, the fluoroquinolones stabilize the broken DNA strands via a ternary complex of DNA-fluoroquinolones-topoisomerase, followed by a double strand break via the denaturation of topoisomerase.[15]

The aminoglycosides are natural and semisynthetic antibiotics derived from *Actinomycetes sp*, the most notable aminoglycoside being streptomycin (a broad spectrum antibiotic isolated from *Streptomyces griseus* in 1944). Kanamycin and amikacin (isolated in 1957 and 1972, respectively) are other notable examples from this class of compounds (Figure 3). Structurally, the aminoglycosides are characterized by amino sugars connected by glycosidic linkages.The aminoglycosides work by inhibiting protein synthesis in bacteria. They bind with high affinity to the A site of the 16S ribosomal RNA of the 30S ribosome.[16] As a result of this binding, the A-sites conformation changes, which causes mistranslation (via codon misreading) and, ultimately, death.

The oxazolidinones were originally discovered in 1987. In particular, DuP-721 was effective against multiply-resistant gram negative bacteria, but suffered from cytotoxicity issues, so it was abandoned. In 1994 and 1995, the Upjohn company entered clinical trials with eperezolid and linezolid for the treatment of gram positive bacteria.[17] At the time, testing thousands of gram positive bacteria against the oxazolidinones and resulted in almost no resistant strains, implying a very interesting mechanism of action. The mechanism of action for the oxazolidinones is similar to the aminoglycosides in that they inhibit protein synthesis. They bind to the P site of the ribosomal 50S subunit, giving similar conformation changes in the subunit, inhibiting protein synthesis.

Other therapeutics are utilized as well in the post first line set of TB/antibacterial drugs. bedaquiline, delamanid, and capreomycin are just a few examples (Figure 3). Despite the myriad of various activities and mechanisms of action, resistance is still a growing problem and more therapeutics with novel/different mechanisms of action are needed to combat the growing problem. Bedaquiline inhibits ATP generation by interfering with F-ATP synthase.[18] Delamanid inhibits mycobacterial cell wall development by inhibiting mycolic acid synthesis via generation of nitrous oxide.[19] Lastly, capreomycin acts on *Mtb* by inhibiting protein synthesis via binding to the 70S ribosomal unit.

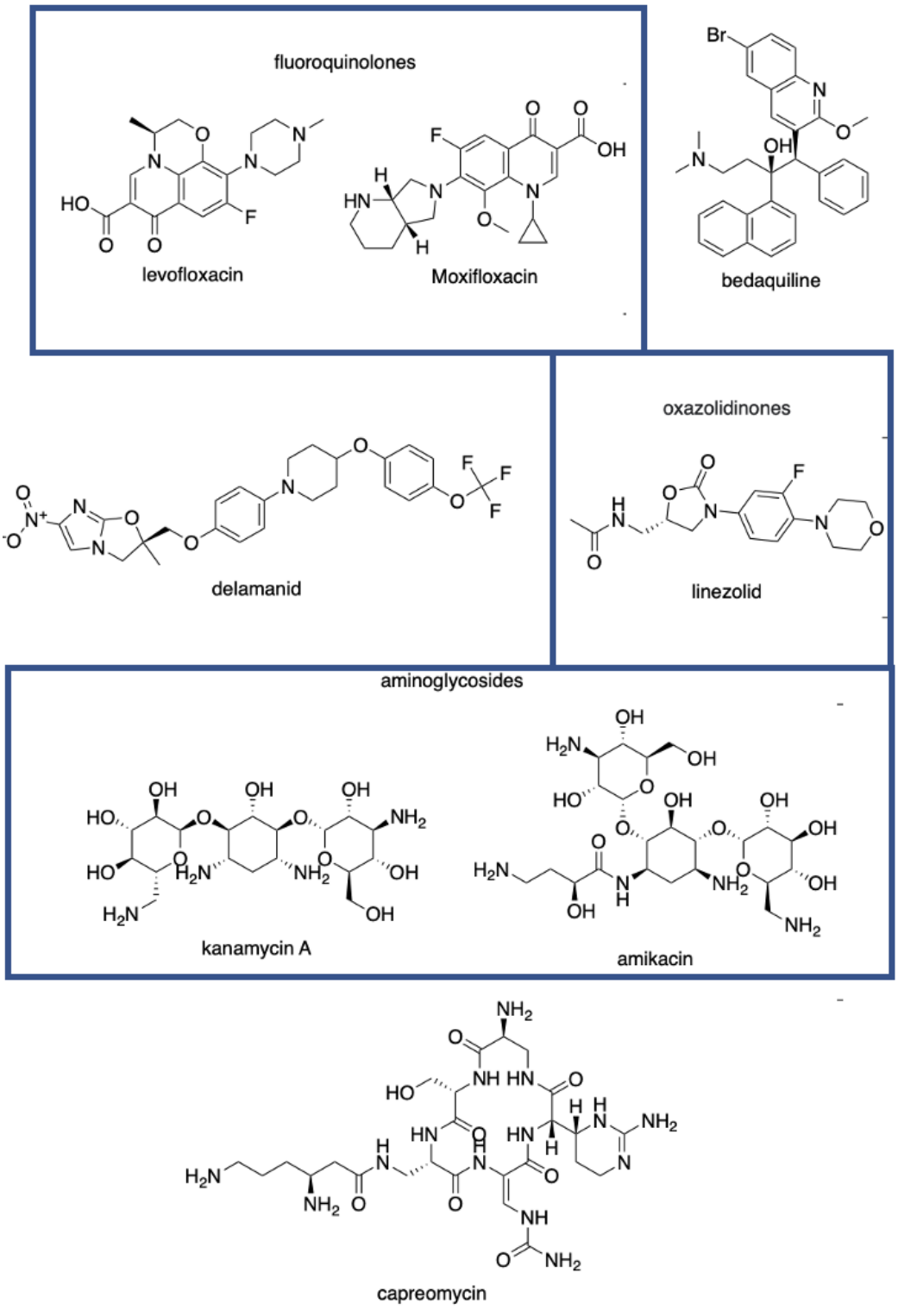

Figure 3. Second Line and Higher Line TB Drugs.

2.2.4 Resistance

As alluded to earlier, resistance with previous and current anti-tuberculosis drugs has been rising as of late. TB resistance has risen for a multitude of reasons. More recently, *Mtb* infection has been prevalent in developing countries and less so in the developed world. When the treatment is not taken for its full course, resistant strains of TB can spread rapidly. Prescribing the wrong treatment for a particular strain can also cause a rise in resistance. Finally, when drugs used for treatment are of poor quality, which is a problem in less wealthy countries and causes dosage problems, a rapid rise in resistance can be seen as well. When *Mtb* strains are resistant to isoniazid and rifampin, they are referred to as multi-drug resistant *Mtb*. Rifampin and isoniazid resistance occur as a result of mutations that change the structure of RNA polymerase and mutation of the *katG* gene, respectively. These resistant strains are harder to deal with but can still be treated with a combination of other TB drugs. Extensively drug resistant TB is more extreme and pressing in today's world. These strains are classified by resistance to both isoniazid and rifampin as well as the fluoroquinolones and one of the injectable drugs (e.g. kanamycin, amikacin, and capreomycin).[20] As a result, it is necessary to find novel drugs with varying mechanisms of action to combat this growing problem. Screening efforts to find novel and repurposed drugs for targeting TB have been ongoing (*In silico* and phenotypic). For example, Schiebler *et al.* performed a high-throughput screen of 214 molecules and found that

carbamazepine aids in the removal of *Mtb* via the stimulation of macrophages.[21] By promoting the innate immune response and improving adaptive immunity, the goal was to limit mechanisms of resistance and make targeting *Mtb* more facile. Despite the progress that has been made with the disease over the years, continued work and perseverance are needed to combat growing resistance and access to those in developing countries.

2.3 Oxazinin A

Oxazinin A (**2.1**) was isolated from an *Euritiomycetes* fungal straistrain by the Schmidt lab at the University of Utah in 2014. It was isolated from the fungal Euritiomycetes strain 110162 on the ascidian *Lissoclinum patella* that was collected in Papua New Guinea.[22] It was isolated using traditional natural products isolation: the fungal strain was incubated in agar and transferred to a liquid media mix for 25 days; the broth centrifuged and extracted with resin; extracted with organic solvent; then purified with multiple rounds of reverse phase chromatography and finally reverse phase HPLC to get the natural product. Oxazinin A was isolated as a racemic mixture, and as shared later, a mixture of diastereomers. One of the features that we have observed in molecules that involve one or more non-enzymatic steps is racemic mixtures. As such, both the Schmidt lab as well as our lab proposed that oxazinin A is formed non-enzymatically. Figure 4 shows the Schmidt lab proposal for the non-enzymatic step in the biosynthesis of oxazinin A.

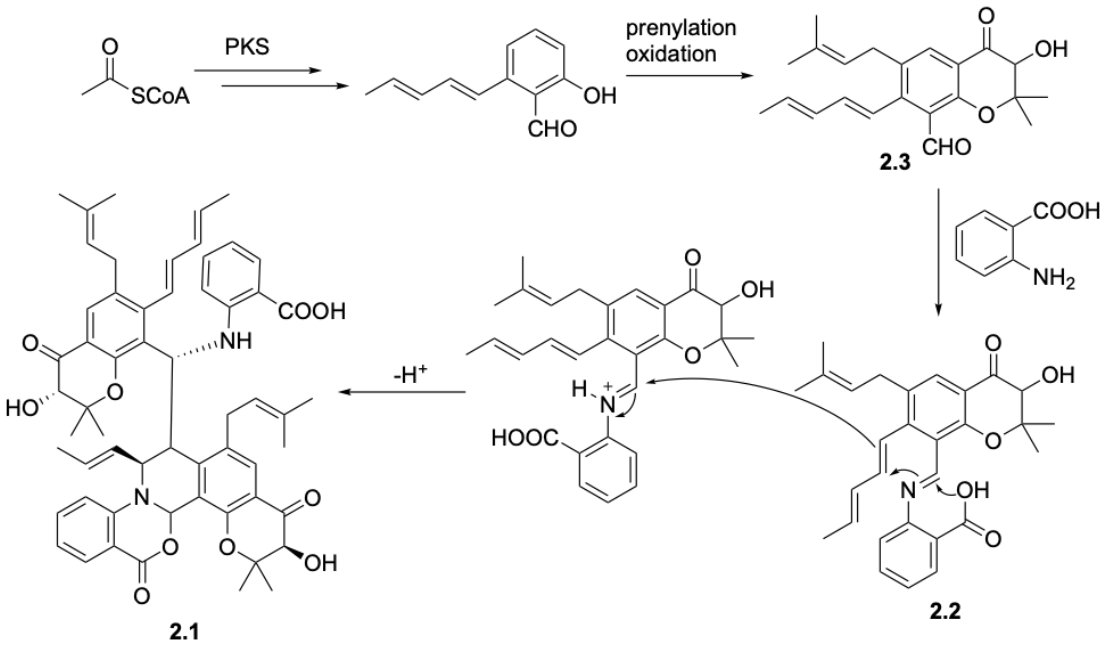

Figure 4. Proposed Biosynthesis of oxazinin A.

Following canonical acetyl CoA biosynthesis of an alkylated salicylaldehyde, an enzymatic prenylation and oxidation shortly follow, giving prenylated polyketide **2.3**. Aldehyde **2.3** then reacts with an equivalent of anthranilic acid (a common tryptophan catabolite) to give imine **2.2**, which then catalyzes a cascade heterodimerization to form oxazinin A.

Following isolation, oxazinin A was then tested to see its activity. It was tested for inhibitory activity against *Mtb*, *Pseudomonas aeruginosa*, *Bacillus subtilis*, and *Burkholderia cepacia*, as well as cytotoxicity against T-cell leukemia cells, and, finally, against ion channel receptors). Oxazinin A was shown to have modest activity against *Mtb* (2.9 μM) however, compared to other indications a value of 2.9 μM is a reasonable starting point for further investigation. This makes oxazinin A not only an interesting synthetic challenge

and molecule to explore non-enzymatically, but also a potential starting point for therapeutic development against a particularly troubling bacterium.

2.3.1 Synthesis of oxazinin A Foreword

The synthesis of the prenylated polyketide that makes up the major component(s) of oxazinin A was tumultuous and required many synthetic schemes and adjustments in order to identify a successful synthetic pathway. From a bird's eye view, the highly substituted aromatic structure contains two unsaturated groups, a reactive aldehyde, and an alpha-oxidized chromanone group on the other side of the aromatic ring. Installation of all of the groups with their conflicting reactivity, as well as ultimately creating a penta-substituted aromatic ring had obvious challenges. Now, I will show a few synthetic pathways that made major contributions to the final synthetic scheme in the total synthesis of oxazinin A.

2.3.2 Original Schemes

When originally approaching oxazinin A, the thought was to have an easy handle with which to install the pentadiene as well as an easy method to form the chromanone on the right side of the ring. With that in mind, we began with the commercially available 4-bromoacetophenone as the starting point of the synthesis. Scheme 1 shows the synthetic plan for construction of oxazinin A from this starting material.

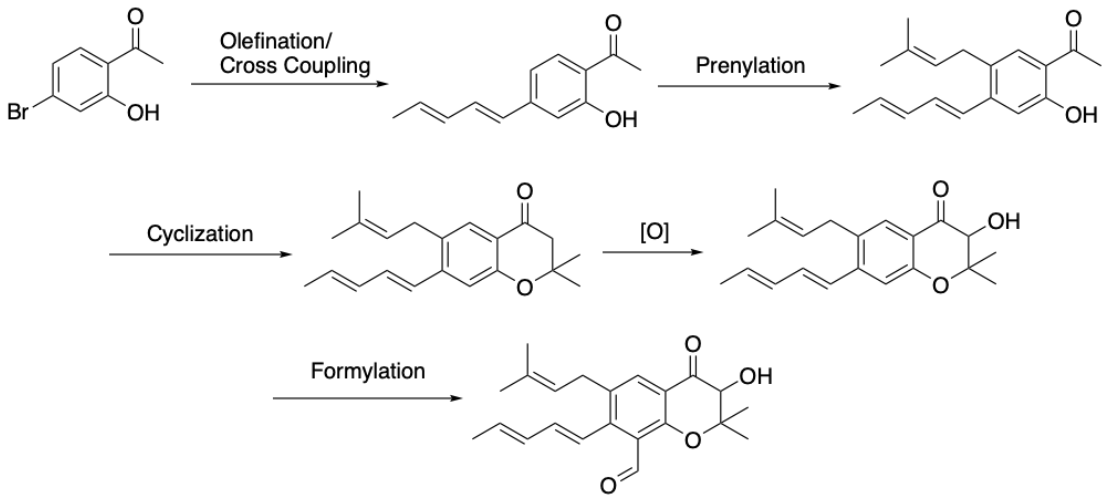

Scheme 1. General Synthetic Route to oxazinin A.

Beginning from 4-bromoacetophenone (**2.4**), the plan was to install the pentadiene via Suzuki cross coupling. For initial model studies, 1-pentenylboronic acid was used instead of the diene equivalent due to ease of access (Scheme 2). Using PEG:H_2O as the solvent system furnished the alkylated product **5** in 87% yield. The next step was to then prenylate the ring para to the hydroxyl group. This was done using prenol in the presence of $ZnCl_2$ in ethyl acetate. Unfortunately, prenylation occurred para and ortho to the hydroxyl group, effectively lowering the overall yield of (**2.6**, 20% yield). This was followed by acetone-derived cyclization with $ZnCl_2$ and pyrrolidine to give the tetrasubstituted aromatic ring **2.7** in moderate yield (50%).

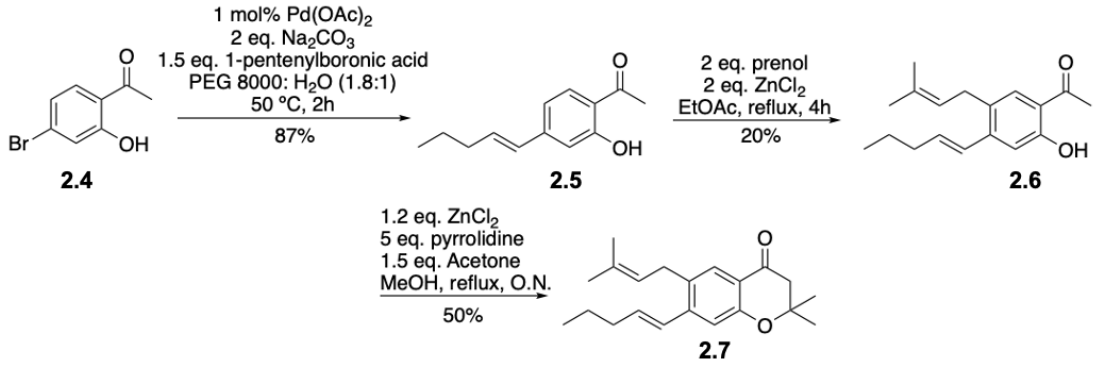

Scheme 2. First Synthetic Route to oxazinin A

To complete the polyketide moiety, we ideally envisioned an alpha-oxidation of the ketone, followed by a formylation to obtain the penultimate product. Unfortunately, attempts at oxidations, such as *m*CPBA in acetic acid and oxone/TFAA were either too harsh and led to reaction of the alkenes and/or a rearrangement of the geminal dimethyl groups. To move **2.7** forward, we decided to attempt formylation first and attempt oxidation at a later stage (Scheme 3). Table 1 shows the attempts at formylation reactions, however none led to a viable product.

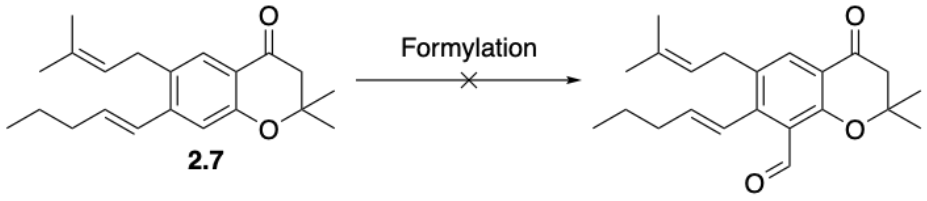

Scheme 3. Formylation of 2.7.

Table 1. Formylation Conditions of 2.7	
Condition	**Result**
$COCl_2$ in DMF (0 °C → 55 °C)	No reaction at 0 °C; small conversion at 55 °C
$TiCL_4$ with Dichloromethyl methyl ether (0 °C)	SM degradation
$AlCl_3$ with paraformaldehyde (rt)	No reaction
nBuLi in DMF (-78 °C → rt)	SM degradation

Table 1. Formylation Conditions of Compound 2.7.

Initially, we attempted to insert the aldehyde using traditional methods of aromatic formylation**.** The first attempts were the creation of highly electrophilic aldehyde mimics: Vilsmeier Haack reagent, dichloromethyl methyl ether, paraformaldehyde. Those showed little to no efficacy in aldehyde installation. Another common method of formylation is the creation of an anionic aromatic ring via deprotonation with *n*BuLi or other strong alkyl bases and quenching the anion with DMF or another aldehyde precursor. The result of which was the degradation of the starting material with no aldehyde present. In the electrophilic aldehyde precursors, the aromatic ring was not electron rich enough to undergo the reactions. In the *n*BuLi reaction, the starting material may have been too reactive on other parts of the ring, particularly the

chromanone portion of the ring. Although the scheme ultimately failed, it provided valuable lessons and established a foundation for future experimentation: oxidation at the later stages will prove difficult in future experiments and formylation via electrophilic aromatic substitution on this ring requires an electron donating/directing handle.

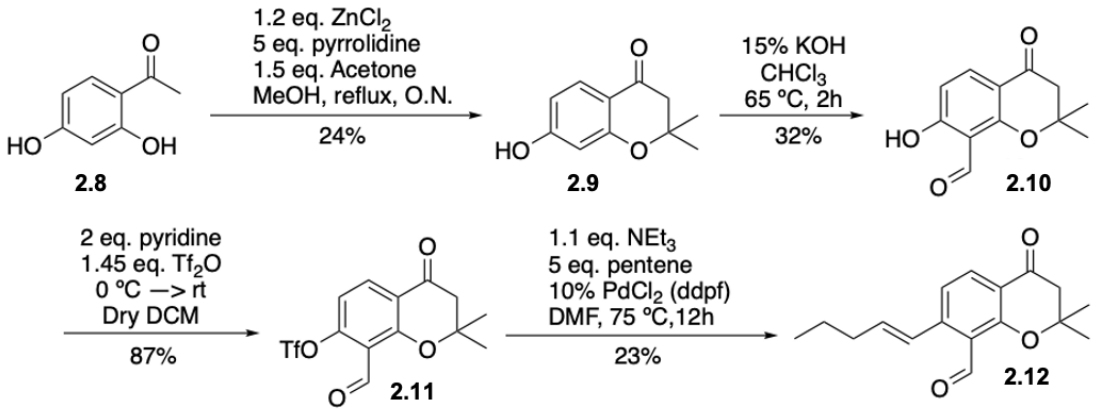

Scheme 4. Second Synthetic Scheme for oxazinin A.

Scheme 4 shows the next pathway towards oxazinin A. To alleviate problems with formylation reactions, the bromine para to the methyl ketone was changed to another hydroxyl group since there is a plethora of literature on hydroxy-mediated ortho formylations. In this pathway, the starting material 4-hydroxyacetophenone (**2.8**) was transformed into the chromanone using the same acetone/pyrrolidine-based cyclization as before to give cyclized product **2.9** (24% yield). **2.9** was then formylated via a Reimer-Tiemann reaction in 32% yield to furnish **2.10**. The free phenol was then converted into triflate **2.11** (87% yield) and finally cross-coupled to 1-pentene, via a Heck Reaction, to give

aldehyde **2.12** in 23% yield. Unfortunately, prenylation using $ZnCl_2$ and prenol did not give the desired product, and the starting material was recovered unreacted. While disappointing, we were able to use **2.12** as a model to look at the non-enzymatic formation of the oxazinin A scaffolding. To that end, compound **2.12** was taken and added to an NMR tube with anthranilic acid in d_6-DMSO and DMAP without stirring or agitation of any kind (in reference to previous work in the lab on the discoipyrroles). A ^{1}H NMR was taken every hour for 126 hours and monitored for the disappearance of aldehyde and the appearance of any intermediates or the dimer **2.12a**. The reaction proceeded sluggishly with the addition of DMAP, so the study was run again with 2% formic acid instead.

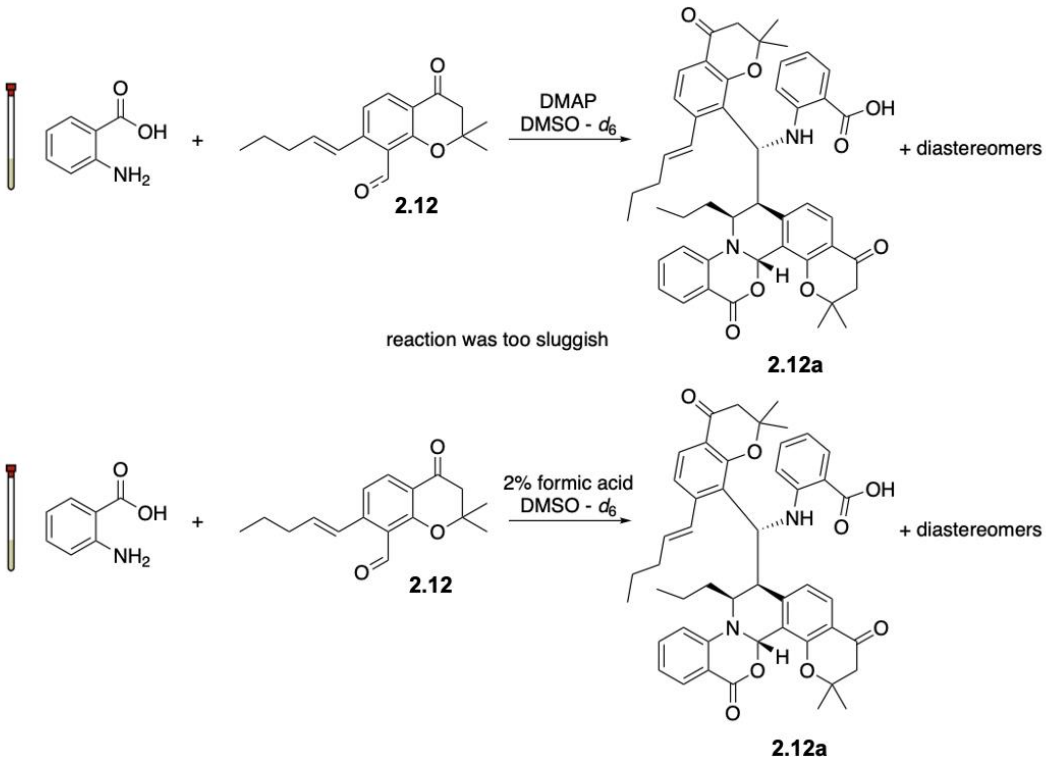

Figure 5 (Previous Page). Model Dimerization Reaction Conditions.

Figure 6. NMR Monitoring of Model oxazinin A System for 126 Hours.

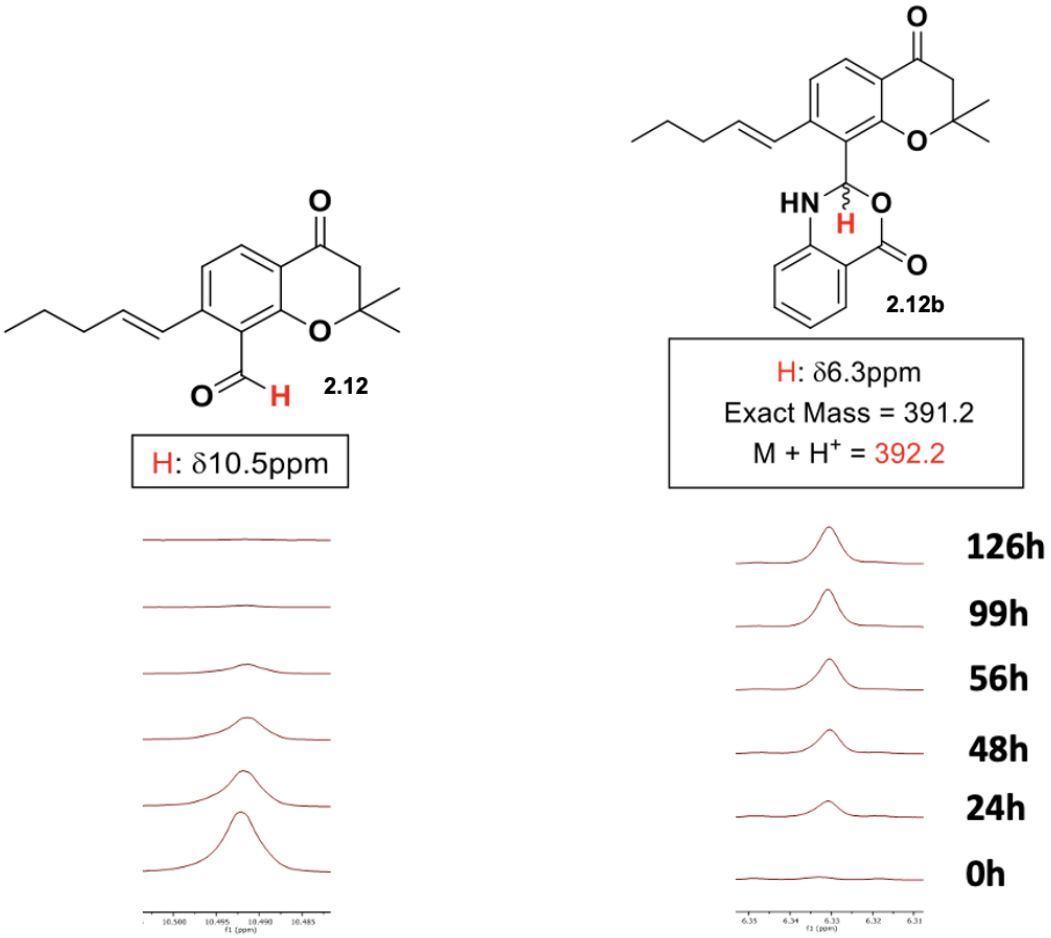

Figure 6 shows the reaction at various time points and the qualitative disappearance of starting aldehyde **2.12** and the formation of a hemiaminal intermediate using the formic acid methodology. Conversion of the aldehyde **2.12** into **2.12b** occurred at around 24 hours and **2.12** converted completely to **2.12b** at approximately hour 99. During this point in the reaction, there was no sign of an imine intermediate like we expected. Moreover, although **2.12** was being converted into **2.12b**, **2.12b** was not being converted into **2.12a**. It

appeared as if intermediate **2.12b** was a dead end and did not lead to the cyclization that forms oxazinin A. We utilized LC-MS to correlate what was observed in NMR to *m/z* values found in the LC traces. As demonstrated in Figure 7, we were able to observe the correct *m/z* for **2.12b** as the major species, while also observing a small quantity of the desired **2.12a**. This was a promising result as it demonstrated that oxazinin A can indeed dimerize non-enzymatically, although further optimization of the dimerization reaction was needed in order to improve conversion to the dimer.

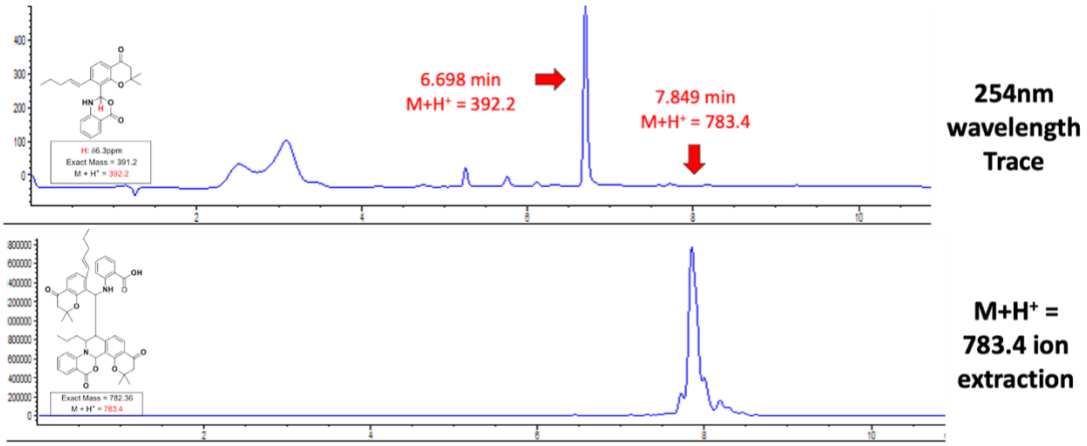

Figure 7. Mass Spectrometry Showing Formation of Intermediate Monomer and Dimer.

After synthesizing that first model system and carrying out preliminary NMR studies, we wanted to go back to the original task of generating the necessary prenylated polyketide. The last synthetic scheme showed that prenylation was best done at the beginning of the synthesis when the ring was still relatively electron rich with the two phenols and only one electron withdrawing group present (the methyl ketone). To that end, compound **2.8** was

prenylated using the earlier methodology consisting of $ZnCl_2$ and prenol in ethyl acetate (scheme 5). This gave compound **2.13** in 20% yield because of prenylation on either side of the para hydroxyl group as well as an O-alkylation product. This prenylated phenol was then cyclized using the same pyrrolidine-mediated methodology (**2.14** in 24% yield). Phenol **2.14** is then formylated via Reimer-Tiemann (KOH, CHCl3) in 33% yield. Finally, the phenol is transformed into the triflate via pyridine and triflic anhydride in 77% yield. Unfortunately, under Heck and Suzuki conditions, no cross-coupling occurred. Instead, the triflate was hydrolyzed back to the phenol in almost all conditions. This demonstrated that for this synthesis to work, there needed to be a handle for both the prenyl and pentadiene, and the aldehyde needed to be installed early (and possibly protected). All the individual steps were successful, but the order of operations and the scaffold needed to be modified for this molecule to be synthesized.

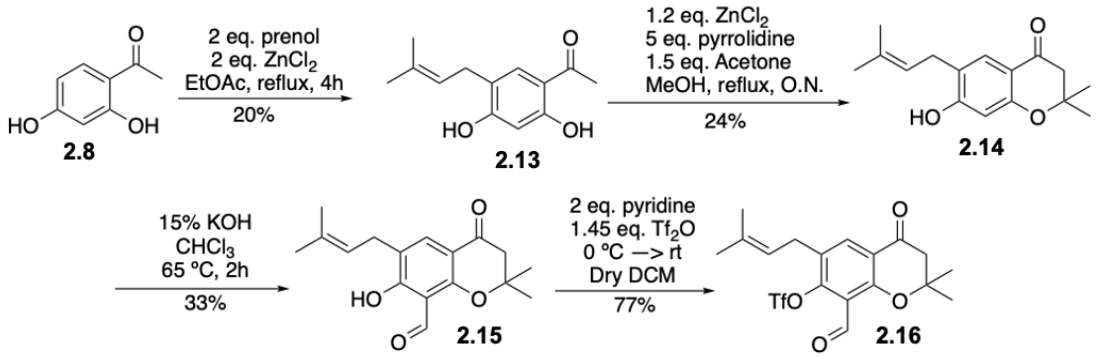

Scheme 5. Third Synthetic Scheme for oxazinin A.

2.3.3 Final Schemes

With all of these lessons in mind, a new synthetic strategy was designed. The aldehyde would be installed at the beginning and protected as a lactone. There would also be handles for alkylating transformations - a bromine handle for prenylation and the lactone acts as a handle for a late stage Wittig olefination. With this new strategy and the previous synthetic experiences in hand, synthesis of oxazinin A was undertaken once more. Scheme 6 shows the synthetic route to common intermediate **2.23**.

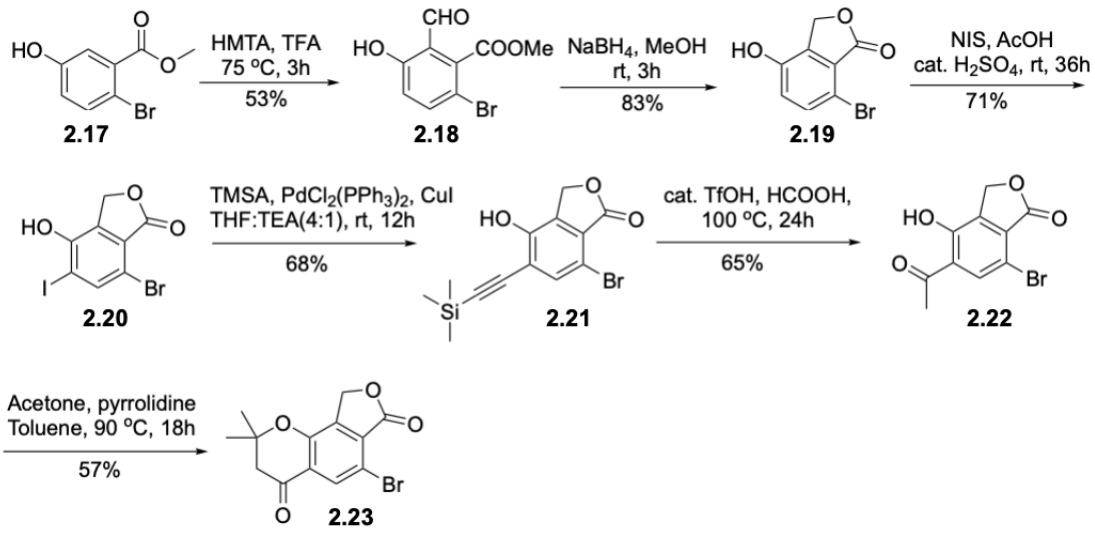

Scheme 6. Synthetic Route to Common Intermediate 2.23.

Beginning from commercially available starting material **2.17**, the new pathway was implemented. Following a Duff formylation (HMTA in neat TFA) to give an aldehyde between the hydroxyl group and the ester (**2.18**, 53% yield), the aldehyde is “protected” as a lactone via reduction with sodium borohydride in MeOH in 83% yield (**2.19**). The lactone is utilized to carry the aldehyde

throughout the entire synthesis. The goal at this step was to take the reduced aldehyde **2.19** all the way to methyl ketone **2.22** but direct acylation proved too difficult using a myriad of methods (Friedel Crafts Acylation, Fries Rearrangement, and other similar methods). To work around this issue and alleviate electrophilic aromatic substitution problems, **2.19** was halogenated with NIS in Acetic Acid (**2.20**, 71% yield) and coupled with a silyl acetylene via Sonogashira Coupling (**2.21**, 68% yield). This silyl acetylene is then hydrolyzed to the methyl ketone with catalytic triflic acid in formic acid (**2.22**, 65% yield). Finally, the methyl ketone was cyclized using a modified version of the acetone/pyrrolidine-mediated cyclization (changing the solvent from methanol to toluene improved the yield of the reaction) to give the tricyclic intermediate **2.23** (57% yield).

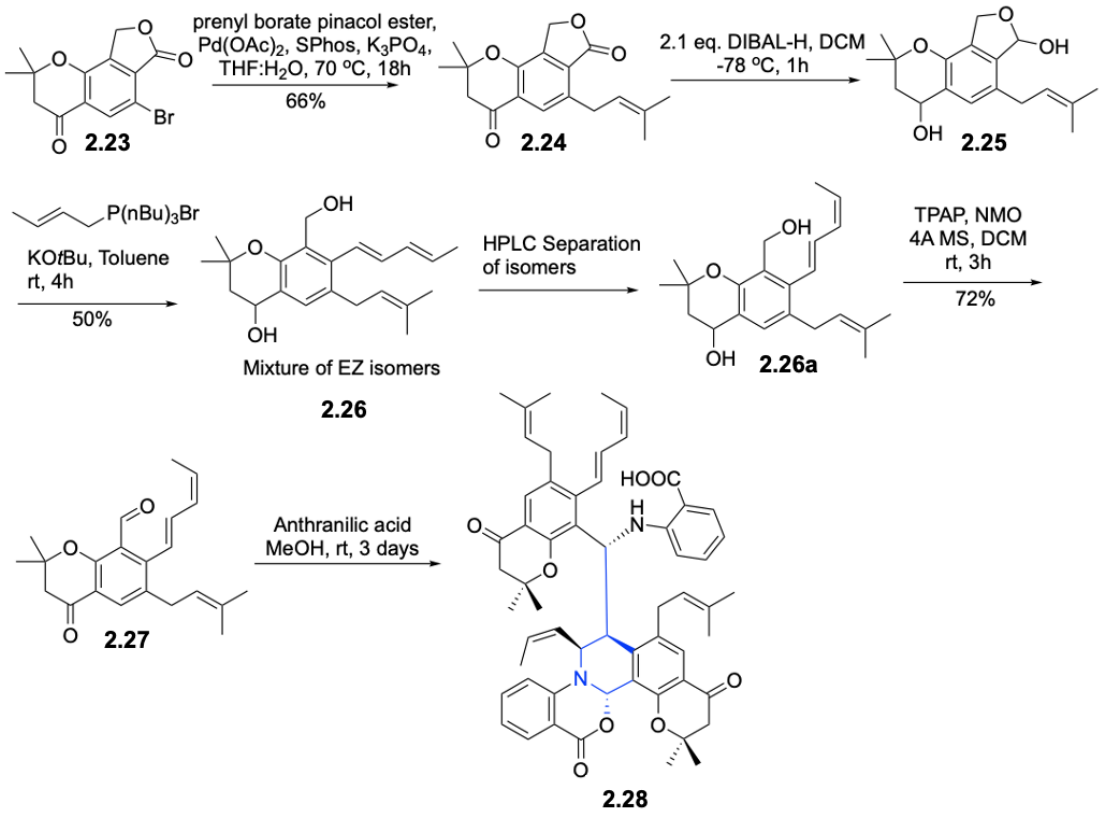

Scheme 7. Route to Non-Hydroxylated EZ Stereoisomeric oxazinin A 2.28.

From there, the prenyl group was installed via Suzuki Coupling with the bromine handle (**2.24**, 66% yield) (Scheme 7). The lactone was then reduced to the lactol via DIBAL-H reduction at -78 °C (**2.25**). The lactol is in an equilibrium between its “open” and “closed” forms. When it is in its open form, it exists as a free aldehyde and primary alcohol. We used this to our advantage by performing a Wittig Olefination on the lactol. As the open form of the lactol reacts with the Wittig salt, the equilibrium will be driven more to the open aldehyde form, giving the desired pentadiene. Despite the successful C-C cross coupling, several stereoisomers of the pentadiene were obtained. After

multiple, successive HPLC purifications, the major fraction containing two stereoisomers was obtained. The identity of the stereoisomer was elucidated using a 1D ^{1}H homonuclear decoupling NMR experiment. By irradiating the terminal methyl group of the pentadiene, its coupling to the other protons on the alkyl chain is removed, and we were able to get coupling constants for the double bonds. For the major stereoisomer in the mixture, the coupling constant of the double bond furthest from the ring and closest to the methyl group was 10.8 Hz, which demonstrates that the protons of that double bond are in a cis configuration and the geometry of the double bond is Z. The other double bond closest to the aromatic ring had a coupling constant of 16.1 Hz, showing a trans configuration of the protons and an E geometry of the double bond. The minor stereoisomer was unidentified as the homonuclear decoupling experiment did not allow for the clear identification of the double bond configuration. Since the EZ stereoisomer was elucidated and the major product of the reaction, it was taken forward in the synthesis (**2.26a**, 50% yield). Following HPLC purification and elucidation of the Wittig Olefination product, **2.26a** was taken and the alcohols oxidized to the benzylic ketone and aldehyde with tetrapropylammonium perruthenate (TPAP) with N-methylmorpholine oxide in DCM (**2.27**, 72% yield). This analog of **2.3** was then taken and used in the oxazinin A dimerization reaction to form the analog **2.28**. Originally, DMSO was used in the dimerization reaction, but we found that in methanol the

dimerization occurred within 3 days rather than the sluggish original dimerization reaction in the previous pathway.

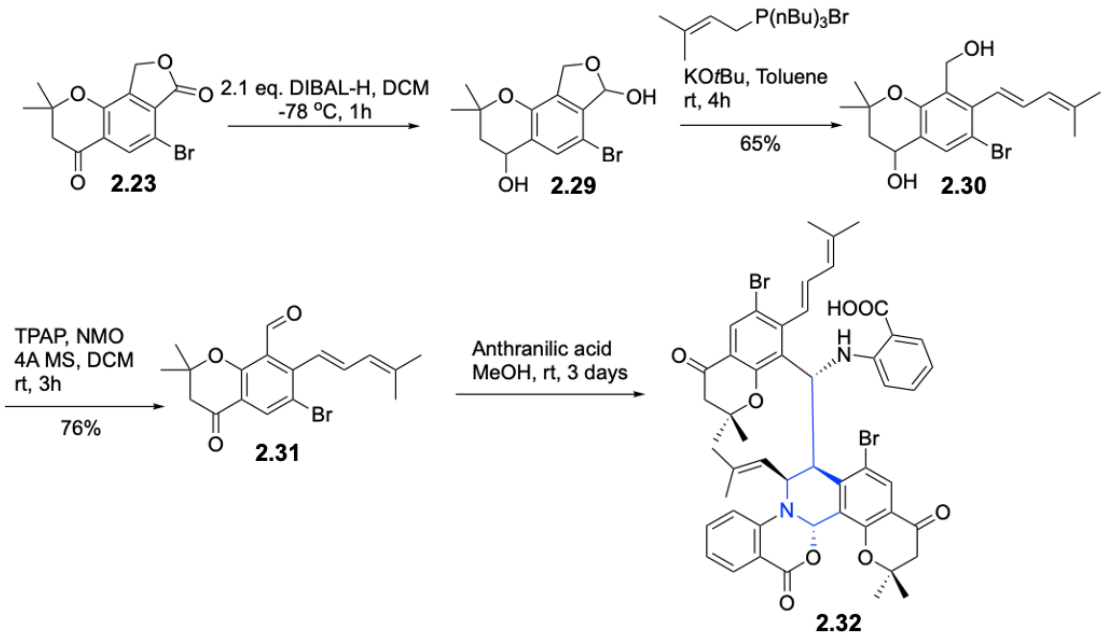

Scheme 8. Route From 2.23 to Brominated oxazinin A Analog 2.32.

Following a similar pathway, a brominated dimer analog was synthesized as well. Rather than performing the suzuki reaction, **2.23** was reduced straightaway using DIBAL-H in DCM to give **2.29**. To alleviate the inherent problems with stereoselectivity with the Wittig Olefination, a methyl capped Wittig salt was used instead of the original salt. By adding the extra methyl group at the end of the salt, the stereoselectivity problems were resolved as only the EE stereoisomer was seen after the reaction (**2.30**, 65% yield). After the primary and secondary alcohols are oxidized with TPAP/NMO to form **2.31** (76% yield), it was subjected to dimerization conditions with anthranilic acid (methanol, 3 days) to give a diastereomeric mixture of dimer products. The

diastereomeric ratio was found to be 1.0:0.44:0.15, however they were separable by HPLC. Serendipitously, the bromine handle allowed for more amenable crystallization of the dimer in hexanes/DCM. With a crystal structure in hand, we were able to confidently assign relative stereochemistry of the major dimer diastereomer and confirm the dimer product (Figure 8, stick model).

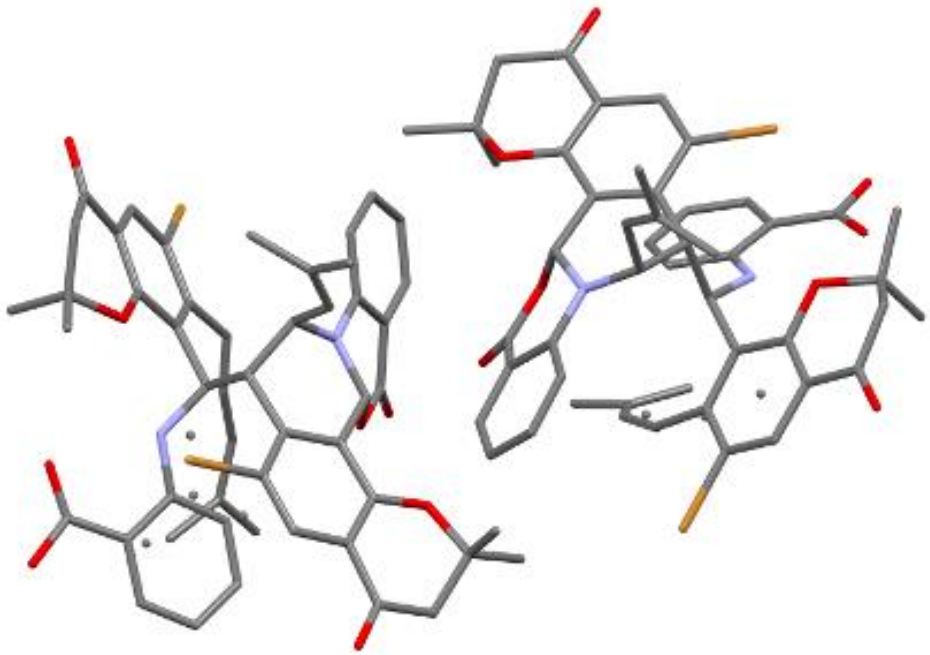

Figure 8. Crystal structure of compound 2.32 (enantiomers).

With most of the reactions figured out, the synthesis of **2.3** was completed (scheme 9). From **2.23**, the alpha position of the ketone was oxidized using $Pb(OAc)_4$ in benzene (**2.33**, 80% yield). Originally, we wanted to perform the Suzuki Coupling with the alpha OH protected with a TBS (*tert* butyl dimethyl silyl) group, but we noticed that not only were we getting coupling

at the bromine position, but also coupling at the alpha position next to the ketone, forming a quaternary center. To avoid this reactivity, the ketone was reduced with $NaBH_4$ and the acetate protecting group was cleaved using LiOH in THF: H_2O (**2.34**, 71% yield). The resulting diol was protected as an acetonide via dimethoxypropane (**2.35**, 42% yield).

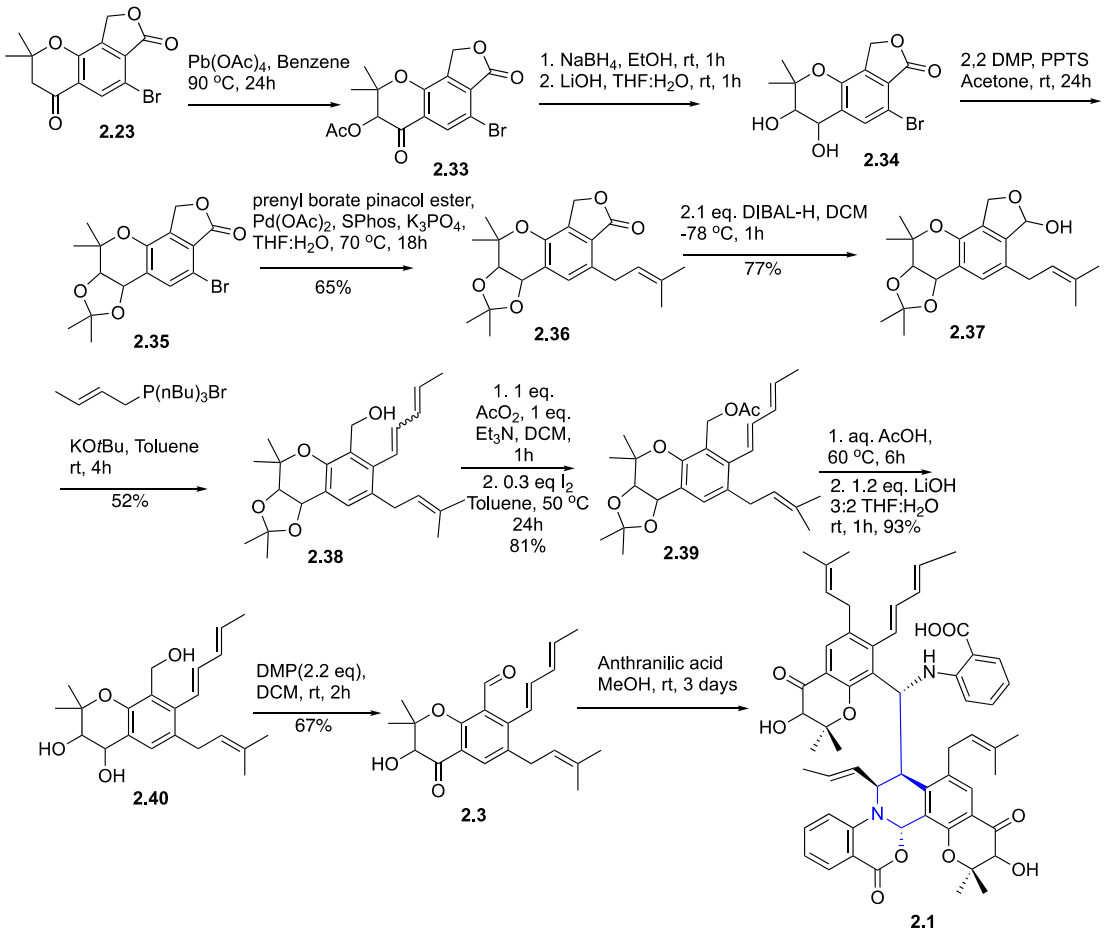

Scheme 9. Final Route to oxazinin A (2.1).

With the chromanone part of the molecule protected, the Suzuki Coupling was performed to give **2.36** (62% yield). The resulting prenylated lactone is reduced with DIBAL-H and the Wittig was performed (**2.38**, 52%

yield). The stereoisomers from before had persisted, but literature had shown that it was possible to convert Z alkenes to E alkenes with catalytic amounts of Iodine in toluene. After HPLC purification of the major stereoisomer (EZ plus the unknown stereoisomer), we attempted this isomerization. First, we protected the primary alcohol as an acetate to avoid any iodine mediated cyclizations that could occur with the alkene and the free alcohol. Then we added in the catalytic iodine and stirred at 50 °C in toluene. To our delight, this converted most of the Z alkene to the E alkene (**2.39**). The mixture was then separated on semi-preparative HPLC. From there the acetonide and the acetate protecting group are removed using aqueous acetic acid at 60 °C (**2.40**). Finally, the benzylic alcohols are selectively oxidized using DMP in DCM to give **2.3**. Similar to before, **2.3** is added with anthranilic acid in methanol and stirred for 3 days to give oxazinin A (**2.1**). The table below shows key comparisons between our synthetic oxazinin A and the oxazinin A isolated by the Schmidt lab (Figure 9). As shown below, our synthetic oxazinin A matches us well with the original isolation and provides confidence in a correct synthesis (full NMR comparison table in spectra and data).

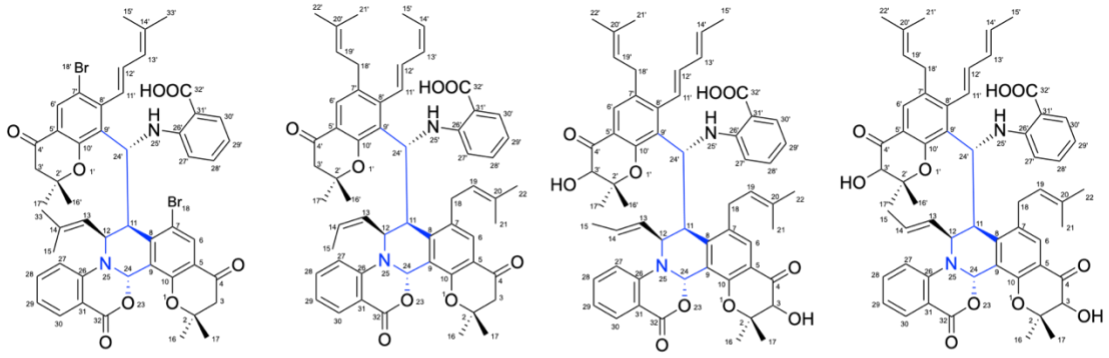

Dehydroxy Bromo Oxa A

No	1H NMR	13 CNMR
24	6.43 (s, 1H)	80.02
11	4.50 (dd, *J* = 10.42, 1.84 Hz, 1H)	49.44
12	3.97 (d, *J* = 8.43 Hz, 1H)	54.74
13	4.74(d, *J* = 8.93 Hz, 1H)	121.50
24'	6.20 (t, *J* = 10.56 Hz, 1H)	56.73

Dehydroxy EZ Oxa A

No	1H NMR	13 CNMR
24	6.44 (s, 1H)	80.21
11	4.34 (dd, *J* = 10.0, 1.04 Hz, 1H)	45.08
12	4.05 (d, *J* = 8.77 Hz, 1H)	53.37
13	5.08(m, *J* = 10.17, 1.21 Hz, 1H)	128.42
24'	5.92 (t, *J* = 10.1 Hz, 1H)	55.68

Synthetic Oxa A

No	1H NMR	13 CNMR
24	6.45 (s, 1H)	80.3
11	4.49 (m, 1H)	45.7
12	3.83 (brs, 1H)	59.0
13	5.20 (dd, J = 15.8, 5.0, 1H)	129.4
24'	5.80 (dd, *J* = 10.4, 10.4 Hz, 1H)	56.4

Oxazinin A

No	1H NMR	13 CNMR
24	6.44 (s, 1H)	80.0
11	4.47 (m, 1H)	45.5
12	3.82 (brs, 1H)	58.6
13	5.19 (dd, J = 15.8, 4.3 Hz, 1H)	128.4
24'	5.82 (dd, J = 10.4, 10.1 Hz, 1H)	55.7

Figure 9. Key NMR Comparisons Across oxazinin A Analogs and the Isolated Natural Product.

2.4 Conclusion

The synthesis of oxazinin A was the culmination of years of effort and systematic scheme design/modification. With the successful completion of the synthesis of oxazinin A, more analogs can be made that ideally have improved activity against *Mycobacterium tuberculosis* and can be a foothold or inspiration for future scientists to tackle this disease.

2.5 Experimental Procedures

(*E*)-1-(2-hydroxy-4-(pent-1-en-1-yl)phenyl)ethan-1-one

Chemical Formula: $C_{13}H_{16}O_2$

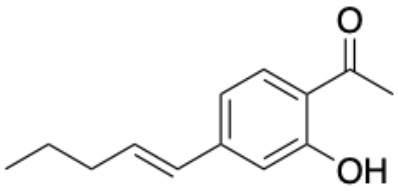

To a flame-dried round bottom flask in a nitrogen atmosphere was added 4-bromoacetophenone (1.74 g, 8.1 mmol), $Pd(OAc)_2$ (18.2 mg, 0.081 mmol), Na_2CO_3 (1.72 g, 16.2 mmol), 1-pentenylboronic acid (1.38 g, 12.1 mmol), 28.2 g of PEG 8000, and 24.1 mL of degassed H_2O (1.2:1 ratio). This was added to an oil bath preheated to 50 °C. The reaction was allowed to stir for 2 hours. Upon completion of reaction, the black slurry was extracted with diethyl ether (2 x 50mL). The crude mixture was dried down and purified via silica column chromatography (7:3 Hexanes: Ethyl Acetate) to give **2.5** in 87% yield.

1H NMR (500 MHz, $CDCl_3$) δ 12.3 (s, 1H), 7.64 (d, 1H, 8.3 Hz), 6.91 (d, 1H, J = 1.7 Hz), 6.88 (dd, 1H, 1.7 Hz, 8.3 Hz), 2.6 (s, 3H), 6.37 (m, 2H), 2.22 (q, 2H, *J* = 7.2 Hz), 1.51 (sextet, 2H, J = 7.5 Hz), 0.96 (t, 3H, *J* = 7.5 Hz)

(*E*)-1-(2-hydroxy-5-(3-methylbut-2-en-1-yl)-4-(pent-1-en-1-yl)phenyl)ethan-1-one

Chemical Formula: $C_{18}H_{24}O_2$

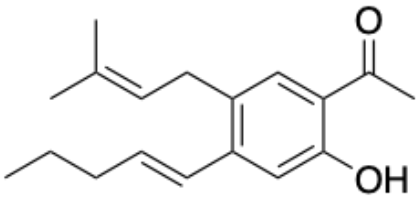

To a flame-dried round bottom flask was added **2.5** (1.4 g, 7.01 mmol), $ZnCl_2$ (1.94 g, 14.01 mmol) in EtOAc (40 mL). This solution was stirred and heated to 40 °C. After stirring for 30 minutes, prenol (1.38 mL, 14.01 mmol) in EtOAc (20 mL) was added dropwise over a period of 10 minutes. Following addition of prenol, the solution was heated to reflux and allowed to stir for 4 hours. Once completed, the solution was quenched with water and extracted with EtOAc. The organic layers were dried down and purified via silica column chromatography (9:1 Hexanes:Ethyl Acetate) to give **2.6** in 20% yield.

1H NMR (500 MHz, $CDCl_3$) δ 12.05 (s, 1H), 7.44 (s, 1H), 7.03 (s, 1H), 6.25 (m, 1H), 6.53 (d, 1H, 15.7 Hz), 5.19 (qt, 1H, *J* = 1.3 Hz, 7.0 Hz), 2.58 (s, 3H), 3.31 (d, 2H, *J* = 7.0 Hz), 2.22 (dq, 2H, *J* = 1.3 Hz, 7.5 Hz), 1.74 (doublet, 6H, *J* = 4.8 Hz), 1.51 (sextet, 2H, *J* = 7.5 Hz), 0.96 (t, 3H, *J* = 7.5 Hz)

(*E*)-2,2-dimethyl-6-(3-methylbut-2-en-1-yl)-7-(pent-1-en-1-yl)chroman-4-one

Chemical Formula: $C_{21}H_{28}O_2$

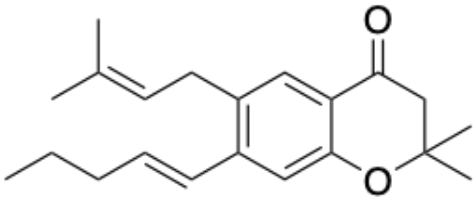

To a flame dried flask containing **2.6** (1.23 g, 4.41 mmol) and $ZnCl_2$ (733 g, 5.3 mmol) in MeOH (15 mL) was added pyrrolidine dropwise (1.82 mL, 22.1 mmol). This solution was allowed to stir for 30 minutes. After stirring, acetone (0.5mL,

6.62mmol) was added dropwise and stirred for 30 more minutes. The solution was then heated to reflux and allowed to heat and stir overnight. The solution was dried down to remove methanol and water/EtOAc were added and the solution was stirred for another 30 minutes. The EtOAc was separated and the water layer was extracted with EtOAc (2 x 30mL). The organic layer was evaporated and purified via silica column chromatography (9:1 Hexanes:Ethyl Acetate) to give **2.7** in 50% yield.

1H NMR (500 MHz, $CDCl_3$) δ 7.60 (s, 1H), 6.98 (s, 1H), 6.53 (d, 1H, *J* = 16.1 Hz), 6.20 (m, 1H), 5.19 (t, 1H, *J* = 7.3 Hz), 3.30 (d, 2H, *J* = 7.3 Hz), 2.66 (s, 2H), 2.20 (dq, 2H, *J* = 1.2 Hz, 7.4 Hz), 1.71 (s, 6H), 1.49 (sextet, 2H, *J* = 7.4 Hz), 1.43 (s, 6H), 0.95 (t, 3H, *J* = 7.5 Hz)

7-hydroxy-2,2-dimethylchroman-4-one

Chemical Formula: $C_{11}H_{12}O_3$

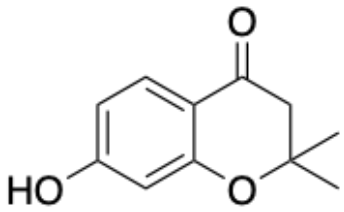

To a flame dried flask containing **2.8** (10 g, 65.7 mmol) and $ZnCl_2$ (10.4 g, 78.8 mmol) in MeOH (145 mL) was added pyrrolidine dropwise (27 mL, 329 mmol). This solution was allowed to stir for 30 minutes. After stirring, acetone (7.3 mL, 99 mmol) was added dropwise and stirred for 30 more minutes. The solution

was then heated to reflux and allowed to heat and stir overnight. The solution was dried down to remove methanol and water/EtOAc were added and the solution was stirred for another 30 minutes. The EtOAc was separated and the water layer was extracted with EtOAc (2 x 50mL). The organic layer was evaporated and purified via silica column chromatography (9:1 Hexanes:Ethyl Acetate) to give **2.9** in 24% yield.

1H NMR (500 MHz, $CDCl_3$) δ 7.79 (d, 1H, 8.7 Hz), 6.46 (dd, 1H, *J* = 2.0 Hz, 8.7 Hz), 6.34 (d, 1H, *J* = 2.0 Hz), 5.46 (br s, 1H), 2.67 (s, 2H), 1.45 (s, 6H)

7-hydroxy-2,2-dimethyl-4-oxochromane-8-carbaldehyde

Chemical Formula: $C_{12}H_{12}O_4$

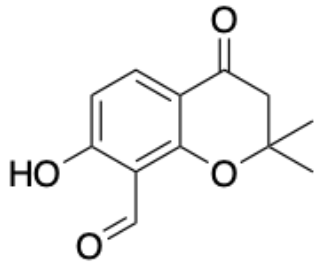

To a flask was added **2.9** (2.21 g, 11.5 mmol) and 15% KOH in water (76 mL). $CHCl_3$ (12 mL) was then added and the solution was heated to 65 °C for two hours. After the allotted time, the reaction was quenched with 1N HCl (30 mL). The aqueous layer was then extracted in $CHCl_3$ (2x 100mL). The organic layers were dried and purified via silica column chromatography (15% Ethyl Acetate in Hexanes) to give **2.10** (32% yield).

1H NMR (500 MHz, $CDCl_3$) δ 12.53 (s, 1H), 10.32 (s, 1H), 8.02 (d, 1H, *J* = 8.8 Hz), 6.56 (d, 1H, *J* = 8.8 Hz), 2.73 (s, 2H), 1.53 (s, 6H)

8-formyl-2,2-dimethyl-4-oxochroman-7-yl trifluoromethanesulfonate

Chemical Formula: $C_{13}H_{11}F_3O_6S$

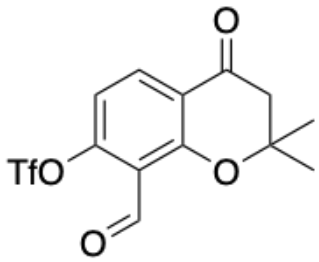

To a flame-dried flask was added **2.10** (90 mg, 0.41 mmol). Dry DCM (2 mL) was added by syringe, and the solution was cooled to 0 °C. Pyridine (66 uL, 0.82 mmol) was added and the solution was stirred for 15 minutes. Tf_2O (99 uL, 0.59 mmol) was then added dropwise at 0 °C. Upon addition of Tf_2O, the solution was allowed to stir for 1 hour. Upon consumption of starting material (via TLC), the solution was quenched with water (2 mL), and the aqueous layer was extracted with DCM (2 x 3mL). The organic layers were dried and the crude mixture was purified via silica column chromatography (x:y Hexanes: Ethyl Acetate) to give **2.11** in 87% yield.

1H NMR (500 MHz, $CDCl_3$) δ 10.42 (s, 1H), 8.14 (d, 1H, *J* = 8.7 Hz), 6.93 (d, 1H, *J* = 8.7 Hz), 2.83 (s, 2H), 1.56 (s, 6H)

(*E*)-2,2-dimethyl-4-oxo-7-(pent-1-en-1-yl)chromane-8-carbaldehyde

Chemical Formula: $C_{17}H_{20}O_3$

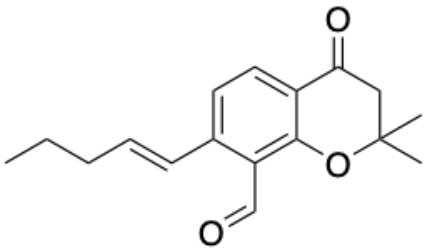

To a flame-dried flask was added **2.11** (507 mg, 1.62 mmol), $PdCl_2$(dppf) (119 mg, 0.162 mmol), NEt_3 (0.25 mL, 1.79 mmol), and 1-pentene (1.8 mL, 16.2 mmol) in DMF (5 mL). The solution was added to a preheated oil bath of 75 °C. The solution was added to a condenser due to the lower boiling point of pentene. The reaction was heated for 12 hours and quenched with water (1 mL). The aqueous layers were extracted with EtOAc (2 x 5mL). The organic layers were then dried. The crude mixture was purified via silica column chromatography (8.5:1.5 Hexanes: Ethyl Acetate) to give **2.12** in 23% yield.

^{1}H NMR (500 MHz, $CDCl_3$) δ 10.6 (s, 1H), 7.96 (d, 1H, *J* = 8.4 Hz), 7.36 (d, 1H, *J* = 16.1 Hz), 7.19 (d, 1H, *J* = 8.4 Hz), 6.37 (m, 1H), 2.78 (s, 2H), 2.26 (dq, 2H, *J* = 1.2 Hz, 7.4 Hz), 1.52 (sextet, 2H, *J* = 7.4 Hz), 1.52 (s, 6H), 0.97 (t, 3H, *J* = 7.7 Hz)

1-(2,4-dihydroxy-5-(3-methylbut-2-en-1-yl)phenyl)ethan-1-one

Chemical Formula: $C_{13}H_{16}O_3$

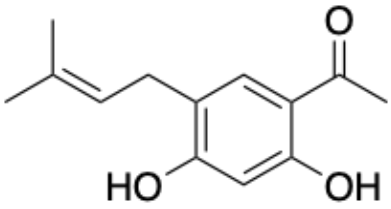

to a flame-dried flask, **2.8** (10 g, 65.7 mmol) and $ZnCl_2$ (18.2 g, 131.5 mmol) were dissolved in EtOAc (400 mL). This solution was stirred and heated to 40 °C when prenol (12.9 mL, 131.5 mmol) in EtOAc (50 mL) were added dropwise. This solution was stirred for 4 h at reflux. Once the reaction is completed, the reaction is quenched with water (200 mL). The aqueous layer was washed with EtOAc (2 x 200 mL). The organic layers were dried down and purified via silica column chromatography (9.5:5 Hexanes:Ethyl Acetate) to afford compound **2.13** (20% yield).

^{1}H NMR (500 MHz, $CDCl_3$) δ 12.50 (s, 1H), 7.44 (s, 1H), 6.36 (s, 1H), 5.7 (s, 1H), 5.29 (t, 1H, *J* = 7.2 Hz), 3.31 (d, 2H, *J* = 7.2 Hz), 2.55 (s, 3H), 1.79 (d, 6H, *J* = 3.47 Hz)

7-hydroxy-2,2-dimethyl-6-(3-methylbut-2-en-1-yl)chroman-4-one

Chemical Formula: $C_{16}H_{20}O_3$

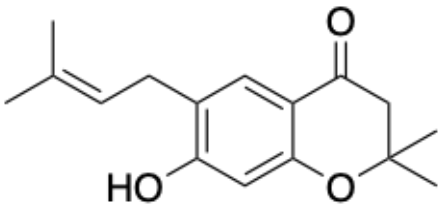

To a flame dried flask containing **2.13** (1.9 g, 8.63 mmol) and $ZnCl_2$ (1.45 g, 10.4 mmol) in MeOH (20 mL) was added pyrrolidine dropwise (8 mL, 97.4 mmol). This solution was allowed to stir for 30 minutes. After stirring, acetone (1.2 mL, 15.6 mmol) was added dropwise and stirred for 30 more minutes. The solution was then heated to reflux and allowed to heat and stir overnight. The

solution was dried down to remove methanol and water/EtOAc were added and the solution was stirred for another 30 minutes. The EtOAc was separated and the water layer was extracted with EtOAc (2 x 30mL). The organic layer was evaporated and purified via silica column chromatography (x:y Hexanes:Ethyl Acetate) to give **2.14** in 24% yield.

^{1}H NMR (500 MHz, $CDCl_3$) δ 7.62 (s, 1H), 6.32 (s, 1H), 5.76 (s, 1H), 5.29 (t, 1H, *J* = 7.3 Hz), 3.31 (s, 2H, *J* = 7.3 Hz), 2.65 (s, 2H), 1.77 (s, 6H), 1.43 (s, 6H)

7-hydroxy-2,2-dimethyl-6-(3-methylbut-2-en-1-yl)-4-oxochromane-8-carbaldehyde

Chemical Formula: $C_{17}H_{20}O_4$

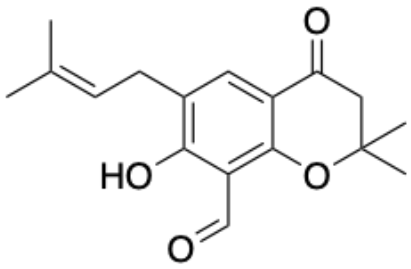

To a flask was added **2.14** (3.4 g, 13.1 mmol) and 15% KOH in water (88 mL). $CHCl_3$ (16 mL) was then added and the solution was heated to 65 °C for two hours. After the allotted time, the reaction was quenched with 1N HCl (40 mL). The aqueous layer was then extracted in $CHCl_3$ (2x 100 mL). The organic layers were dried and purified via silica column chromatography (15% Ethyl Acetate in Hexanes) to give **2.15** (33% yield).

^{1}H NMR (500 MHz, $CDCl_3$) δ 1.51 (s, 6H), 12.86 (s, 1H), 10.30 (s, 1H), 7.86 (s, 1H), 5.27 (t, 1H, 7.4 Hz), 1.70 (s, 3H), 3.25 (d, 2H, *J* = 7.4 Hz), 2.71 (s, 2H), 1.75 (s, 3H)

8-formyl-2,2-dimethyl-6-(3-methylbut-2-en-1-yl)-4-oxochroman-7-yl trifluoromethanesulfonate

Chemical Formula: $C_{18}H_{19}F_3O_6S$

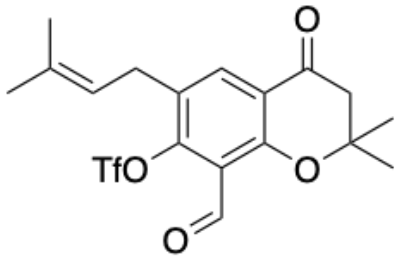

To a flame-dried flask was added **2.15** (154 mg). Dry DCM (1.7 mL, ~2.4 mL/mmol (**2.15**)) was added by syringe, and the solution was cooled to 0 °C. Pyridine (90 uL, 1.07 mmol) was added and the solution was stirred for 15 minutes. Tf_2O (0.13 mL, 0.78 mmol) was then added dropwise at 0 °C. Upon addition of Tf_2O, the solution was allowed to stir for 3 hours. Upon consumption of starting material (via TLC), the solution was dried in silica and purified directly (8:2 Hexanes: Ethyl Acetate) to give **2.16** in 77% yield.

^{1}H NMR (500 MHz, $CDCl_3$) δ 10.40 (s, 1H), 8.01 (s, 1H), 5.20 (t, 1H, *J* = 7.3 Hz), 3.39 (d, 2H, *J* = 7.3 Hz), 2.81 (s, 2H), 1.78 (s, 3H), 1.70 (s, 3H), 1.54 (s, 6H)

Methods and materials for the final scheme

Unless otherwise noted, commercially available materials were used without further purification. Reactions were performed under an atmosphere of nitrogen with magnetic stirring unless noted otherwise. Flash chromatography (FC) was performed using E. Merck silica gel 60 (240–400 mesh). Thin layer chromatography was performed using precoated plates purchased from E. Merck (silica gel 60 PF_{254}, 0.25 mm). Nuclear magnetic resonance (NMR) spectra were recorded on a Bruker Avance III HD 800 MHz and Bruker Avance III HD 500 MHz spectrometer at operating frequencies of 800/500 MHz (^{1}H NMR) or 200/125 MHz (^{13}C NMR). Chemical shifts (δ) are given in ppm relative to residual solvent chloroform ($CDCl_3$: ^{1}H, δ = 7.26 ppm, ^{13}C, δ = 77.16 ppm), dimethyl sulfoxide ($(CD_3)_2SO$:^{1}H, δ = 2.50 ppm, ^{13}C, δ = 39.52 ppm) and coupling constants (*J*) in Hz. Multiplicity is tabulated as s for singlet, d for doublet, t for triplet, q for quadruplet, and m for multiplet and br when the signal in question is broadened. Electrospray ionization mass spectra (ESI-MS) were recorded on a LTQ-Orbitrap Velos Pro MS. Chemicals were purchased from Aldrich, Fisher, Alfa Aesar, TCI, or Oakwood chemicals and used without purification.^{15}N-N_2Na was purchased from Cambridge Isotope Laboratories, Inc. and also used without purification.

Scale up of common tricyclic intermediate

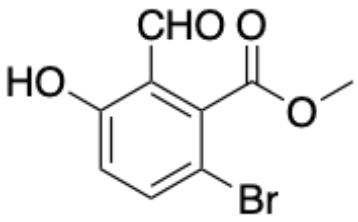

Synthesis of methyl 6-bromo-2-formyl-3-hydroxybenzoate (2.18)

methyl 2-bromo-5-hydroxybenzoate (12 g, 56.3 mmol) was dissolved in anhydrous TFA (120 mL) under N_2, and hexamethylenetetramine (17.3 g, 123.9 mmol) was added in one portion. The yellow solution was heated in an oil bath until all the starting phenol was converted (TLC control, ca. 6 h); the

mixture was then cooled to r.t. The cooled solution was poured into 4 M HCl (200 mL) and stirred for 15 min, the product was extracted with CH_2Cl_2 (2 × 400 mL). The combined organic extracts were washed with water (2 × 200 mL), sat. brine (200 mL), then dried (Na_2SO_4) and the solvent removed in vacuo. The crude residue was purified by column chromatography over silica gel (hexane: ethyl acetate = 8:2), affording **2.18** 7.2 gm (53 % yield) as colorless solid.

^{1}H NMR (500 MHz, $CDCl_3$-*d*) δ 12.38 (s, 1H), 9.74 (s, 1H), 8.19 (s, 1H), 4.02 (s, 3H).

^{13}C NMR (125 MHz, $CDCl_3$-*d*) δ 193.78, 165.53, 160.45, 148.91, 138.96, 117.28, 109.92, 88.96, 53.57.

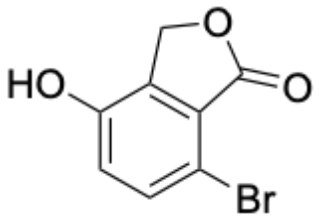

Synthesis of 7-bromo-4-hydroxyisobenzofuran-1(3H)-one (2.19)

methyl 6-bromo-2-formyl-3-hydroxybenzoate (**2.18**) (7 gm, 26.8 mmol) was taken into 100 ml of methanol. To this $NaBH_4$ (1.48 gm, 40.2 mol) was added portion wise at 0 ^oC and the reaction mixture was allowed to warm to room temperature. The reaction mixture was acidified using 1N HCl, with a white precipitate forming. The white solid precipitate was filtered and dried over vacuum to obtain pure product **2.19** (5.1 gm, 83% yield).

^{1}H NMR (500 MHz, DMSO-d_6) δ 10.67 (s (broad), 1H), 7.56 (d, J = 8.4 Hz, 1H), 7.04 (d, J = 8.4 Hz, 1H), 5.24 (s, 2H).

^{13}C NMR (125 MHz, DMSO-d_6) δ 168.24, 151.82, 136.46, 134.33, 124.05, 121.66, 106.97, 66.63.

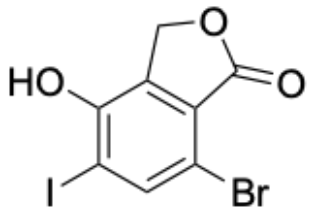

Synthesis of 7-bromo-4-hydroxy-5-iodoisobenzofuran-1(3H)-one (2.20)

7-bromo-4-hydroxyisobenzofuran-1(3H)-one **2.19** (5 gm, 22.0 mmol) and N-Iodosuccinimide (10.8 gm, 48.4 mmol) was taken in glacial acetic acid (100 mL). A catalytic amount of H_2SO_4 (0.5 mL) was then added at room temperature and the reaction mixture was stirred for approximately 2 days. The reaction mixture was then poured on crushed ice and stirred for 30 min. The product was then filtered and dried under vacuum. This solid was washed with toluene 3 times to remove any residual water as well as iodine to obtain pure gray solid product **2.20** (5.6 gm, 71% yield).

^{1}H NMR (500 MHz, DMSO-d_6) δ 11.06 (s, 1H), 8.04 (s, 1H), 5.24 (s, 2H).

^{13}C NMR (125 MHz, DMSO-d_6) δ 167.92, 151.15, 142.30, 135.25, 124.37, 108.16, 94.69, 66.88.

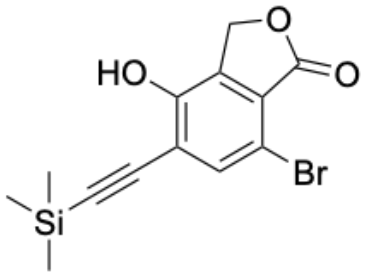

Synthesis of 7-bromo- 4-hydroxy- 5-((trimethylsilyl)ethynyl) isobenzo furan-1(3H)-one

To a solution of 7-bromo-4-hydroxy-5-iodoisobenzofuran-1(3H)-one (**2.20**) (5.3 g, 14.9 mmol) in degassed THF (40 mL) and Et_3N (20 mL) were added $PdCl_2(PPh_3)_2$ (0.419 g, 0.598 mmol) and CuI (0.170 g, 0.898 mmol). Then Trimethylsilylacetylene (2.5 mL, 17.9 mmol) was added, and the reaction was stirred overnight at room temperature. The reaction mixture was diluted with water (100 mL) and acidified (pH 5-6) by adding 1N HCl and extracted with ethyl acetate (2 × 200 mL). The combined organic extracts were washed with water, brine, then dried over sodium sulfate (Na_2SO_4) and the solvent was removed in vacuo. The crude product was purified by silica gel column chromatography (hexanes:ethyl acetate = 7:3) to afford compound **2.21** as light-yellow solid product (3.3 g, 68%).

^{1}H NMR (500 MHz, $CDCl_3$-*d*) δ 7.63 (s, 1H), 6.13 (s, 1H), 5.22 (s, 2H), 0.30 (s, 9H).

^{13}C NMR (125 MHz, $CDCl_3$-*d*) δ 167.99, 150.84, 136.53, 134.52, 125.48, 116.22, 110.00, 107.86, 95.98, 66.22, 0.16.

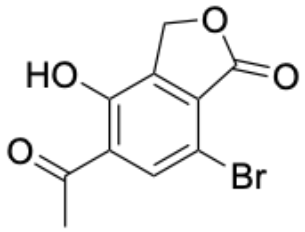

Synthesis of 5-acetyl-7-bromo-4-hydroxyisobenzofuran-1(3H)-one (2.22)

7-bromo-4-hydroxy-5-((trimethylsilyl)ethynyl)isobenzofuran-1(3H)-one **2.21** (3.2 gm, 9.90 mmol) was taken in formic acid (50 mL) and cat. TfOH (171 mg, 1.98 mmol) was added. Reaction mixture was then heated in oil bath at 90 ^{o}C for 18h. The reaction mixture was diluted with water (100 mL) and subsequently extracted with ethyl acetate (150 mL x 2). The combined organic layer was washed with water, brine, dried over sodium sulphate and concentrated in vacuo. The crude product was purified via silica gel column chromatography (hexanes:ethyl acetate = 8:2) to afford compound **2.22** as light brown solid product (2 g, 65%).

^{1}H NMR (500 MHz, $CDCl_3$-*d*) δ 12.28 (s, 1H), 8.00 (s, 1H), 5.27 (s, 2H), 2.73 (s, 3H).

^{13}C NMR (126 MHz, $CDCl_3$-*d*) δ 204.12, 167.52, 156.04, 138.53, 135.61, 130.18, 123.41, 107.85, 66.63, 27.58.

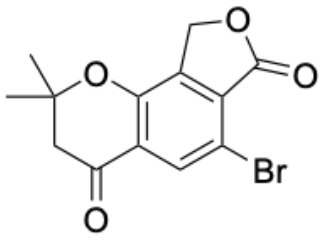

6-bromo-2,2-dimethyl-2,3-dihydro-4H-furo[3,4-h]chromene-4,7(9H)-dione (2.23)

To a well stirred solution of 5-acetyl- 7-bromo- 4-hydroxy isobenzofuran-1(3H)-one (**2.22**) (2 g, 6.47 mmol) and acetone (4.8 mL, 64.7 mmol) in toluene (20 mL), pyrrolidine (0.54 mL, 6.47 mmol) was added at room temperature. After stirring for 10 min AcOH (0.38 mL, 6.47 mmol) was added and the reaction mixture was subsequently heated in an oil bath at 90 ^{o}C for 18h. The reaction mixture was quenched by adding crushed ice then acidified (pH 5-6)with 1N HCl solution. Finally, the aqueous solution was extracted with ethyl acetate (2×100 mL). The organic layer was washed by water, brine and dried over anhydrous sodium sulfate, and the solvent was removed to obtain the crude product. The crude residue was purified by column chromatography over silica gel (hexane:ethyl acetate = 7:3), affording compound **2.23** (1.31 gm, 57%) as a yellow solid.

^{1}H NMR (500 MHz, $CDCl_3$-*d*) δ 8.12 (s, 1H), 5.22 (s, 2H), 2.82 (s, 2H), 1.51 (s, 6H).

^{13}C NMR (125 MHz, $CDCl_3$-*d*) δ 190.16, 167.59, 153.55, 138.95, 132.05, 129.98, 124.21, 110.43, 81.65, 66.29, 48.79, 26.70.

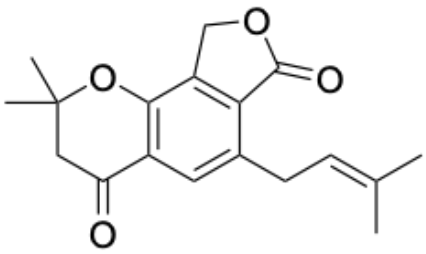

Synthesis of 2,2-dimethyl- 6-(3-methylbut-2-en-1-yl) -2,3-dihydro -4H-furo[3,4-h]chromene-4,7(9H)-dione

In an oven-dried round bottom flask, 6-bromo- 2,2-dimethyl- 2,3-dihydro- 4H-furo[3,4-h]chromene-4,7(9H)-dione (150 mg, 0.485 mmol), was taken in degassed THF and degassed deionized water in the ratio of 2.5:1. THF:H_2O (35 mL). Then 4,4,5,5-tetramethyl- 2-(3-methylbut-2-en-1-yl)- 1,3,2-dioxaborolane (142 mg, 0.728 mmol), palladium acetate (5.4 mg, 0.024 mmol), 2-Dicyclohexyl-phosphino-2′,6′-dimethoxybiphenyl (SPhos, 19 mg, 0.0485 mmol), and potassium phosphate (K_3PO_4, 226 mg, 1.067 mmol) was added under inert atmosphere. The resulting mixture was stirred in an oil bath at 70 ^oC for 16 h. The reaction mixture was diluted with water 20 mL and extracted with ethyl acetate (2 x 100 mL). The organic layer was washed with water, brine and dried over Na_2SO_4. The concentration of the organic layer in vacuo followed by silica gel (60–120) column chromatographic purification of the resulting residue using hexane:ethyl acetate (8:2) as an eluent afforded the pure product **2.24** as white solid (96 mg, 66%).

^{1}H NMR (500 MHz, $CDCl_3$-*d*) δ 7.76 (s, 1H), 5.32 (t, *J* = 8.7 Hz, 1H), 5.22 (s, 2H), 3.76 (d, *J* = 7.3 Hz, 2H), 2.79 (s, 2H), 1.73 (d, *J* = 5.1 Hz, 6H), 1.49 (s, 6H). ^{13}C NMR (125 MHz, $CDCl_3$-*d*) δ 191.72, 170.18, 152.53, 136.52, 134.48, 134.05, 129.50, 127.66, 123.19, 121.44, 80.74, 67.08, 49.13, 28.39, 26.77, 25.96, 18.11.

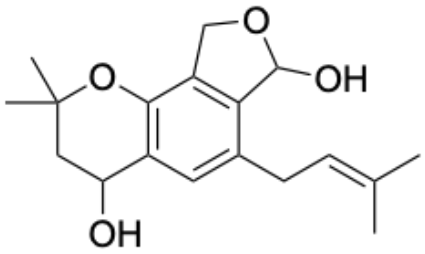

2,2-dimethyl-6-(3-methylbut-2-en-1-yl)-3,4,7,9-tetrahydro-2H-furo[3,4-h]chromene-4,7-diol

DIBALH (1 M/Hexane; 0.513 mL, 0.513 mmol) was added to a solution of the 2,2-dimethyl-6-(3-methylbut-2-en-1-yl)-2,3-dihydro-4H-furo[3,4-h]chromene-4,7(9H)-dione (70 mg, 0.233 mmol) in anhydrous CH_2Cl_2 (5 mL) at -78 ^{o}C. After 1h, the quenched by the addition of a saturated aqueous solution of sodium sulfate (0.5 mL) and allowed to warm to room temperature. Then added anhydrous sodium sulfate to remove excess water and filtered and concentrated in vacuo to afford crude ~60 mg white solid product. The residue used for the next step without further purification.

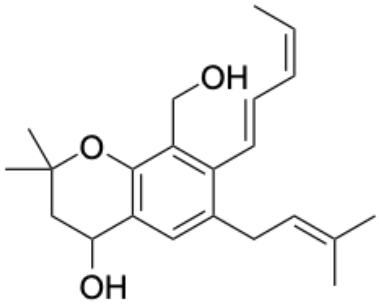

8-(hydroxymethyl)-2,2-dimethyl-6-(3-methylbut-2-en-1-yl)-7-((1E,3E)-penta-1,3-dien-1-yl)chroman-4-ol using HPLC

Phosphonium salt bromo(tributyl)((E)but-2-en-1-yl)phosphane (162 mg, 0.411 mmol) and 2,2-dimethyl-6-(3-methylbut-2-en-1-yl)-3,4,7,9-tetrahydro-2H-furo[3,4-h]chromene-4,7-diol (50 mg, 0.164 mmol) were combined in dry toluene (5 mL). The solution was cooled to 0 °C and *t*-BuOK in 1.0 M in THF (0. 411 mL, 0. 411 mmol) was added slowly dropwise over the period of 10 min. The mixture was allowed to warm to room temperature and stirred for 4 h. Reaction was then quenched by adding saturated solution of NH_4Cl and extracted with ethyl acetate (2 X 10 mL) and washed with water (10 mL) and brine (10 mL). The organic phase was dried (Na_2SO_4), filtered and concentrated. The crude mixture was purified by flash chromatography (hexane:ethyl acetate = 7:3) to afford the coupled product (28 mg, 50%)

HPLC separation protocol: In order to untangle the mixture and ascertain relative ratios of each product, preparative HPLC was used to separate the crude mixture into two peaks, with each containing E/Z stereoisomers. The

major peak of the two was then purified again via semi-preparative, acidless HPLC to give two stereoisomers, and the major peak was taken. That major peak consisted of a single stereoisomer. While it was initially unclear how many stereoisomers were present in the crude mixture, the second round of purification demonstrated that each initial peak presumably had 2 E/Z stereoisomers present. The semi-preparative HPLC purification then further resolved the two stereoisomeric peaks into single stereoisomers.

^{1}H NMR (800 MHz, $CDCl_3$-*d*) δ 7.23 (s, 1H), 6.60 (dd, *J* = 15.8, 11.1 Hz, 1H), 6.55 (d, *J* = 15.9 Hz, 1H), 6.20 – 6.17 (m, 1H), 5.62 – 5.58 (m, 1H), 5.20 (t, *J* = 7.1 Hz, 1H), 4.84 (t, *J* = 6.8 Hz, 1H), 4.72 (s, 2H), 3.27 (d, *J* = 7.0 Hz, 2H), 2.56 (s, 1H), 2.20 (dd, *J* = 13.5, 6.1 Hz, 1H), 1.89 (dd, *J* = 13.4, 8.5 Hz, 1H), 1.78 (dd, *J* = 7.1, 1.3 Hz, 3H), 1.71 (s, 3H), 1.68 (s, 3H), 1.48 (s, 3H), 1.35 (s, 3H).

^{13}C NMR (201 MHz, $CDCl_3$-*d*) δ 150.25, 138.52, 132.22, 132.07, 131.39, 129.64, 128.21, 127.53, 127.26, 126.62, 123.53, 122.87, 75.94, 63.81, 59.26, 42.72, 32.49, 29.12, 26.47, 25.94, 18.08, 13.71.

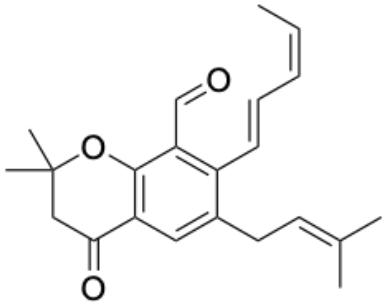

2,2-dimethyl-6-(3-methylbut-2-en-1-yl)-4-oxo-7-((1E,3Z)-penta-1,3-dien-1-yl)chromane-8-carbaldehyde:

The 8-(hydroxymethyl)-2,2-dimethyl-6-(3-methylbut-2-en-1-yl)-7-((1E,3E)-penta-1,3-dien-1-yl)chroman-4-ol (6 mg, 0.017 mmol) was dissolved in dry CH_2C1_2 (5 mL) containing both the 4 Angstrom molecular sieves and NMO (5.1 mg, 0.043 mmol). After stirring the mixture for 10 min, Tetrapropyl ammonium perruthenate (TPAP) (0.6 mg, 0.001 mmol) was added and the reaction stirred for 1h at room temperature. The black reaction mixture is directly loaded on silica gel column and purified to afford pure product (4 mg, 67%).

^{1}H NMR (800 MHz, $CDCl_3$-*d*) δ 10.23 (s, 1H), 7.88 (s, 1H), 6.80 (d, *J* = 15.6 Hz, 1H), 6.54 (ddd, *J* = 15.6, 11.1, 1.0 Hz, 1H), 6.26 – 6.21 (m, 1H), 5.73 (dq, *J* = 10.8, 7.2 Hz, 1H), 5.19 (ddt, *J* = 8.2, 5.4, 1.3 Hz, 1H), 3.33 (d, *J* = 7.0 Hz, 2H), 2.76 (s, 2H), 1.76 (dd, *J* = 7.2, 1.7 Hz, 3H), 1.74 (s, 3H), 1.69 (s, 3H), 1.50 (s, 6H).

^{13}C NMR (200 MHz, $CDCl_3$-*d*) δ 191.70, 190.89, 158.98, 148.04, 134.42, 133.43, 132.99, 131.36, 130.30, 129.18, 127.10, 124.97, 122.48, 119.24, 80.57, 48.74, 31.72, 26.79, 25.92, 18.14, 13.80.

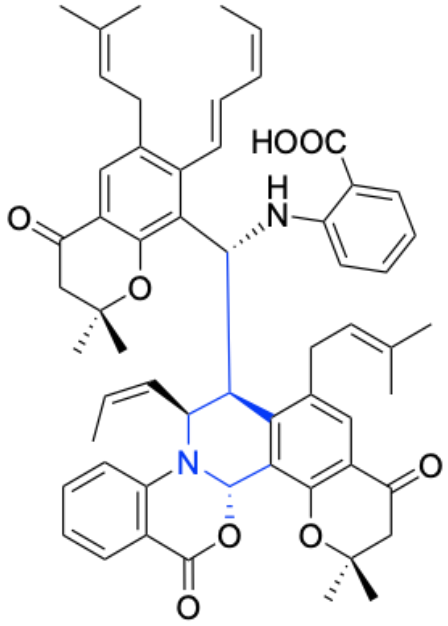

2-(((1R)-(2,2-dimethyl-6-(3-methylbut-2-en-1-yl)-4-oxo-7-((1E,3Z)-penta-1,3-dien-1-yl)chroman-8-yl)((6S,13cS)-12,12-dimethyl-8-(3-methylbut-2-en-1-yl)-10,15-dioxo-6-((Z)-prop-1-en-1-yl)-7,11,12,13c-tetrahydro-6H,10H,15H-benzo[4,5][1,3]oxazino[2,3-a]pyrano[3,2-h]isoquinolin-7-yl)methyl)amino)benzoic acid

2,2-dimethyl-6-(3-methylbut-2-en-1-yl)-4-oxo-7-((1E,3Z)-penta-1,3-dien-1-yl)chromane-8-carbaldehyde (4 mg, 0.0118 mmol) was taken in MeOH and anthranilic acid (1.62 mg, 0.0118 mmol) was added and stirred for three days. After completion of the reaction (via tlc) it was purified by HPLC.

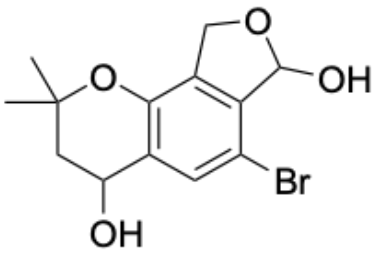

6-bromo-2,2-dimethyl-3,4,7,9-tetrahydro-2H-furo[3,4-h]chromene-4,7-diol

DIBALH (1 M/Hexane; 0.355 mL, 0.355 mmol) was added to a solution of the (6-bromo-2,2-dimethyl-2,3-dihydro-4H-furo[3,4-h]chromene-4,7(9H)-dione (50 mg, 0.16 mmol) in anhydrous CH_2Cl_2 (3 mL) at -78 ^oC. After 1h, the quenched by the addition of a saturated aqueous solution of sodium sulfate (0.5 mL) and allowed to warm to room temperature. Then added anhydrous sodium sulfate to remove excess water and filtered and concentrated in vacuo to afford crude 40 mg white solid product. The residue used for the next step without further purification.

^{1}H NMR (500 MHz, $CDCl_3$-*d*) δ 7.58 (s, 1H), 6.41 (s, 1H), 5.23 (d, *J* = 13.2 Hz, 1H), 4.98 (d, *J* = 13.3 Hz, 1H), 4.91 – 4.81 (m, 1H), 3.03 (t, *J* = 7.9 Hz, 1H), 2.19 (dd, *J* = 18.7, 3.9 Hz, 1H), 1.80 (d, *J* = 7.3 Hz, 1H), 1.43 (s, 3H), 1.30 (s, 3H).

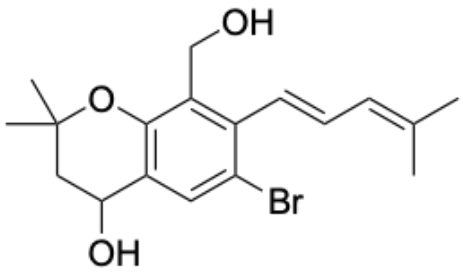

(E)-6-bromo-8-(hydroxymethyl)-2,2-dimethyl-7-(4-methylpenta-1,3-dien-1-yl)chroman-4-ol.

Phosphonium salt bromo(tributyl)(3-methylbut-2-en-1-yl)phosphane (65 mg, 0.160 mmol) and 6-bromo-2,2-dimethyl-3,4,7,9-tetrahydro-2H-furo[3,4-h]chromene-4,7-diol (20 mg, 0.064 mmol) were combined in dry toluene (3 mL). The solution was cooled to 0 °C and t-BuOK in 1.0 M in THF (0.160 mL, 0.160 mmol) was added slowly dropwise over the period of 10 min. The mixture was allowed to warm to room temperature and stirred for 4 h. Reaction was then quenched by adding saturated solution of NH_4Cl and extracted with ethyl acetate (2 X 10 mL) and washed with water (10 mL) and brine (10 mL). The organic phase was dried (Na_2SO_4), filtered and concentrated. The crude mixture was purified by flash chromatography (hexane:ethyl acetate = 7:3) to afford the coupled product (16 mg, 69%)

^{1}H NMR (500 MHz, $CDCl_3$-*d*) δ 7.62 (s, 1H), 6.63 (dd, *J* = 15.7, 11.0 Hz, 1H), 6.43 (d, *J* = 15.7 Hz, 1H), 6.05 (d, *J* = 10.9 Hz, 1H), 4.79 (dd, *J* = 8.8, 6.3 Hz, 1H), 4.72 (s, 2H), 2.16 (q, *J* = 6.7, 6.1 Hz, 2H), 1.85 (s, 3H), 1.81 (s, 3H), 1.46 (s, 3H), 1.32 (s, 3H).

^{13}C NMR (126 MHz, $CDCl_3$-*d*) δ 151.52, 139.42, 138.42, 133.78, 130.73, 128.16, 126.52, 125.23, 124.66, 115.01, 76.68, 63.25, 59.48, 42.35, 29.18, 26.30, 26.09, 18.74.

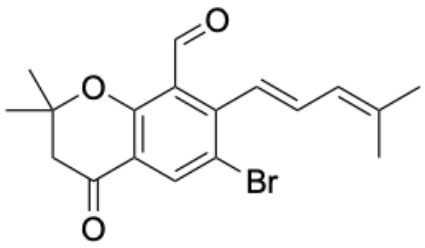

(E)-6-bromo-2,2-dimethyl-7-(4-methylpenta-1,3-dien-1-yl)-4-oxochromane-8-carbaldehyde.

The (E)-6-bromo-8-(hydroxymethyl)-2,2-dimethyl-7-(4-methylpenta-1,3-dien-1-yl)chroman-4-ol (16 mg, 0.045 mmol) was dissolved in dry CH_2C1_2 (5 mL) containing both the 4 Angstrom molecular sieves and NMO (13 mg, 0.112 mmol). After stirring the mixture for 10 min, Tetrapropyl ammonium perruthenate (TPAP) (3 mg, 0.009 mmol) was added and the reaction stirred for 1h at room temperature. The black reaction mixture is directly loaded on silica gel column and purified to afford pure product (12 mg, 76%).

^{1}H NMR (500 MHz, $CDCl_3$-*d*) δ 10.01 (s, 1H), 8.22 (s, 1H), 6.72 – 6.66 (m, 1H), 6.58 (dd, *J* = 15.4, 10.7 Hz, 1H), 6.15 – 6.13 (m, 1H), 2.77 (s, 2H), 1.88 (s, 3H), 1.80 (s, 3H), 1.51 (s, 6H).

^{13}C NMR (125 MHz, $CDCl_3$-*d*) δ 190.35, 189.39, 158.82, 148.32, 142.91, 139.08, 134.13, 126.77, 125.07, 124.77, 120.14, 115.70, 81.16, 48.47, 26.69, 18.92.

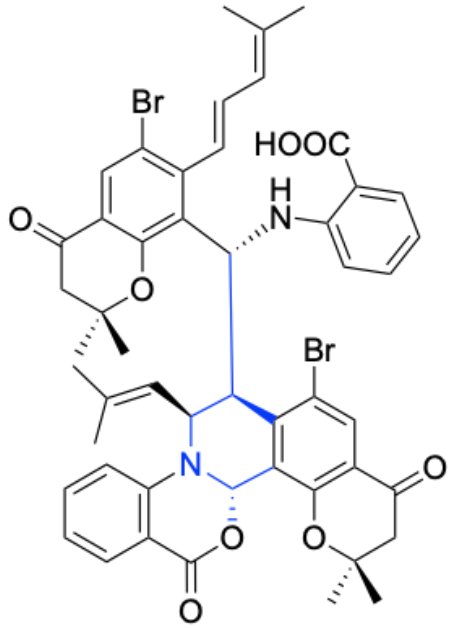

2-(((1R)-((6S,13cS)-8-bromo-12,12-dimethyl-6-(2-methylprop-1-en-1-yl)-10,15-dioxo-7,11,12,13c-tetrahydro-6H,10H,15H-benzo[4,5][1,3]oxazino[2,3-a]pyrano[3,2-h]isoquinolin-7-yl)(6-bromo-2,2-dimethyl-7-((E)-4-methylpenta-1,3-dien-1-yl)-4-oxochroman-8-yl)methyl)amino)benzoic acid

(E)-6-bromo-2,2-dimethyl-7-(4-methylpenta-1,3-dien-1-yl)-4-oxochromane-8-carbaldehyde (9 mg, 0.024 mmol) was taken in MeOH and anthranilic acid (3.39 mg, 0.024 mmol) was added and stirred for three days. After completion of the reaction (via tlc) it was purified by HPLC.

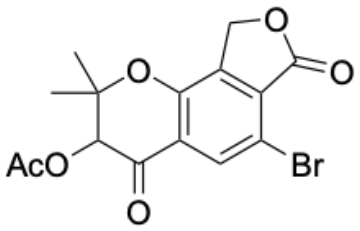

6-bromo-2,2-dimethyl-4,7-dioxo-3,4,7,9-tetrahydro-2H-furo[3,4-h]chromen-3-yl acetate

Lead tetraacetate (4.3 gm, 9.708 mmol) was added in a single portion to a screw-capped vessel containing a solution of the 6-bromo-2,2-dimethyl-2,3-dihydro-4H-furo[3,4-h]chromene-4,7(9H)-dione (1 gm, 3.236) in benzene (30 mL) at room temperature. The reaction vessel was sealed, and the sealed reaction vessel was placed in an oil bath that had been preheated to 82 °C. The reaction mixture was stirred for 48 h at 82 °C. The product mixture was cooled to 23 °C over 30 min. The cooled product mixture was filtered through a short pad of Celite. The filter cake was rinsed with ethyl acetate (3 × 30 mL). The filtrates were combined, and the combined filtrates were diluted sequentially with water (40 mL) and saturated aqueous sodium bicarbonate solution (20 mL). The diluted product mixture was transferred to a separatory funnel and the layers that formed were separated. The aqueous layer was extracted with ethyl acetate (2 × 100 mL). The organic layers were combined, and the combined organic layers were washed with brine. The washed organic layer was dried over sodium sulfate. The dried solution was filtered, and the filtrate was concentrated. The residue obtained was purified by flash-column

chromatography (hexanes: ethyl acetate = 7:3) to provide the acetate product as a yellow solid (950 mg, 80%).

^{1}H NMR (500 MHz, $CDCl_3$-*d*) δ 8.06 (s, 1H), 5.63 (s, 1H), 5.23 (d, *J* = 5.7 Hz, 2H), 2.25 (s, 3H), 1.59 (s, 3H), 1.39 (s, 3H).

^{13}C NMR (126 MHz, $CDCl_3$-*d*) δ 186.47, 169.42, 167.23, 152.57, 138.68, 132.36, 130.43, 123.85, 111.36, 83.62, 76.61, 66.13, 26.04, 20.61, 19.75.

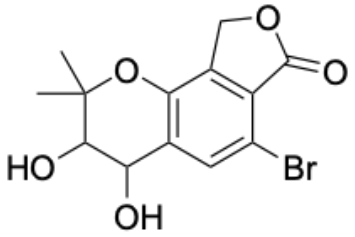

6-bromo-3,4-dihydroxy-2,2-dimethyl-3,4-dihydro-2H-furo[3,4-h]chromen-7(9H)-one

6-bromo-2,2-dimethyl-4,7-dioxo-3,4,7,9-tetrahydro-2H-furo[3,4-h]chromen-3-yl acetate (900 mg, 2.439 mmol) was taken in methanol and $NaBH_4$ (135 mg, 3.658 mmol) was added in portions at 0 ^{o}C. The reaction was quenched by adding sat. solution of NH_4Cl (10 mL) then extracted with ethyl acetate (20 mL x 3). The reaction mixture was diluted with water and extracted with ethyl acetate (20 mL). The combined organic layers were washed with water, brine and dried over Na_2SO_4. The organic layer was then concentrated in vacuo to obtain crude product (820 mg 90% crude yield). The crude product (820 mg,

2.210 mmol) was then dissolved in 10 mL of THF:H_2O (5:2) and to it LiOH (181 mg, 4.420 mmol) was added and stirred at rt for 1h. Finally, the reaction was acidified with 1N HCl then diluted with water (10 mL) and extracted with ethyl acetate (30 mL x 2). The combined organic layers were washed with water, brine and dried over Na_2SO_4. The concentration of the organic layer in vacuo to obtain crude product (580 mg 79 % crude yield). The crude product was taken forward without further purification

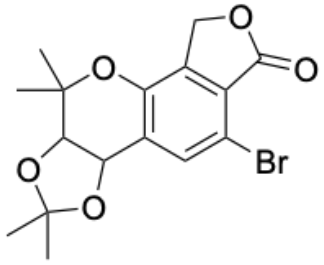

5-bromo-2,2,10,10-tetramethyl-10,10a-dihydro-8H-[1,3]dioxolo[4,5-c]furo[3,4-h]chromen-6(3aH)-one

To a stirred solution of 6-bromo-3,4-dihydroxy-2,2-dimethyl-3,4-dihydro-2H-furo[3,4-h]chromen-7(9H)-one (550 mg, 1.681 mmol) and 2,2-dimethoxypropane (2.05 mL, 16.819 mmol) in acetone (5 mL) was added (Pyridinium p-toluenesulfonate) PPTS (42 mg, 0.168 mmol) at rt. After being stirred at rt for 24 h, the reaction mixture was concentrated under reduced pressure to give the crude residue, which was purified via silica gel column chromatography (30 % ethyl acetate in hexanes) to give pure product (260 mg, 42%).

^{1}H NMR (500 MHz, $CDCl_3$-*d*) δ 7.66 (s, 1H), 5.22 – 5.15 (m, 2H), 5.11 (d, *J* = 5.9 Hz, 1H), 4.18 (d, *J* = 5.7 Hz, 1H), 1.53 (s, 3H), 1.42 (s, 3H), 1.28 (s, 3H), 1.16 (s, 3H).

^{13}C NMR (125 MHz, $CDCl_3$-*d*) δ 168.42, 146.36, 137.46, 135.21, 128.75, 125.03, 111.05, 110.44, 77.71, 77.26, 69.65, 66.49, 27.84, 26.52, 24.91, 23.62.

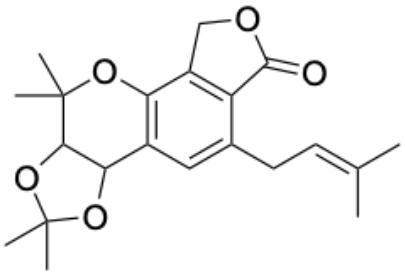

2,2,10,10-tetramethyl-5-(3-methylbut-2-en-1-yl)-10,10a-dihydro-8H-[1,3]dioxolo[4,5-c]furo[3,4-h]chromen-6(3aH)-one:

In an oven-dried round bottom flask, 5-bromo-2,2,10,10-tetramethyl-10,10a-dihydro-8H-[1,3]dioxolo[4,5-c]furo[3,4-h]chromen-6(3aH)-one (160 mg, 0.434 mmol), was taken in degassed THF and degassed deionized water in the ratio of 2.5:1. THF:H_2O (35 mL). Then 4,4,5,5-tetramethyl-2-(3-methylbut-2-en-1-yl)-1,3,2-dioxaborolane (127 mg, 0.652 mmol), palladium acetate (4.8 mg, 0.021 mmol), 2-Dicyclohexyl-phosphino-2′,6′-dimethoxybiphenyl (SPhos, 17 mg, 0.043 mmol), and potassium phosphate (K_3PO_4, 230 mg, 1.086 mmol) was added under inert atmosphere. The resulting mixture was stirred in an oil bath

at 70 ^{o}C for 16 h. The reaction mixture was diluted with water 20 mL and extracted with ethyl acetate (2 x 100 mL). The organic layer was washed with water, brine and dried over Na_2SO_4. The concentration of the organic layer in vacuo followed by silica gel (60–120) column chromatographic purification of the resulting residue using hexane:ethyl acetate (8:2) as an eluent afforded the pure product **10** as white solid (97 mg, 62%).

^{1}H NMR (500 MHz, $CDCl_3$-*d*) δ 7.28 (s, 1H), 5.33 (t, *J* = 7.24 Hz, 1H), 5.23 – 5.15 (m, 2H), 5.15 – 5.11 (m, 2H), 4.17 (d, *J* = 5.8 Hz, 1H), 3.83 (dd, *J* = 15.9, 7.1 Hz, 1H), 3.66 (dd, *J* = 15.9, 7.5 Hz, 1H), 1.74 (s, 3H), 1.72 (s, 3H), 1.50 (s, 3H), 1.43 (s, 3H), 1.26 (s, 3H), 1.16 (s, 3H).

^{13}C NMR (125 MHz, $CDCl_3$-*d*) δ 171.04, 144.98, 135.29, 135.02, 133.43, 130.95, 126.96, 123.99, 122.04, 110.61, 78.16, 76.58, 70.28, 67.23, 28.54, 27.71, 26.56, 25.97, 24.86, 23.77, 18.10.

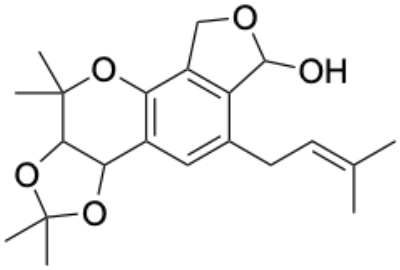

2,2,10,10-tetramethyl-5-(3-methylbut-2-en-1-yl)-3a,6,10,10a-tetrahydro-8H-[1,3]dioxolo[4,5-c]furo[3,4-h]chromen-6-ol

DIBALH (1 M/Hexane; 0.737 mL, 0.737 mmol) was added to a solution of the 2,2,10,10-tetramethyl-5-(3-methylbut-2-en-1-yl)-10,10a-dihydro-8H-

[1,3]dioxolo[4,5-c]furo[3,4-h]chromen-6(3aH)-one (110 mg, 0.307 mmol) in anhydrous CH_2Cl_2 (5 mL) at -78 ^oC. After 1h, the quenched by the addition of a saturated aqueous solution of sodium sulfate (0.5 mL) and allowed to warm to room temperature. Then added anhydrous sodium sulfate to remove excess water and filtered and concentrated in vacuo to afford crude (85 mg, 77%) white solid product. The residue used for the next step without further purification.

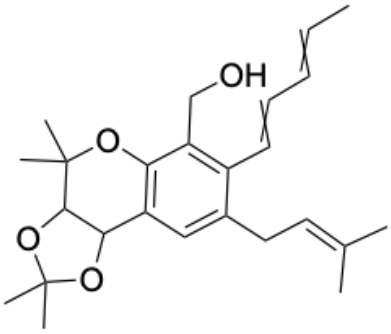

(2,2,4,4-tetramethyl-8-(3-methylbut-2-en-1-yl)-7-(penta-1,3-dien-1-yl)-3a,9b-dihydro-4H-[1,3]dioxolo[4,5-c]chromen-6-yl)methanol

Phosphonium salt bromo(tributyl)((E)but-2-en-1-yl)phosphane (0.416 mmol) and 2,2,10,10-tetramethyl-5-(3-methylbut-2-en-1-yl)-3a,6,10,10a-tetrahydro-8H-[1,3]dioxolo[4,5-c]furo[3,4-h]chromen-6-ol (0.138 mmol) were combined in dry toluene (5 mL). The solution was cooled to 0 °C and *t*-BuOK in 1.0 M in THF (0.416 mL, 0.416 mmol) was added slowly dropwise over the period of 10 min. The mixture was allowed to warm to room temperature and stirred for 4 h. Reaction was then quenched by adding saturated solution of NH_4Cl and extracted with ethyl acetate (2 X 10 mL) and washed with water (10 mL) and

brine (10 mL). The organic phase was dried (Na_2SO_4), filtered and concentrated. The crude mixture was purified by flash chromatography (hexane:ethyl acetate = 8:2) to afford the coupled product (52%)

^{1}H NMR (500 MHz, $CDCl_3$-*d*) δ 7.12 (d, *J* = 9.6 Hz, 1H), 6.67 – 6.40 (m, 2H), 6.29 – 6.17 (m, 1H), 5.83 – 5.56 (m, 1H), 5.19 (t, *J* = 6.3 Hz, 1H), 5.11 (t, *J* = 5.1 Hz, 1H), 4.73 (q, *J* = 9.0, 6.1 Hz, 2H), 4.15 (q, *J* = 4.2, 3.3 Hz, 1H), 3.26 (d, *J* = 6.3 Hz, 2H), 2.47 (s, 1H), 1.80 (dd, *J* = 11.7, 7.1 Hz, 3H), 1.72 (s, 3H), 1.68 (s, 3H), 1.47 (s, 3H), 1.44 (s, 3H), 1.29 (s, 3H), 1.24 (s, 3H).

^{13}C NMR (125 MHz, $CDCl_3$-*d*) δ 149.42, 138.62, 133.12, 132.00, 131.90, 131.35, 130.64, 129.71, 129.27, 128.19, 127.50, 126.92, 126.20, 123.52, 120.36, 110.04, 78.43, 76.35, 70.89, 58.94, 32.54, 27.44, 26.41, 25.92, 24.37, 18.07, 13.73.

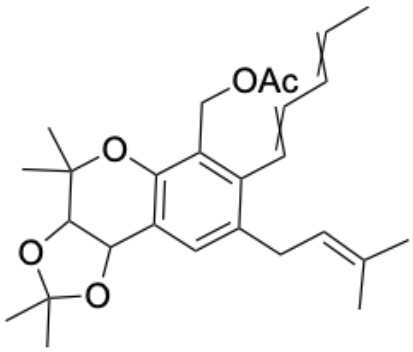

(2,2,4,4-tetramethyl-8-(3-methylbut-2-en-1-yl)-7-(penta-1,3-dien-1-yl)-3a,9b-dihydro-4H-[1,3]dioxolo[4,5-c]chromen-6-yl)methyl acetate

To a solution of (2,2,4,4-tetramethyl-8-(3-methylbut-2-en-1-yl)-7-(penta-1,3-dien-1-yl)-3a,9b-dihydro-4H-[1,3]dioxolo[4,5-c]chromen-6-yl)methanol (25 mg, 0.062 mmol) in dry CH_2Cl_2 (5 mL) was added triethylamine (83 mg, 0.628 mmol) followed by acetic anhydride (29 mg, 0.314 mmol) under nitrogen atmosphere at room temperature. The resulting mixture was stirred at room temperature for 30 min. After completion of the reaction (TLC analysis), saturated $NaHCO_3$ solution (4 mL) was added, the aqueous phase was separated and extracted with CH_2Cl_2 (2 x 10 mL). The combined organic extracts were dried over Na_2SO_4, filtered and concentrated. Purification of the residue by flash chromatography on SiO_2 (ethyl acetate:hexane=1:9) to afford pure product (22 mg, 81%).

^{1}H NMR (500 MHz, $CDCl_3$-*d*) δ 7.19 (d, *J* = 9.2 Hz, 1H), 6.62 – 6.31 (m, 2H), 6.23 – 6.14 (m, 1H), 5.79 – 5.53 (m, 1H), 5.21 (dd, *J* = 11.0, 6.9 Hz, 2H), 5.14 – 5.08 (m, 2H), 4.14 (dd, *J* = 6.4, 3.9 Hz, 1H), 3.26 (t, *J* = 6.8 Hz, 2H), 2.05 (d, *J* = 4.0 Hz, 3H), 1.83 – 1.73 (m, 3H), 1.72 (s, 3H), 1.68 (s, 3H), 1.44 (s, 3H), 1.40 (s, 3H), 1.27 (s, 3H), 1.25 (s, 3H). ^{13}C NMR (125 MHz, $CDCl_3$-*d*) δ 170.93, 150.12, 140.34, 136.12, 132.82, 132.10, 131.92, 131.07, 130.63, 130.47, 130.36, 129.73, 128.01, 127.44, 125.97, 123.41, 121.64, 120.67, 109.93, 78.53, 76.20, 70.98, 59.96, 32.47, 27.33, 26.26, 25.92, 24.50, 24.12, 21.23, 18.07, 13.58.

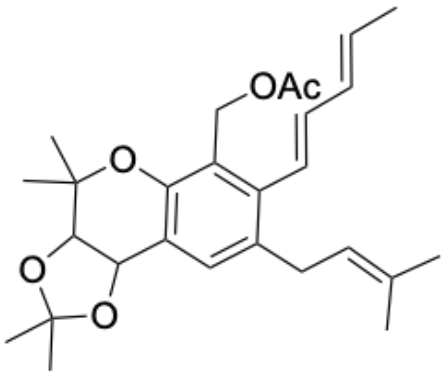

Iodine catalyzed isomerization of diene:

Iodine (1.26 mg, 0.005 mmol) was added to a solution of (2,2,4,4-tetramethyl-8-(3-methylbut-2-en-1-yl)-7-(penta-1,3-dien-1-yl)-3a,9b-dihydro-4H-[1,3]dioxolo[4,5-c]chromen-6-yl)methyl acetate (22 mg, 0.05 mmol) in toluene (2.5 mL) at room temperature. The resulting deep-red solution was warmed to 50 °C in an oil bath and was stirred at this temperature for 24 h. The reaction mixture was diluted with water (5 mL) and extracted with ethyl acetate (2 x 10 mL), and the combined organic phases were dried over anhydrous sodium sulfate and the filtrate was concentrated in vacuo. ^{1}H NMR analysis of the crude product mixture indicated the reversal of the EZ to EE ratio.

^{1}H NMR (500 MHz, $CDCl_3$-*d*) δ 7.18 (d, *J* = 9.2 Hz, 1H), 6.72 – 6.37 (m, 1H), 6.25 – 6.11 (m, 2H), 5.77 – 5.50 (m, 1H), 5.21 (dd, *J* = 11.0, 6.9 Hz, 2H), 5.16 – 5.04 (m, 2H), 4.17 – 4.09 (m, 1H), 3.26 (t, *J* = 6.4 Hz, 2H), 2.05 (s, 3H), 1.83 – 1.74 (m, 3H), 1.72 (s, 3H), 1.68 (s, 3H), 1.43 (s, 3H), 1.39 (s, 3H), 1.26 (s, 3H), 1.24 (s, 3H). ^{13}C NMR (125 MHz, $CDCl_3$-*d*) δ 171.04, 150.03, 140.25,

136.13, 132.81, 132.07, 131.92, 130.63, 130.36, 125.98, 123.41, 121.69, 120.55, 109.91, 78.55, 76.17, 71.00, 59.84, 32.36, 27.32, 26.27, 25.93, 24.48, 24.12, 21.17, 18.36, 18.10.

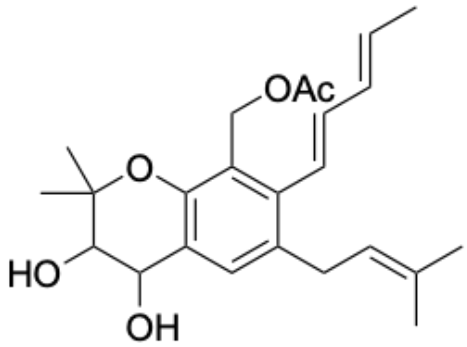

(3,4-dihydroxy-2,2-dimethyl-6-(3-methylbut-2-en-1-yl)-7-(penta-1,3-dien-1-yl)chroman-8-yl)methyl acetate

A solution of (2,2,4,4-tetramethyl-8-(3-methylbut-2-en-1-yl)-7-(penta-1,3-dien-1-yl)-3a,9b-dihydro-4H-[1,3]dioxolo[4,5-c]chromen-6-yl)methyl acetate (18 mg, 0.0409 mmol) in 60 % aqueous acetic acid (2 mL) was stirred for 6 h at 60 °C in oil bath. The reaction mixture was then concentrated in vacuo and purified by flash chromatography on SiO_2 (ethyl acetate:hexane=6:4) to afford pure product (13 mg, 79%).

^{1}H NMR (500 MHz, $CDCl_3$-*d*) δ 7.37 (d, *J* = 9.3 Hz, 1H), 6.60 – 6.38 (m, 1H), 6.25 – 6.13 (m, 2H), 5.80 – 5.56 (m, 1H), 5.19 (t, *J* = 7.0 Hz, 1H), 5.16 (d, *J* = 3.8 Hz, 2H), 4.77 (s, 1H), 3.69 (d, *J* = 3.8 Hz, 1H), 3.26 (d, *J* = 6.9 Hz, 2H), 2.69 (s, 1H), 2.14 (s, 1H), 2.04 (s, 3H), 1.78 (dd, *J* = 29.0, 6.9 Hz, 3H), 1.72 (s, 3H),

1.69 (s, 3H), 1.45 (s, 3H), 1.26 (s, 3H). ^{13}C NMR (125 MHz, $CDCl_3$-*d*) δ 171.05, 149.52, 140.35, 136.26, 132.89, 132.21, 131.82, 130.85, 129.68, 125.78, 123.26, 121.00, 120.94, 71.60, 65.44, 59.96, 25.93, 24.77, 23.64, 21.13, 18.37, 18.10.

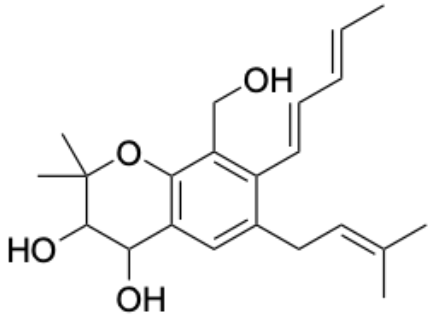

8-(hydroxymethyl)-2,2-dimethyl-6-(3-methylbut-2-en-1-yl)-7-(penta-1,3-dien-1-yl)chromane-3,4-diol

(3,4-dihydroxy-2,2-dimethyl-6-(3-methylbut-2-en-1-yl)-7-(penta-1,3-dien-1-yl)chroman-8-yl)methyl acetate (12 mg, 0.03 mmol) was then dissolved in 4 mL of THF:H_2O (3:2) and to it LiOH (1.5 mg, 0.036 mmol) was added and stirred at rt for 1h. Finally, the reaction was acidified with 1N HCl then diluted with water (5 mL) and extracted with ethyl acetate (10 mL x 2). The combined organic layers were washed with water, brine and dried over Na_2SO_4. The concentration of the organic layer in vacuo to obtain crude product (10 mg 93% crude yield). The crude product was further purified by HPLC.

^{1}H NMR (500 MHz, $CDCl_3$-*d*) δ 7.24 (s, 1H), 6.41 (d, *J* = 14.7 Hz, 1H), 6.31 – 6.17 (m, 2H), 5.79 (dq, *J* = 13.7, 6.7 Hz, 1H), 5.18 (t, *J* = 6.9 Hz, 1H), 4.73 (d,

J = 11.7 Hz, 2H), 4.65 (d, *J* = 11.6 Hz, 1H), 3.63 (s, 1H), 3.25 (qd, *J* = 15.5, 7.2 Hz, 2H), 2.74 (s, 1H), 2.54 (s, 1H), 1.81 (d, *J* = 6.7 Hz, 3H), 1.72 (s, 3H), 1.69 (s, 3H), 1.48 (s, 3H), 1.26 (s, 3H). ^{13}C NMR (125 MHz, $CDCl_3$-*d*) δ 149.12, 138.62, 136.27, 132.98, 132.08, 131.88, 130.80, 128.40, 126.05, 123.39, 120.71, 78.25, 71.48, 65.30, 58.74, 32.51, 25.94, 25.08, 23.76, 18.40, 18.12.

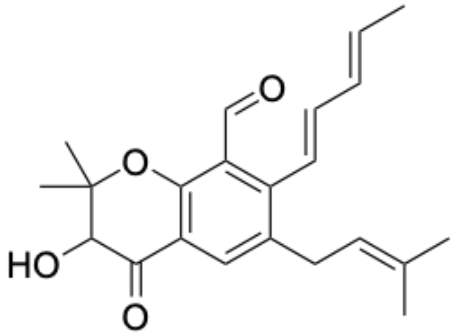

3-hydroxy-2,2-dimethyl-6-(3-methylbut-2-en-1-yl)-4-oxo-7-((1E,3E)-penta-1,3-dien-1-yl)chromane-8-carbaldehyde

To a solution of 8-(hydroxymethyl)-2,2-dimethyl-6-(3-methylbut-2-en-1-yl)-7-((1E,3E)-penta-1,3-dien-1-yl) chromane-3,4-diol (6 mg, 0.0167 mmol) in dry CH_2Cl_2 (5 mL) at 0 °C was added Dess–Martin periodinane (17 mg, 0.0402 mmol) under nitrogen atmosphere. The resulting mixture was stirred at room temperature for 3 h. After completion of the reaction (TLC analysis), saturated $NaHCO_3$ solution (4 mL) was added, the aqueous phase was separated and extracted with CH_2Cl_2 (2 x 10 mL). The combined organic extracts were dried over Na_2SO_4, filtered and concentrated. Purification of the residue by flash

chromatography on SiO_2 (ethyl acetate:hexane=2:8) to afford pure product (4 mg, 67%).

^{1}H NMR (800 MHz, $CDCl_3$-*d*) δ 10.17 (s, 1H), 7.79 (s, 1H), 6.68 (d, *J* = 15.6 Hz, 1H), 6.31 – 6.26 (m, 1H), 6.19 (dd, *J* = 15.6, 10.5 Hz, 1H), 5.88 (dq, *J* = 13.8, 6.8 Hz, 1H), 5.18 (t, *J* = 7.1 Hz, 1H), 4.45 (s, 1H), 3.32 (p, *J* = 8.8 Hz, 2H), 2.62 (s, 6H), 1.84 (d, *J* = 6.7 Hz, 3H), 1.75 (s, 3H), 1.70 (s, 6H), 1.23 (s, 3H). ^{13}C NMR (200 MHz, $CDCl_3$-*d*) δ 193.68, 190.44, 158.61, 148.63, 140.23, 134.24, 133.79, 133.64, 131.36, 130.94, 125.00, 124.64, 122.01, 117.60, 84.78, 41.19, 31.52, 26.88, 25.92, 18.57, 18.16, 17.55.

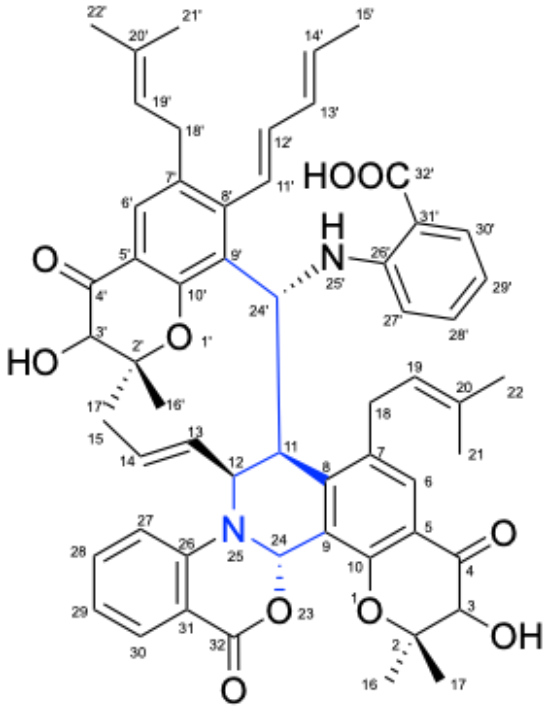

Oxazinin A (1)

Synthesis of oxazinin A

3-hydroxy-2,2-dimethyl-6-(3-methylbut-2-en-1-yl)-4-oxo-7-((1E,3E)-penta-1,3-dien-1-yl) chromane-8-carbaldehyde (3 mg, 0.008 mmol) was taken in MeOH and anthranilic acid (1.04 mg, 0.007 mmol) was added and stirred for three days. After completion of the reaction (via tlc) it was purified by HPLC to afford pure 1 mg of the product.

2.6 References

(1) Tuberculosis https://www.who.int/news-room/fact-sheets/detail/tuberculosis (accessed 2022 -01 -18).

(2) Dragotakes, Q.; Stouffer, K. M.; Fu, M. S.; Sella, Y.; Youn, C.; Yoon, O. I.; De Leon-Rodriguez, C. M.; Freij, J. B.; Bergman, A.; Casadevall, A. Macrophages Use a Bet-Hedging Strategy for Antimicrobial Activity in Phagolysosomal Acidification. *J. Clin. Invest.* **2020**, *130* (7), 3805–3819.

(3) Delogu, G.; Sali, M.; Fadda, G. The Biology of Mycobacterium Tuberculosis Infection. *Mediterr. J. Hematol. Infect. Dis.* **2013**, *5* (1). https://doi.org/10.4084/MJHID.2013.070.

(4) Maitra, A.; Munshi, T.; Healy, J.; Martin, L. T.; Vollmer, W.; Keep, N. H.; Bhakta, S. Cell Wall Peptidoglycan in Mycobacterium Tuberculosis: An Achilles'

Heel for the TB-Causing Pathogen. *FEMS Microbiology Reviews*. 2019, pp 548–575. https://doi.org/10.1093/femsre/fuz016.

(5) Kieser, K. J. *Spatiotemporal Control of Mycobacterium Tuberculosis Cell Wall Biogenesis by the Peptidoglycan Synthase PonA1*; 2015.

(6) Treating and Managing Tuberculosis https://www.lung.org/lung-health-diseases/lung-disease-lookup/tuberculosis/treating-and-managing#:~:text=If%20you%20have%20an%20active,%E2%80%94rifampin%2C%20pyrazinamide%20and%20ethambutol. (accessed 2022 -01 -25).

(7) Unissa, A. N.; Subbian, S.; Hanna, L. E.; Selvakumar, N. Overview on Mechanisms of Isoniazid Action and Resistance in Mycobacterium Tuberculosis. *Infect. Genet. Evol.* **2016**, *45*, 474–492.

(8) Heifets, L. B. Antimycobacterial Drugs. *Semin. Respir. Infect.* **1994**, *9* (2), 84–103.

(9) Sensi, P. History of the Development of Rifampin. *Rev. Infect. Dis.* **1983**, *5 Suppl 3*, S402–S406.

(10) Wehrli, W. Rifampin: Mechanisms of Action and Resistance. *Clinical Infectious Diseases*. 1983, pp S407–S411. https://doi.org/10.1093/clinids/5.supplement_3.s407.

(11) Chakraborty, S.; Rhee, K. Y. Tuberculosis Drug Development: History and Evolution of the Mechanism-Based Paradigm. *Cold Spring Harb. Perspect. Med.* **2015**, *5* (8), a021147.

(12) Takiff, H.; Guerrero, E. Current Prospects for the Fluoroquinolones as First-Line Tuberculosis Therapy. *Antimicrob. Agents Chemother.* **2011**, *55* (12), 5421–5429.

(13) Bouza, E.; Garcia-Garrote, F.; Cercenado, E.; Marin, M.; Diaz, M. S. Pseudomonas Aeruginosa: A Survey of Resistance in 136 Hospitals in Spain. The Spanish Pseudomonas Aeruginosa Study Group. *Antimicrob. Agents Chemother.* **1999**, *43* (4), 981–982.

(14) Takiff, H. E.; Salazar, L.; Guerrero, C.; Philipp, W.; Huang, W. M.; Kreiswirth, B.; Cole, S. T.; Jacobs, W. R., Jr; Telenti, A. Cloning and Nucleotide Sequence of Mycobacterium Tuberculosis gyrA and gyrB Genes and Detection of Quinolone Resistance Mutations. *Antimicrob. Agents Chemother.* **1994**, *38* (4), 773–780.

(15) Hooper, D. C. Mechanisms of Action of Antimicrobials: Focus on Fluoroquinolones. *Clin. Infect. Dis.* **2001**, *32 Suppl 1*, S9–S15.

(16) Kotra, L. P.; Haddad, J.; Mobashery, S. Aminoglycosides: Perspectives on Mechanisms of Action and Resistance and Strategies to Counter Resistance. *Antimicrob. Agents Chemother.* **2000**, *44* (12), 3249–3256.

(17) Shinabarger, D. Mechanism of Action of the Oxazolidinone Antibacterial Agents. *Expert Opinion on Investigational Drugs*. 1999, pp 1195–1202. https://doi.org/10.1517/13543784.8.8.1195.

(18) Sarathy, J. P.; Gruber, G.; Dick, T. Re-Understanding the Mechanisms of Action of the Anti-Mycobacterial Drug Bedaquiline. *Antibiotics (Basel)* **2019**, *8* (4). https://doi.org/10.3390/antibiotics8040261.

(19) Khoshnood, S.; Taki, E.; Sadeghifard, N.; Kaviar, V. H.; Haddadi, M. H.; Farshadzadeh, Z.; Kouhsari, E.; Goudarzi, M.; Heidary, M. Mechanism of Action, Resistance, Synergism, and Clinical Implications of Delamanid Against Multidrug-Resistant Mycobacterium Tuberculosis. *Frontiers in Microbiology*. 2021. https://doi.org/10.3389/fmicb.2021.717045.

(20) CDCTB. Drug-Resistant TB https://www.cdc.gov/tb/topic/drtb/default.htm (accessed 2022 -01 -27).

(21) Schiebler, M.; Brown, K.; Hegyi, K.; Newton, S. M.; Renna, M.; Hepburn, L.; Klapholz, C.; Coulter, S.; Obregón-Henao, A.; Henao Tamayo, M.; Basaraba, R.; Kampmann, B.; Henry, K. M.; Burgon, J.; Renshaw, S. A.; Fleming, A.; Kay, R. R.; Anderson, K. E.; Hawkins, P. T.; Ordway, D. J.; Rubinsztein, D. C.; Floto, R. A. Functional Drug Screening Reveals Anticonvulsants as Enhancers of mTOR-Independent Autophagic Killing of Mycobacterium Tuberculosis through Inositol Depletion. *EMBO Mol. Med.* **2015**, *7* (2), 127–139.

(22) Lin, Z.; Koch, M.; Abdel Aziz, M. H.; Galindo-Murillo, R.; Tianero, M. D.; Cheatham, T. E.; Barrows, L. R.; Reilly, C. A.; Schmidt, E. W. Oxazinin A, a Pseudodimeric Natural Product of Mixed Biosynthetic Origin from a Filamentous Fungus. *Org. Lett.* **2014**, *16* (18), 4774–4777.

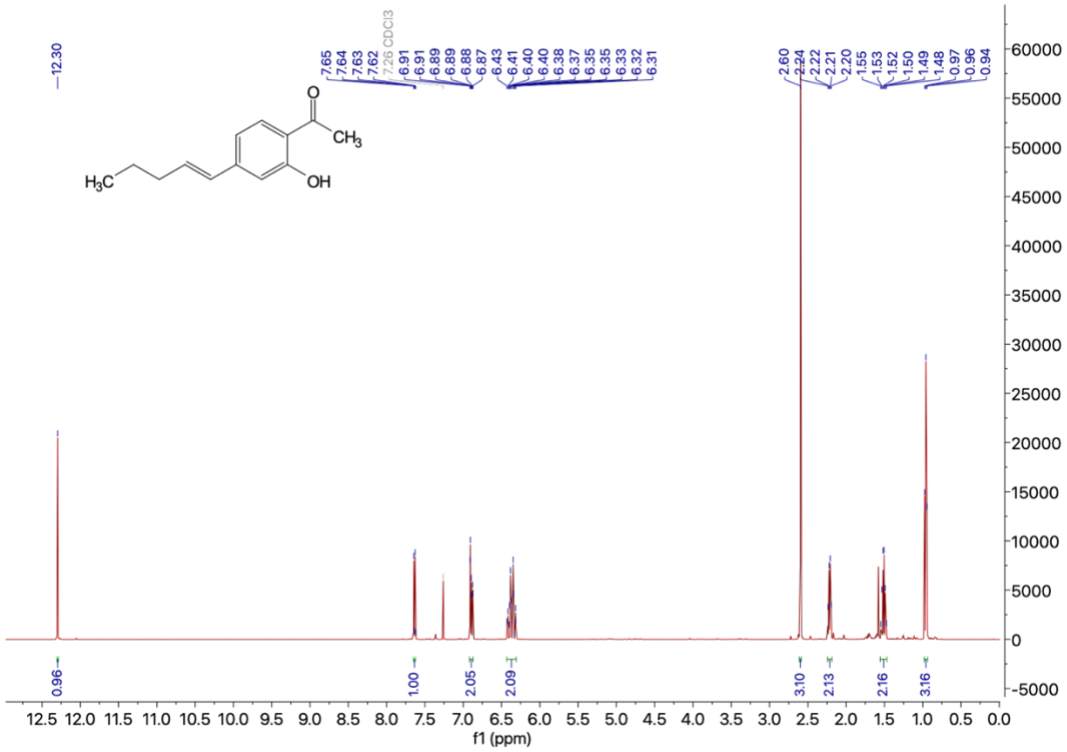
12.30
7.65
7.64
7.63
7.62
7.26 CDCl3
6.91
6.89
6.89
6.88
6.87
6.43
6.41
6.40
6.40
6.38
6.37
6.35
6.35
6.33
6.32
6.31
2.60
2.24
2.22
2.21
2.20
1.55
1.53
1.52
1.50
1.49
1.48
0.97
0.96
0.94
O
CH3
H3C
OH
0.96
1.00
2.05
2.09
3.10
2.13
2.16
3.16
f1 (ppm)

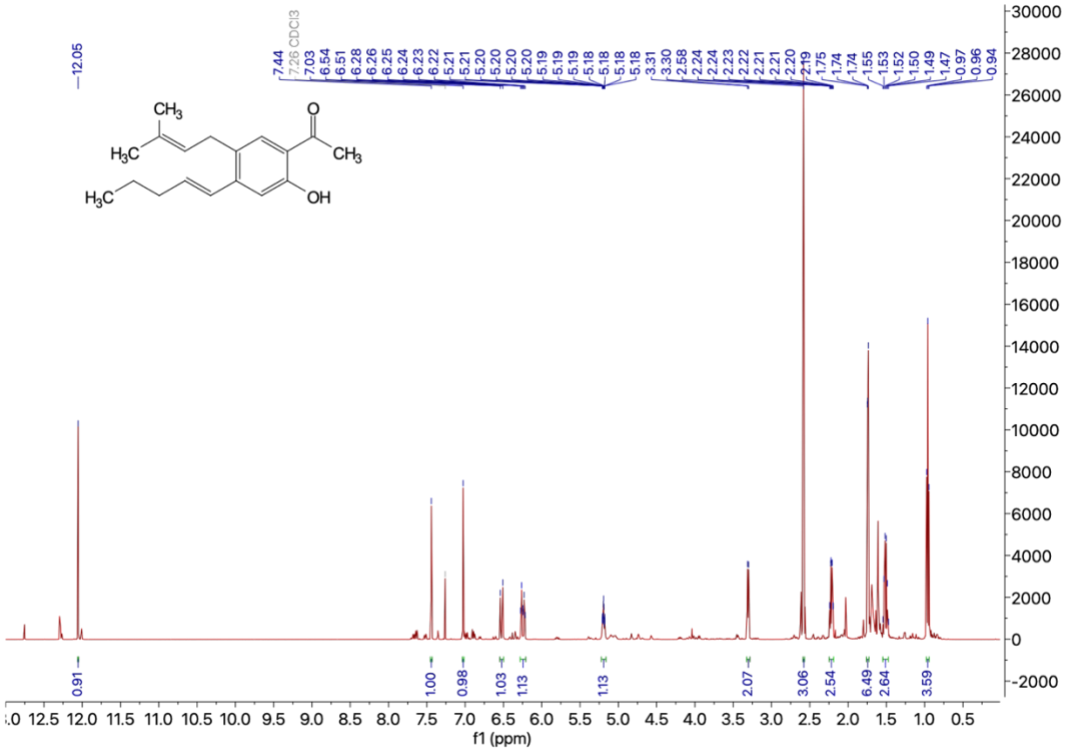
12.05
7.44
7.26 CDCl3
7.03
6.54
6.51
6.28
6.26
6.25
6.24
6.23
6.22
5.21
5.21
5.20
5.20
5.20
5.20
5.19
5.19
5.19
5.18
5.18
5.18
3.31
3.30
2.58
2.24
2.24
2.23
2.22
2.21
2.21
2.20
2.19
1.75
1.74
1.74
1.55
1.53
1.52
1.50
1.49
1.47
0.97
0.96
0.94
CH3
H3C
O
CH3
H3C
OH
0.91
1.00
0.98
1.03
1.13
1.13
2.07
3.06
2.54
6.49
2.64
3.59
f1 (ppm)

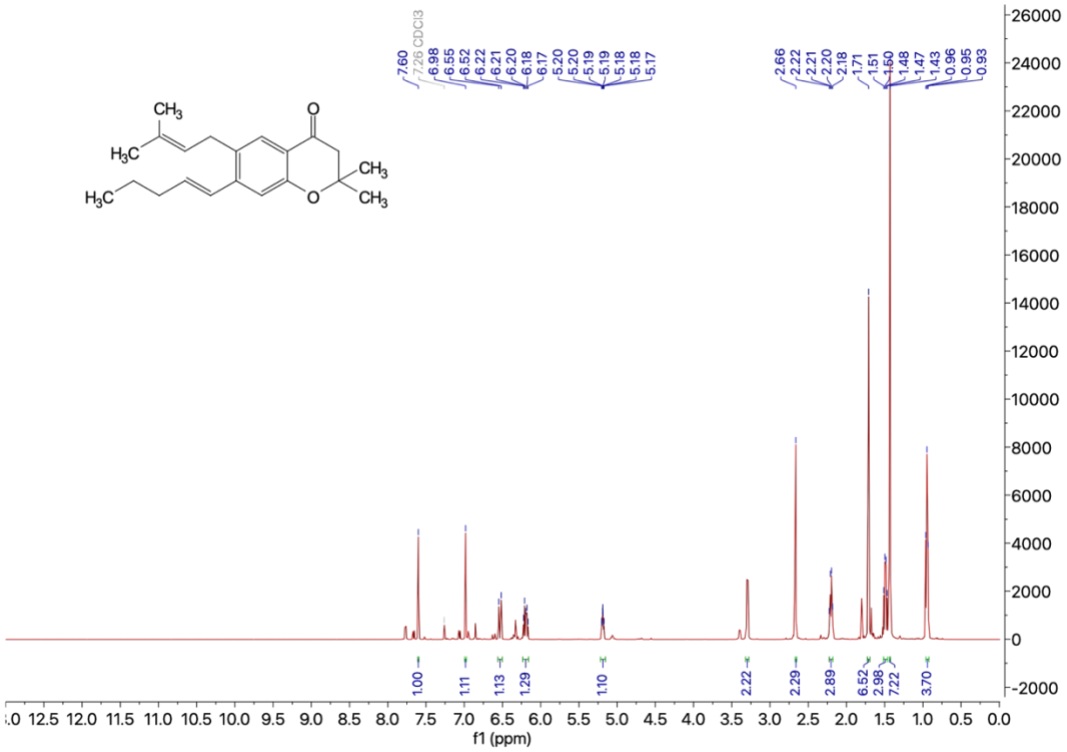
7.60
7.26 CDCl3
6.98
6.55
6.52
6.22
6.21
6.20
6.18
6.17
5.20
5.20
5.19
5.19
5.18
5.18
5.17
2.66
2.22
2.21
2.20
2.18
1.71
1.51
1.50
1.48
1.47
1.43
0.96
0.95
0.93
CH3
H3C
O
CH3
H3C
O
CH3
1.00
1.11
1.13
1.29
1.10
2.22
2.29
2.89
6.52
2.98
7.22
3.70
f1 (ppm)

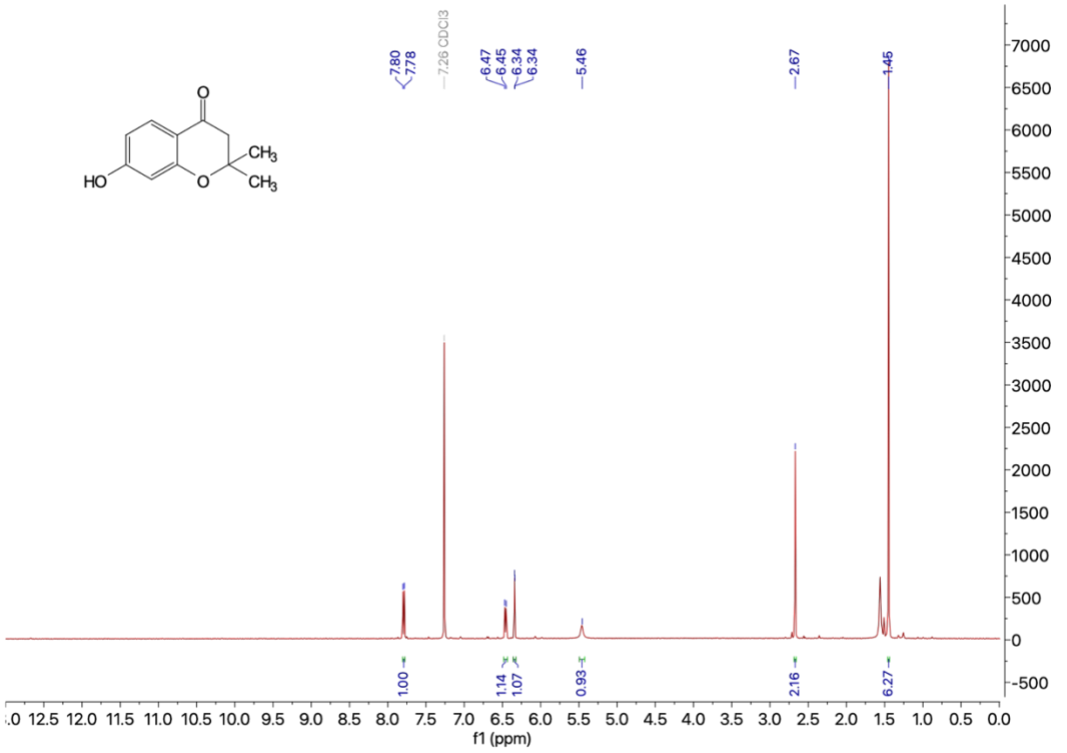
7.80
7.78
7.26 CDCl3
6.47
6.45
6.34
6.34
5.46
2.67
1.45
O
CH3
HO
O
CH3
1.00
1.14
1.07
0.93
2.16
6.27
f1 (ppm)

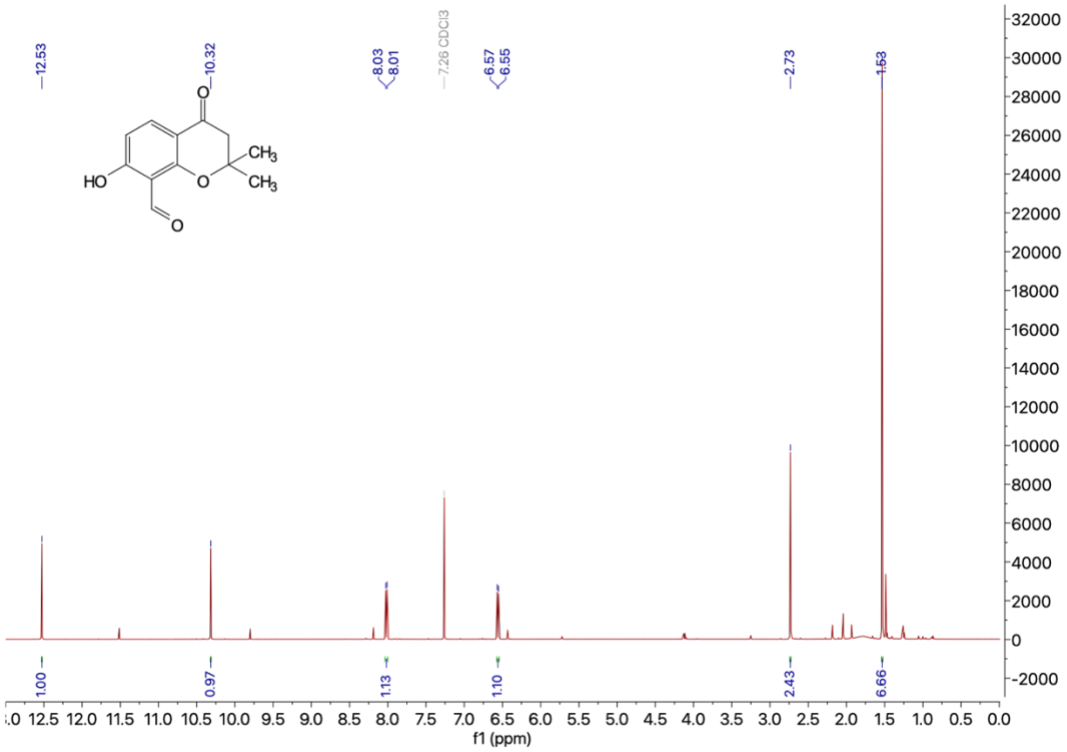
12.53
10.32
8.03
8.01
7.26 CDCl3
6.57
6.55
2.73
1.53
HO
O
CH3
CH3
1.00
0.97
1.13
1.10
2.43
6.66
f1 (ppm)

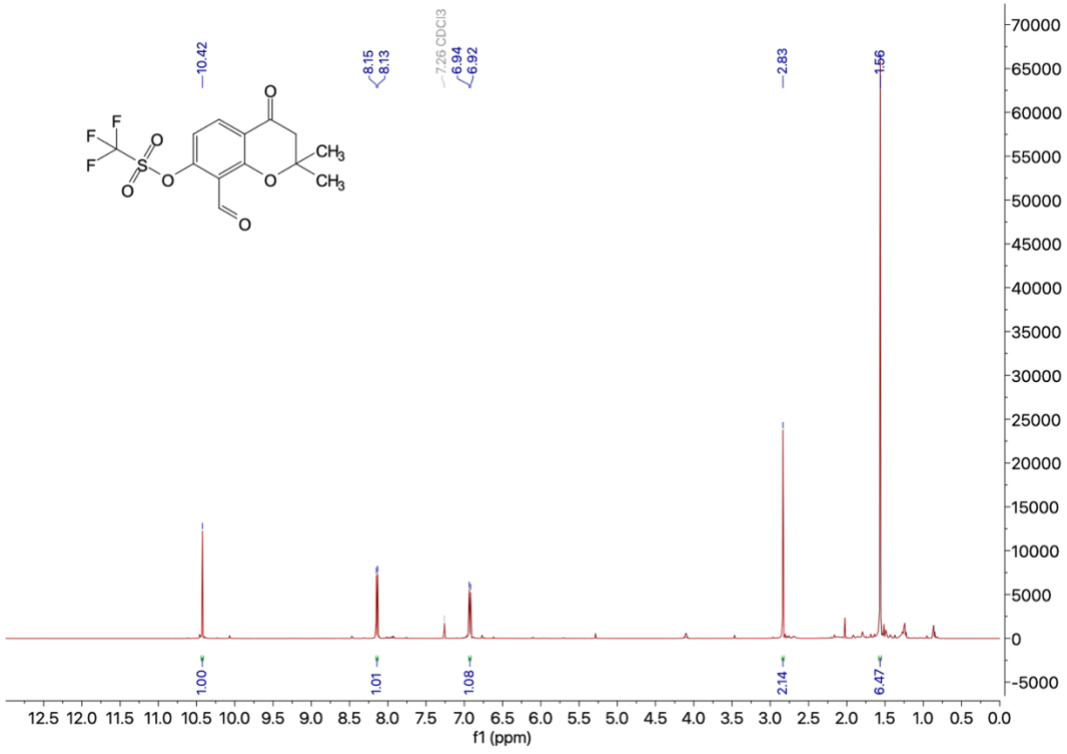
10.42
8.15
8.13
7.26 CDCl3
6.94
6.92
2.83
1.56
F
F
F
S
O
CH3
CH3
1.00
1.01
1.08
2.14
6.47
f1 (ppm)

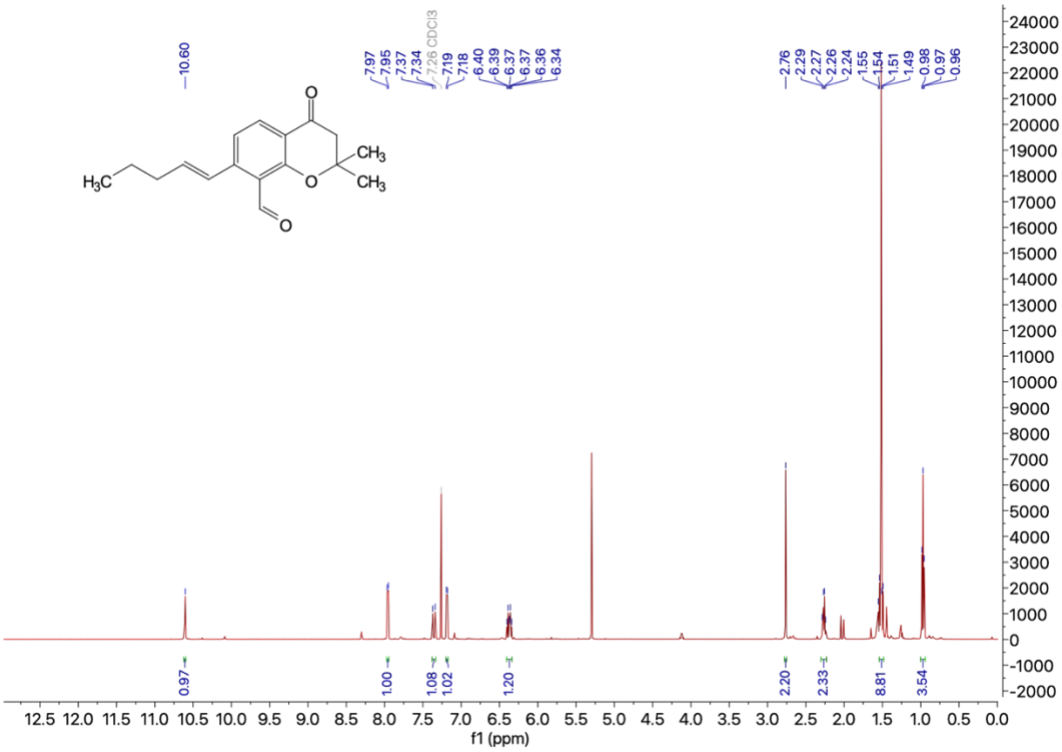
10.60
7.97
7.95
7.37
7.34
7.26 CDCl3
7.19
7.18
6.40
6.39
6.37
6.37
6.36
6.34
2.76
2.29
2.27
2.26
2.24
1.55
1.54
1.51
1.49
0.98
0.97
0.96
O
CH3
H3C
O
CH3
O
0.97
1.00
1.08
1.02
1.20
2.20
2.33
8.81
3.54
f1 (ppm)

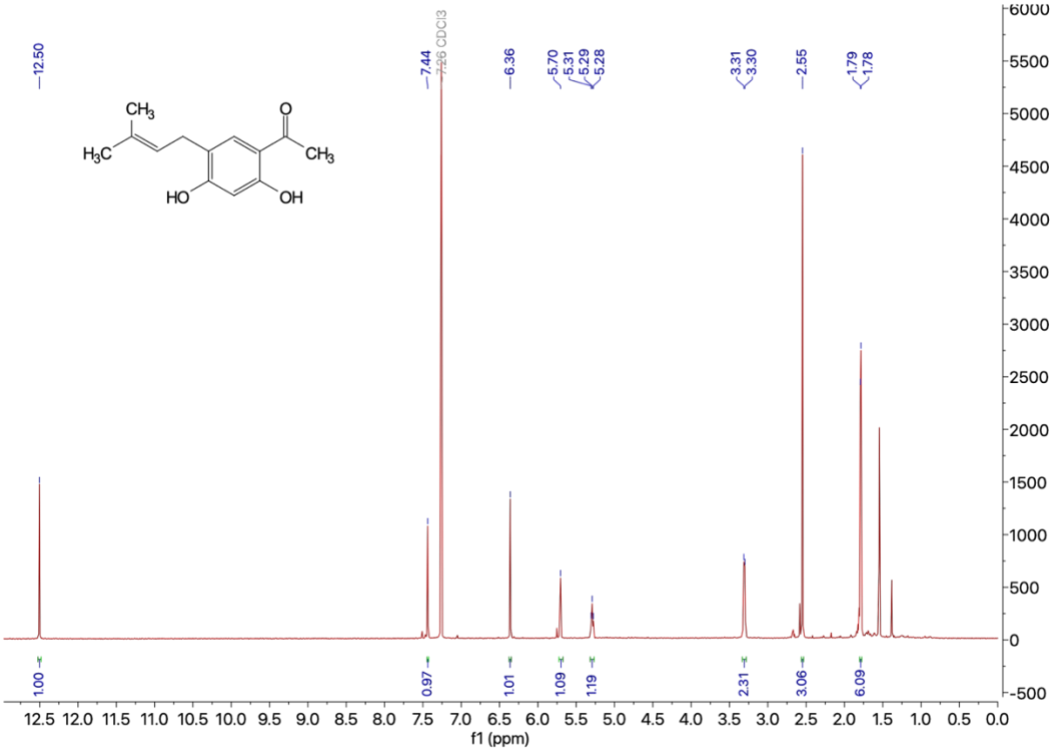
12.50
7.44
7.26 CDCl3
6.36
5.70
5.31
5.29
5.28
3.31
3.30
2.55
1.79
1.78
CH3
O
H3C
CH3
HO
OH
1.00
0.97
1.01
1.09
1.19
2.31
3.06
6.09
f1 (ppm)

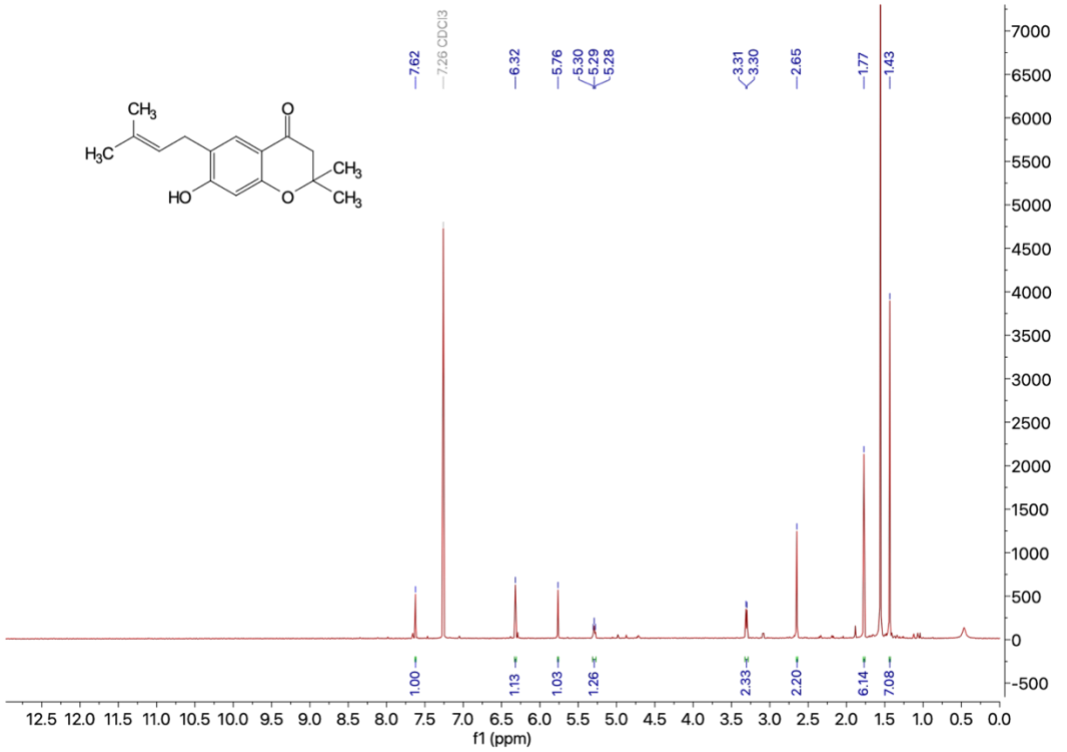
7.62
7.26 CDCl3
6.32
5.76
5.30
5.29
5.28
3.31
3.30
2.65
1.77
1.43
1.00
1.13
1.03
1.26
2.33
2.20
6.14
7.08
f1 (ppm)

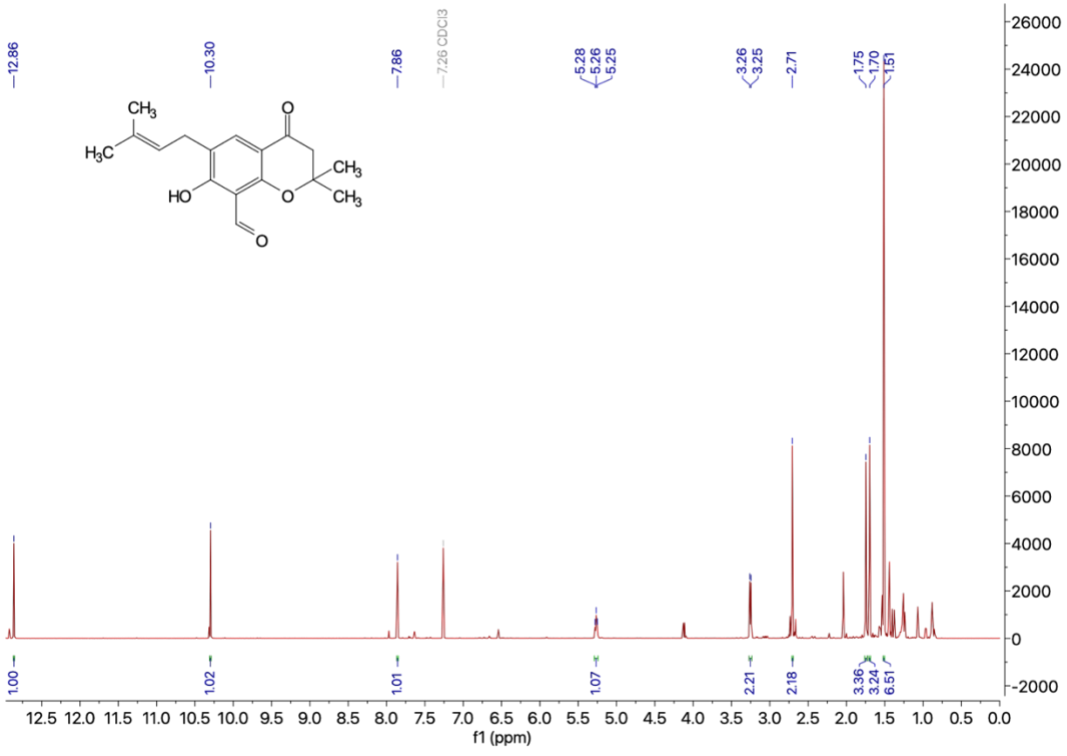
12.86
10.30
7.86
7.26 CDCl3
5.28
5.26
5.25
3.26
3.25
2.71
1.75
1.70
1.51
1.00
1.02
1.01
1.07
2.21
2.18
3.36
3.24
6.51
f1 (ppm)

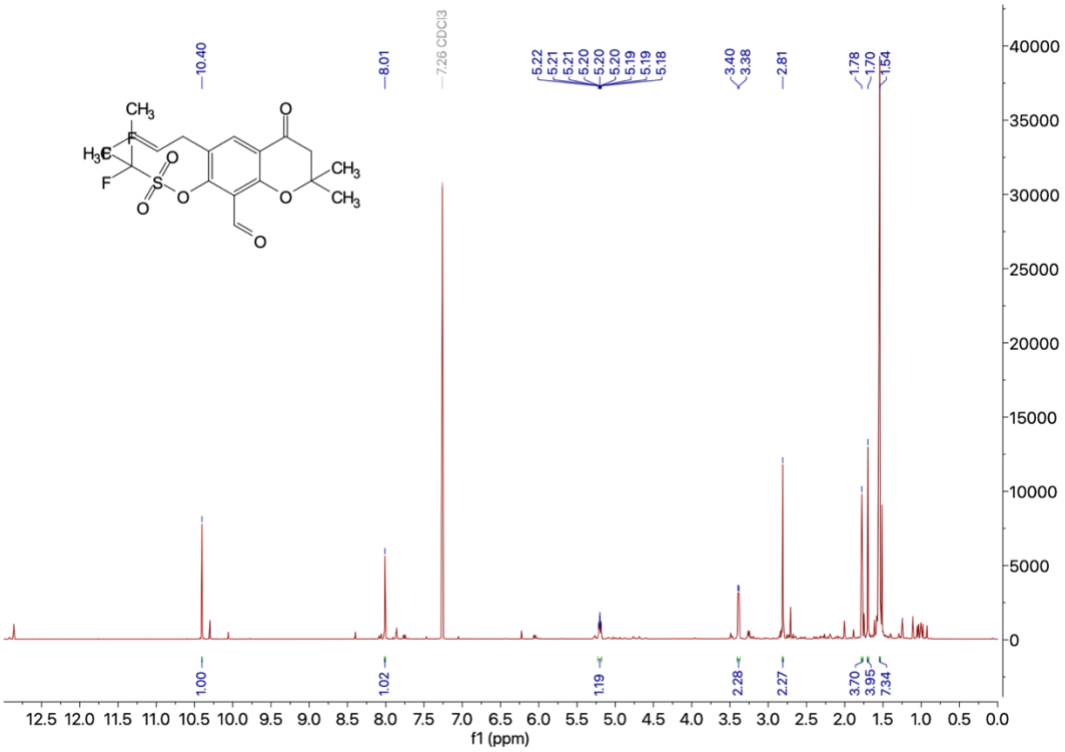
10.40
8.01
7.26 CDCl3
5.22
5.21
5.21
5.20
5.20
5.20
5.19
5.19
5.18
3.40
3.38
2.81
1.78
1.70
1.54
1.00
1.02
1.19
2.28
2.27
3.70
3.95
7.34
f1 (ppm)

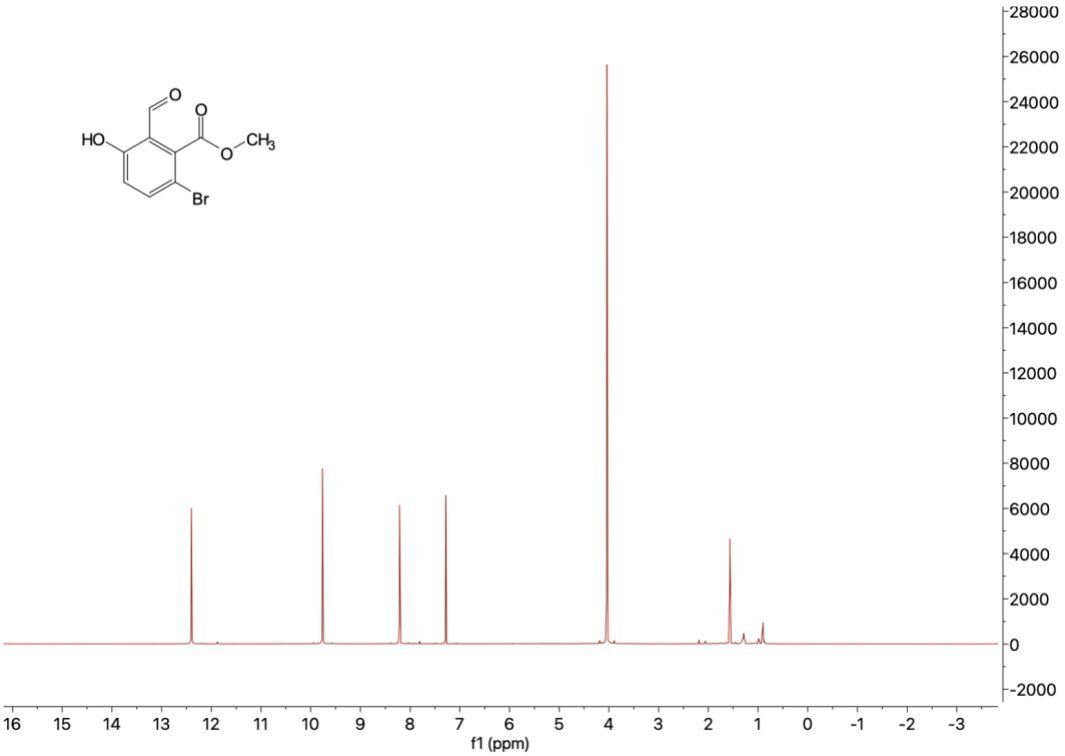
f1 (ppm)

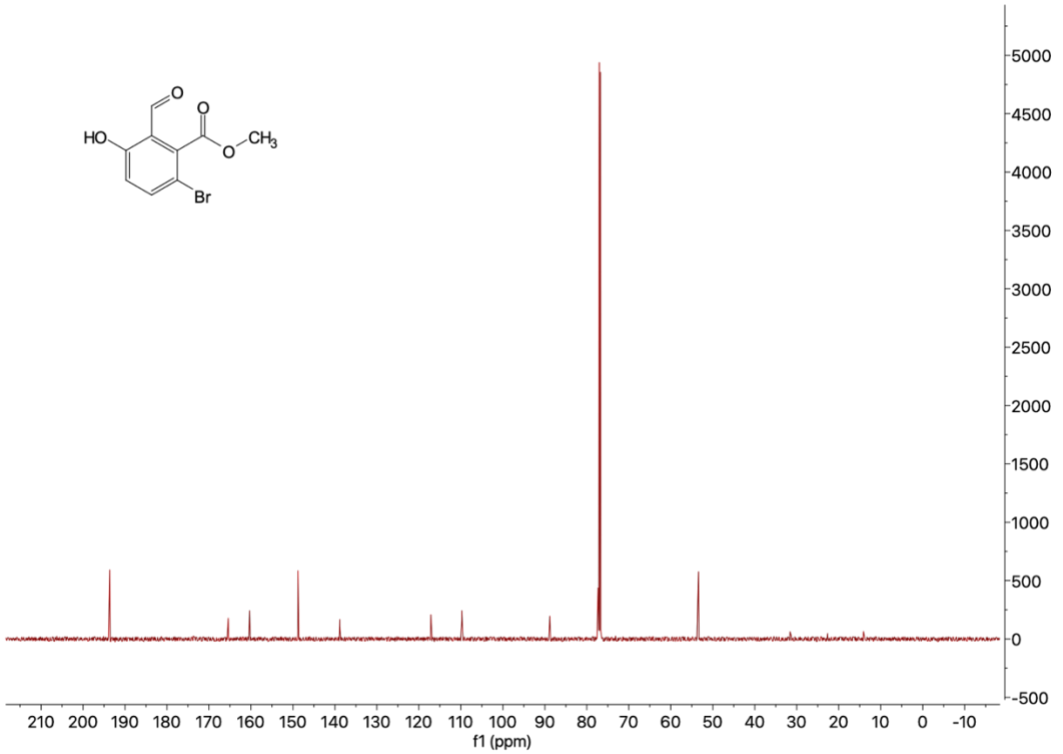
HO
O
O
O
CH3
Br
5000
4500
4000
3500
3000
2500
2000
1500
1000
500
0
-500
210 200 190 180 170 160 150 140 130 120 110 100 90 80 70 60 50 40 30 20 10 0 -10
f1 (ppm)

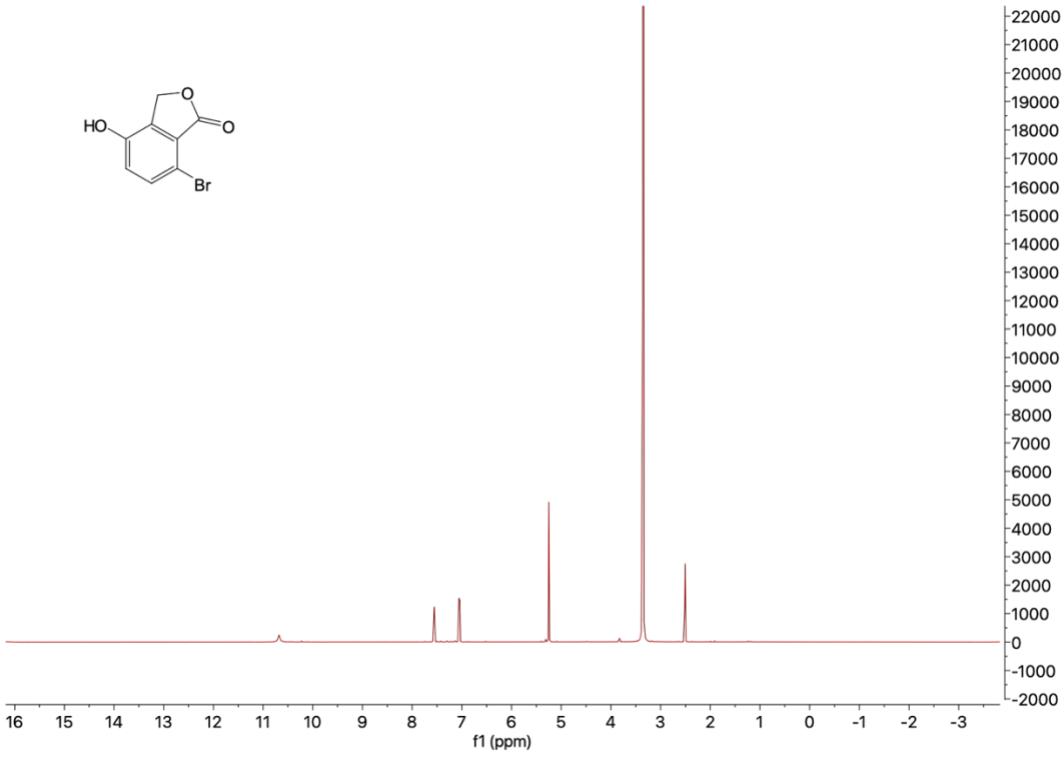
HO
O
O
Br
22000
21000
20000
19000
18000
17000
16000
15000
14000
13000
12000
11000
10000
9000
8000
7000
6000
5000
4000
3000
2000
1000
0
-1000
-2000
16 15 14 13 12 11 10 9 8 7 6 5 4 3 2 1 0 -1 -2 -3
f1 (ppm)

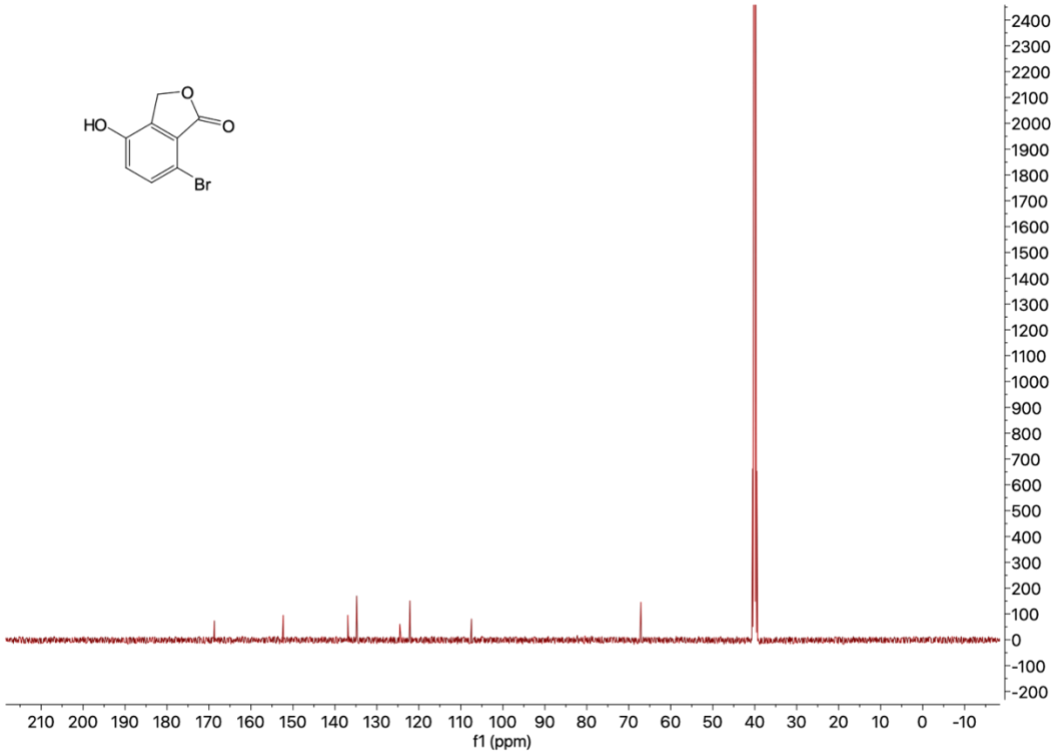
HO
O
O
Br
2400
2300
2200
2100
2000
1900
1800
1700
1600
1500
1400
1300
1200
1100
1000
900
800
700
600
500
400
300
200
100
0
-100
-200
210 200 190 180 170 160 150 140 130 120 110 100 90 80 70 60 50 40 30 20 10 0 -10
f1 (ppm)

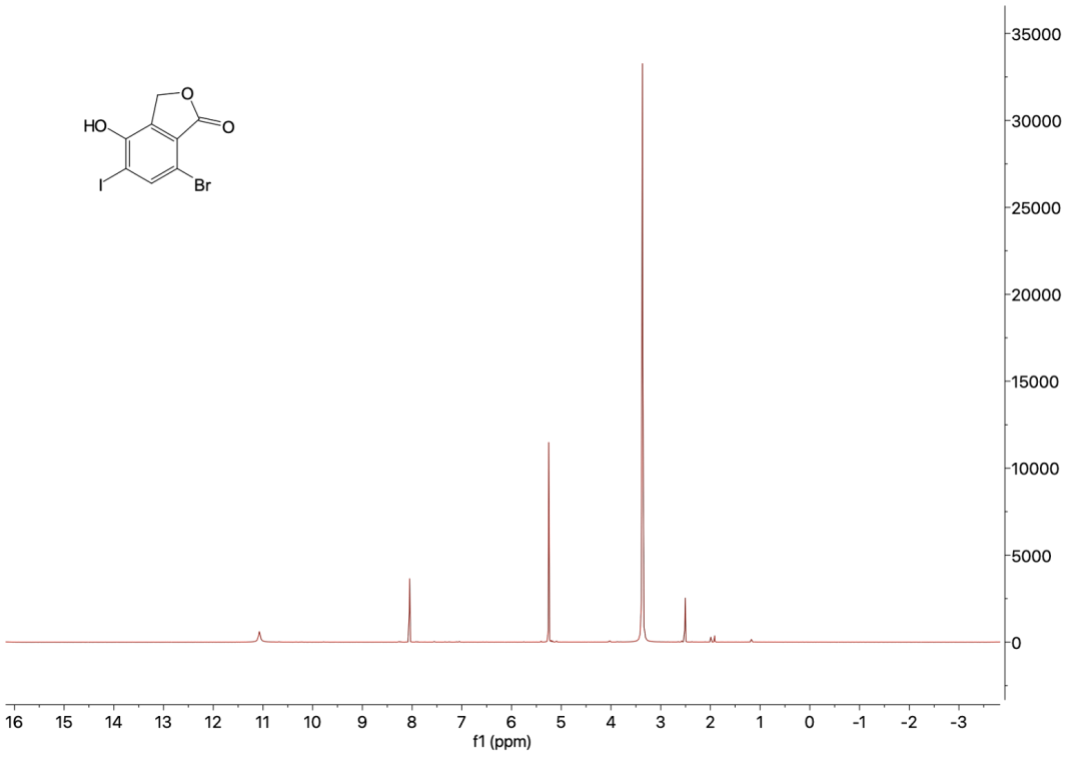
HO
O
O
I
Br
35000
30000
25000
20000
15000
10000
5000
0
16 15 14 13 12 11 10 9 8 7 6 5 4 3 2 1 0 -1 -2 -3
f1 (ppm)

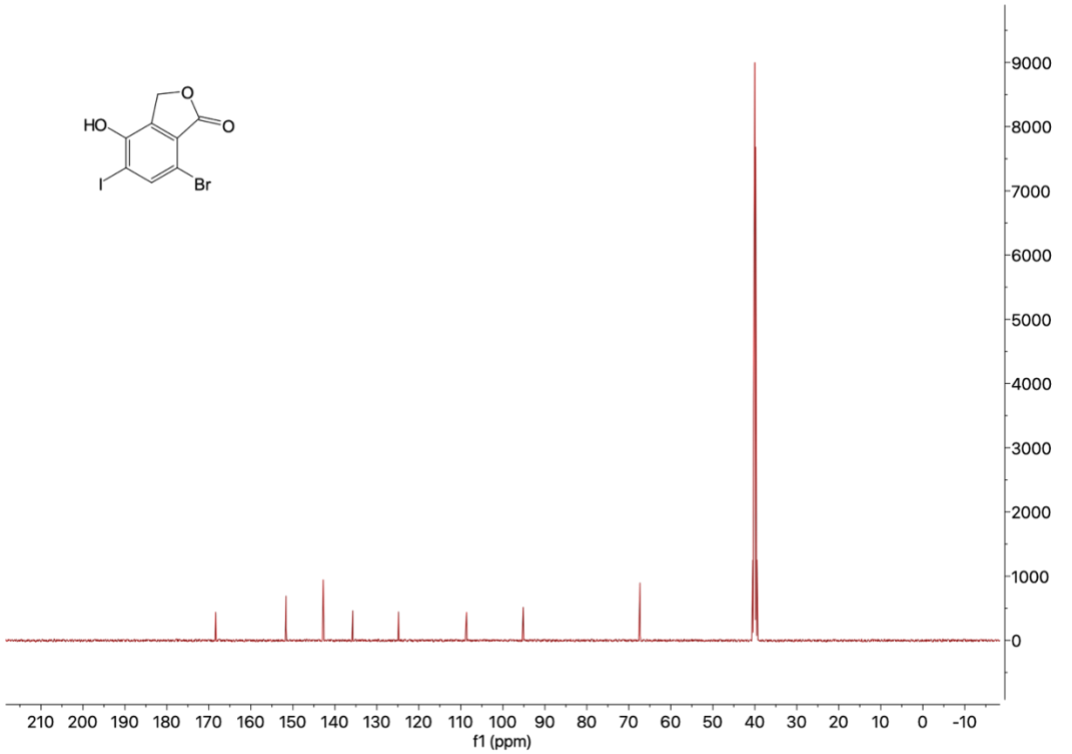
HO
O
O
I
Br
9000
8000
7000
6000
5000
4000
3000
2000
1000
0
210 200 190 180 170 160 150 140 130 120 110 100 90 80 70 60 50 40 30 20 10 0 -10
f1 (ppm)

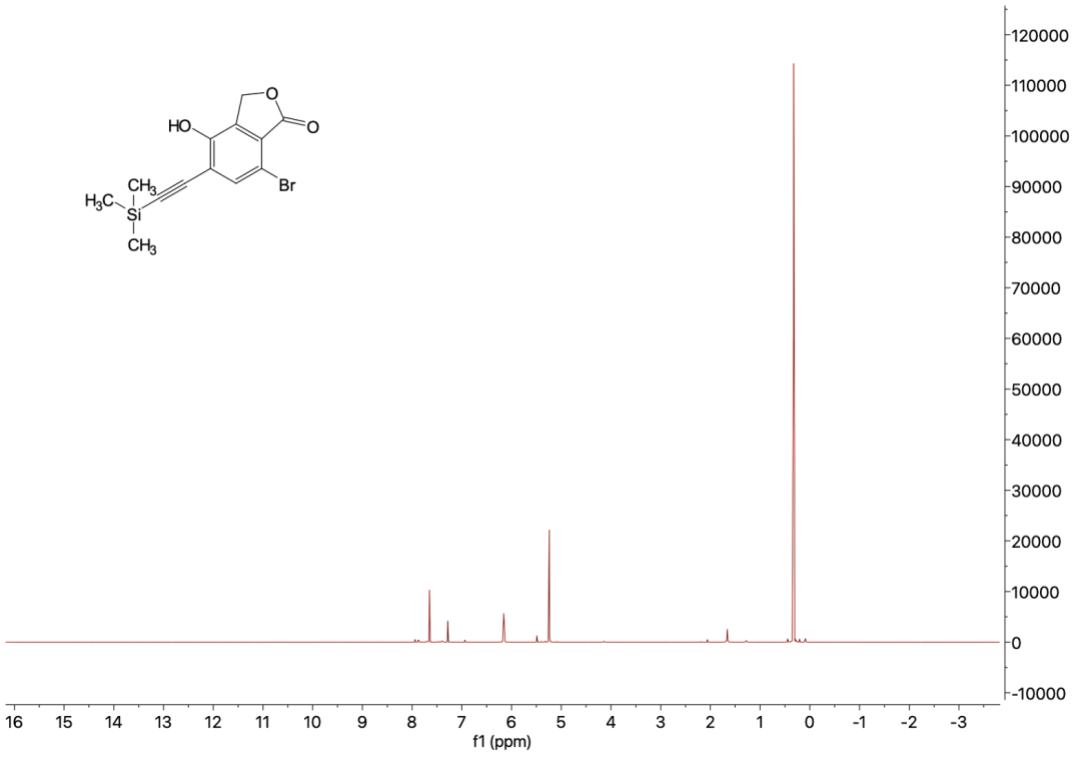
HO
O
O
Br
CH3
H3C
Si
CH3
120000
110000
100000
90000
80000
70000
60000
50000
40000
30000
20000
10000
0
-10000
16 15 14 13 12 11 10 9 8 7 6 5 4 3 2 1 0 -1 -2 -3
f1 (ppm)

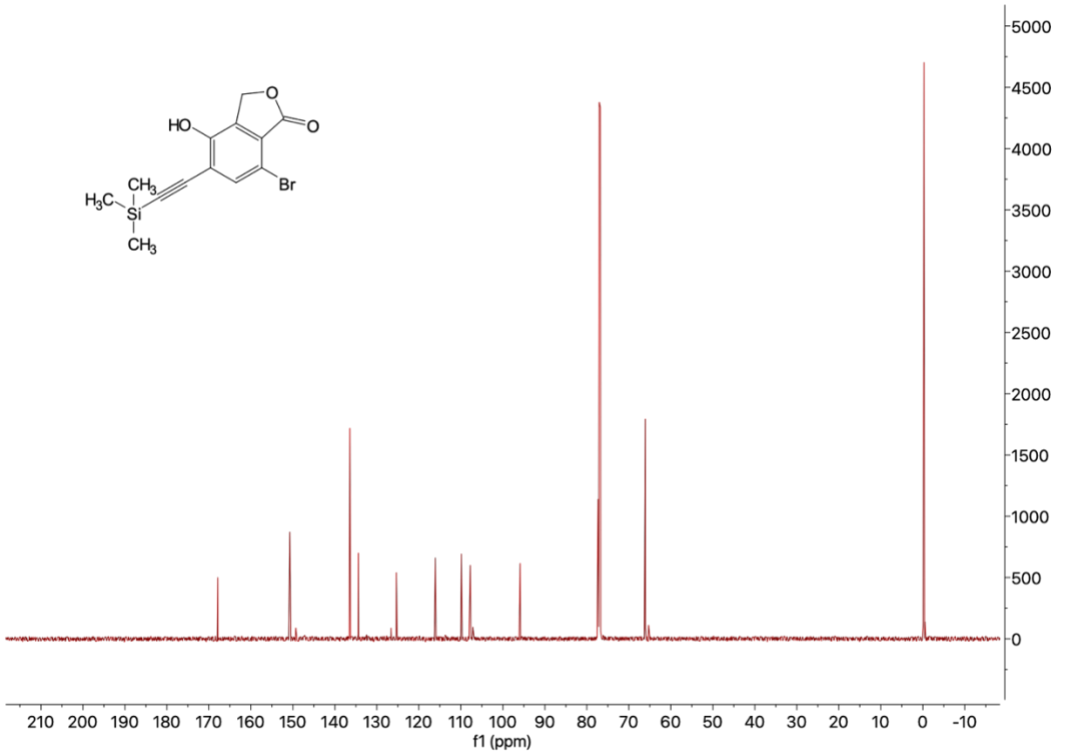
HO
O
O
Br
CH3
H3C
Si
CH3
5000
4500
4000
3500
3000
2500
2000
1500
1000
500
0
210 200 190 180 170 160 150 140 130 120 110 100 90 80 70 60 50 40 30 20 10 0 -10
f1 (ppm)

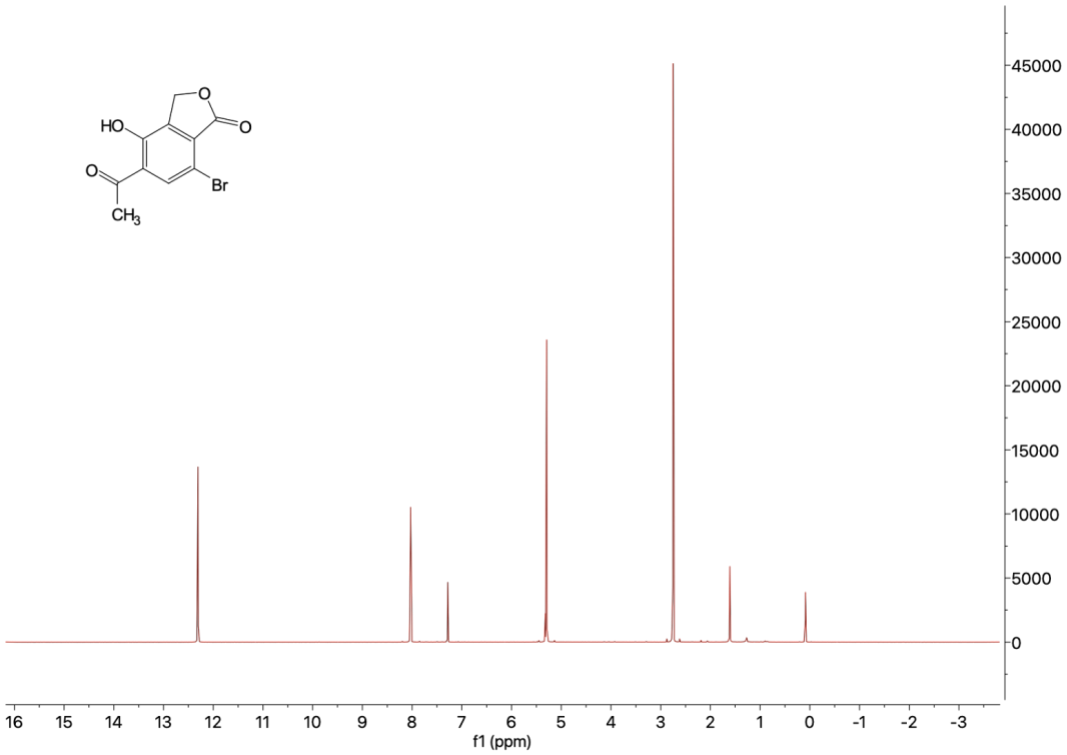
HO
O
O
O
Br
CH3
45000
40000
35000
30000
25000
20000
15000
10000
5000
0
16 15 14 13 12 11 10 9 8 7 6 5 4 3 2 1 0 -1 -2 -3
f1 (ppm)

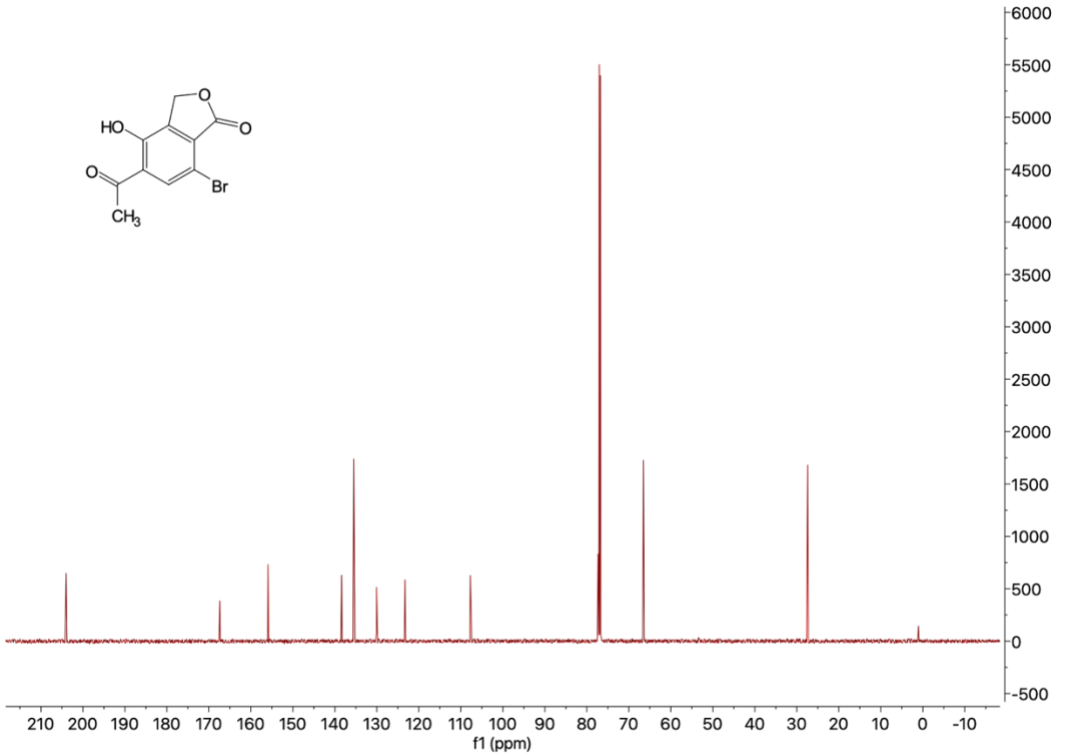
HO
O
O
O
Br
CH3
6000
5500
5000
4500
4000
3500
3000
2500
2000
1500
1000
500
0
-500
210 200 190 180 170 160 150 140 130 120 110 100 90 80 70 60 50 40 30 20 10 0 -10
f1 (ppm)

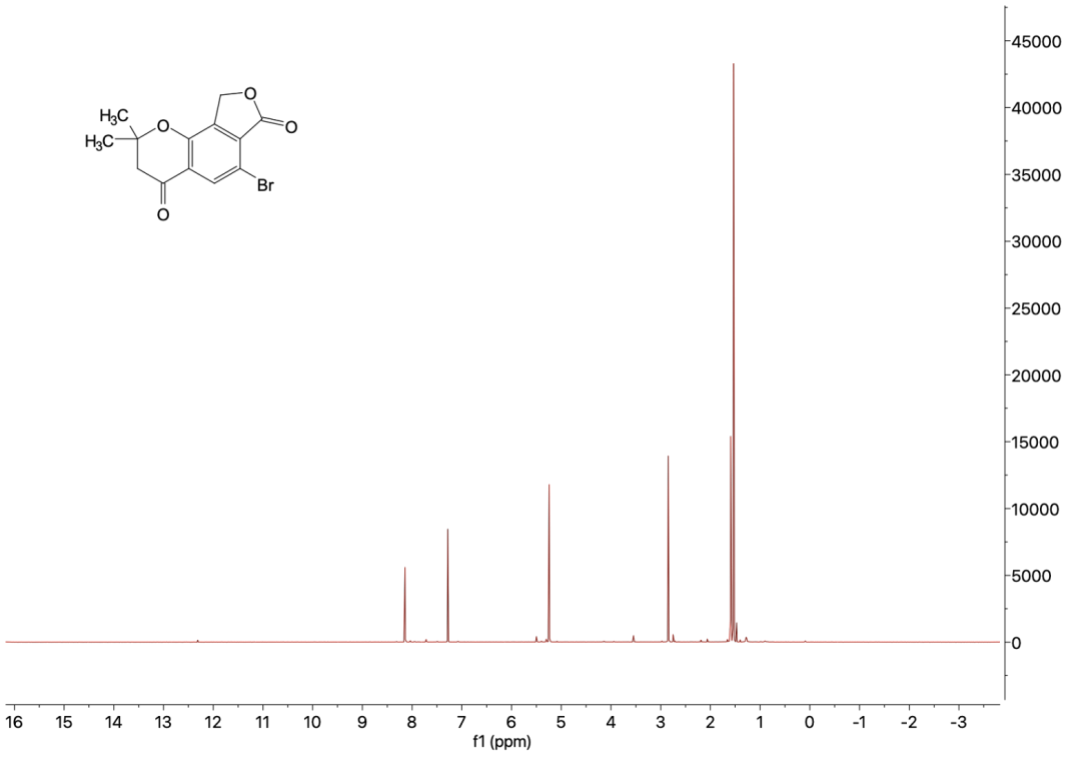
H3C
H3C
O
O
O
Br
45000
40000
35000
30000
25000
20000
15000
10000
5000
0
16 15 14 13 12 11 10 9 8 7 6 5 4 3 2 1 0 -1 -2 -3
f1 (ppm)

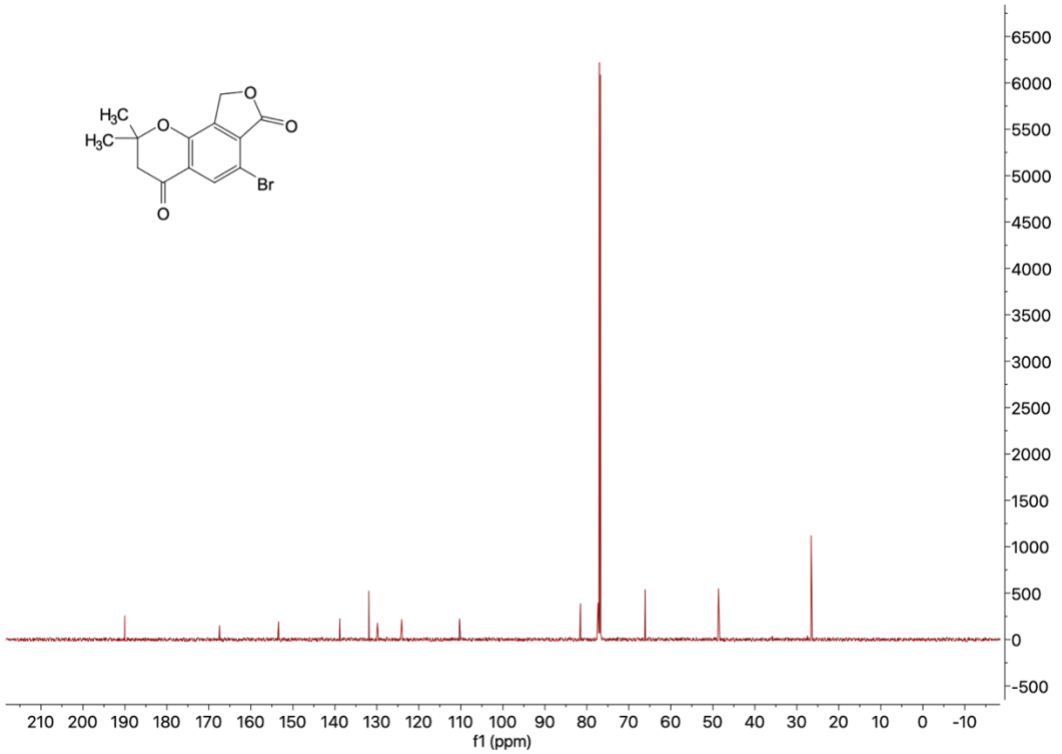
H3C
H3C
O
O
O
Br
O
6500
6000
5500
5000
4500
4000
3500
3000
2500
2000
1500
1000
500
0
-500
210 200 190 180 170 160 150 140 130 120 110 100 90 80 70 60 50 40 30 20 10 0 -10
f1 (ppm)

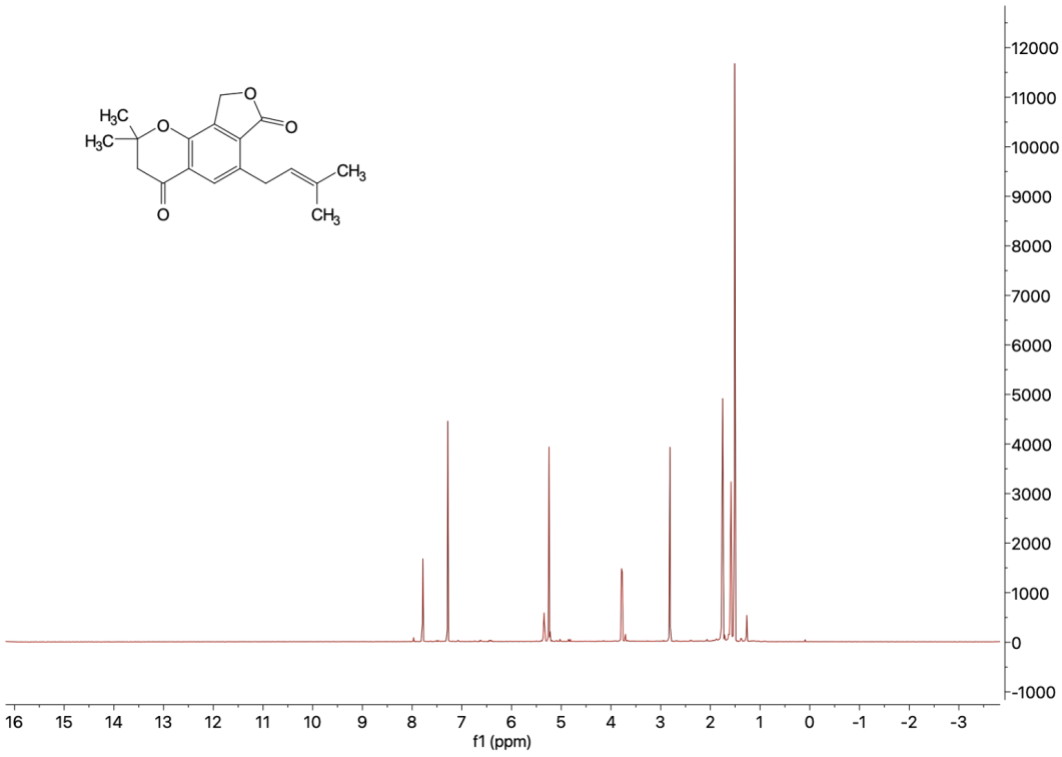
H3C
H3C
O
O
O
CH3
CH3
12000
11000
10000
9000
8000
7000
6000
5000
4000
3000
2000
1000
0
-1000
16 15 14 13 12 11 10 9 8 7 6 5 4 3 2 1 0 -1 -2 -3
f1 (ppm)

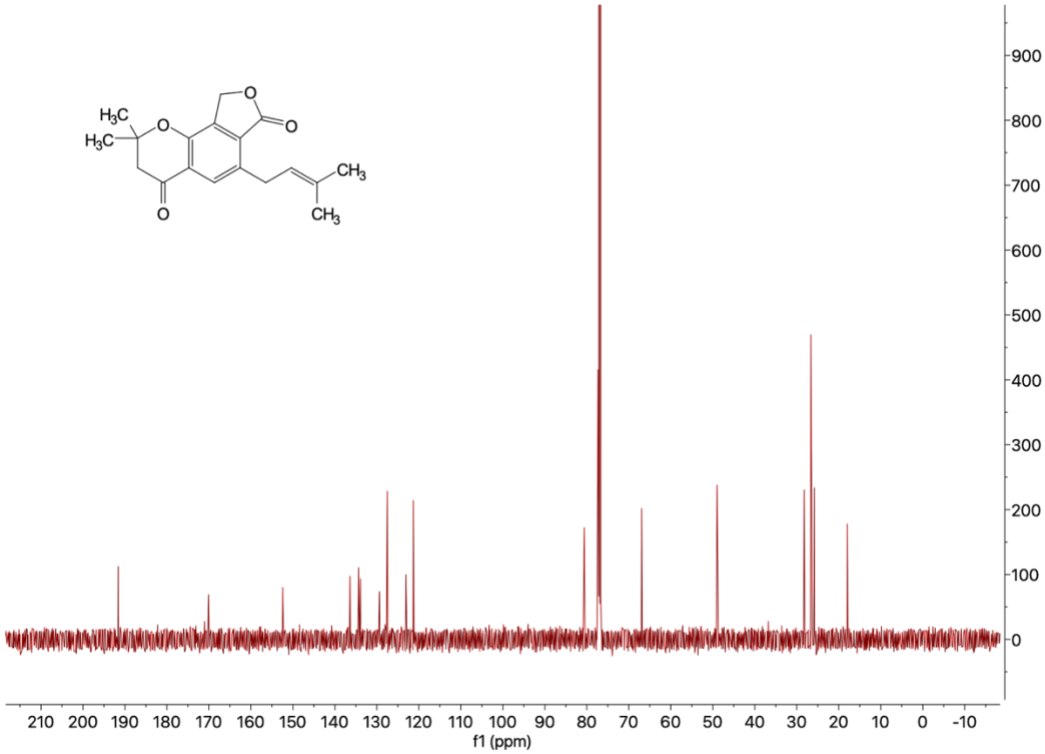
H3C
H3C
O
O
O
O
CH3
CH3
900
800
700
600
500
400
300
200
100
0
210 200 190 180 170 160 150 140 130 120 110 100 90 80 70 60 50 40 30 20 10 0 -10
f1 (ppm)

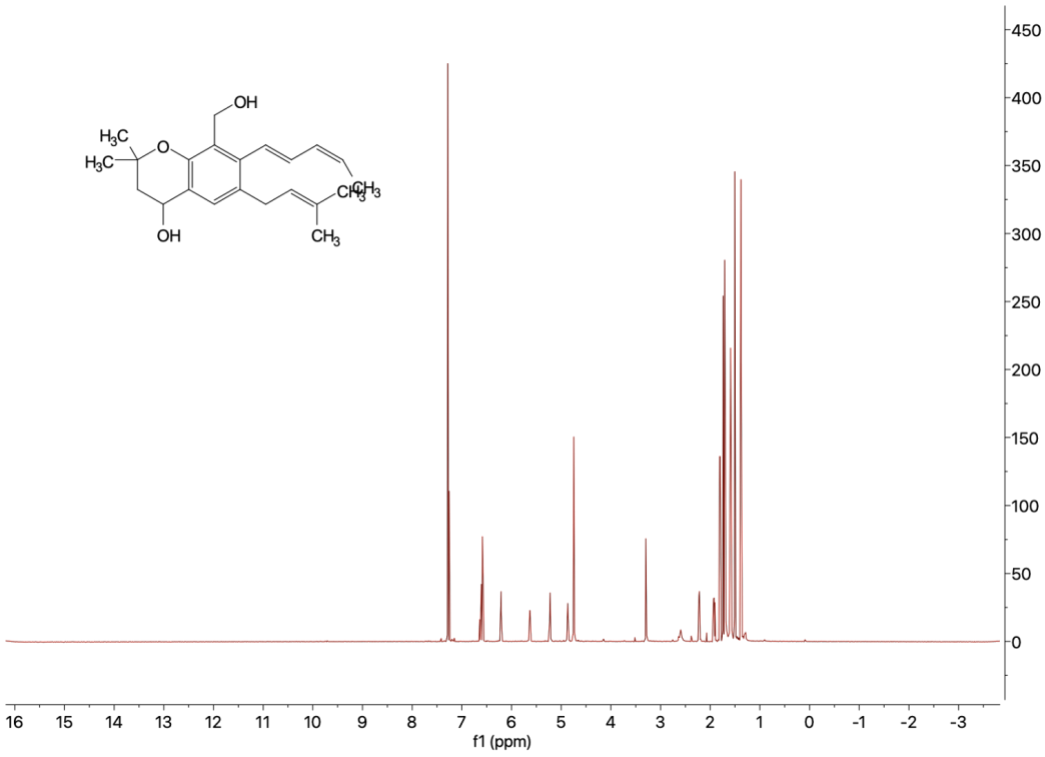
OH
H3C
H3C
O
OH
CH3
CH3
450
400
350
300
250
200
150
100
50
0
16 15 14 13 12 11 10 9 8 7 6 5 4 3 2 1 0 -1 -2 -3
f1 (ppm)

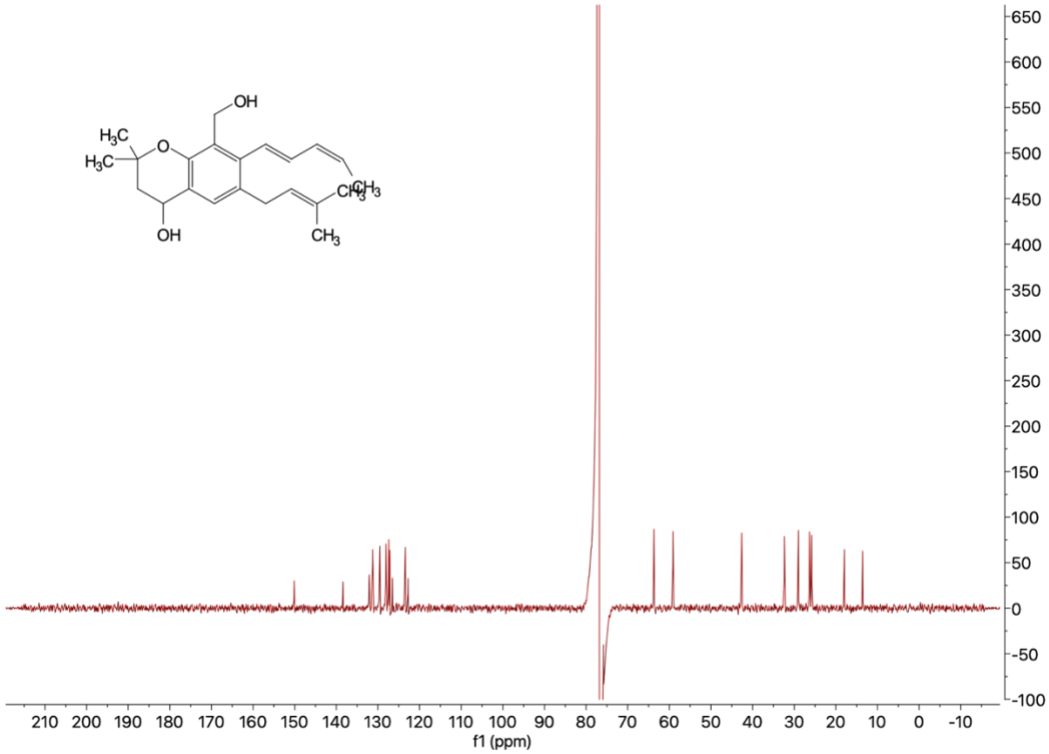
OH
H3C
H3C
O
CH3
CH3
OH
650
600
550
500
450
400
350
300
250
200
150
100
50
0
-50
-100
210 200 190 180 170 160 150 140 130 120 110 100 90 80 70 60 50 40 30 20 10 0 -10
f1 (ppm)

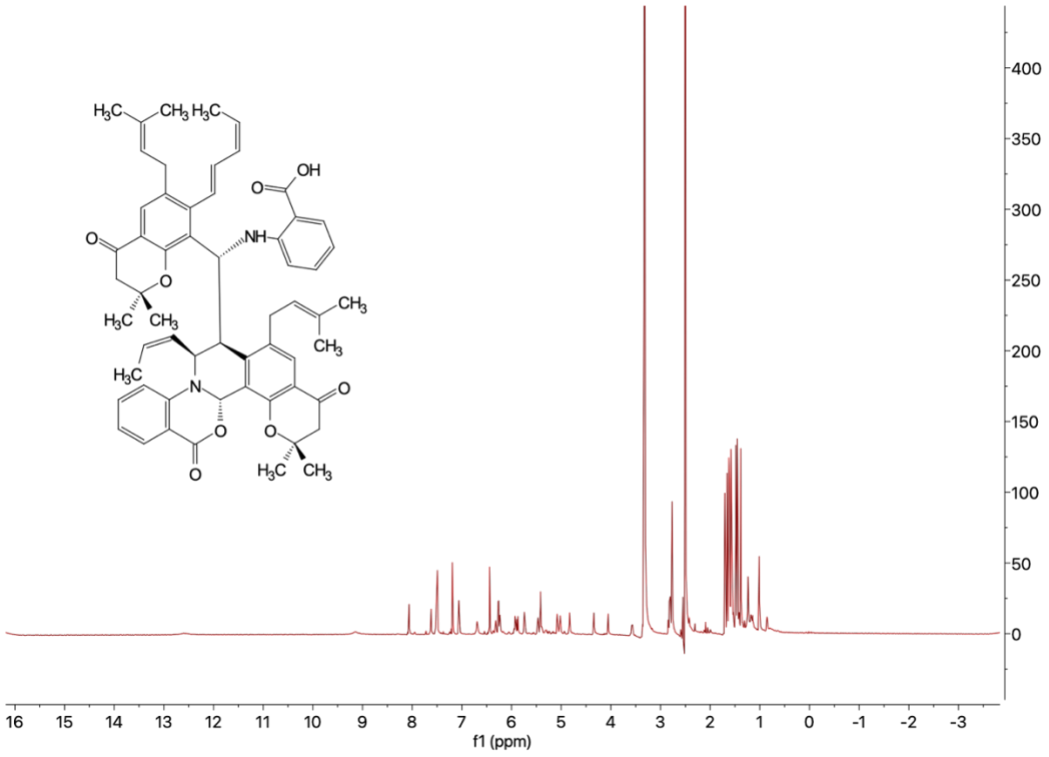
H3C
CH3
H3C
OH
O
NH
O
O
H3C
CH3
CH3
CH3
H3C
N
O
O
O
O
H3C
CH3
400
350
300
250
200
150
100
50
0
16 15 14 13 12 11 10 9 8 7 6 5 4 3 2 1 0 -1 -2 -3
f1 (ppm)

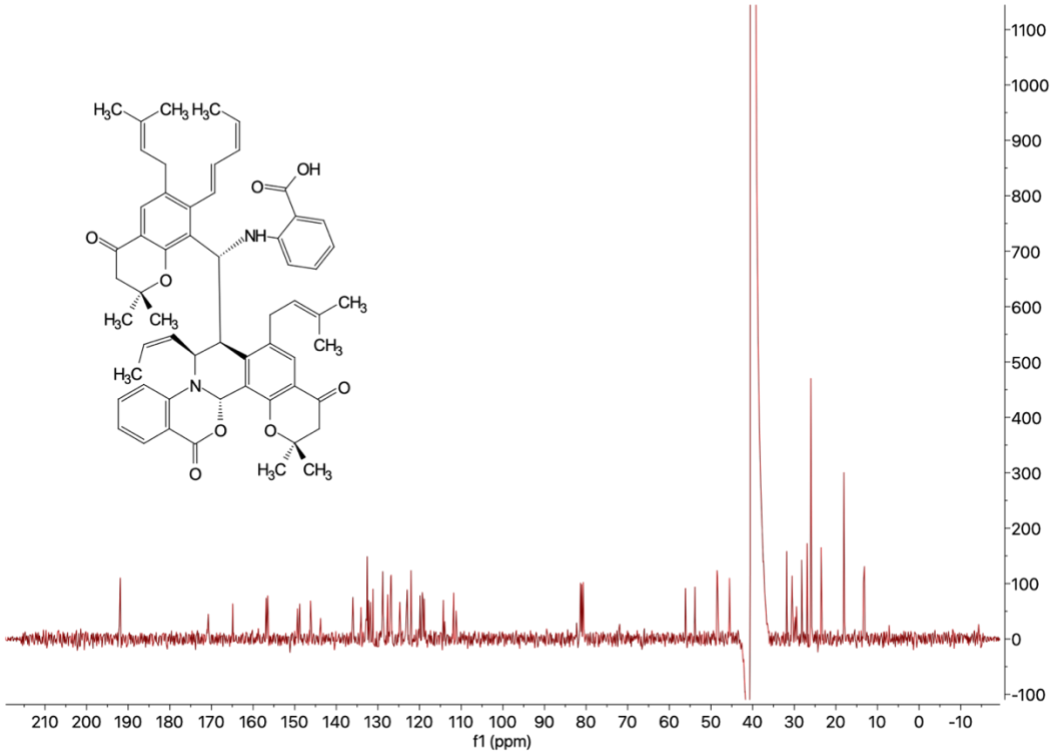
H3C CH3 H3C
OH
O
NH
O
H3C CH3
CH3
CH3
H3C
N
O
O
O
O
O
H3C CH3
1100 1000 900 800 700 600 500 400 300 200 100 0 -100
210 200 190 180 170 160 150 140 130 120 110 100 90 80 70 60 50 40 30 20 10 0 -10
f1 (ppm)

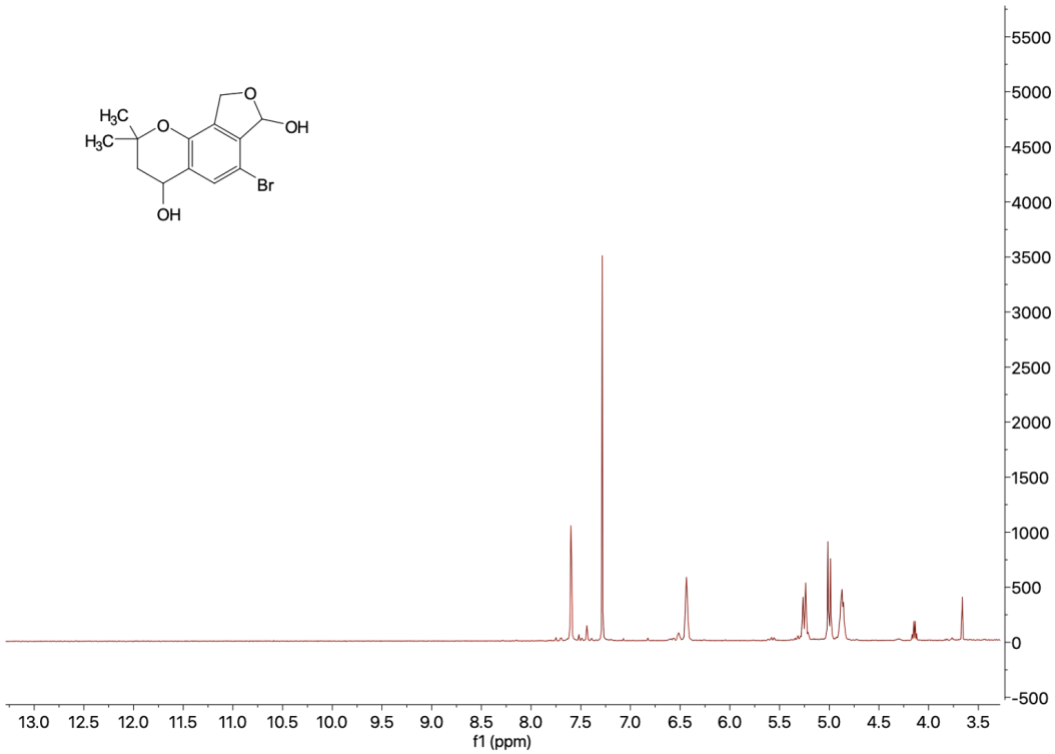
H3C
H3C
O
O
OH
Br
OH
5500 5000 4500 4000 3500 3000 2500 2000 1500 1000 500 0 -500
13.0 12.5 12.0 11.5 11.0 10.5 10.0 9.5 9.0 8.5 8.0 7.5 7.0 6.5 6.0 5.5 5.0 4.5 4.0 3.5
f1 (ppm)

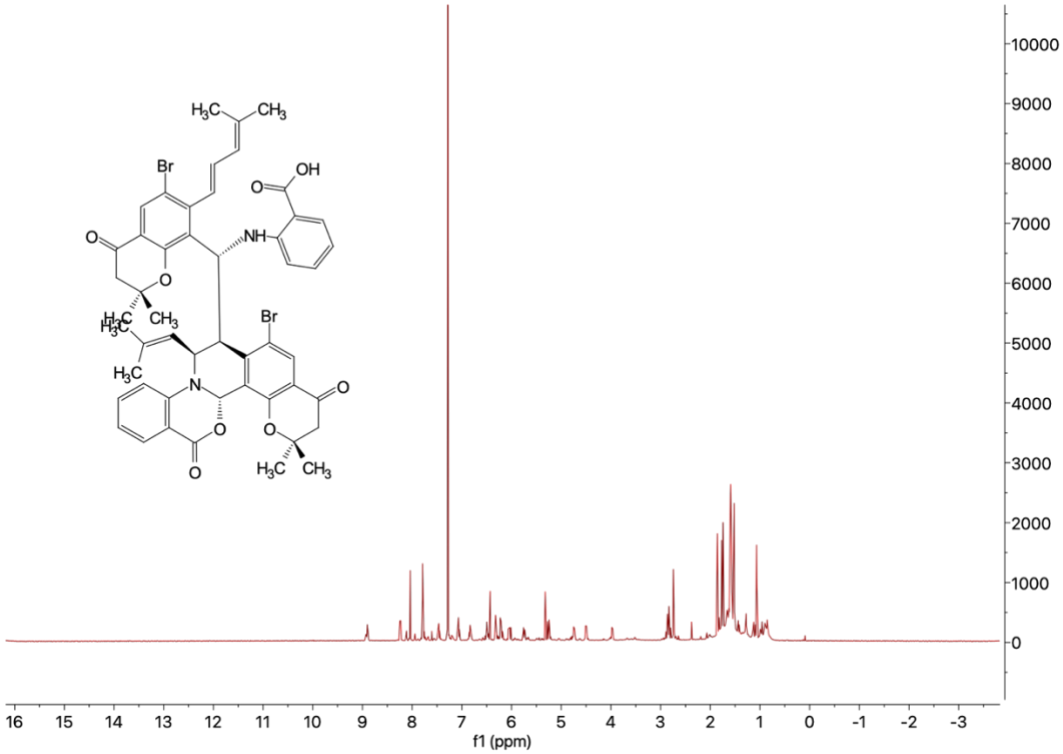
10000
9000
8000
7000
6000
5000
4000
3000
2000
1000
0
16 15 14 13 12 11 10 9 8 7 6 5 4 3 2 1 0 -1 -2 -3
f1 (ppm)

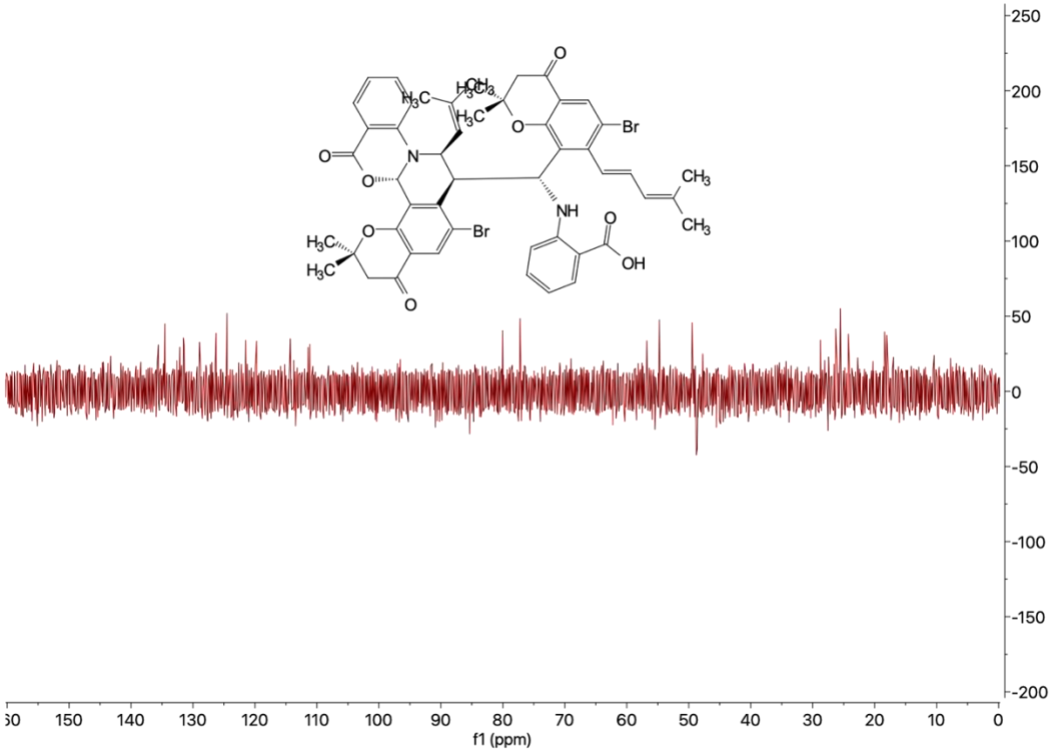
250
200
150
100
50
0
-50
-100
-150
-200
150 140 130 120 110 100 90 80 70 60 50 40 30 20 10 0
f1 (ppm)

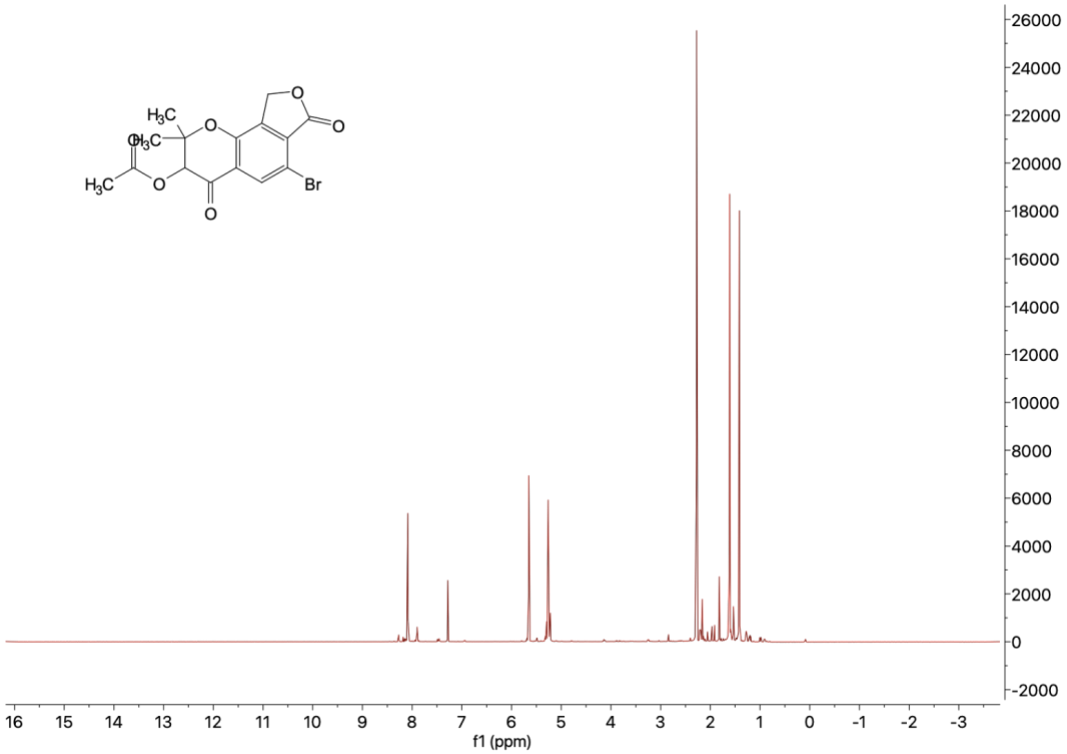
H3C
CH3
O
O
O
O
H3C
O
Br
O
26000
24000
22000
20000
18000
16000
14000
12000
10000
8000
6000
4000
2000
0
-2000
16 15 14 13 12 11 10 9 8 7 6 5 4 3 2 1 0 -1 -2 -3
f1 (ppm)

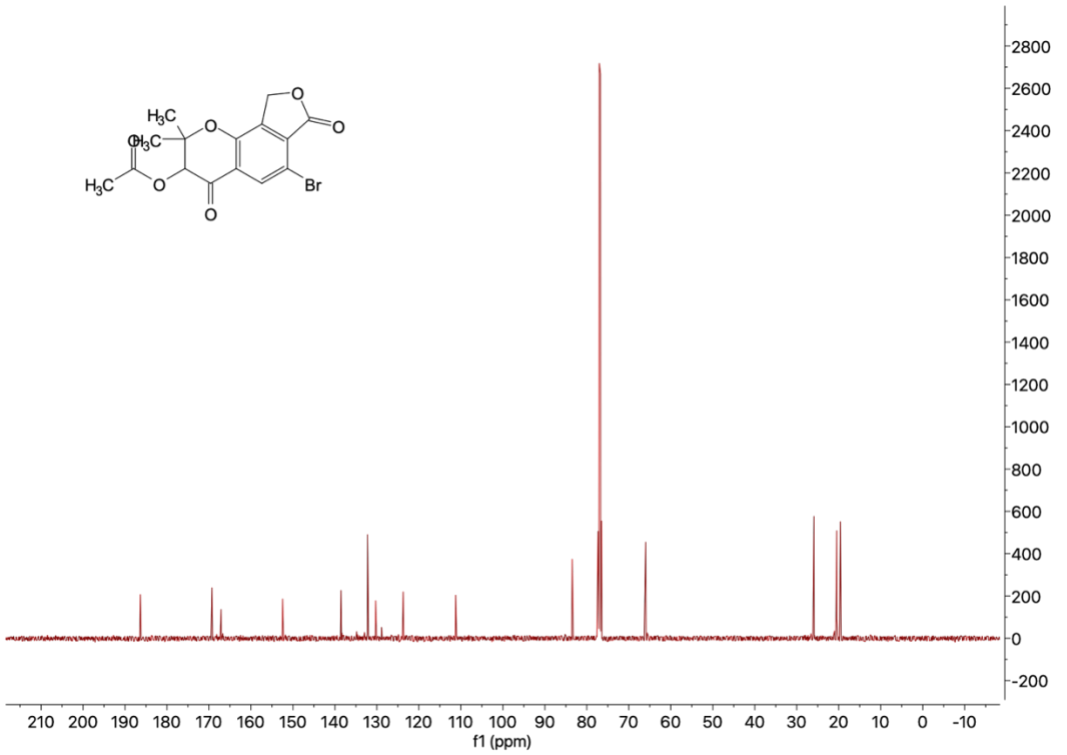
H3C
CH3
O
O
O
O
H3C
O
Br
O
2800
2600
2400
2200
2000
1800
1600
1400
1200
1000
800
600
400
200
0
-200
210 200 190 180 170 160 150 140 130 120 110 100 90 80 70 60 50 40 30 20 10 0 -10
f1 (ppm)

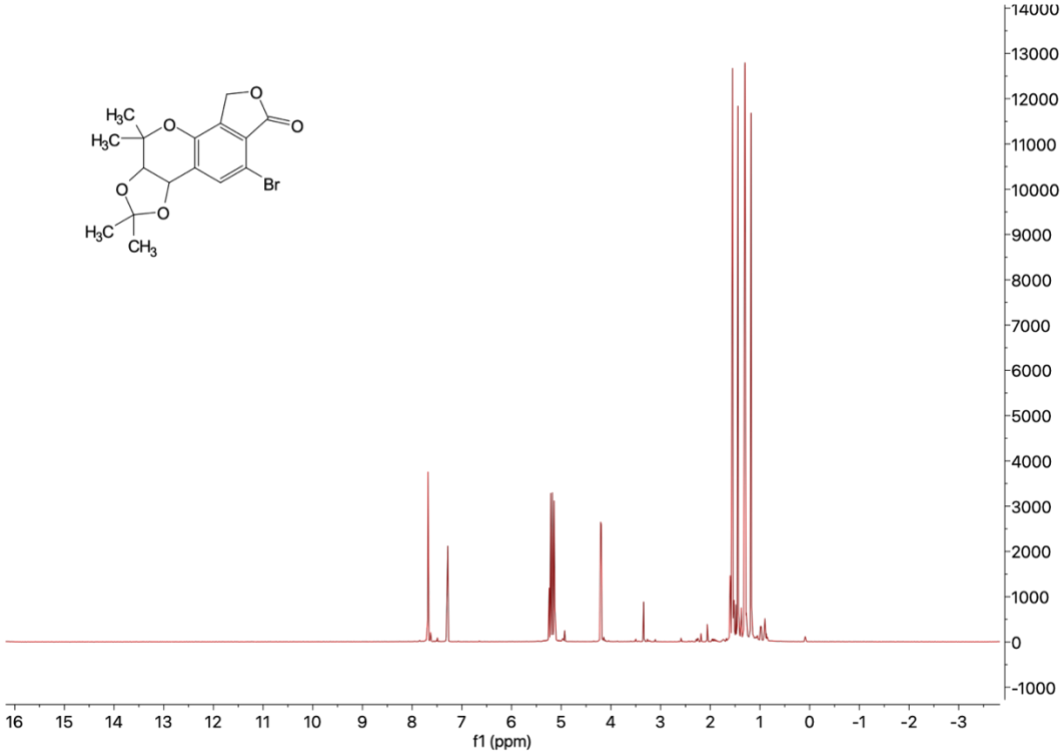
H3C
H3C
O
O
O
Br
O
O
H3C
CH3
14000
13000
12000
11000
10000
9000
8000
7000
6000
5000
4000
3000
2000
1000
0
-1000
16 15 14 13 12 11 10 9 8 7 6 5 4 3 2 1 0 -1 -2 -3
f1 (ppm)

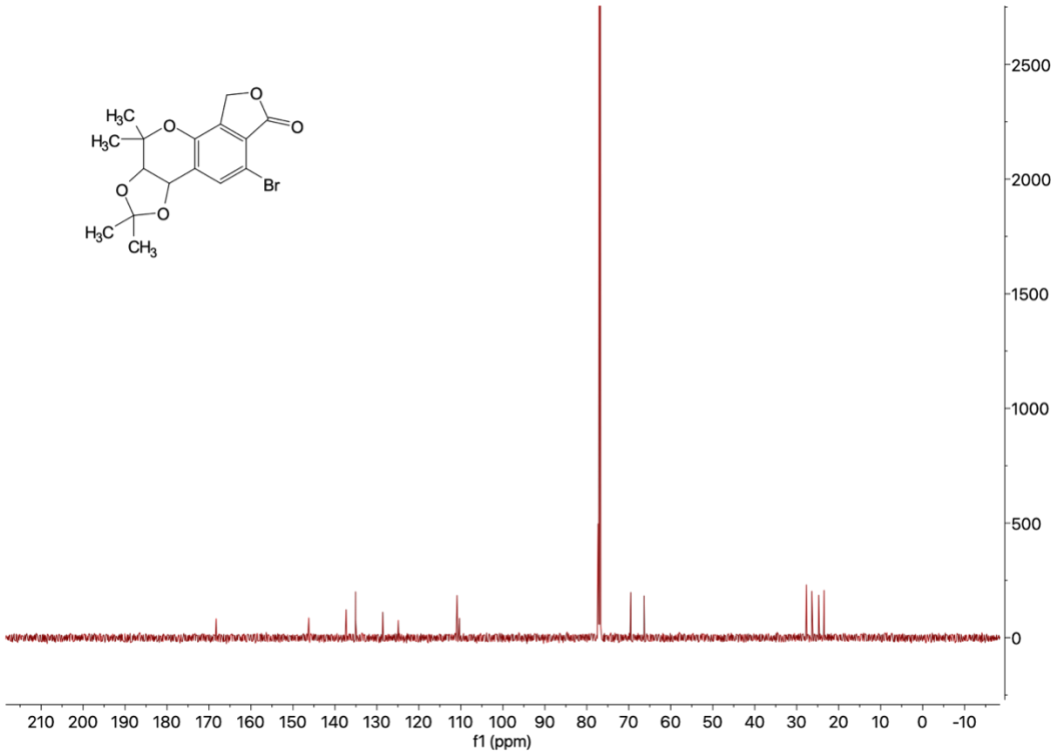
H3C
H3C
O
O
O
Br
O
O
H3C
CH3
2500
2000
1500
1000
500
0
210 200 190 180 170 160 150 140 130 120 110 100 90 80 70 60 50 40 30 20 10 0 -10
f1 (ppm)

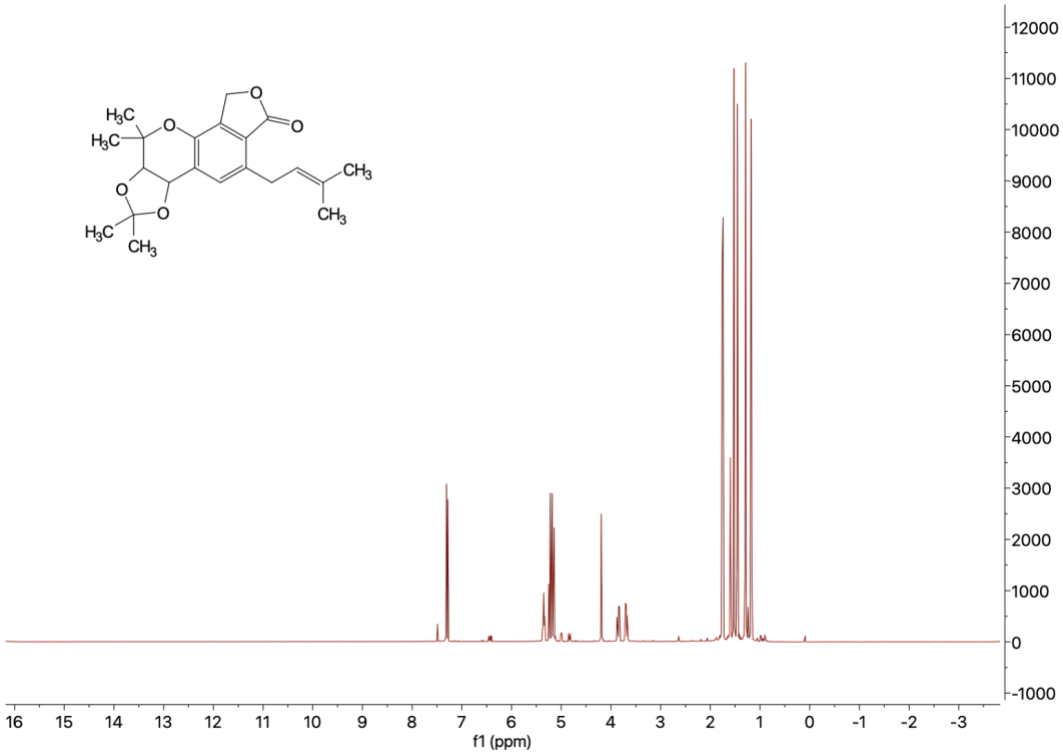
H3C
H3C
O
O
O
O
H3C
CH3
CH3
CH3
12000
11000
10000
9000
8000
7000
6000
5000
4000
3000
2000
1000
0
-1000
16 15 14 13 12 11 10 9 8 7 6 5 4 3 2 1 0 -1 -2 -3
f1 (ppm)

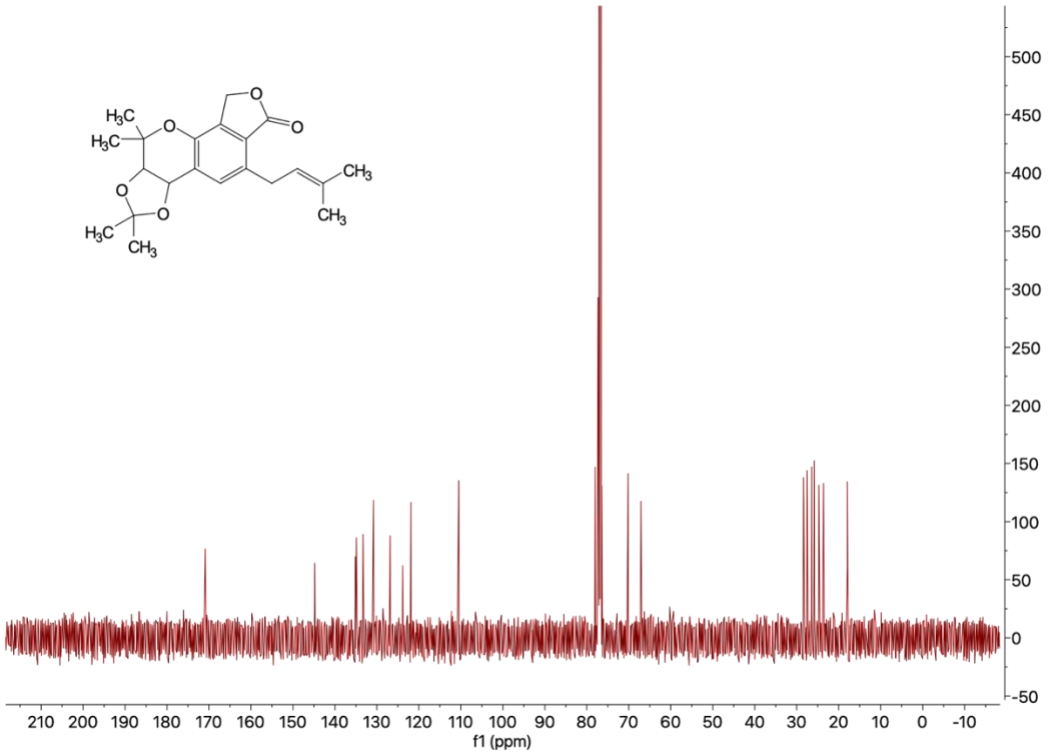
H3C
H3C
O
O
O
O
H3C
CH3
CH3
CH3
500
450
400
350
300
250
200
150
100
50
0
-50
210 200 190 180 170 160 150 140 130 120 110 100 90 80 70 60 50 40 30 20 10 0 -10
f1 (ppm)

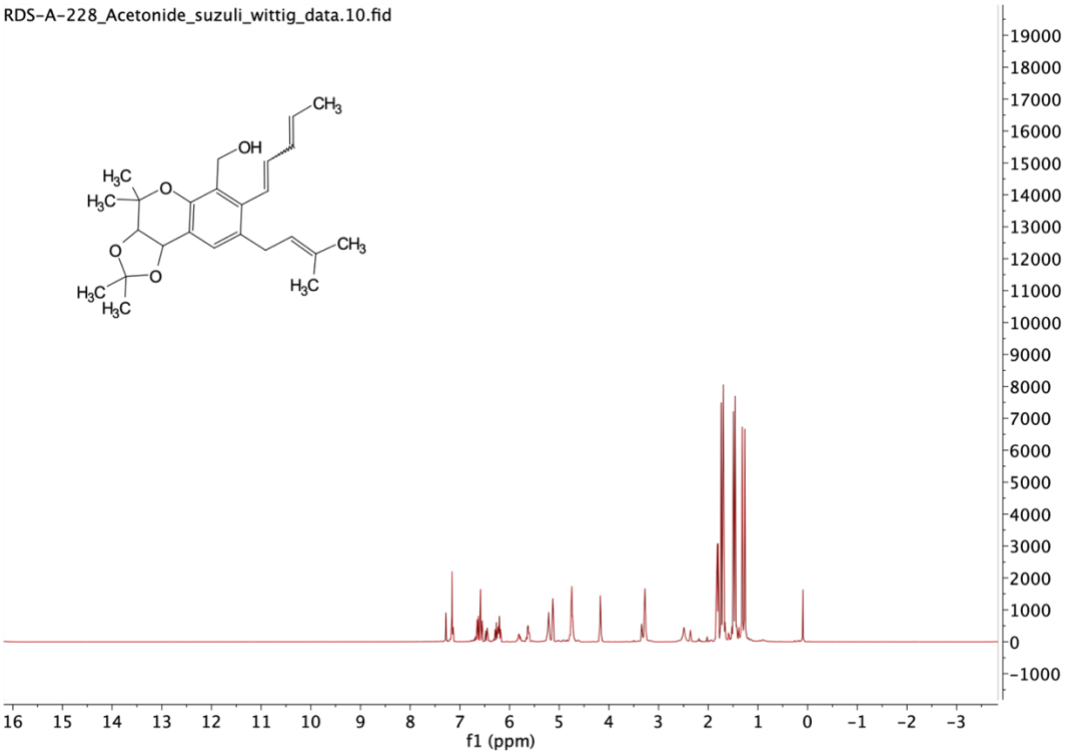
RDS-A-228_Acetonide_suzuli_wittig_data.10.fid
OH
CH3
H3C
O
CH3
H3C
f1 (ppm)

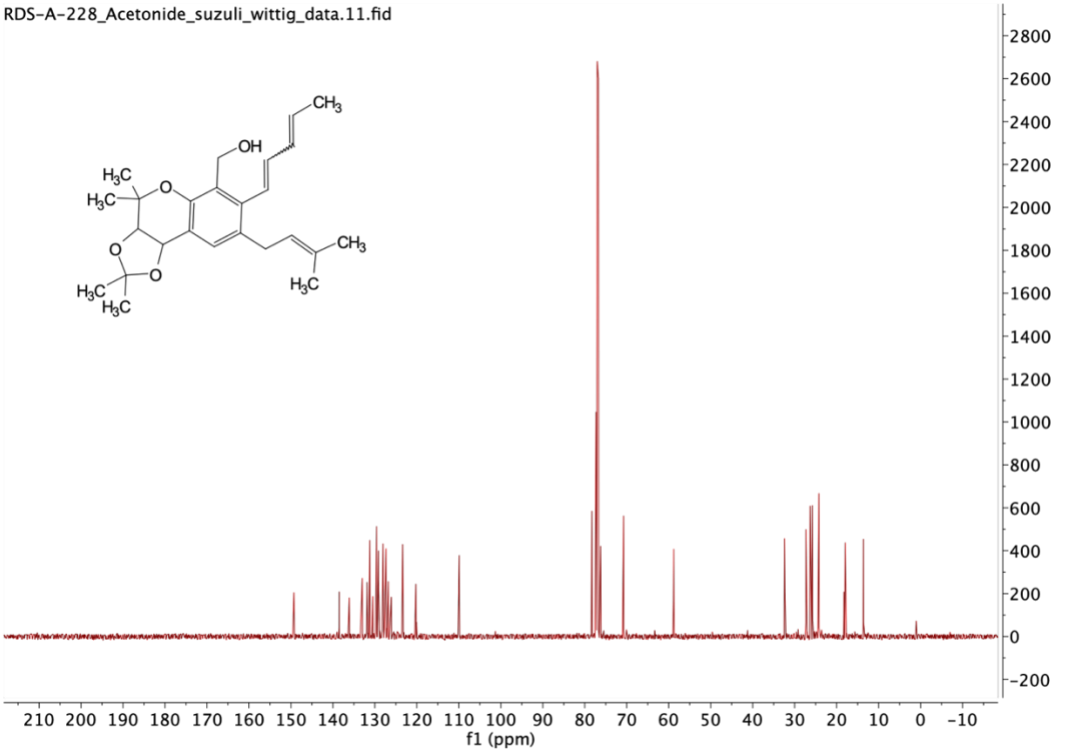
RDS-A-228_Acetonide_suzuli_wittig_data.11.fid
OH
CH3
H3C
O
CH3
H3C
f1 (ppm)

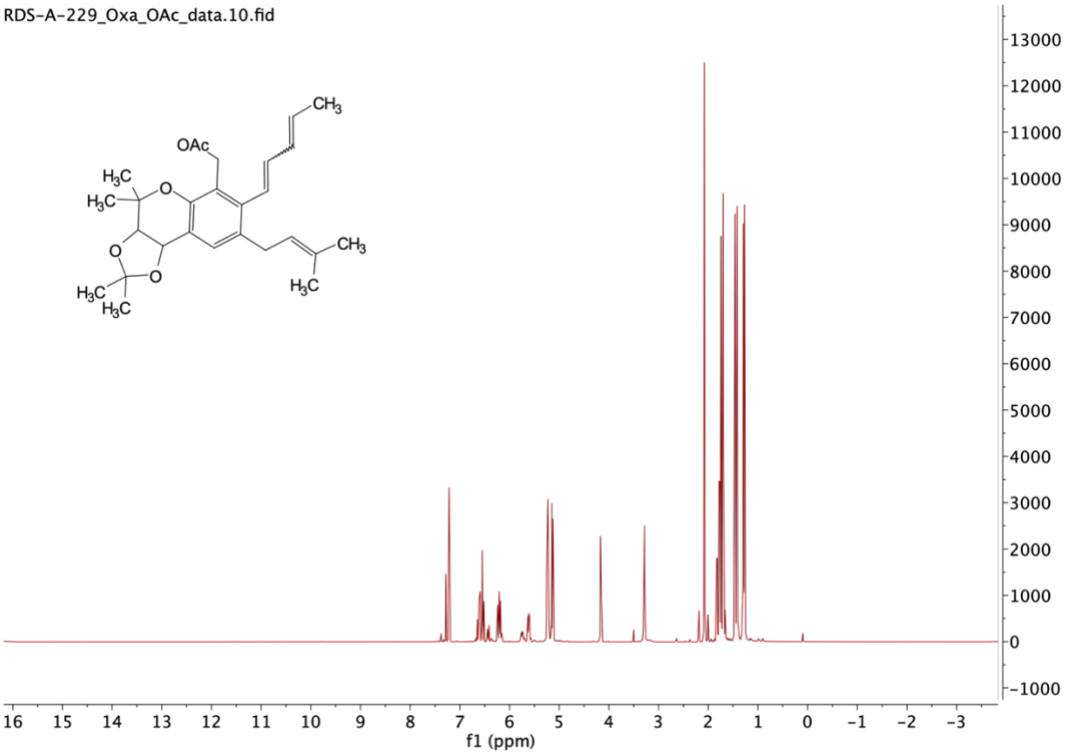
RDS-A-229_Oxa_OAc_data.10.fid
OAc
CH3
H3C
H3C
O
O
O
H3C
H3C
CH3
H3C
13000
12000
11000
10000
9000
8000
7000
6000
5000
4000
3000
2000
1000
0
-1000
16 15 14 13 12 11 10 9 8 7 6 5 4 3 2 1 0 -1 -2 -3
f1 (ppm)

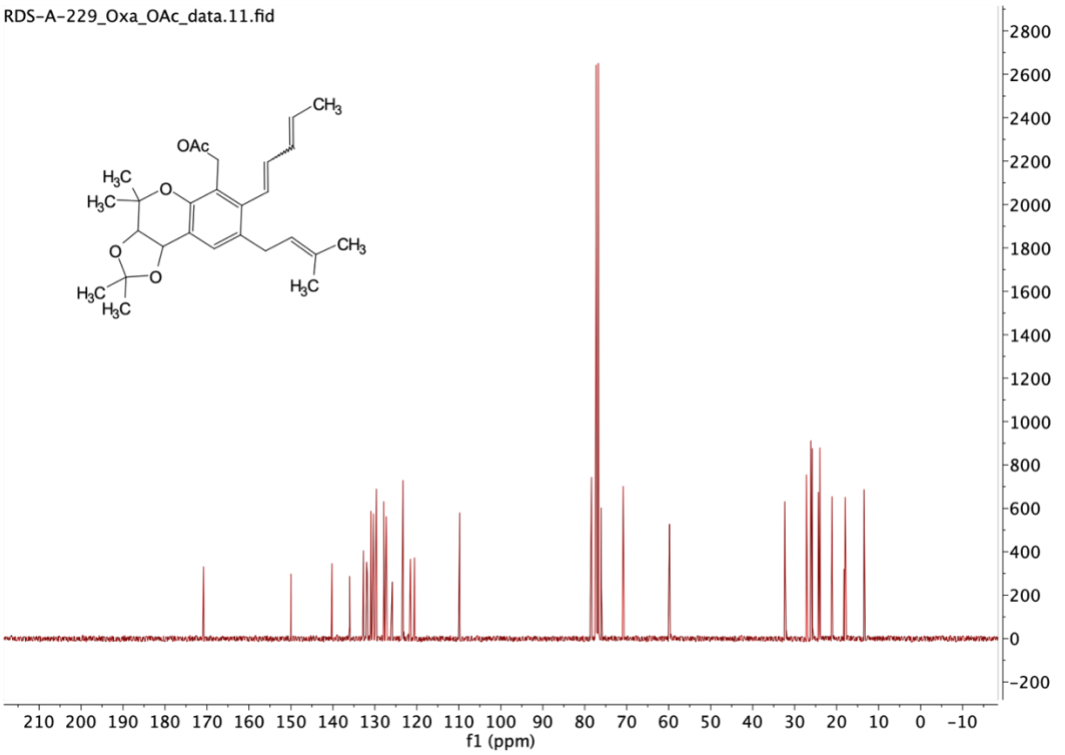
RDS-A-229_Oxa_OAc_data.11.fid
OAc
CH3
H3C
H3C
O
O
O
H3C
H3C
CH3
H3C
2800
2600
2400
2200
2000
1800
1600
1400
1200
1000
800
600
400
200
0
-200
210 200 190 180 170 160 150 140 130 120 110 100 90 80 70 60 50 40 30 20 10 0 -10
f1 (ppm)

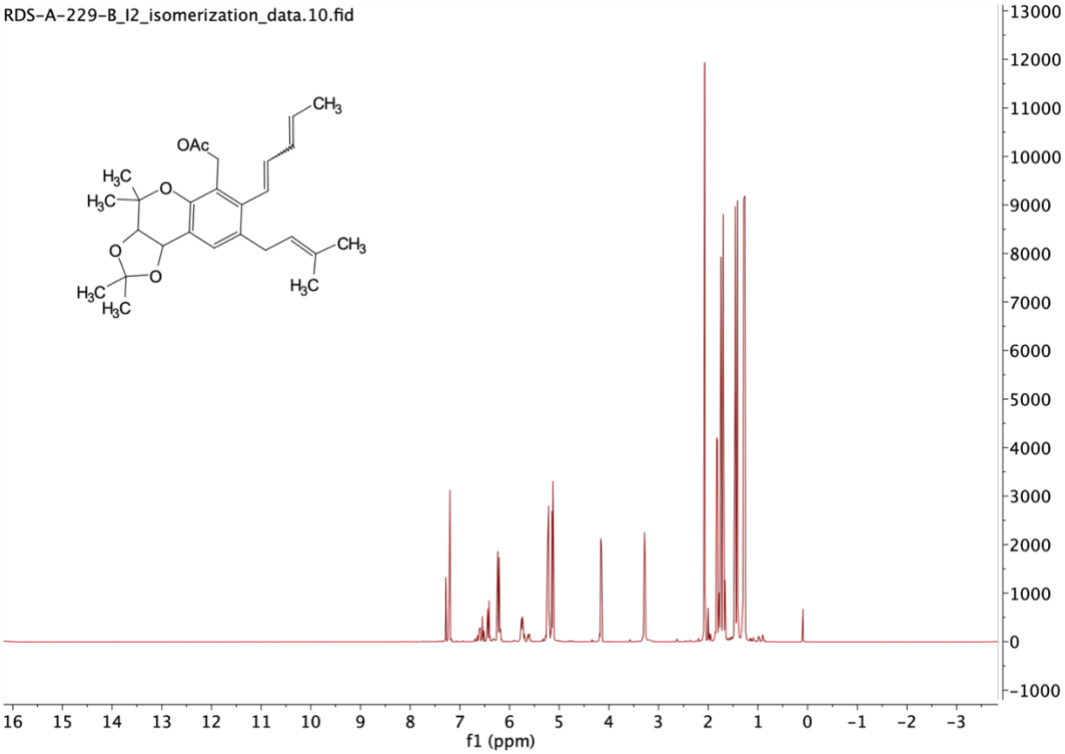
RDS-A-229-B_I2_isomerization_data.10.fid
OAc
CH3
H3C
H3C
O
O
O
H3C
H3C
CH3
H3C
13000
12000
11000
10000
9000
8000
7000
6000
5000
4000
3000
2000
1000
0
-1000
16 15 14 13 12 11 10 9 8 7 6 5 4 3 2 1 0 -1 -2 -3
f1 (ppm)

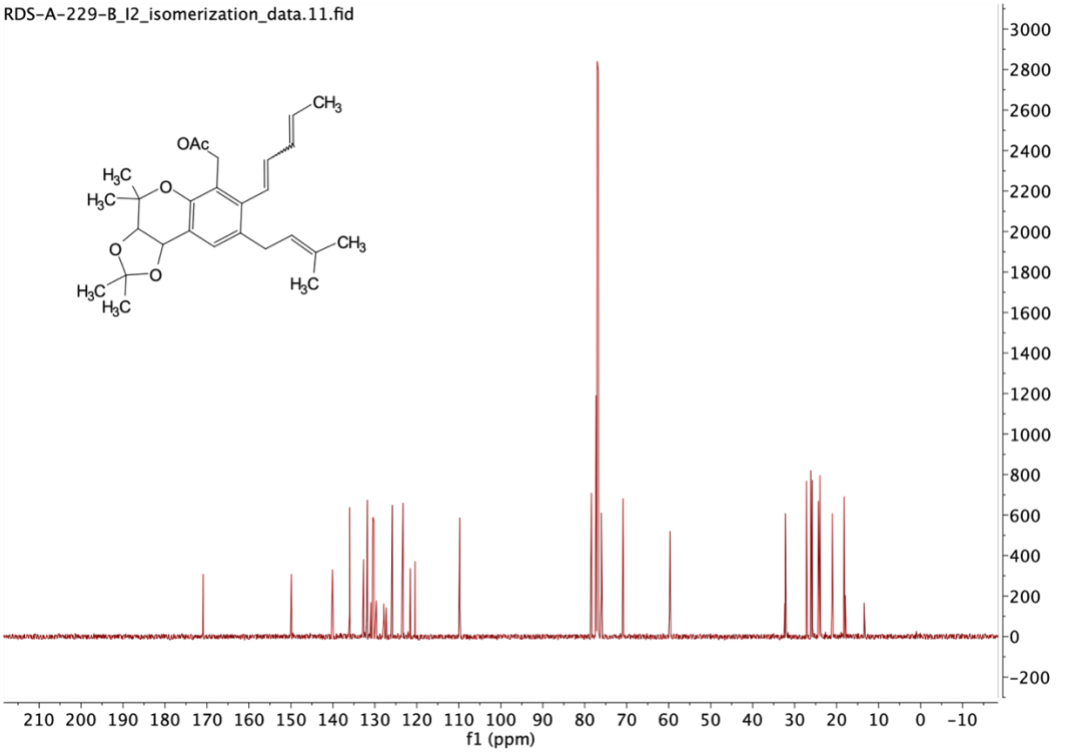
RDS-A-229-B_I2_isomerization_data.11.fid
OAc
CH3
H3C
H3C
O
O
O
H3C
H3C
CH3
H3C
3000
2800
2600
2400
2200
2000
1800
1600
1400
1200
1000
800
600
400
200
0
-200
210 200 190 180 170 160 150 140 130 120 110 100 90 80 70 60 50 40 30 20 10 0 -10
f1 (ppm)

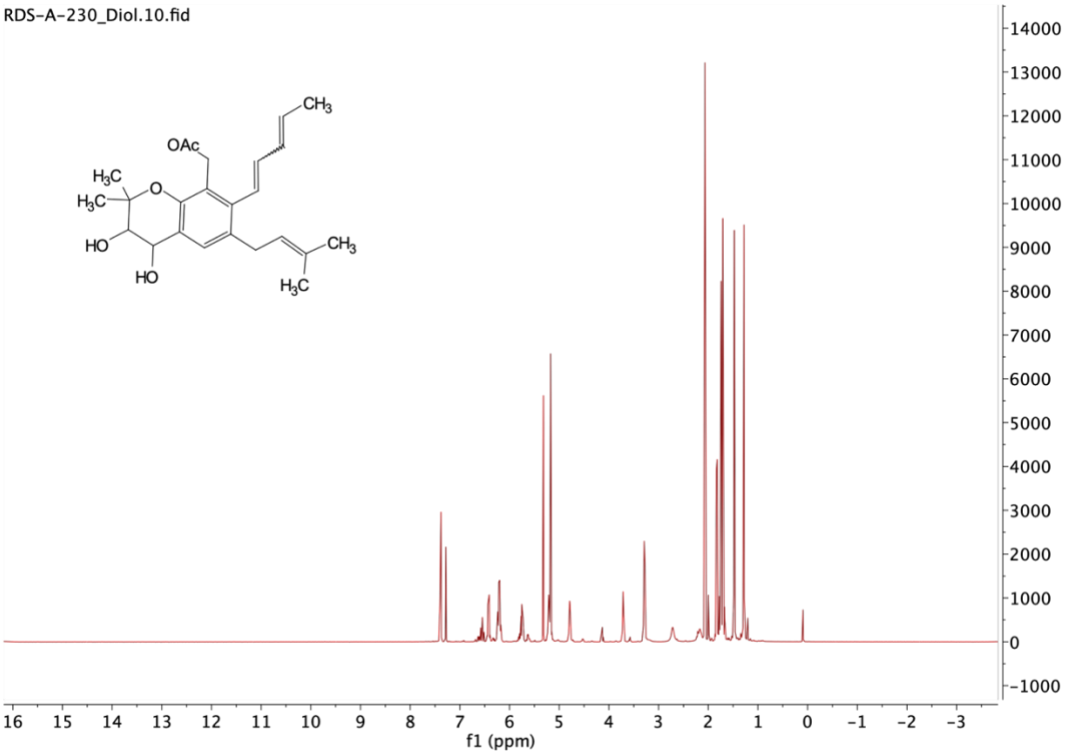
RDS-A-230_Diol.10.fid
OAc
CH3
H3C
H3C
O
HO
HO
CH3
H3C
14000
13000
12000
11000
10000
9000
8000
7000
6000
5000
4000
3000
2000
1000
0
-1000
16 15 14 13 12 11 10 9 8 7 6 5 4 3 2 1 0 -1 -2 -3
f1 (ppm)

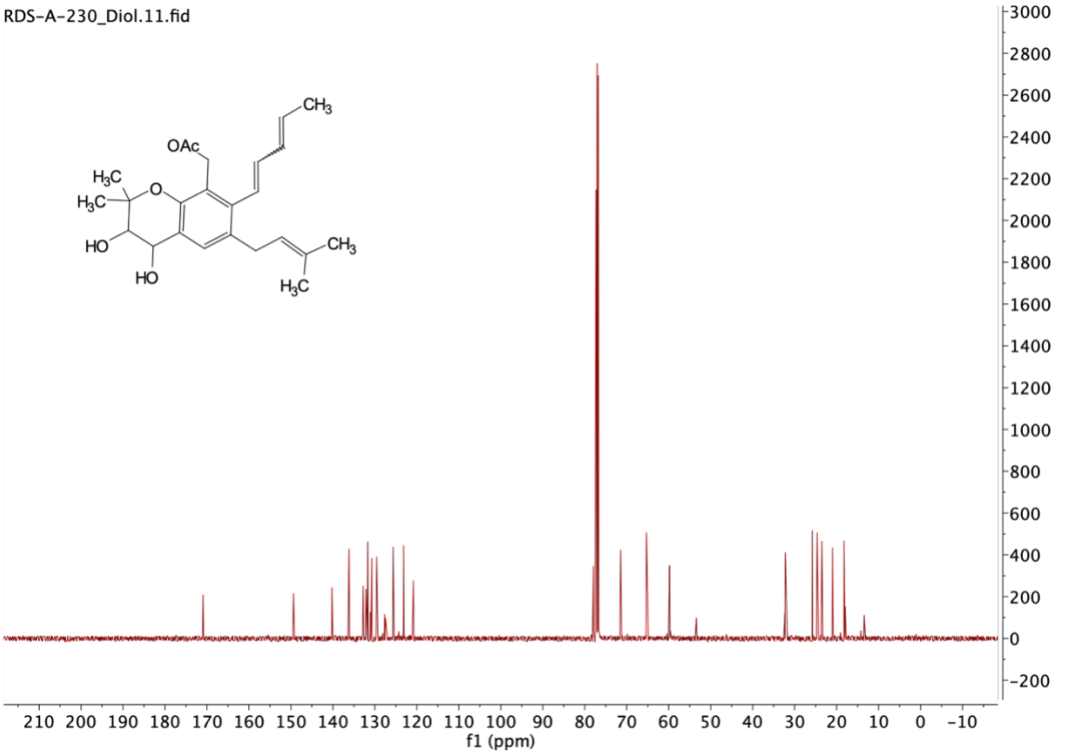
RDS-A-230_Diol.11.fid
OAc
CH3
H3C
H3C
O
HO
HO
CH3
H3C
3000
2800
2600
2400
2200
2000
1800
1600
1400
1200
1000
800
600
400
200
0
-200
210 200 190 180 170 160 150 140 130 120 110 100 90 80 70 60 50 40 30 20 10 0 -10
f1 (ppm)

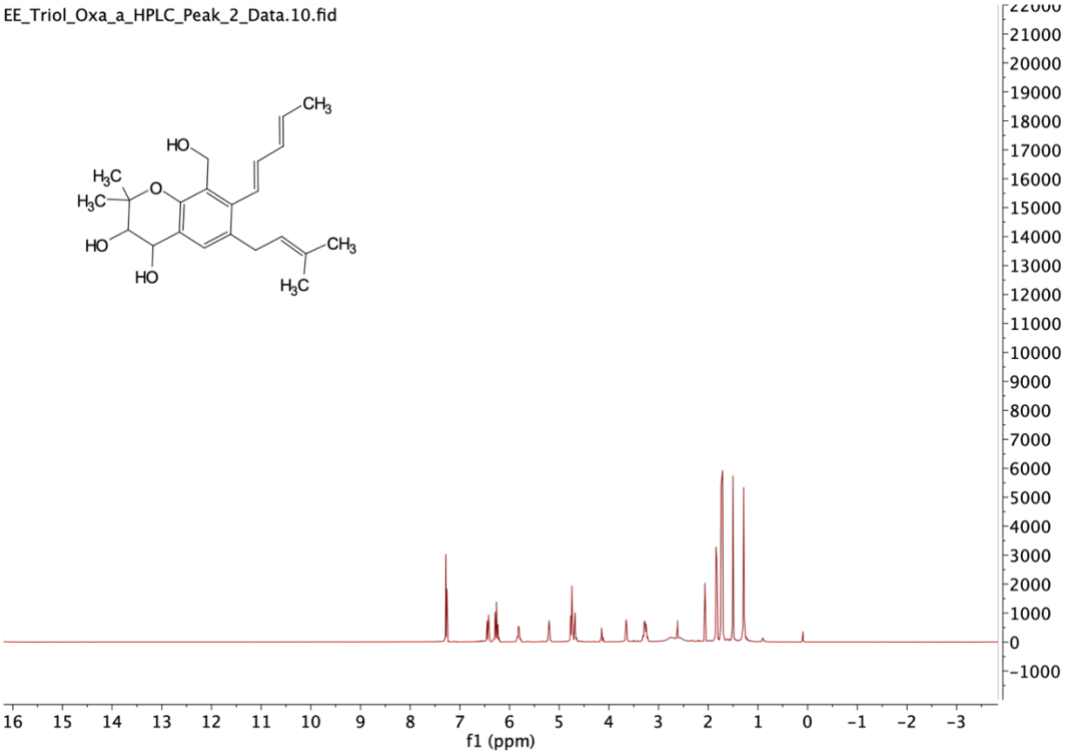
EE_Triol_Oxa_a_HPLC_Peak_2_Data.10.fid
f1 (ppm)

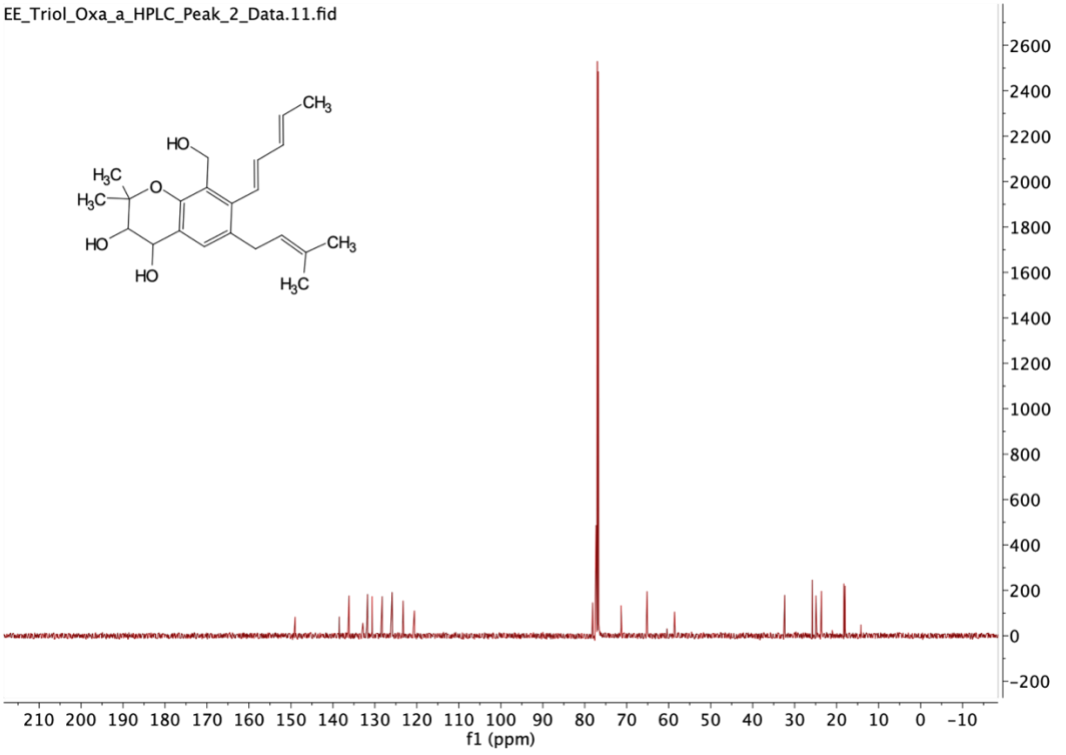
EE_Triol_Oxa_a_HPLC_Peak_2_Data.11.fid
f1 (ppm)

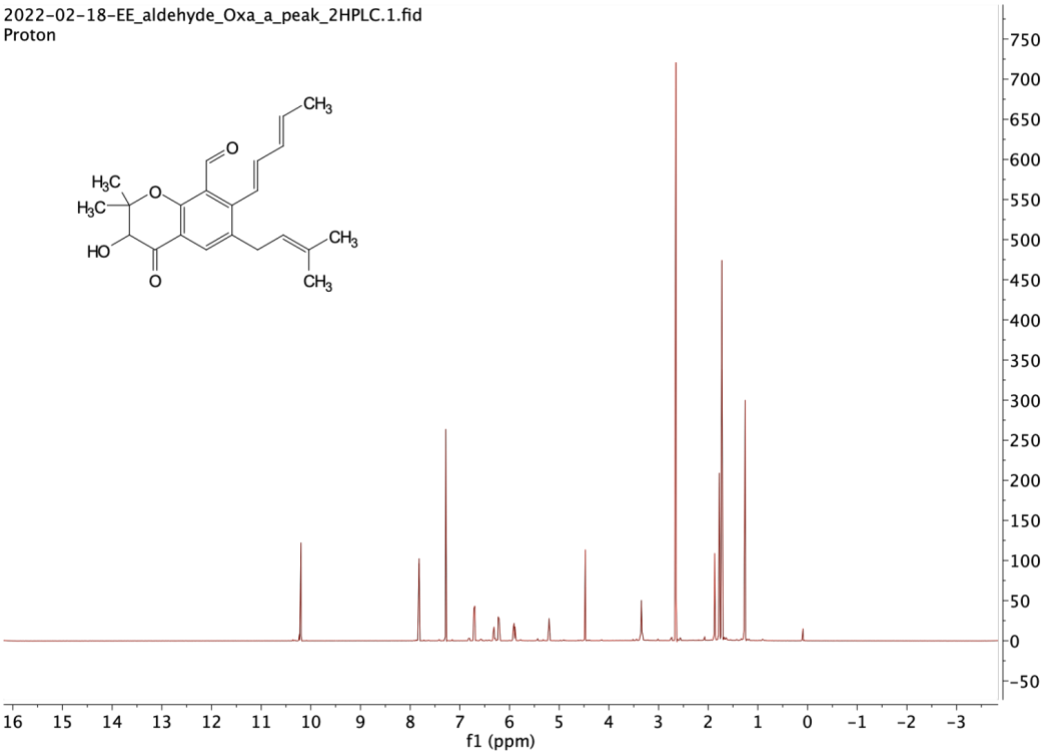
2022-02-18-EE_aldehyde_Oxa_a_peak_2HPLC.1.fid
Proton
f1 (ppm)

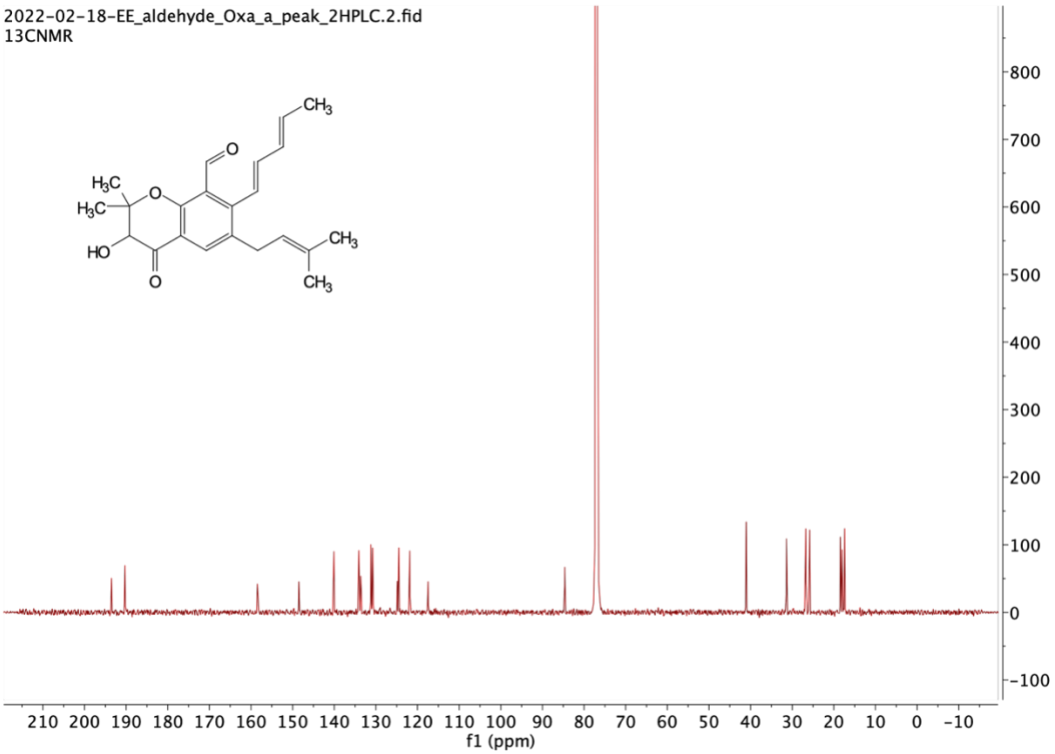
2022-02-18-EE_aldehyde_Oxa_a_peak_2HPLC.2.fid
13CNMR
f1 (ppm)

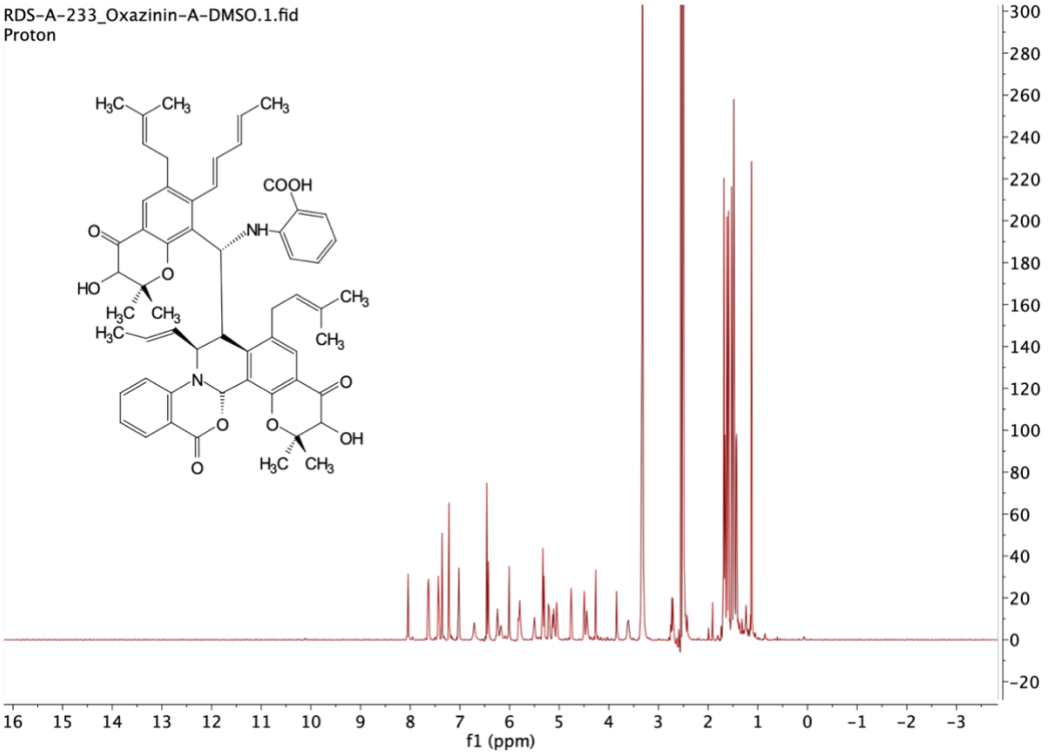
RDS-A-233_Oxazinin-A-DMSO.1.fid
Proton
f1 (ppm)

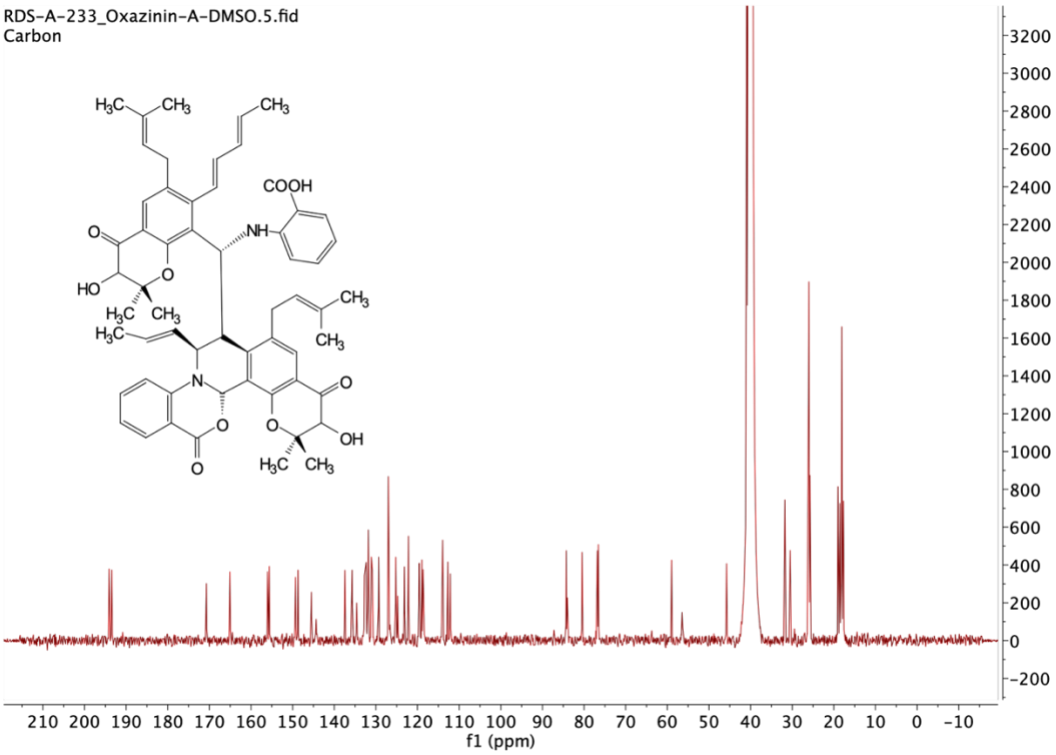
RDS-A-233_Oxazinin-A-DMSO.5.fid
Carbon
f1 (ppm)

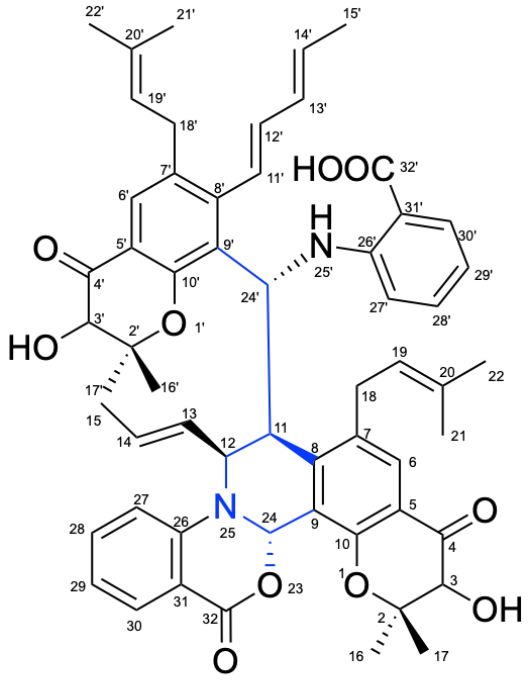

Oxazinin A

No.	Synthetic oxazinin A In DMSO-*d*6		Isolated oxazinin A In DMSO-*d*6	
	1H NMR (*J* in Hz)	13C NMR	1H NMR (*J* in Hz)	13C NMR
2		84.3 C		84.6
3	4.26 d (5.0)	76.6 CH	4.22 d (5.0)	76.1 CH
3-OH	6.00 d (5.2)		5.99 d (4.8)	
4		193.3 C		193.7 C
5		ND		ND

6	**7.21 s**	**127.0 CH**	**7.18 s**	**126.2**
7		**134.6 C**		**135.2 C**
8		**144.4 C**		**144.3 C**
9		**119.0 C**		**119.8 C**
10		**155.6 C**		**156.1 C**
11	**4.49 m**	**45.7 CH**	**4.47 m**	**45.5 CH**
12	**3.83 brs**	**59.0 CH**	**3.82 brs**	**58.6 CH**
13	**5.20 dd (15.8, 5.0)**	**129.4 CH**	**5.19 dd (15.8, 4.3)**	**128.4 CH**
14	**5.32 dq (16.2 , 6.3)**	**127.0 CH**	**5.30 dq (15.8, 5.9)**	**126.2 CH**
15	**1.42 d (6.1)**	**17.7 CH3**	**1.40 d (6.0)**	**17.6 CH3**
16	**1.52 s**	**25.7 CH3**	**1.50 s**	**26.0 CH3**
17	**1.12 s**	**18.7 CH3**	**1.11 s**	**19.1 CH3**
18a	**3.6 brd (16.3)**	**30.4 CH2**	**3.54 dd (16.3, 4.2)**	**29.7 Ch2**
18b	**Under solvent peak**	**30.4 CH_2**	**3.27 m**	**29.7 CH2**
19	**5.04 brt (6.5)**	**123.1 CH**	**5.01 t (6.5)**	**122.3 CH**

20		**132.7 C**		**133.1 C**
21	**1.58 s**	**18.2 CH3**	**1.60 s**	**18.1 CH3**
22	**1.68 s**	**26.0 CH3**	**1.67 s**	**25.9 CH3**
24	**6.45 s**	**80.3 CH**	**6.44 s**	**80.0 CH**
25		**-**		**-**
26		**148.7 C**		**148.9 C**
27	**6.42d (8.1)**	**112.7 CH**	**6.41 d (8.0)**	**111.9 CH**
28	**7.43 dd (7.9, 7.7)**	**135.7 CH**	**7.42 dd (7.9, 7.6)**	**135.0 CH**
29	**7.01 dd (7.6, 7.5)**	**119.7 CH**	**7.00 dd (7.6, 7.5)**	**118.8 CH**
30	**8.04 d (8.00)**	**130.8 CH**	**8.04 d (8.00)**	**130.1 CH**
31		**114.0 C**		**114.0 C**
32		**165.1 C**		**165.2 C**
2'		**84.3 C**		**84.6 C**
3'	**4.44 brm**	**76.8 CH**	**4.46 m**	**76.2 CH**
3'-OH	**6.00**		**6.00 d (4.9)**	
4'		**194.1 C**		**194.5C**

5’		**118.7 C**		**119.3 C**
6’	**7.35 s**	**124.7 CH**	**7.35 s**	**124.1 CH**
7’		**132.6 C**		**132.6 C**
8’		**145.5 C**		**145.5 C**
9’		**126.6 C**		**126.3 C**
10’		**156.0 C**		**156.4 C**
11’	**5.31 d (15.8)**	**125.3 CH**	**5.29 d (15.6)**	**124.5 CH**
12’	**5.49 dd (15.6, 10.8)**	**137.4 CH**	**5.50 dd (15.6, 11.0)**	**136.5 CH**
13’	**5.81 dd (15.2, 11.1)**	**130.9 CH**	**5.80 dd (15.6, 11.0)**	**130.2 CH**
14’	**5.10 dq (14.5, 6.7)**	**131.9 CH**	**5.10 dq (14.6, 6.1)**	**131.3 CH**
15’	**1.65 d (6.5)**	**18.6 CH3**	**1.64 d (6.4)**	**18.7 CH3**
16’	**1.68 s**	**26.1 CH3**	**1.66 s**	**26.4 CH3**
17’	**1.47 s**	**18.6 CH3**	**1.44 s**	**18.5 CH3**
18’	**2.71 m**	**31.7 CH2**	**2.71 m**	**31.8 CH2**

19’	**4.76 t (7.3)**	**122.2 CH**	**4.74 t (7.3)**	**121.3 CH**
20’		**132.9 C**		**133.3 C**
21’	**1.47 s**	**19.0 CH3**	**1.50 s**	**19.2 CH3**
22’	**1.62 s**	**26.0 CH3**	**1.57 s**	**26.2 CH3**
24’	**5.80 dd (10.4, 10.4)**	**56.4 CH**	**5.82 dd (10.4, 10.1)**	**55.7 CH**
25’	**br 9.00-9.30**	**NH**	**9.01 d (10.4)**	
26’		**149.3 C**		**150.3 C**
27’	**6.17 brm**	**112.1 CH**	**6.22 d (8.0)**	**111.5 CH**
28’	**6.71 brm**	**ND CH**	**6.75 dd (8.0, 7.9)**	**132.8 CH**
29’	**6.24 dd (7.7, 7.5)**	**114.0 CH**	**6.25 dd (7.6, 7.5)**	**113.7 CH**
30’	**7.63 d (7.7)**	**131.8 CH**	**7.62 d (7.7)**	**131.1 CH**
31’		**ND**		**109.5 C**
32’		**170.8 C**		**171.8 C**

32'-OH	**12.56 s**	**-**	**12.53 s**	**-**

Chapter Three: Synthesis and Mechanistic Elucidation of the pyonitrins and aerupyrroles

The text of this dissertation [or thesis] includes reprint[s] of the following previously published material: Org. Lett. ***2020****, 22, 4, 1516–1519. The co-author listed in this publication directed and supervised the research which forms the basis for the dissertation [or thesis]*

3.1 Abstract

The pyonitrins, antifungal compounds formed from the non-enzymatic reaction of two bacterial metabolites (aeruginaldehyde and pyrrolnitrin(s)) are synthesized. This synthesis inspired the creation of hybrid natural products using aeruginaldehyde from the pyonitrins and anthranilic acid and 4-methoxy sattabacin from the discoipyrroles. The generation of these hybrid structures, based on our understanding of the non-enzymatic origins, provides a framework for exploring future combinatorial chemistry efforts with functional groups identified in these studies.

3.2 Introduction

Fungal infections, like bacterial infections, come from a myriad of sources, can cause a plethora of health problems, and are much more common than many think. We typically think of fungal infections in relation to plants but are an increasing problem within humans as well. Fungal infections can range from the more common ailments such as athlete's foot (fungal infection that occurs between the toes of infected individuals) to mucormycotic (rare fungal infection that can be present in the lungs, skin, brain, or gastrointestinal system). In fact, superficial fungal infection of the skin and nails affects 25% of the world population (approximately 1.7 billion people).[1] These infections have been

relatively under looked in comparison to other ailments. The World Health Organization (WHO) has just recently begun to create a fungal pathogens list in addition to having its first meeting of antifungal experts in 2020. While not talked about as much as other pathogenic infections, studies show that these infections are just as deadly.

Invasive fungal infections are not as pervasive as superficial infections but are more dangerous and have much higher mortality rates. Fungal infections kill over one and a half million people a year, and 90% of all fungal deaths are from these four genera: *Cryptococcus*, *Candida*, *Aspergillus*, and *Pneumocystis*.[2] Aspergillosis, for example, infects more than 200,000 people a year worldwide and has a 30-95% mortality rate in infected populations. In addition, Candidiasis, caused by *Candida albicans*, infects more than 400,000 people a year worldwide and has a 45-75% mortality rate. Although less fatal (20-70% fatality rate), Cryptococcosis, infects more than a million people a year. The fatality rates occur with such large ranges due to reporting and diagnostic inadequacies but still point toward the growing threat of invasive fungal infections on human health.

Fungal infections have always been difficult to treat. Almost 7% of all blood *Candida* samples are resistant to the antifungal drug fluconazole.[2] Moreover, *Candida albicans* is the common cause of all severe *Candida* infections. Other *Candida* species such as *Candida auris* have also shown to have increased resistance to current treatments. The classes of drugs currently

used to treat fungal infections are the polyenes, azoles, allylamines, flucytosine, and echinocandins.[3] The azoles and the allylamines inhibit ergosterol biosynthesis; the polyenes bind to ergosterol in the plasma membrane; flucytosine inhibits DNA synthesis; the echinocandins inhibit cell wall synthesis within fungi.[4] Common forms of resistance to these mechanisms include membrane-associated drug efflux that move the drug outside of the cell, site specific mutations that change the binding of the drug to the target, and the development of biofilms that make it difficult for a drug to penetrate and localize in the correct area. As a result, it is crucially important to have effective treatments against fungal infections.

3.3 Introduction to the pyonitrins

In the Clardy lab at Harvard, Mevers et al. discovered a series of natural products from extracts of insect-derived bacteria that had activity against *Candida albicans*.[5] The compounds were isolated from the organism *Pseudomonas protegens* and were found to have both *in vitro* activity against *Candida albicans* cultures as well as *in vivo* activity in a murine model of *C. albicans* infection. Pyonitrins A-D (**3.1** – **3.4**) were eventually isolated and were determined to have structural similarities to two known metabolites that are observed in *Pseudomonas spp.*: pyrrolnitrin and pyochelin (Figure 1).

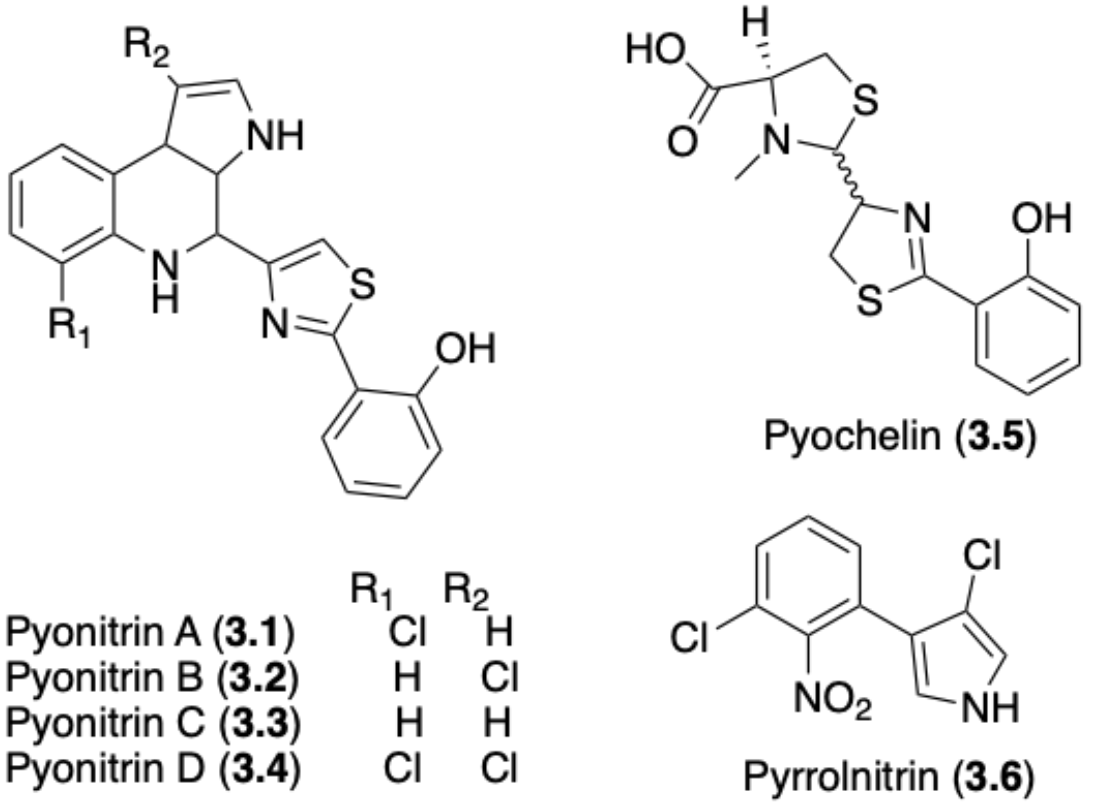

	R_1	R_2
Pyonitrin A (**3.1**)	Cl	H
Pyonitrin B (**3.2**)	H	Cl
Pyonitrin C (**3.3**)	H	H
Pyonitrin D (**3.4**)	Cl	Cl

Figure 1. The pyonitrins and the metabolites they are derived from.

The chemical structure of the pyonitrins resembled both pyrrolnitrin and pyochelin, demonstrating that the pyonitrins were derived from a chemical reaction of the metabolites or their precursors. Using the bioinformatic tool, antiSMASH, analysis showed that the biosynthetic gene clusters are separated by 89kb, which they hypothesized was too large of a gap for the formation of the pyonitrins to be related to the biosynthetic pathway of the pyrrolnitrins or the pyochelins. Genomic studies showed that one piece comes from the shunt product of pyochelin synthesis, aeruginaldehyde and the other comes from amine intermediates in the pyrrolnitrin biosynthesis. Our hypothesis, based on

this information, was that aeruginaldehyde (**3.7**) and amino pyrrolnitrin intermediates undergo a non-enzymatic Pictet-Spengler condensation to give the pyonitrins. Interestingly, this demonstrates the power of non-enzymatic chemistry: a suite of compounds that have activity against *Candida albicans* arose from the serendipitous protein-independent reaction between a shunt product and a biosynthetic intermediate. The chemistry itself is straightforward, relying on the inherent reactivity of the functional groups present in the molecule, but the implications are profound, and can lead to more interesting scaffolds and bioactivity.

3.4 Synthesis of the pyonitrins

As shown above, the pyonitrins were postulated to be produced in the fermentation conditions via a non-enzymatic Pictet-Spengler condensation between aeruginaldehyde and various amino pyrrolnitrin intermediates. The amounts obtained via traditional isolation by the Clardy lab was approximately 0.5mg of pyonitrins A and B and only trace amounts of pyonitrins C and D. A biomimetic total synthesis would alleviate the quantity issues for additional testing, but we also wanted to look at the non-enzymatic Pictet-Spengler reaction that forms the compounds. Using the ^{15}N-based NMR studies the lab has used in the past with the discoipyrroles, we also wanted to elucidate the non-enzymatic mechanism of pyonitrin formation.[6] This would allow us to see the particular way the molecule comes together as well as determine structural

components of the molecule that are necessary for the reaction in order to make interesting synthetic analogs. We modeled the synthesis after the Clardy biosynthetic pathway. By synthesizing the aminopyrrolnitrins and aeruginaldehyde, we were able to obtain the pyonitrins in the same manner (Figure 2).

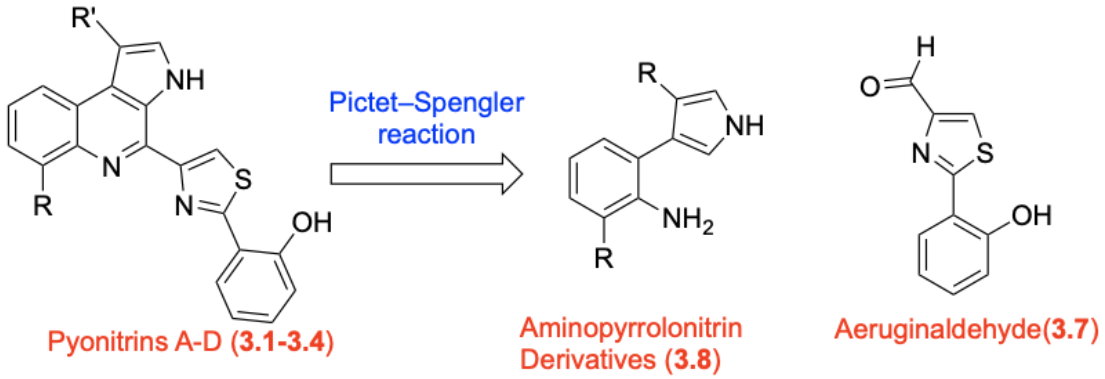

Figure 2. Retrosynthesis of the pyonitrins.

Synthesis of **3.7** was started from condensation of L-cysteine methyl ester hydrochloride (**3.9**) and 2-hydroxy cyanobenzene (**3.10**) to afford thiazoline derivative (**3.11**) in 77% yield.[7] Dehydrogenation of **3.11** with bromotrichloromethane and DBU at −20 °C gave thiazole (**3.12**) as a sole product in quantitative yield.[8] The methyl ester was hydrolyzed to the acid using lithium hydroxide and transformed into a Weinreb amide (**3.13**) using standard conditions. Reduction of **3.13** with Lithium Aluminum Hydride afforded **7** in excellent yield (Scheme 1).

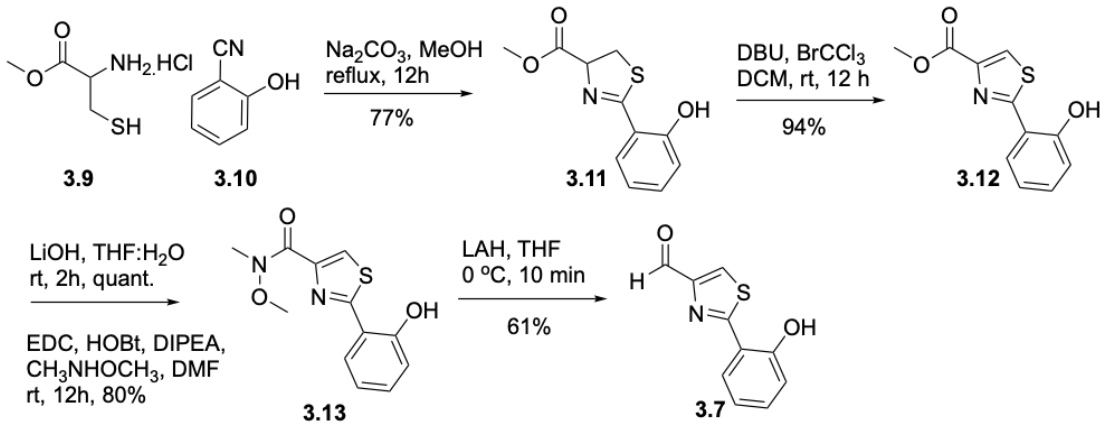

Scheme 1. Synthesis of aeruginaldehyde.

Synthesis of pyonitrins A–D began with Suzuki–Miyaura cross-couplings of the pyrrolepinacolboronote esters (**3.16–3.17**) and the corresponding aniline (**3.14–3.15**) derivatives in the presence of catalytic palladium diacetate (SPhos, K_3PO4, aq. nBuOH at rt) to obtain compounds **3.18–3.21** in 65–90% yield.[9] Final preparation of the aminopyrrolnitrin analogs **3.22–3.25** with differing chlorination patterns was achieved by removal of the silyl protecting group using TBAF. With the coupling partners in hand, we turned our attention to the final Pictet–Spengler reaction. To mimic the aqueous fermentation conditions, we attempted the Pictet–Spengler reaction of **3.22** and **3.7** in water at room temperature for 36 hours under acidic conditions (10% TFA).[10] Under these conditions, **3.1** precipitated out of the aqueous solution with an overall yield of 56%.

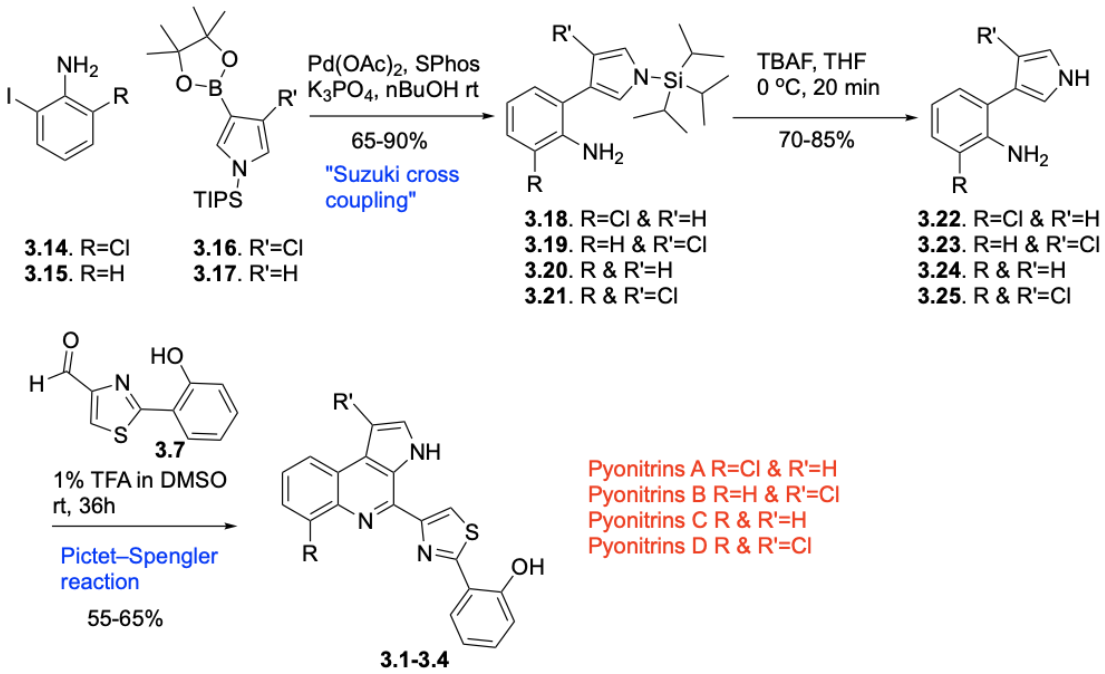

Scheme 2. Synthesis of the aminopyrrolnitrins.

While conditions for the Pictet–Spengler reaction could clearly be optimized, we were looking for conditions that would be compatible with NMR studies, such as $^{1}H–^{15}N$ HMBC NMR spectroscopy, to resolve the reaction pathway. As the aqueous conditions led to precipitation of **3.1**, we looked to the use of organic solvent to keep the product in solution. The Pictet–Spengler reaction of **3.22** and **3.7** in DMSO with TFA (1%) at room temperature for 36 hours led to the production of pyonitrin A in 61% yield. The structure of synthetic pyonitrin A was confirmed by comparison of our NMR and high-resolution mass spectral data with the literature report (Table 1). The synthesis of the remaining pyonitrins B–D from the corresponding aminopyrrolnitrins **3.23**, **3.24**, and **3.25** and **3.7** was achieved using the developed Pictet–Spengler reaction protocol (1% TFA in DMSO solvent for 36 hours) (Scheme 2).

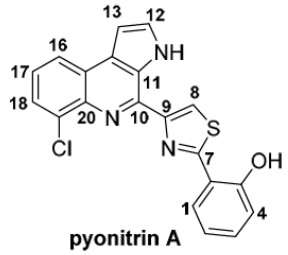

pyonitrin A

No	^{1}H NMR natural (600 MHz)	^{1}H NMR synthetic (500 MHz)	Difference in ppm	^{13}C NMR natural (600 MHz)	^{13}C NMR synthetic (500 MHz)	Difference in ppm
1	8.70 (d, 7.8)	8.75 (dd, *J* = 7.8, 1.2 Hz, 1H)	0.05	128.7 CH	128.5	0.2
2	7.00 (t, 7.5)	7.10 (t, *J* = 8.1 Hz, 1H)	0.10	118.9 CH	119.5	0.6
3	7.34 (t, 7.6)	7.39 (m, 1H),	0.05	131.6 CH	131.1	0.5
4	7.07 (t, 8.2)	7.08 (t, *J* = 7.2 Hz, 1H)	0.01	117.1 CH	116.2	0.9
5				157.3 C	155.1	2.2
6				119.9 C	119.4	0.5
7				164.4 C	163.5	0.9
8	8.64 (s)	8.70 (s, 1H)	0.06	121.4 C	121.4	-
9				153.2 C	152.9	0.3
10				139.8 C	139.2	0.6
11				126.7 C	126.2	0.5
12	7.85 (d, 2.9)	7.85 (t, *J* = 2.7 Hz, 1H)	-	130.1 CH	129.6	0.5
13	7.29 (d, 2.9)	7.31 (t, *J* = 2.0 Hz, 1H)	0.02	101.7 CH	101.3	0.4
14				130.2 C	129.6	0.6
15				125.1 C	125.5	0.4
16	8.32 (d, 8.0)	8.34 (dd, *J* = 8.1, 1.1 Hz, 1H)	0.02	122.9 CH	122.5	0.4
17	7.54 (d, 7.8)	7.55 (t, *J* = 7.8 Hz, 1H)	0.01	126.1 CH	125.6	0.5
18	7.76 (d, 7.4)	7.77 (dd, *J* = 7.4, 1.0 Hz, 1H)	0.01	126.7 CH	126.2	0.5
19				132.8	132.4	0.4
20				138.2	137.7	0.5
NH	11.69 (bs)	11.68	0.01			
OH		11.18				

Table 1. NMR data comparison of synthesized pyonitrin A and literature values.

In natural product biosynthesis, the Pictet–Spengler condensation is typically a highly regulated enzyme catalyzed process, and **3.1–3.4** are the first examples of the nonenzymatic Pictet–Spengler condensation in natural products.[5] Similar to our previous work on nonenzymatic

condensation/cyclization transformations, such as the discoipyrroles, our goal was to monitor the formation and disappearance of key intermediates in the nonenzymatic formation of the pyonitrins in real time. We wanted to exploit the large chemical shift range of ^{15}N NMR due to the electronic interactions involving the lone pair of electrons on the nitrogen atoms.[11] To this end, we have utilized heteronuclear multiple-bond correlation (HMBC) NMR experiments to identify ^{1}H–^{15}N heteronuclear correlation of key intermediates formed in real time. To create a probe for both structural changes and intermolecular interactions in compounds that contain nitrogen atoms with changing chemical environments, an ^{15}N-labeled starting material was required. As a result, we began our NMR study of the abiotic formation of the pyonitrins with the synthesis and utilization of ^{15}N-labeled aminopyrrolnitrin (**3.26**), whereby the aniline contained the ^{15}N isotope label.

All the NMR experiments were performed using **3.26** (1 equiv) and **3.7** (1 equiv) in 1% TFA in 700 µL of DMSO-d_6. Experimentally we began by carrying out the Pictet–Spengler condensation with **3.26** and conducted continuous reaction monitoring in 30-minute intervals for 48 hours using 1H–15N HMBC. **3.26** has a ^{15}N shift of 57.8 ppm and a strong correlation to aromatic protons of the aniline ring at 6.60 and 7.09 ppm (Figure 3). Immediately (30 min) after addition of **3.26** and **3.7** in 1% trifluoroacetic acid in DMSO-d_6, a new, strong signal appeared at δ ^{15}N 70.7 ppm with HMBC correlation to protons at 6.09, 6.57, 6.95, 6.96, 7.13, and 7.18 ppm suggesting the formation of a 1,2-

dihydroquinoline moiety (**3.28**). The cross peak with a $^{1}H–^{15}N$ shift of 11.00 and 151.73 ppm corresponds to nitrogen of the pyrrole on **3.28**. This was surprising since we expected to see the formation of the imine intermediate (**3.27**) prior to cyclization. After 90 min, the $^{1}H–^{15}N$ HMBC correlations showed a new ^{15}N signal at 270 ppm appears with correlations to protons at 8.70, 8.34, 7.78, 7.54 ppm, representing formation of ^{15}N-labeled pyonitrin A (**3.29**). These were the only intermediates observed in the reaction. We stopped the NMR experiment after 48 hours, and the ratio of the product to **3.28** was determined to be 1:2 via a ^{1}H NMR (Figure 3 and video 1 (added as a supplemental file)). The reaction was allowed to continue for an additional 48 hours to obtain complete conversion to **3.29**.

Figure 3 (next page) NMR study of ^{15}N aminopyonitrin and aeruginaldehyde. (a) Formation of pyonitrin A along with the intermediates. (b) Representative time points from $^{1}H–^{15}N$ HMBC experiments.

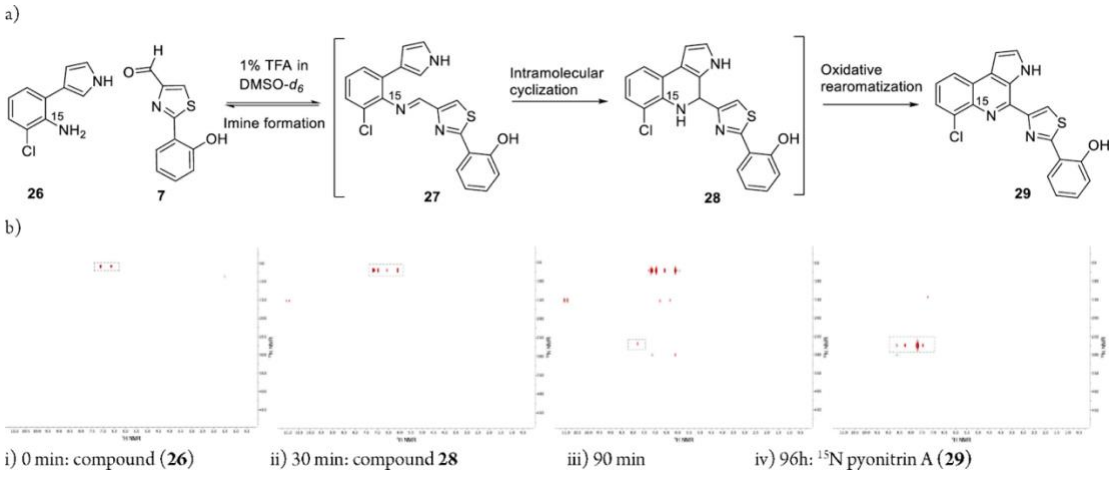

When compared to the media fermentation conditions, a 1% solution of TFA in DMSO-d_6 is far too acidic and might promote the rapid cyclization of **3.27** to **3.28**. We decided to lower the percentage of TFA and redo the reaction to try and detect the formation of **3.27**. With samples of ^{15}N-labeled aminopyrrolnitrin **3.26**, aeruginaldehyde **3.7**, pyonitrin A, and 1,2-dihydroquinoline **3.28** we reran the experiment using only ^{1}H NMR. The experimental design was as follows: Using **3.26** (1 equiv) and **3.7** (1 equiv) in 0.05% TFA in DMSO-d_6, an array of 1 scan ^{1}H NMR experiments were run and the spectra were compared against the starting materials and products, including the dihydroquinoline intermediate **3.28** (Figure 4). Interestingly, as soon as the starting materials were added together, we could immediately see the formation of **3.28** and not **3.27** like we expected. This might be because as soon as the imine intermediate is formed, the inherent reactivity and proximity of the imine allow for immediate cyclization to **3.28**.

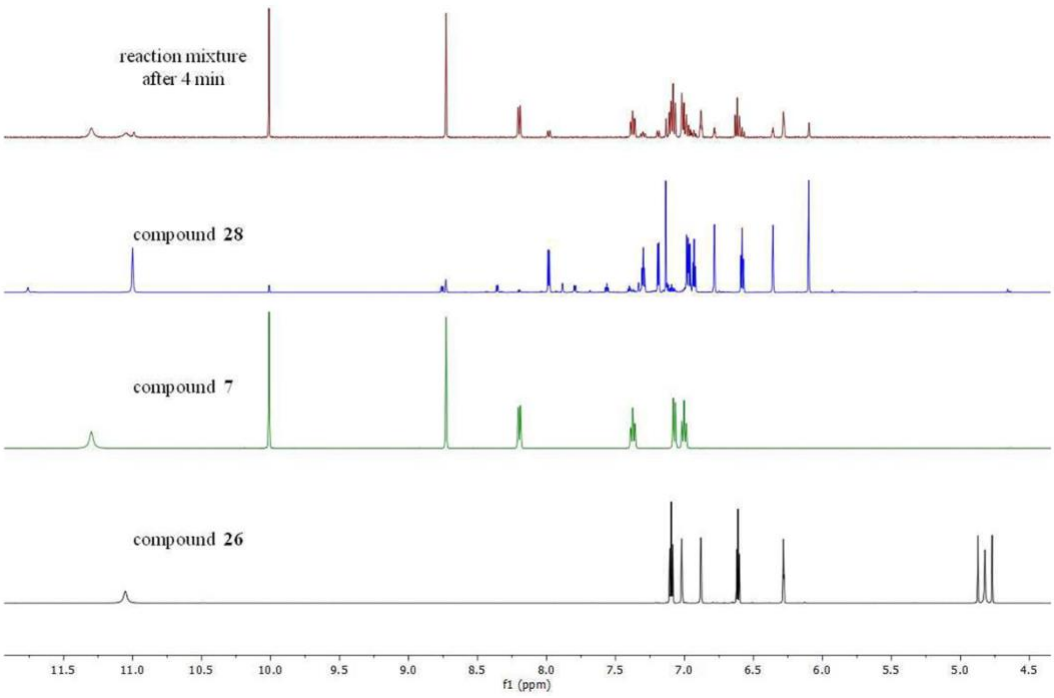

Figure 4. Real time investigation of imine 3.27 formation by comparison of 1H NMR of starting materials 3.26, 3.7 and intermediate 3.28.

We believe this is significant in context to the biological system since the imine intermediate that is formed from the reaction of aminopyrrolnitrin and aeruginaldehyde is not observed in the study. The low probability that two biosynthetic intermediates come together in the bacterial milieu to form the imine intermediate makes the inherent reactivity of the two starting materials imperative for pyonitrin formation. Interaction between the two starting materials in the biological system and subsequent imine formation is the limiting factor in the formation of pyonitrin A. As a result, potential reversibility of imine formation would hinder conversion to the final product. The fast and

spontaneous cyclization of the imine drives formation of the pyonitrin A from any aminopyrrolnitrin and aeruginaldehyde molecules.

Several microbial fermentations lead to the co-occurrence of aldehydes and amines. Many of these, however, do not lead to the production of a new chemical. A vast number of aldehyde and amine reactions are in equilibrium with the imine product. Depending on the conditions, the equilibrium can lie with the starting materials. For these reactions to proceed efficiently, especially in the case of starting materials in low concentrations, a strong driving force is needed to shift the equilibrium toward the imine. In the case of the pyonitrins, irreversible cyclization causes the equilibrium to shift toward a novel natural product.

3.5 Synthesis of pyonitrin/discoipyrrole chimeras

With the non-enzymatic mechanism of the pyonitrins as well as the discoipyrroles (from previous lab work) in hand, we thought to create novel unnatural natural products by exploiting common non-enzymatic mechanisms (aldehyde reacting with an amine). In the discoipyrrole A mechanism, 4-hydroxysattabacin reacts with 4-hydroxybenzaldehyde and anthranilic acid to give the natural product. To create these new chimeric natural products, we exchanged the 4-hydroxybenzaldehyde in the discoipyrrole mechanism with aeruginaldehyde in the pyonitrin synthesis (Figure 5).

Figure 5. Non-enzymatic reaction to form discoipyrrole A and discoipyrrole/pyonitrin hybrid.

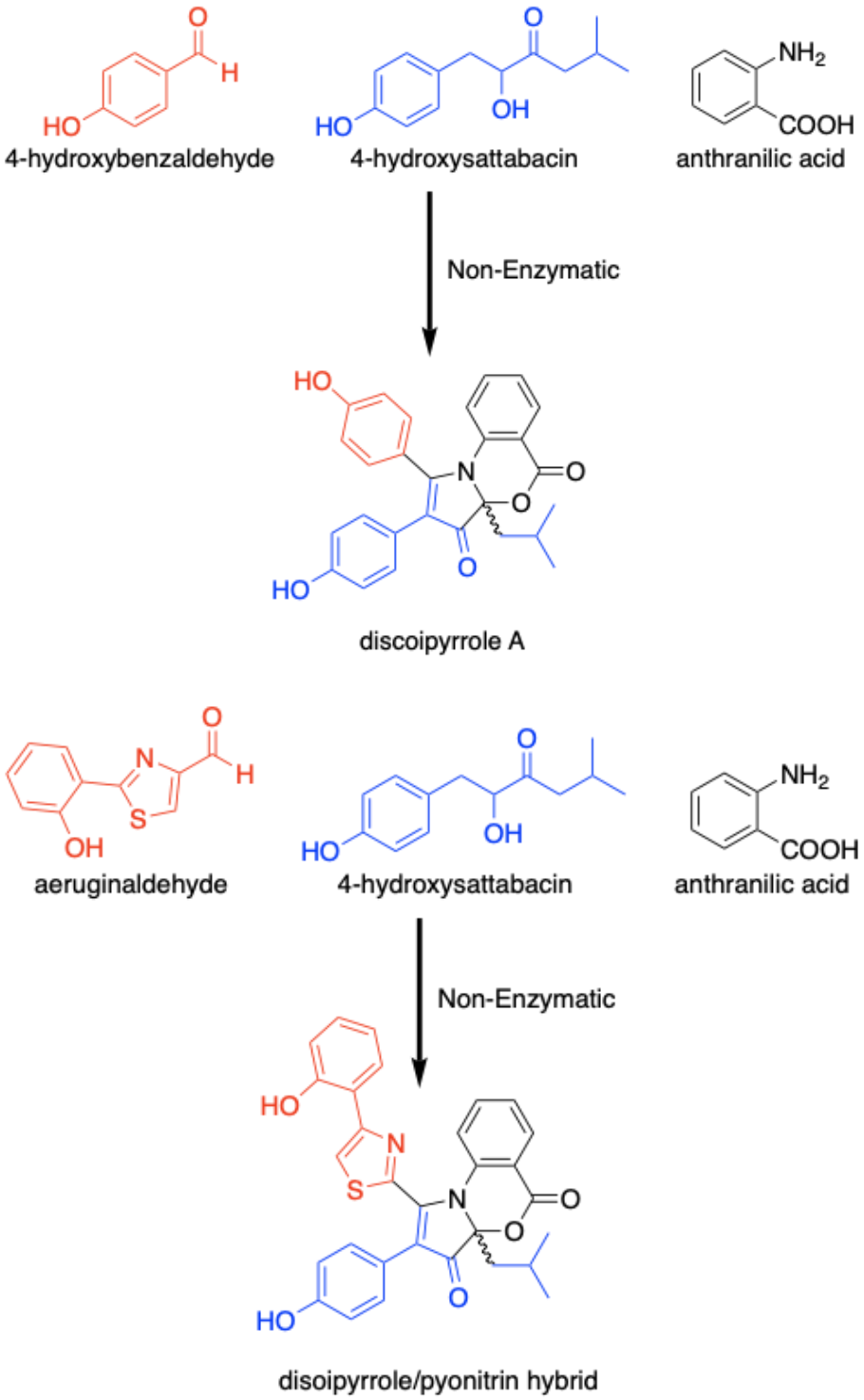

Aeruginaldehyde was synthesized in the same manner as the pyonitrin synthesis. Another aeruginaldehyde analog was created by replacing the hydroxyl group of **3.10** with a chlorine. The synthesis was analogous to that of the hydroxyl aeruginaldehyde and is shown below (scheme 3).

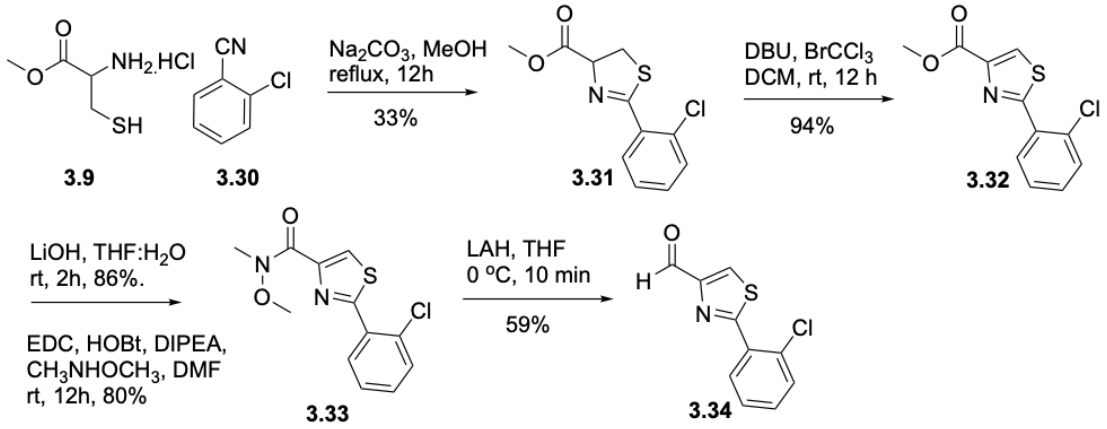

Scheme 3: Synthesis of chloroaeruginaldehyde.

4-methoxy sattabacin was synthesized in lieu of the hydroxyl version for ease of synthesis (Scheme 4).[12]

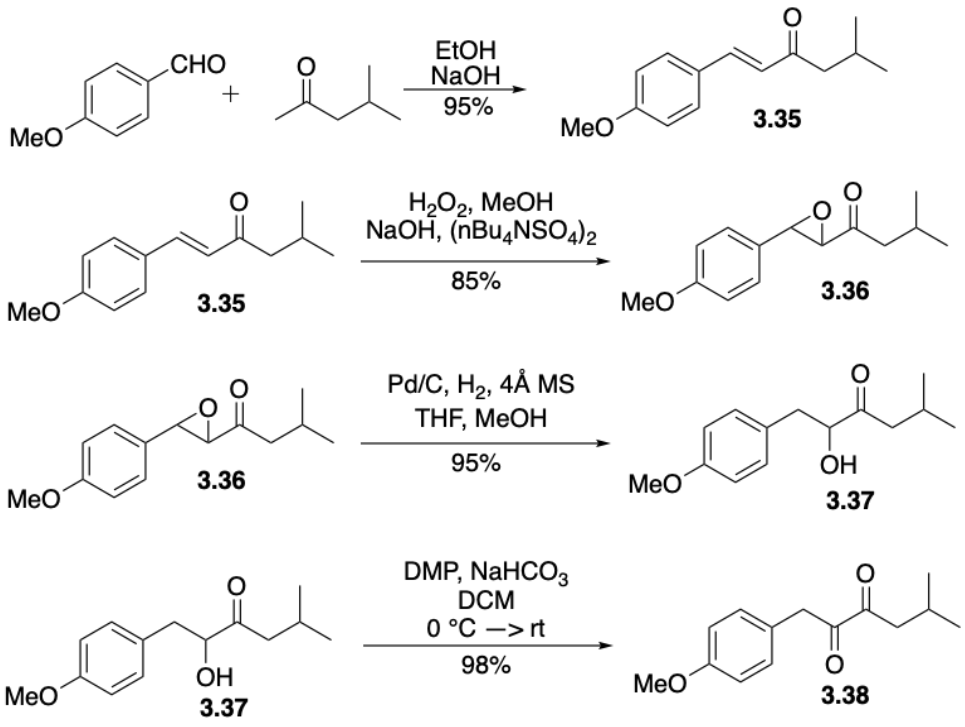

Scheme 4. Synthesis of oxidized 4-methoxy sattabacin.

4-methoxybenzaldehyde underwent a aldol condensation with 4-methyl 2-pentanone with NaOH in ethanol in excellent yield (**3.35**, 95% yield). **3.35** was then oxidized using hydrogen peroxide and tertbutylammonium peroxysulfate with NaOH in MeOH to give the epoxide **3.36** in 85% yield. The epoxide is reduced via 10% Palladium on carbon in a THF:MeOH mixture to give **3.37** in 95% yield. FInally, the hydroxyl is oxidized using DMP to give the 1,2-diketone **3.38** in 98% yield. The diketone was used instead of the alpha hydroxyl because in the discoipyrrole system, the diketone is the active molecule in the reaction. The alpha hydroxyl gets oxidized in air to the diketone in order to begin the non-enzymatic reaction. To alleviate the need for an air oxidation, 4-

methoxy sattabacin was oxidized to the diketone prior to the reaction. With 4-methoxy sattabacin and both the chloro- and hydroxy- aeruginaldehyde in hand, the discoipyrrole-like multicomponent reaction was run (Scheme 5). Unlike the discoipyrroles, the anthranilic acid did not fully cyclize with the pyrrole core to give the expected product. Fortunately, the rest of the core was intact. The new hybrid unnatural natural products were coined the aerupyrroles.

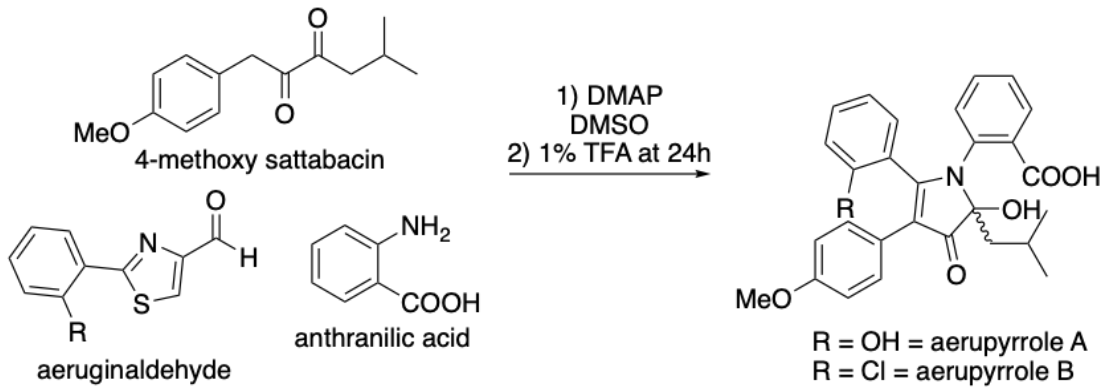

Scheme 5. Synthesis of aerupyrroles.

3.6 Conclusion

The formation of the pyonitrins and the aerupyrroles represent a way to create natural products without performing total or semi-synthesis. By exploiting the non-enzymatic chemistry inherently present in the discoipyrroles and the pyonitrins of these molecules, new scaffolds were able to be created. This methodology of fusion can be used for other natural products that contain non-enzymatic steps in their biosynthesis or even shunt metabolites or

intermediates. More work needs to be done, but there also is potential for ameliorated or new bioactivity because of these chimeric additions.

3.7 Experimental Procedures

Methods and Materials

Unless otherwise noted, commercially available materials were used without further purification. Reactions were performed under an atmosphere of nitrogen with magnetic stirring unless noted otherwise. Flash chromatography (FC) was performed using E. Merck silica gel 60 (240–400 mesh). Thin layer chromatography was performed using precoated plates purchased from E. Merck (silica gel 60 PF_{254}, 0.25 mm). Nuclear magnetic resonance (NMR) spectra were recorded on a Bruker Avance III HD 800 MHz and Bruker Avance III HD 500 MHz spectrometer at operating frequencies of 800/500 MHz (^{1}H NMR) or 200/125 MHz (^{13}C NMR). Chemical shifts (δ) are given in ppm relative to residual solvent chloroform ($CDCl_3$: ^{1}H, δ = 7.26 ppm, ^{13}C, δ = 77.16 ppm), dimethyl sulfoxide ($(CD_3)_2SO$:

^{1}H, δ = 2.50 ppm, ^{13}C, δ = 39.52 ppm) and coupling constants (*J*) in Hz. Multiplicity is tabulated as s for singlet, d for doublet, t for triplet, q for quadruplet, and m for multiplet and br when the signal in question is broadened. Electrospray ionization mass spectra (ESI-MS) were recorded on a LTQ-Orbitrap Velos Pro MS. Chemicals were purchased from Aldrich, Fisher, Alfa

Aesar, TCI, or Oakwood chemicals and used without purification. ^{15}N-N_2Na was purchased from Cambridge Isotope Laboratories, Inc. and also used without purification.

General procedures:

General procedure 1. Suzuki cross-coupling.

In an oven-dried round bottom flask, aromatic halide (1.0 equiv), N-(TIPS) pyrrole pinacol boronate (1.2 equiv), palladium acetate [$Pd(OAc)_2$, 0.05 equiv], 2-Dicyclohexyl-phosphino-2′,6′-dimethoxybiphenyl (SPhos, 0.10 equiv), and potassium phosphate (K_3PO_4, 2.0 equiv) was added under inert atmosphere followed by addition of the solvent system (2.0 mL/mmol aryl halide), consisting of degassed *n*-butanol (*n*-BuOH) and degassed deionized water in the ratio of 2.5:1. The resulting mixture was stirred at room temperature for 16 h. The crude reaction mixture was then filtered through a plug of silica gel using EtOAc eluent and concentrated in vacuo. Purification by column chromatography over silica gel eluting with ethyl acetate and hexanes provided the desired TIPS-protected phenylpyrrole.

General procedure 2. Removal of silyl protecting group using TBAF.

To a solution of TIPS-protected phenylpyrrole (1.0 equiv) in THF (2.0 mL/mmol SM) at 0 ^oC was added tetrabutylammonium fluoride (TBAF, 1.0 M in THF, 2.0 equiv) dropwise. Allow to stir reaction mixture for 15 min at same temperature the reaction progress monitored by TLC. The reaction mixture was quenched

with saturated ammonium chloride (NH_4Cl) solution and the resulting biphasic mixture was transferred to a separatory funnel. The organic and aqueous layers were separated, and the aqueous layer was extracted with ethyl acetate. The organic layers were combined and washed with saturated sodium chloride, dried with sodium sulfate, and concentrated under reduced pressure to afford the crude product. Subsequent purification by column chromatography over deactivated silica gel (5% NEt_3), eluting with ethyl acetate and hexanes afforded the desilylated product

General procedure 3. Pictet-Spengler reaction.

1% solution of TFA in DMSO (1 mL), aldehyde (1 eq) and pyrrole aniline (1 eq) were added at rt. The mixture was further stirred at ambient temperature and the progress of reaction was monitored by TLC. Upon completion of the reaction, saturated aqueous $NaHCO_3$ was added to quench the acid in the reaction mixture. The product was extracted using ethyl acetate (20 mL) and the organic layer was washed with water (2 x 10 mL), brine solution (1 x 10 mL) and finally dried over anhydrous sodium sulfate. It was then evaporated in vacuo to obtain a residue and purified by column chromatography eluting with ethyl acetate and hexanes to afford pure pyonitrins.

General 2D ^{1}H-^{15}N HMBC monitoring of Pictet-Spengler condensation:

^{15}N-dechloroaminopyrrolnitrin **3.26**, and aeruginaldehyde **3.7** was added to 700 µL of 1% TFA in DMSO-d_6 in a 5 mm thin wall, 8 inch NMR tube (Wilmad) and inserted Bruker Avance III HD 800 MHz instrument. The ^{1}H-^{15}N HMBC experiment was optimized for $^{N}J_{NH}$ = 5 Hz. The ^{1}H-^{15}N HMBC data were acquired as 2048 x 172 points with 8 transients per t1 increment. A delay of 1 second was used between transients taking 27 minutes and 43 seconds per spectrum. Instrument was tuned, locked, and shimmed. NMR experiments were then queued to run in the following order: ^{1}H NMR experiment (32 scans taking 2 minutes and 15 seconds) followed by ^{1}H-^{15}N HMBC (8 scans of 86 increments taking 27 minutes and 43 seconds). Therefore, a single ^{1}H NMR spectrum was collected once every 30 min along with one HMBC spectra constantly for 48 hours.

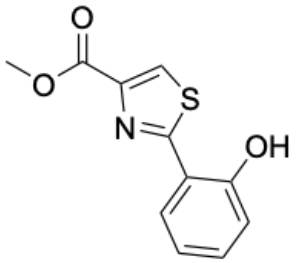

Synthesis of methyl 2-(2-hydroxyphenyl)thiazole-4-carboxylate (3.12)

To the anhydrous methanol solution (50 mL) of the 2-hydroxybenzonitrile **3.10** (2 gm, 16.8 mmol) and anhydrous Na_2CO_3 (1.7 gm, 16.8 mmol) the L-Cysteine methyl ester hydrochloride **3.9** (7.1 gm 42.01 mmol) was added, then the resulting mixture was stirred at 80 ^{o}C in oil bath for 12 h, cooled to room temperature. The insoluble solid was filtered and the filtrate was then

concentrated. The crude product was dissolved in water (30 mL) and extracted with ethyl acetate (2 x 50 mL). The combined organics were then washed with brine and dried over sodium sulfate and concentrated to obtain pure thiazoline product **3.11** (3 gm, 77% yield) was used for next step without further purification.

Thiazoline **3.11** (3 gm, 0.012 mol) was dissolved in dry CH_2Cl_2 (150 mL) and cooled to -20 °C. DBU (1.2 mL, 0.012 mol) was added and the reaction mixture was stirred for 5 min. at -20 °C, treated with $BrCCl_3$ 3 (3.8 mL, 0.025 mol) and stirred at room temperature for 12h. The reaction mixture was then diluted with ammonium chloride (50 mL) and the aqueous layer was extracted with dichloromethane (3 x 100 mL each). After drying over sodium sulfate the solvent was removed under reduced pressure, and purified by column chromatography over silica gel, eluting with ethyl acetate and hexanes to furnished 2.8 gm of methyl 2-(2-hydroxyphenyl)thiazole-4-carboxylate **3.12** (94% yield) as a colorless solid.

^{1}H NMR (500 MHz, $CDCl_3$) δ 11.84 (s, 1H), 8.11 (s, 1H), 7.62 (dd, *J* = 7.8, 1.2 Hz, 1H), 7.36 (td, *J* = 7.7, 1.2 Hz, 1H), 7.09 (d, *J* = 8.3 Hz, 1H), 6.93 (td, *J* = 7.7, 0.9 Hz, 1H), 3.97 (s, 3H).

^{13}C NMR (125 MHz, $CDCl_3$) δ 169.7, 161.1, 157.2, 145.9, 132.7, 127.5, 125.3, 119.7, 118.3, 116.4, 52.6.

HRMS (ESI) *m/z*: $[M + H]^+$ Calcd for $C_{11}H_{10}NO_3S$ 236.0381; Found 236.0372

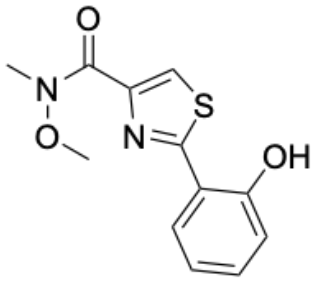

Synthesis of 2-(2-hydroxyphenyl)-N-methoxy-N-methylthiazole-4-carboxamide (3.13)

Methyl 2-(2-hydroxyphenyl) thiazole-4-carboxylate **3.12** (2.8 gm, 0.011 mol) was taken into 50 ml mixture of THF:H_2O:CH_3OH (3:2:1). To this lithium hydroxide (1.0 gm, 0.025 mol) was added and the reaction mixture was stirred at room temperature for 2h. The solvent was removed via rotovap and the reaction mixture was acidified using 1N HCl. The white solid precipitate was filtered and dried over vacuum to obtain (2.6 gm, 98% yield) pure thiazole acid product.

The acid product (2.5 gm, 0.011 mol) was then dissolved in dry DMF (30 mL).To this EDC (2.5 gm, 0.013 mol), HOBt (3.35 gm, 0.024 mol), *N,O*-Dimethylhydroxylamine hydrochloride (1.31 gm, 0.013 mol) and DIPEA (10 mL, 0.056 mol) were added at 0 ^oC and the reaction mixture was stirred at room temperature for 12h. The reaction mixture was diluted with water (50 mL) and extracted with ethyl acetate (100 mL x 2). The combined organic layer was washed with water (50 mL) and brine (50 mL) and dried over sodium sulfate and concentrated to obtain pure white solid product **3.13** (2.4 gm, 80% yield)

^{1}H NMR (500 MHz, $CDCl_3$) δ 11.94 (s, 1H), 8.02 (s, 1H), 7.64 (dd, *J* = 7.8, 1.3 Hz, 1H), 7.35 (td, *J* = 7.9, 1.4 Hz, 1H), 7.07 (dd, *J* = 8.3, 0.7 Hz, 1H), 6.93 (td, *J* = 7.6, 1.0 Hz, 1H), 3.81 (s, 3H), 3.43 (s, 3H).

^{13}C NMR (125 MHz, $CDCl_3$) δ 168.7, 161.7, 157.0, 147.6, 132.5, 127.5, 123.9, 119.7, 118.1, 116.7, 62.0, 34.0

HRMS (ESI) *m/z*: $[M + H]^+$ Calcd for $C_{12}H_{13}N_2O_3S$ 265.0646; Found 265.0635

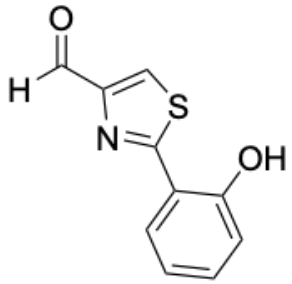

Synthesis of 2-(2-hydroxyphenyl)thiazole-4-carbaldehyde (3.7)

2-(2-hydroxyphenyl)-N-methoxy-N-methylthiazole-4-carboxamide **3.13** (100 mg, 0.37 mmol) was taken in dry THF (5 mL) and to it 2M solution of lithium aluminium hydride (0.284 mL, 0.56 mmol) was added at 0 ^{o}C. After 10 min the reaction was quenched by adding a saturated solution of ammonium chloride (10 mL) and extracted with ethyl acetate (30 mL x 2). The combined organic layer was washed with water (30 mL) and brine (30 mL) and dried over sodium sulfate and concentrated to obtain pure yellow solid product **3.7** (60 mg, 61% yield).

^{1}H NMR (500 MHz, $CDCl_3$) δ 11.60 (s, 1H), 10.06 (s, 1H), 8.13 (s, 1H), 7.64 (dd, *J* = 7.8, 1.2 Hz, 1H), 7.39 (td, *J* = 7.8, 1.2 Hz, 1H), 7.10 (dd, *J* = 8.3, 0.7 Hz, 1H), 6.95 (td, *J* = 7.6, 0.8 Hz, 1H).

^{13}C NMR (125 MHz, $CDCl_3$) δ 183.5, 170.6, 157.0, 153.7, 133.0, 127.7, 125.2, 119.9, 118.3, 116.2.

HRMS (ESI) *m/z*: $[M + H]^+$ Calcd for $C_{10}H_8NO_2S$ 206.0275; Found 206.0272

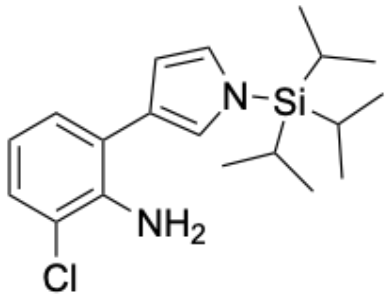

2-chloro-6-(1-(triisopropylsilyl)-1H-pyrrol-3-yl)aniline (3.18)

Following general procedure 1, Compound **3.18** was prepared from 2-chloro-6-iodoaniline **3.14** (250 mg, 0.99 mmol) and **3.17** (415 mg, 1.19 mmol). The crude residue was purified by column chromatography over silica gel (hexane/ethyl acetate = 9/1), affording **3.18** 264 mg (75% yield) as colorless oil.

^{1}H NMR (500 MHz, $CDCl_3$) δ 7.17 (d, *J* = 7.8 Hz, 2H), 6.99 (t, *J* = 1.9 Hz, 1H), 6.88 (t, *J* = 2.2 Hz, 1H), 6.71 (t, *J* = 7.8 Hz, 1H), 6.52 (dd, *J* = 1.5, 2.4 Hz, 1H), 4.39 (s, 2H), 1.50 (sept, *J* = 7.4 Hz, 3H), 1.15 (d, *J* = 7.6 Hz, 18H).

^{13}C NMR (125 MHz, $CDCl_3$) δ 140.6, 128.2, 127.1, 125.1, 124.0, 123.6, 122.7, 119.7, 118.3, 110.8, 17.9, 11.8.

HRMS (ESI) *m/z*: $[M + H]^+$ Calcd for $C_{19}H_{30}ClN_2Si$ 349.1866; Found 349.1869

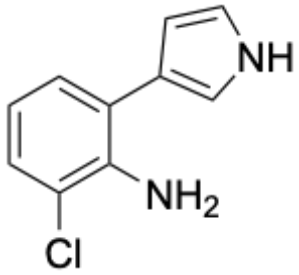

2-chloro-6-(1H-pyrrol-3-yl)aniline (3.22)

Following general procedure 2, **3.22** was prepared from 2-chloro-6-(1-(triisopropylsilyl)-1H-pyrrol-3-yl)aniline **3.18** (50 mg, 0.14 mmol). The crude residue was purified by column chromatography over deactivated silica gel (5% NEt_3) (hexane/ethyl acetate = 2/8), affording compound **3.22** (21 mg) as colorless oil in 76% yield.

^{1}H NMR (500 MHz, $CDCl_3$) δ 8.43 (s, 1H), 7.19 (d, *J* = 8.0 Hz, 1H), 7.15 (d, *J* = 7.5 Hz, 1H), 6.99 (d, *J* = 1.3 Hz, 1H), 6.88 (d, *J* = 1.9 Hz, 1H), 6.71 (t, *J* = 7.8 Hz, 1H), 6.45 (d, *J* = 1.2 Hz, 1H), 4.39 (s, 2H).

^{13}C NMR (125 MHz, $CDCl_3$) δ 140.7, 128.4, 127.3, 123.7, 121.5, 119.7, 118.8, 118.4, 116.5, 108.7.

HRMS (ESI) *m/z*: $[M + H]^+$ Calcd for $C_{10}H_{10}ClN_2$ 193.0532; Found 193.0531

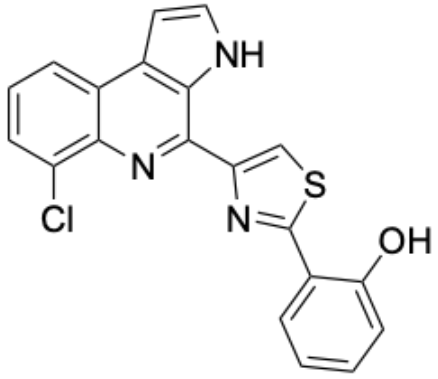

pyonitrin A (3.1)

Following general procedure 3, pyonitrin A was prepared from 2-chloro-6-(1H-pyrrol-3-yl)aniline **3.22** (2 mg, 0.01 mmol) and **3.7** (2.1 mg, 0.01 mmol). The crude residue was purified by column chromatography over silica gel (hexane/ethyl acetate = 4/6), affording pyonitrin A (2.4 mg) as a yellow solid in 61% yield.

^{1}H NMR (500 MHz, DMSO-d_6) δ 11.68 (s, 1H), 11.18 (s, 1H), 8.75 (dd, J = 7.8, 1.2 Hz, 1H), 8.70 (s, 1H), 8.34 (dd, J = 8.1, 1.1 Hz, 1H), 7.85 (t, J = 2.7 Hz, 1H), 7.77 (dd, J = 7.4, 1.0 Hz, 1H), 7.55 (t, J = 7.8 Hz, 1H), 7.39 (m, 1H), 7.31 (t, J = 2.0 Hz, 1H), 7.10 (t, J = 8.1 Hz, 1H), 7.08 (t, J = 7.2 Hz, 1H)

^{13}C NMR (125 MHz, DMSO-d_6) δ 163.5, 155.1, 152.9, 139.3, 137.7, 132.4, 131.2, 129.8, 129.6, 128.5, 126.2, 125.6, 124.7, 122.5, 121.4, 119.5, 119.4, 116.2, 101.3.

HRMS (ESI) m/z: $[M + H]^+$ Calcd for $C_{20}H_{13}ClN_3OS$ 378.0467; Found 378.0460

Synthesis of pyonitrin B:

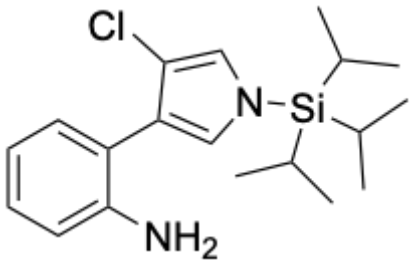

2-(4-chloro-1-(triisopropylsilyl)-1H-pyrrol-3-yl)aniline (3.19)

Following general procedure 1, **3.19** was prepared from 2-iodoaniline **3.15** (180mg, 0.82 mmol) and **3.16** (377 mg, 0.98 mmol). The crude residue was purified by column chromatography over silica gel (hexane/ethyl acetate = 9/1), affording **3.19** (192 mg) as colorless oil in 67% yield.

^{1}H NMR (500 MHz, $CDCl_3$) δ 7.21 (d, *J* = 7.5 Hz, 1H), 7.14 (t, *J* = 7.2 Hz, 1H), 6.79 (m, 4H), 3.81 (s, 2H), 1.45 (Sept, *J* = 7.4 Hz, 3H), 1.13 (d, *J* = 7.5 Hz, 18H).

^{13}C NMR (125 MHz, $CDCl_3$) δ 144.9, 131.6, 128.4, 123.7, 121.8, 121.7, 119.5, 118.3, 115.5, 113.8, 17.9, 11.7.

HRMS (ESI) *m/z*: $[M + H]^+$ Calcd for $C_{19}H_{30}ClN_2Si$ 349.1866; Found 349.1868

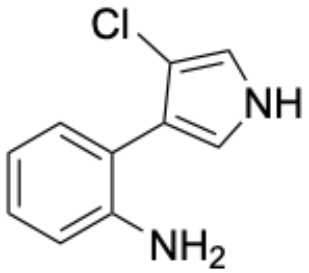

2-(4-chloro-1H-pyrrol-3-yl)aniline (3.23)

Following general procedure 2, **3.23** was prepared from 2-(4-chloro-1-(triisopropylsilyl)-1H-pyrrol-3-yl)aniline **3.19** (60 mg, 0.17 mmol). The crude residue was purified by column chromatography over deactivated silica gel (5% NEt_3) (hexane/ethyl acetate = 2/8), affording **3.23** (28 mg) as colorless oil in 84% yield.

^{1}H NMR (500 MHz, $CDCl_3$) δ 8.39 (s, 1H), 7.20 (dd, *J* = 7.4, 1.0 Hz, 1H), 7.16 (td, *J* = 7.9, 1.3 Hz, 1H), 6.83 – 6.75 (m, 4H), 3.83 (s, 2H).

^{13}C NMR (125 MHz, $CDCl_3$) δ 144.9, 131.8, 128.6, 119.7, 119.3, 118.4, 117.2, 116.1, 115.5, 112.1.

HRMS (ESI) *m/z*: $[M + H]^+$ Calcd for $C_{10}H_{10}ClN_2$ 193.0532; Found 193.0530

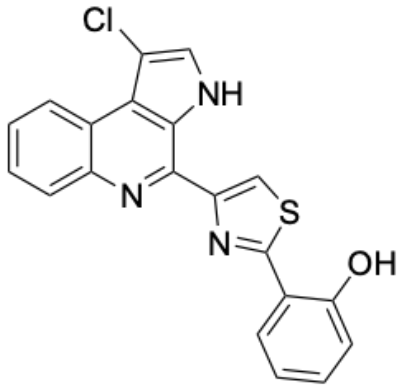

pyonitrin B (3.2)

Following general procedure 3, **3.2** was prepared from 2-(4-chloro-1H-pyrrol-3-yl)aniline **3.23** (14 mg, 0.07 mmol) and **7** (15 mg, 0.07 mmol). The crude residue was purified by column chromatography over silica gel (hexane/ethyl acetate = 4/6), affording pyonitrin B (15 mg) as a colorless oil in 55% yield.

^{1}H NMR (800 MHz, DMSO-*d*$_6$) δ 11.83 (s, 1H), 11.20 (s, 1H), 8.86 (dd, *J* = 7.5, 1.4 Hz, 1H), 8.71 (s, 1H), 8.70 (d, *J* = 6.8, 1H), 8.15 (dd, *J* = 7.6, 1.2 Hz, 1H), 7.89 (d, *J* = 2.8 Hz, 1H), 7.70 – 7.67 (m, 2H), 7.40 (dt, *J* = 7.5, 1.4 Hz, 1H), 7.11 (d, *J* = 8.1 Hz, 1H), 7.09 (t, *J* = 7.4 Hz, 1H).

^{13}C NMR (200 MHz, DMSO-*d*$_6$) δ 163.5, 155.1, 152.5, 142.1, 139.3, 131.2, 129.4, 128.5, 126.5, 126.2, 126.0, 125.2, 123.1, 122.3, 121.8, 121.2, 119.5, 119.4, 116.2, 105.2.

HRMS (ESI) *m/z*: $[M + H]^+$ Calcd for $C_{20}H_{13}ClN_3OS$ 378.0467; Found 378.0464

Table 2: Comparisons of NMR data of pyonitrin B isolated and synthetic sample in DMSO-*d_6*

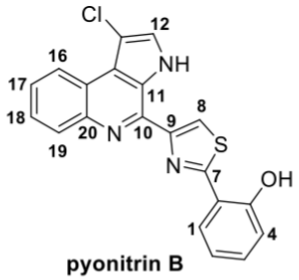

pyonitrin B

No	^{1}H NMR natural (600 MHz)	^{1}H NMR synthetic (500 MHz)	Difference in ppm	^{13}C NMR natural (600 MHz)	^{13}C NMR synthetic (500 MHz)	Difference in ppm
1	8.64 (d, 7.3)	8.70 (dd, *J* = 6.8, 1H)	0.06	128.6	128.5	0.1
2	7.09 (t, 7.7)	7.11 (d, *J* = 8.1 Hz, 1H),	0.02	117.6	116.2	1.4
3	7.30 (t, 7.3)	7.40 (dt, *J* = 7.5, 1.4 Hz, 1H)	0.10	131.5	131.2	0.3
4	6.93 (t, 7.1)	7.09 (t, *J* = 7.4 Hz, 1H)	0.16	118.1	119.4	1.3
5				158.0	155.05	2.95
6				119.8	119.5	0.3
7				164.6	163.5	1.1
8	8.62 (s)	8.71 (s, 1H),	0.09	121.1	121.2	0.1
9				152.7	152.5	0.2
10				140.0	139.3	0.7
11				123.4	121.8	1.6
12	7.88 (s)	7.88 (d, *J* = 2.8 Hz, 1H)	--	126.8	126.5	0.3
13				105.6	105.2	0.4
14				125.8	125.2	0.6
15				123.0	123.1	0.1
16	8.85 (d, 7.9)	8.86 (dd, *J* = 7.5, 1.4 Hz, 1H)	0.01	122.3	122.3	--
17	7.65 (m)	7.70 – 7.67 (m, 2H)	-	126.4	126.0	0.4
18	7.68 (m)		-	126.9	126.2	0.7
19	8.14 (d, 7.7)	8.16 (dd, *J* = 7.6, 1.2 Hz, 1H)	0.02	129.9	129.4	0.3
20				142.7	142.1	0.6
NH		11.83				
OH		11.20				

Synthesis of pyonitrin C:

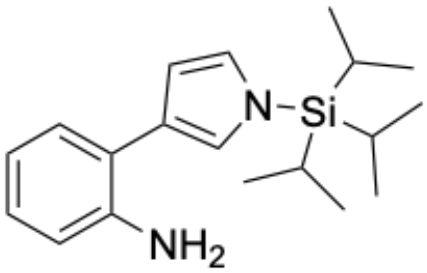

2-(1-(triisopropylsilyl)-1H-pyrrol-3-yl)aniline (3.20)

Following general procedure 1, **3.20** was prepared from 2-iodoaniline **3.15** (150 mg, 0.68 mmol) and **3.17** (286 mg, 0.82 mmol). The crude residue was purified by column chromatography over silica gel (hexane/ethyl acetate = 9/1), affording **3.20** (180 mg) as a colorless oil in 83% yield.

^{1}H NMR (500 MHz, $CDCl_3$) δ 7.26 (dd, *J* = 7.4, 1.2 Hz, 1H), 7.05 (td, *J* = 7.8, 1.4 Hz, 1H), 6.96 (s, 1H), 6.85 (s, 1H), 6.78 (td, *J* = 7.5, 1.0 Hz, 1H), 6.75 (dd, *J* = 7.8, 0.8 Hz, 1H), 6.51 (dd, *J* = 2.4, 1.2 Hz, 1H), 3.94 (s, 2H), 1.48 (sept, *J* = 7.6 Hz, 3H), 1.13 (d, *J* = 7.5 Hz, 18H).

^{13}C NMR (125 MHz, $CDCl_3$) δ 143.8, 129.9, 127.1, 124.9, 124.0, 122.8, 122.5, 118.7, 115.6, 110.9, 18.0, 11.9.

HRMS (ESI) *m/z*: $[M + H]^+$ Calcd for $C_{19}H_{31}N_2Si$ 315.2256; Found 315.2274

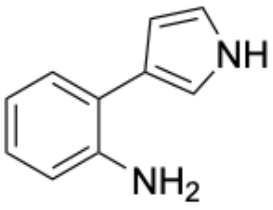

2-(1H-pyrrol-3-yl)aniline (3.24)

Following general procedure 2, **3.24** was prepared from 2-(1-(triisopropylsilyl)-1H-pyrrol-3-yl) aniline **3.20** (50mg, 0.15 mmol). The crude residue was purified by column chromatography over deactivated silica gel (5% NEt_3) (hexane/ethyl acetate = 2/8), affording **3.24** (22 mg) as a colorless oil in 87% yield.

^1H NMR (500 MHz, $CDCl_3$) δ 8.39 (s, 1H), 7.26 (dd, *J* = 7.4, 1.2 Hz, 1H), 7.09 (td, *J* = 7.7, 1.2 Hz, 1H), 7.01 (s, 1H), 6.88 (m, 1H), 6.82-6.77 (m, 2H), 6.47 (m, 1H), 3.73 (s, 2H).

^{13}C NMR (125 MHz, $CDCl_3$) δ 143.9, 130.0, 127.3, 122.4, 122.1, 118.8, 118.6, 116.3, 115.7, 108.9.

HRMS (ESI) *m/z*: $[M + H]^+$ Calcd for $C_{10}H_{11}N_2$ 159.0922; Found 159.0917

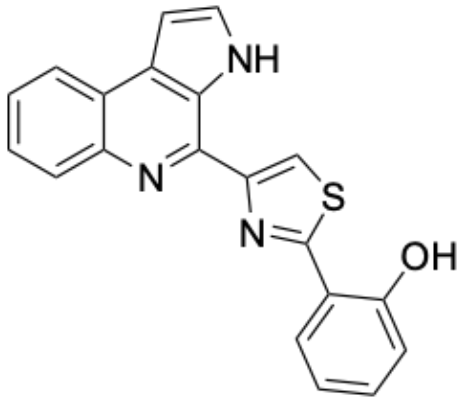

pyonitrin C

Following general procedure 3, pyonitrin C was prepared from 2-(1H-pyrrol-3-yl)aniline **3.24** (10 mg, 0.06 mmol) and **3.7** (13 mg, 0.06 mmol). The crude residue was purified by column chromatography over silica gel (hexane/ethyl acetate = 4/6), affording pyonitrin C (12 mg) as a yellow solid in 55% yield.

^{1}H NMR (800 MHz, DMSO-d_6) δ 11.59 (s, 1H), 8.72 (dd, *J* = 7.8, 1.6 Hz, 1H), 8.65 (s, 1H), 8.33 (dd, *J* = 7.8, 1.3 Hz, 1H), 8.09 (d,*J*= 7.5 Hz, 1H), 7.79 (t, *J* = 2.7 Hz, 1H), 7.62 – 7.56 (m, 2H), 7.37 (t, *J* = 7.3 Hz, 1H), 7.25 (s, 1H), 7.11 (d, *J* = 8.1 Hz, 1H), 7.05 (d, *J* = 7.4 Hz, 1H).

^{13}C NMR (200 MHz, DMSO-d_6) δ 163.4, 153.1, 141.9, 139.2, 131.0, 129.3, 129.0, 128.6, 128.4, 126.0, 125.9, 125.5, 123.2, 123.1, 120.3, 119.5, 119.1, 116.4, 100.8.

HRMS (ESI) *m/z*: $[M + H]^+$ Calcd for $C_{20}H_{14}N_3OS$ 344.0857; Found 344.0844

Synthesis of pyonitrin D:

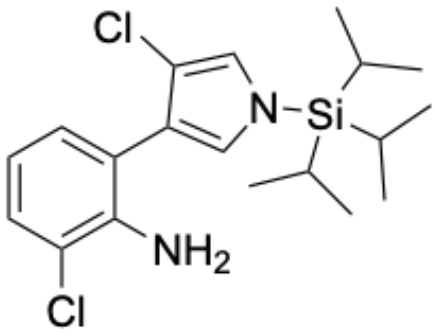

2-chloro-6-(4-chloro-1-(triisopropylsilyl)-1H-pyrrol-3-yl)aniline (3.21)

Following general procedure 1, **3.21** was prepared from 2-chloro-6-iodoaniline **3.14** (190 mg, 0.75 mmol) and **3.16** (345 mg, 0.90 mmol). The crude residue was purified by column chromatography over silica gel (hexane/ethyl acetate = 9/1), affording **3.21** (211 mg) as a colorless oil in 73% yield.

^{1}H NMR (500 MHz, $CDCl_3$) δ 7.23 (dd, *J* = 8.0, 1.2 Hz, 1H), 7.12 (dd, *J* = 7.6, 1.2 Hz, 1H), 6.85 – 6.80 (m, 2H), 6.72 (t, *J* = 7.8 Hz, 1H), 4.23 (s, 2H), 1.45 (sept, *J* = 7.6 Hz, 3H), 1.13 (d, *J* = 7.5 Hz, 18H).

^{13}C NMR (125 MHz, $CDCl_3$) δ 141.7, 130.0, 128.4, 123.4, 122.1, 121.1, 120.7, 119.5, 118.0, 113.7, 17.9, 11.7.

HRMS (ESI) *m/z*: $[M + H]^+$ Calcd for $C_{19}H_{29}Cl_2N_2Si$ 383.1477; Found 383.1479

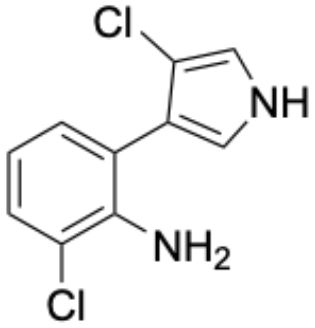

2-chloro-6-(4-chloro-1H-pyrrol-3-yl)aniline (3.25)

Following general procedure 2, **25** was prepared from 2-chloro-6-(4-chloro-1-(triisopropylsilyl)-1H-pyrrol-3-yl) aniline **3.21** (100 mg, 0.26 mmol). The crude residue was purified by column chromatography over deactivated silica gel (5% NEt_3) (hexane/ethyl acetate = 2/8), affording **3.25** (48 mg) as a colorless oil in 81% yield.

^{1}H NMR (500 MHz, $CDCl_3$) δ 8.43 (s, 1H), 7.24 (dd, *J* = 8.0, 1.3 Hz, 1H), 7.09 (dd, *J* = 7.6, 1.2 Hz, 1H), 6.86 (t, *J* = 2.6 Hz, 1H), 6.82 (t, *J* = 2.7 Hz, 1H), 6.72 (t, *J* = 7.8 Hz, 1H), 4.23 (s, 2H).

^{13}C NMR (125 MHz, $CDCl_3$) δ 141.8, 130.2, 128.6, 120.3, 119.5, 119.3, 118.0, 117.3, 116.3, 112.2.

HRMS (ESI) *m/z*: $[M + H]^+$ Calcd for $C_{10}H_9Cl_2N_2$ 227.0142; Found 227.0137

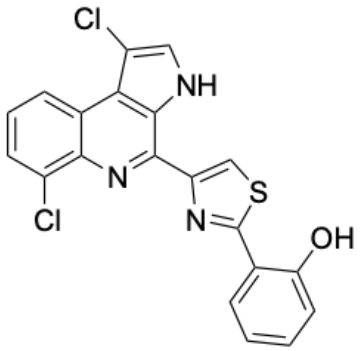

pyonitrin D (3.4)

Following general procedure 2, pyonitrin D was prepared from 2-chloro-6-(4-chloro-1H-pyrrol-3-yl) aniline **3.25** (10 mg, 0.04 mmol) and **3.7** (9 mg, 0.04 mmol). The crude residue was purified by column chromatography over silica gel (hexane/ethyl acetate = 4/6), affording pyonitrin D (12 mg) as a yellow solid in 66% yield.

^{1}H NMR (500 MHz, DMSO-*d*$_6$) δ 11.91 (s, 1H), 11.28 (s, 1H), 8.84 (dd, *J* = 8.3, 1.0 Hz, 1H), 8.73 (s, 1H),8.72 (m, 1H), 7.95 (s, 1H), 7.86 (dd, *J* = 7.5, 1.0 Hz, 1H), 7.64 (t, *J* = 7.9 Hz, 1H), 7.39 (dt, *J* = 8.1, 1.0 Hz, 1H), 7.11 (d, *J* = 8.3 Hz, 1H), 7.08 (t, *J* = 7.5 Hz, 1H).

^{13}C NMR (125 MHz, DMSO-*d*$_6$) δ 163.8, 152.3, 139.4, 138.0, 132.7, 131.2, 128.5, 127.2, 126.9, 126.2, 125.4, 123.8, 123.4, 122.1, 121.0, 119.4, 116.3, 105.5.

HRMS (ESI) *m/z*: $[M + H]^+$ Calcd for $C_{20}H_{12}Cl_2N_3OS$ 412.0078; Found 412.0075

Synthesis of ^{15}N labeled pyonitrin A:

^{15}N labeled 2-chloro-6-iodoaniline (3.26a)

A solution of 2-chloro-6-iodobenzoic acid (281 mg 1.0 mmol) in concentrated sulfuric acid (2.5 mL) was heated to 60^{o}C in oil bath for 1 h. The solution was then cooled to rt before addition of sodium azide [^{15}N] (66 mg, 1.0 mmol). The resulting mixture was left to stir at rt for 42 h before cooling to 0^{o}C and basifying with concentrated ammonium hydroxide. The organics were extracted with ethyl acetate (2 x 20 mL). The organic layers were combined and washed with brine solution (1 x 20 mL), dried over sodium sulfate and concentrated under reduced pressure and purified by column chromatography over silica gel (hexane/ethyl acetate = 7/3), to afford the pure ^{15}N labeled 2-chloro-6-iodoaniline **3.26a** as brown solid (210 mg) in 82% yield.

^{1}H NMR (500 MHz, $CDCl_3$) δ 7.54 (d, *J* = 7.9 Hz, 1H), 7.23 (d, *J* = 7.9 Hz, 1H), 6.41 (t, *J* = 7.9 Hz, 1H), 4.64 - 4.41 (m, 2H).

^{13}C NMR (125 MHz, $CDCl_3$) δ 143.5, 137.6, 129.7, 120.0, 118.0, 83.6.

HRMS (ESI) *m/z*: $[M + H]^+$ Calcd for $C_6H_6ClI^{15}N$ 254.9233; Found 254.9203

Note: We have observed multiplate for NH_2 in proton because equal possibility of the nucleophilic attack of ^{15}N labeled as well as ^{14}N nitrogen from the sodium azide ($Na^{15}NN_2$) in the reaction. The same was confirmed by high resolution mass spectroscopy showed the mass for both ^{14}N and ^{15}N products. HRMS (ESI) *m/z*: $[M + H]^+$ Calcd for C_6H_6ClIN- 253.9233; Found 253.9232

^{15}N labeled 2-chloro-6-(1-(triisopropylsilyl)-1H-pyrrol-3-yl)aniline (3.26b)

Following general procedure 1, **3.26b** was prepared from ^{15}N labelled 2-chloro-6-iodoaniline **3.26a** (100 mg, 0.39 mmol) and **3.17** (164 mg, 0.47 mmol). The crude residue was purified by column chromatography over silica gel (hexane/ethyl acetate = 9/1), affording **3.26b** (111 mg) as a colorless oil in 81% yield.

^{1}H NMR (500 MHz, $CDCl_3$) δ 7.16-7.14 (m, 2H), 6.96 (s, 1H), 6.86 (t, *J* = 2.2 Hz, 1H), 6.69 (t, *J* = 7.8 Hz, 1H), 6.50 (dd, *J* = 2.4, 1.2 Hz 1H), 4.37 (m, 2H), 1.48 (sept, *J* = 7.6 Hz, 3H), 1.13 (d, *J* = 7.5 Hz, 18H)

^{13}C NMR (125 MHz, $CDCl_3$) δ 140.6, 128.2, 127.1, 125.1, 124.1, 123.6, 122.7, 119.7, 118.4, 110.8, 18.0, 11.8.

HRMS (ESI) *m/z*: $[M + H]^+$ Calcd for $C_{19}H_{30}Cl^{15}NNSi$ 350.1866; Found 350.1847 (^{15}N product)

HRMS (ESI) *m/z*: $[M + H]^+$ Calcd for $C_{19}H_{30}ClN_2Si$ 349.1866; Found 349.1871 (^{14}N product)

^{15}N labeled 2-chloro-6-(1H-pyrrol-3-yl)aniline (3.26)

Following general procedure 2, **3.26** was prepared from ^{15}N labelled 2-chloro-6-(1-(triisopropylsilyl)-1H-pyrrol-3-yl)aniline **3.26b** (55 mg, 0.15 mmol). The crude residue was purified by column chromatography over deactivated silica

gel (5% NEt_3) (hexane/ethyl acetate = 2/8), affording **3.26** (22 mg) as a colorless oil in 73% yield.

^{1}H NMR (800 MHz, DMSO-d_6) δ 11.05 (s, 1H), 7.10-7.08 (m, 2H), 7.01 (q, *J* = 1.8 Hz, 1H), 6.87 (q, *J* = 2.5 Hz, 1H), 6.60 (t, *J* = 7.7 Hz, 1H), 6.27 (q, *J* = 2.4 Hz, 1H), 4.87 – 4.76 (m, 2H).

^{13}C NMR (200 MHz, DMSO-d_6) δ 140.6, 127.8, 126.3, 123.6, 120.1, 118.6, 118.2, 117.3, 116.2, 107.3.

HRMS (ESI) *m/z*: $[M + H]^+$ Calcd for $C_{10}H_{10}Cl^{15}NN$ 194.0532; Found 194.0499 (^{15}N product)

HRMS (ESI) *m/z*: $[M + H]^+$ Calcd for $C_{10}H_{10}ClN_2$ 193.0532; Found 193.0428 (^{14}N product)

^{15}N labeled pyonitrin A (3.29)

Following general procedure 3, **3.29** was prepared from ^{15}N labeled 2-chloro-6-(1H-pyrrol-3-yl)aniline **3.26** (10 mg, 0.05 mmol) and **3.7** (10.6 mg, 0.05 mmol). The crude residue was purified by column chromatography over silica gel (hexane/ethyl acetate = 4/6), affording ^{15}N labeled pyonitrin A (14 mg) as a yellow solid in 71% yield.

^{1}H NMR (500 MHz, DMSO-d_6) δ 11.69 (s, 1H), 11.18 (s, 1H), 8.75 (dd,*J* = 7.8, 1.1 Hz, 1H), 8.70 (s, 1H), 8.34 (dd, *J* = 8.1, 1.0 Hz, 1H), 7.85 – 7.83 (m, 1H), 7.78 (d, *J* = 7.4 Hz, 1H), 7.54 (t, *J* = 7.8 Hz, 1H), 7.39 (dt, *J* = 8.2, 1.3 Hz, 1H), 7.31 (s, 1H), 7.11 (d, *J* = 8.0 Hz, 1H), 7.09 (t, *J* = 7.4 Hz, 1H).

^{13}C NMR (125 MHz, DMSO-d_6) δ 163.5, 155.1, 152.9, 139.3, 137.7, 132.4, 131.2, 129.8, 129.6, 128.5, 126.2, 125.6, 124.7, 122.5, 121.4, 119.5, 119.4, 116.2, 101.3.

HRMS (ESI) *m/z*: $[M + H]^+$ Calcd for $C_{20}H_{13}Cl^{15}NN_2OS$ 379.0467; Found 379.0438 (^{15}N product)

HRMS (ESI) *m/z*: $[M + H]^+$ Calcd for $C_{20}H_{13}ClN_3OS$ 378.0467; Found 378.0457 (^{14}N product)

Synthesis and isolation of ^{15}N labeled intermediate (3.28)

1% solution of TFA in DMSO (1 mL), ^{15}N labeled 2-chloro-6-(1H-pyrrol-3-yl)aniline **3.26** (5 mg, 0.025 mmol) and 2-(2-hydroxyphenyl)thiazole-4-carbaldehyde **3.7** (5.31 mg, 0.025 mmol) were added at rt. The mixture was further stirred at ambient temperature for 45 min. Then saturated aqueous $NaHCO_3$ was added to quench the acid in the reaction mixture. The product was extracted using ethyl acetate (10 mL x 2) and the organic layer was washed with water (10 mL x 2), brine solution (10 mL x 1) and finally dried over anhydrous sodium sulfate. It was then evaporated in vacuo to obtain a residue and purified by flash column chromatography silica gel (hexane/ethyl acetate = 4/6), to afford pure ^{15}N labeled intermediate **3.28** (7 mg, 71%).

^{1}H NMR (500 MHz, DMSO-d_6) δ 11.27 (s, 1H), 10.98 (s, 1H), 7.97 (dd, *J* = 7.9, 1.5 Hz, 1H), 7.36 – 7.24 (m, 1H), 7.18 (d, *J* = 6.8 Hz, 1H), 7.12 (s, 1H), 7.00 –

6.94 (m, 2H), 6.92 (t, *J* = 7.5 Hz, 1H), 6.77 (t, *J* = 2.6 Hz, 1H), 6.58 (t, *J* = 7.7 Hz, 1H), 6.35 (t, *J* = 2.4 Hz, 1H), 6.09 (d, *J* = 2.5 Hz, 1H).

^{13}C NMR (125 MHz, DMSO-d_6) δ 165.2, 158.1, 155.3, 136.5, 131.2, 127.5, 125.1, 125.0, 121.0, 119.9, 119.4, 119.3, 118.3, 117.4, 116.8, 116.5, 114.2, 114.0, 102.0, 51.3.

HRMS (ESI) *m/z*: $[M + H]^+$ Calcd for $C_{20}H_{15}Cl^{15}NN_2OS$ 381.0624; Found 381.0600 (^{15}N product)

HRMS (ESI) *m/z*: $[M + H]^+$ Calcd for $C_{20}H_{15}ClN_3OS$ 380.0624; Found 380.0622 (^{14}N product)

Synthesis of Diketone 3.37

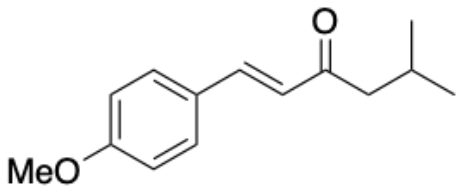

(E)-1-(4-methoxyphenyl)-5-methylhex-1-en-3-one

A solution of p-anisaldehyde (6ml, 50 mmol, 1 equiv) and isobutyl methyl ketone (7.6 ml, 60 mmol, 1.2 equiv) in 50 ml of ethanol was added 10 ml of water and 25 ml of 2.5N NaOH at 0 ºC. The reaction was warm up to room temperature and stirring 24 hours. To the reaction mixture was cool down to 0 ºC and add 2.5N HCl slowly until pH = 7. The crude reaction was concentrated via rotary evaporation. The crude product was recovered by filtration. The

collect product was washed with cold ethanol and water to give pure (E)-1-(4-methoxyphenyl)-5-methylhex-1-en-3-one as light yellow solid (10.5 g, 47.5 mmol, 95% yield) 1H NMR (500 MHz, CDCl3) δ 7.54-7.48 (m, 3H), 6.91 (d, J =8.4Hz,2H), 6.63(d, J = 16.0 Hz, 1H), 3.85 (s, 3H), 2.51 (d, J = 6.9 H z, 2H), 2.23 (m, 1H), 0.98 (d, J= 6.9 Hz, 6H). 13CNMR(125.77 MHz, CDCl3) δ 200.8, 161.9, 142.6, 130.4,127.7, 124.9, 114.8, 55.8, 50.3, 25.8, 23.1.

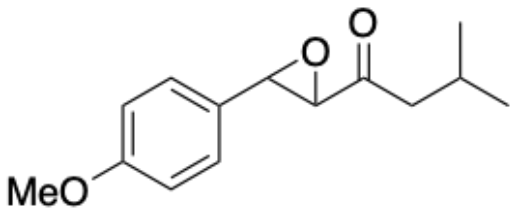

1-(3-(4-methoxyphenyl)oxiran-2-yl)-3-methylbutan-1-one

To a stirred solution of (E)-1-(4-methoxyphenyl)-5-methylhex-1-en-3-one (5.46 g, 25 mmol, 1 equiv) in 100 ml of methanol was added tetrabutylammonium peroxydisulfate (16.7g, 25 mmol, 1 equiv), H2O2 (2.5 ml, 25 mmol, 30% in H2O) and NaOH (1g, 25mmol, 1 equiv) at room temperature. The reaction mixture was stirring for 12 hours. The reaction was added saturated NH4Cl solution (100ml) and extracted with diethyl ether (100ml x 6). The combined ethereal layers were washed with brine, dried over anhydrous MgSO4, and concentrated via rotary evaporation to give pure 1-(3-(4methoxyphenyl)oxiran-2-yl)-3-methylbutan-1-one as white solid. (4.98g, 21.3mmol, 85% yield)

1H NMR (500 MHz, CDCl3) δ 7.20 (d, J = 8.9 Hz, 2H), 6.89 (d, J = 8.9 Hz, 2H), 3.90(d, J = 1.8 Hz, 1H), 3.81 (s,3H),3.50 (d, J = 1.8 Hz, 1H), 2.44 (dd, J = 16.0, 6.4 Hz, 1H), 2.29-2.15 (m, 2H), 1.00-0.94 (m, 6H). 13C NMR (125.77 MHz, CDCl3) δ 206.1, 160.4, 127.3, 114.4, 63.4, 58.0, 55.5, 46.8, 24.4, 22.8, 22.7.

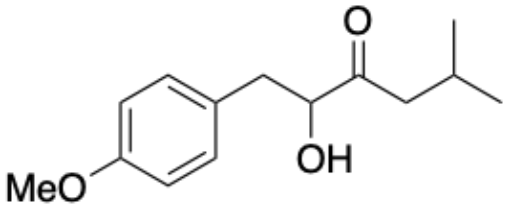

2-hydroxy-1-(4-methoxyphenyl)-5-methylhexan-3-one

To a 250 ml flask equipped with a stir bar was added 4Å powdered molecular sieves (5g) and the flask was flamed-dried under high vacuum. The flask was cooled to room temperature and back filled with argon.1-(3-(4-methoxyphenyl)oxiran-2-yl)-3methylbutan-1-one (4.7g, 20 mmol, 1 equiv), THF (80 ml), methanol (40 ml), and 10%palladium/carbon cat alyst (1g, 0.05 equiv) were added carefully. The mixture was saturated by hydrogen gas and stirred under hydrogen atmosphere for 3 hours. The mixture was filtered through celite, and the filter was wash with 250 ml of ethyl acetate. The crude reaction mixture was concentrated and purified via flash column

chromatography on silica gel with 10 to 15% ethyl acetate in hexanes as eluents. (4.5 g,19 mmol, 95%, yellow oil)

1H NMR (500 MHz, CDCl3) δ 7.11 (m, 2H), 6.80 (m, 2H), 4.26 (m, 1H), 3.72 (s, 3H), 3.54 (d, J = 5.5 Hz, 1H), 3.01 (dd, J = 14.2 Hz, 4.1 Hz, 1H), 2.73 (dd, J = 14.2, 7.3 Hz, 1H), 2.33 (d, J = 6.9 Hz, 2H), 2.13 (m, 1H),0.89 (d, J = 6.8 Hz, 6H). 13C NMR (125.77 MHz, CDCl3) δ 211.3, 158.4, 130.2, 128.6, 113.8, 77.5, 55.0, 47.2, 39.0, 24.3, 22.5, 22.4.

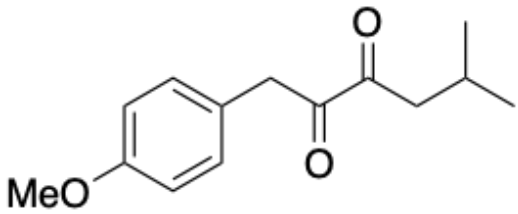

1-(4-methoxyphenyl)-5-methylhexane-2,3-dione

To a 100 ml flame-dried flask was added 2-hydroxy-1-(4-methoxyphenyl)- 5-methylhexan3

one (2.88 g, 12.2 mmol, 1 equiv), dichloromethane (50 ml), and sodiu m bicarbonate (1.23 g, 14.6 mmol, 1.2 equiv). The reaction was cool down to 0 ºC and stirred for 5 minutes, then added DessMartin periodinane (6.2g, 14.6 mmol, 1.2 equiv). The reaction was warmed up to room temperature and stirred for 4 hours. The reaction mixture was filter through celite and concentrated. The crude mixture was dissolved by 100 ml of hexanes and filter through celite, and the filter was washed with 50 ml of hexanes three

times. The organic solution was concentrated and gave pure diketone product. (2.8 g, 12.0 mmol, 98% yield, yellow oil)

1H NMR (500 MHz, CDCl3) δ 7.12 (d, J = 8.7 Hz, 2H), 6.85 (d, J = 8.7 Hz, 2H), 3.96 (s, 2H), 3.79 (s, 3H), 2.57(d, J= 6.9 Hz, 2H) , 2.05 (m, 1H), 0.86 (d, J = 6.8 Hz, 6H). 13CNMR(125 MHz, CDCl3) δ 200.1, 196.9,159.0, 131.0, 130.4,124.3, 114.4, 55.4, 45.2, 42.1, 24.7, 22.6.

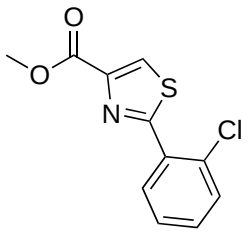

methyl 2-(2-chlorophenyl)thiazole-4-carboxylate

To the anhydrous methanol solution (50 mL) of the 2-chlorobenzonitrile (16.8 mmol) and anhydrous Na_2CO_3 (1.7 gm, 16.8 mmol) the L-Cysteine methyl ester hydrochloride (7.1 gm 42.01 mmol) was added, then the resulting mixture was stirred at 80 ^oC in oil bath for 12 h, cooled to room temperature. The insoluble solid was filtered and the filtrate was then concentrated. The crude product was dissolved in water (30 mL) and extracted with ethyl acetate (2 x 50 mL). The combined organics were then washed with brine and dried over sodium sulfate and concentrated to obtain pure thiazoline product (33% yield) was used for next step without further purification.

Thiazoline (0.012 mol) was dissolved in dry CH_2Cl_2 (150 mL) and cooled to -20 °C. DBU (1.2 mL, 0.012 mol) was added, and the reaction mixture was

stirred for 5 min. at -20 °C, treated with $BrCCl_3$ 3 (3.8 mL, 0.025 mol) and stirred at room temperature for 12h. The reaction mixture was then diluted with ammonium chloride (50 mL) and the aqueous layer was extracted with dichloromethane (3 x 100 mL each). After drying over sodium sulfate the solvent was removed under reduced pressure, and purified by column chromatography over silica gel, eluting with ethyl acetate and hexanes to furnished methyl 2-(2-chlorophenyl)thiazole-4-carboxylate (94% yield) as a colorless solid.

^{1}H NMR (500 MHz, $CDCl_3$) δ 8.32 (s, 1H), 8.29 (m, 1H), 7.50 (m,1H), 7.39 (m, 2H), 3.98 (s, 3H).

^{13}C NMR (125 MHz, $CDCl_3$) δ 164.3, 162.0, 146.4, 132.1, 131.5, 131.2, 131.1, 130.6, 128.8, 127.2, 52.5

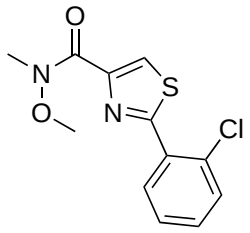

2-(2-chlorophenyl)-*N*-methoxy-*N*-methylthiazole-4-carboxamide

methyl 2-(2-chlorophenyl)thiazole-4-carboxylate (0.011 mol) was taken into 50 ml mixture of $THF:H_2O:CH_3OH$ (3:2:1). To this lithium hydroxide (1.0 gm, 0.025 mol) was added and the reaction mixture was stirred at room temperature for 2h. The solvent was removed via rotovap and the reaction mixture was acidified

using 1N HCl. The white solid precipitate was filtered and dried over vacuum to obtain (86% yield) pure thiazole acid product.

The acid product (0.011 mol) was then dissolved in dry DMF (30 mL). To this EDC (2.5 gm, 0.013 mol), HOBt (3.35 gm, 0.024 mol), *N,O*-Dimethylhydroxylamine hydrochloride (1.31 gm, 0.013 mol) and DIPEA (10 mL, 0.056 mol) were added at 0 ^{o}C and the reaction mixture was stirred at room temperature for 12h. The reaction mixture was diluted with water (50 mL) and extracted with ethyl acetate (100 mL x 2). The combined organic layer was washed with water (50 mL) and brine (50 mL) and dried over sodium sulfate and concentrated to obtain pure white solid product (80% yield)

^{1}H NMR (500 MHz, $CDCl_3$) δ 8.25 (m, 1H), 8.15 (s, 1H), 7.50 (m, 1H), 7.37 (m, 2H), 3.86 (s, 3H), 3.50 (brs, 3H).

^{13}C NMR (125 MHz, $CDCl_3$) δ 162.7, 148.5, 132.1, 131.5, 131.1, 130.7, 127.2, 126.5, 61.7, 41.0.

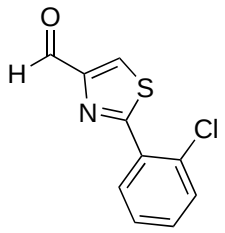

2-(2-chlorophenyl)thiazole-4-carbaldehyde

2-(2-chlorophenyl)-N-methoxy-N-methylthiazole-4-carboxamide (0.37 mmol) was taken in dry THF (5 mL) and to it 2M solution of lithium aluminium hydride (0.284 mL, 0.56 mmol) was added at 0 ^{o}C. After 10 min the reaction was

quenched by adding a saturated solution of ammonium chloride (10 mL) and extracted with ethyl acetate (30 mL x 2). The combined organic layer was washed with water (30 mL) and brine (30 mL) and dried over sodium sulfate and concentrated to obtain pure yellow solid product (59% yield).

^{1}H NMR (500 MHz, $CDCl_3$) δ 10.13 (s, 1H), 8.29 (m, 2H), 7.51 (m, 1H), 7.39 (m, 2H)

^{13}C NMR (125 MHz, $CDCl_3$) δ 180.1, 164.8, 154.2, 132.2, 131.2, 131.2, 131.0, 130.7, 128.1, 127.3

(1) Havlickova, B.; Czaika, V. A.; Friedrich, M. Epidemiological Trends in Skin Mycoses Worldwide. *Mycoses* **2008**, *51 Suppl 4*, 2–15.

(2) Antifungal Resistance in Candida https://www.cdc.gov/fungal/diseases/candidiasis/antifungal-resistant.html#:~:text=About%207%25%20of%20all%20Candida,Candida%20glabrata%2C%20and%20Candida%20parapsilosis. (accessed 2022 -02 -08).

(3) Kathiravan, M. K.; Salake, A. B.; Chothe, A. S.; Dudhe, P. B.; Watode, R. P.; Mukta, M. S.; Gadhwe, S. The Biology and Chemistry of Antifungal Agents: A Review. *Bioorg. Med. Chem.* **2012**, *20* (19), 5678–5698.

(4) Cowen, L. E.; Sanglard, D.; Howard, S. J.; Rogers, P. D.; Perlin, D. S. Mechanisms of Antifungal Drug Resistance. *Cold Spring Harb. Perspect. Med.* **2014**, *5* (7), a019752.

(5) Mevers, E.; Saurí, J.; Helfrich, E. J. N.; Henke, M.; Barns, K. J.; Bugni, T. S.; Andes, D.; Currie, C. R.; Clardy, J. Pyonitrins A–D: Chimeric Natural Products Produced by Pseudomonas Protegens. *Journal of the American Chemical Society*. 2019, pp 17098–17101. https://doi.org/10.1021/jacs.9b09739.

(6) Colosimo, D. A.; MacMillan, J. B. Detailed Mechanistic Study of the Non-Enzymatic Formation of the Discoipyrrole Family of Natural Products. *J. Am. Chem. Soc.* **2016**, *138* (7), 2383–2388.

(7) Tan, F.; Shi, B.; Li, J.; Wu, W.; Zhang, J. Design and Synthesis of New 2-Aryl-4,5-Dihydro-Thiazole Analogues: In Vitro Antibacterial Activities and Preliminary Mechanism of Action. *Molecules* **2015**, *20* (11), 20118–20130.

(8) Williams, D. R.; Lowder, P. D.; Gu, Y.-G.; Brooks, D. A. Studies of Mild Dehydrogenations in Heterocyclic Systems. *Tetrahedron Letters*. 1997, pp 331–334. https://doi.org/10.1016/s0040-4039(96)02344-1.

(9) Morrison, M. D.; Hanthorn, J. J.; Pratt, D. A. Synthesis of Pyrrolnitrin and Related Halogenated Phenylpyrroles. *Org. Lett.* **2009**, *11* (5), 1051–1054.

(10) Saha, B.; Sharma, S.; Sawant, D.; Kundu, B. Water as an Efficient Medium for the Synthesis of Tetrahydro-β-Carbolines via Pictet—Spengler Reactions. *ChemInform*. 2007. https://doi.org/10.1002/chin.200722147.

(11) Marek, R.; Lycka, A.; Kolehmainen, E.; Sievanen, E.; Tousek, J. 15N NMR Spectroscopy in Structural Analysis: An Update (2001 - 2005). *Curr. Org. Chem. 11* (13), 1154–1205.

(12) Shih, J.-L.; Nguyen, T. S.; May, J. A. Organocatalyzed Asymmetric Conjugate Addition of Heteroaryl and Aryl Trifluoroborates: A Synthetic Strategy for Discoipyrrole D. *Angew. Chem. Int. Ed Engl.* **2015**, *54* (34), 9931–9935.

^{1}H NMR spectrum of **12** (500 MHz, $CDCl_3$)

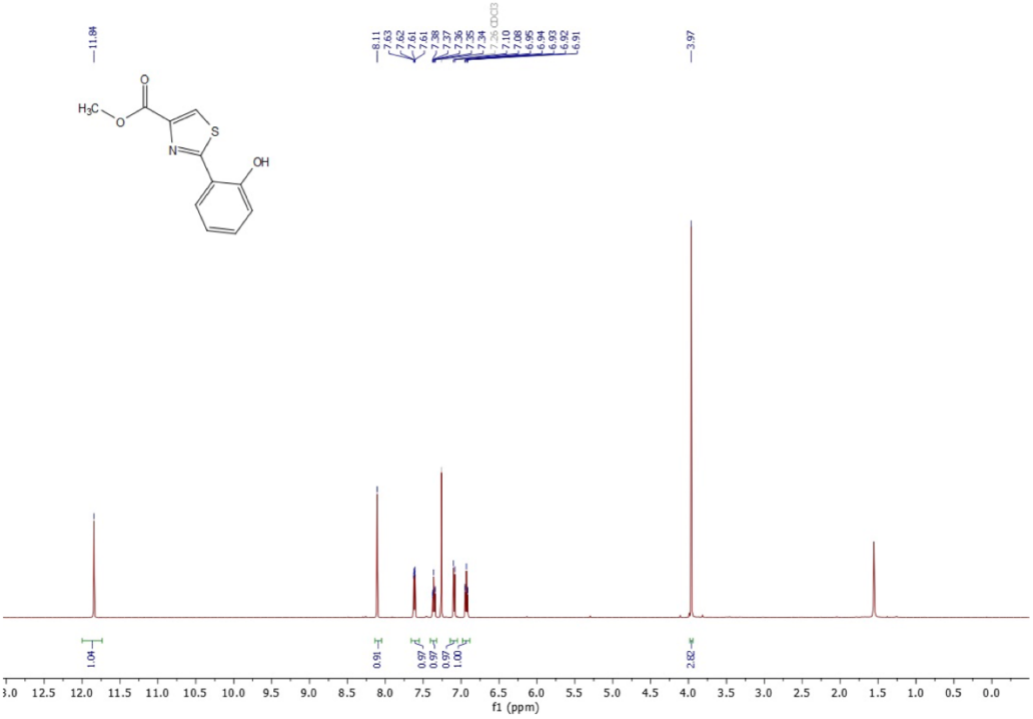

S17

^{13}C NMR spectrum of **12** (125 MHz, $CDCl_3$)

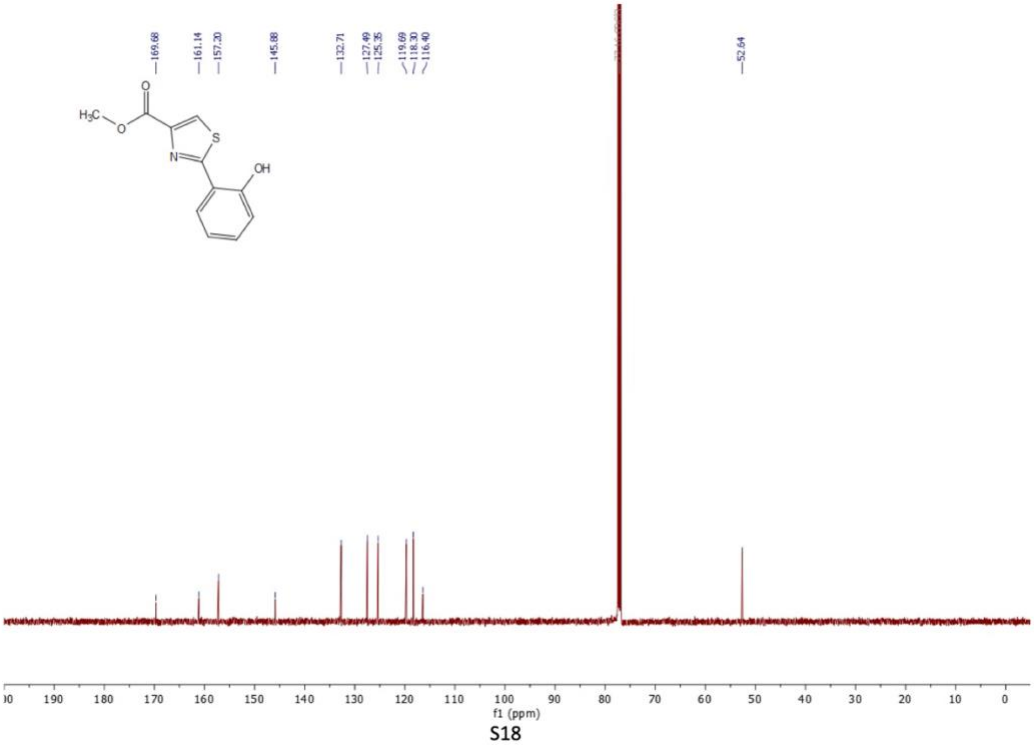

S18

^{1}H NMR spectrum of **13** (500 MHz, $CDCl_3$)

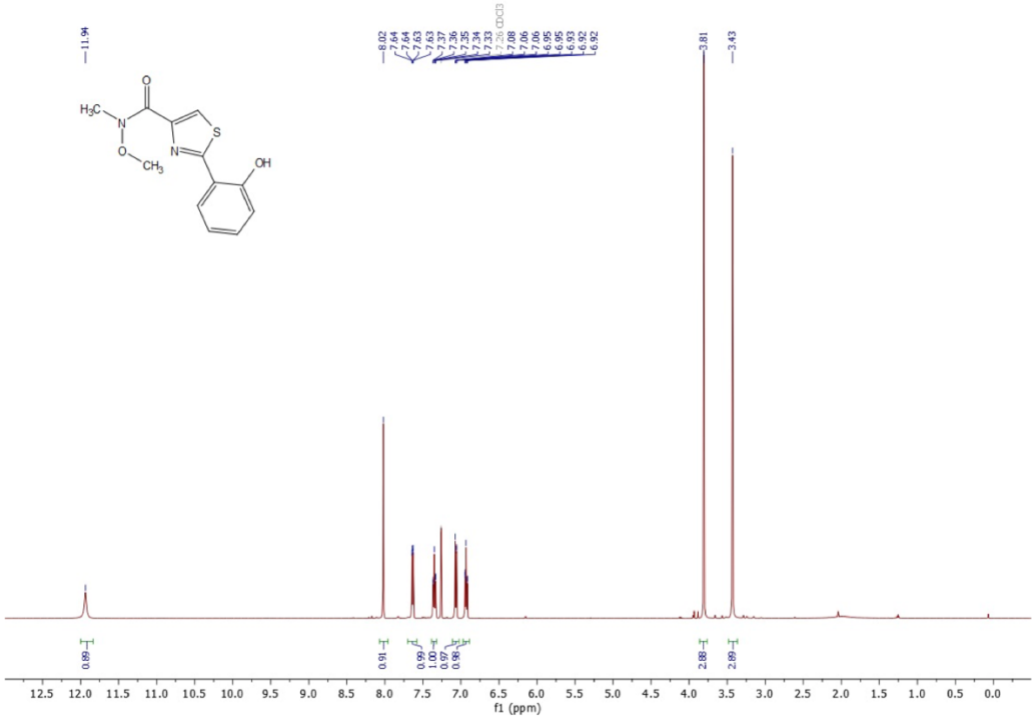

S19

^{13}C NMR spectrum of **13** (125 MHz, $CDCl_3$)

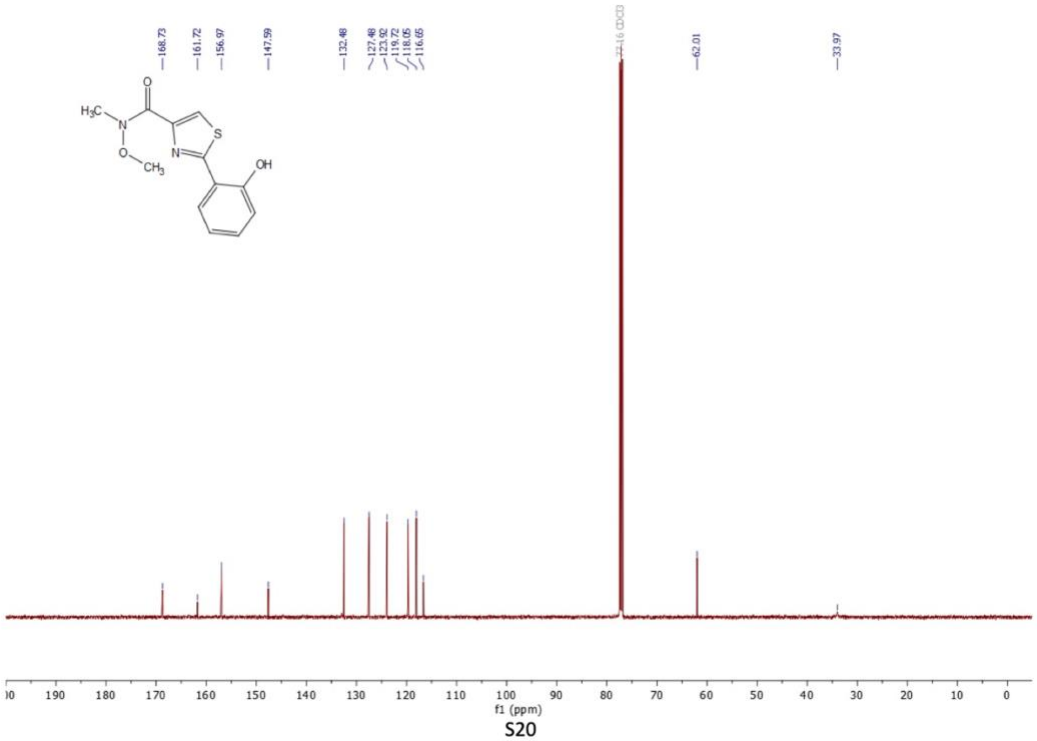

S20

^{1}H NMR spectrum of **7** (500 MHz, $CDCl_3$)

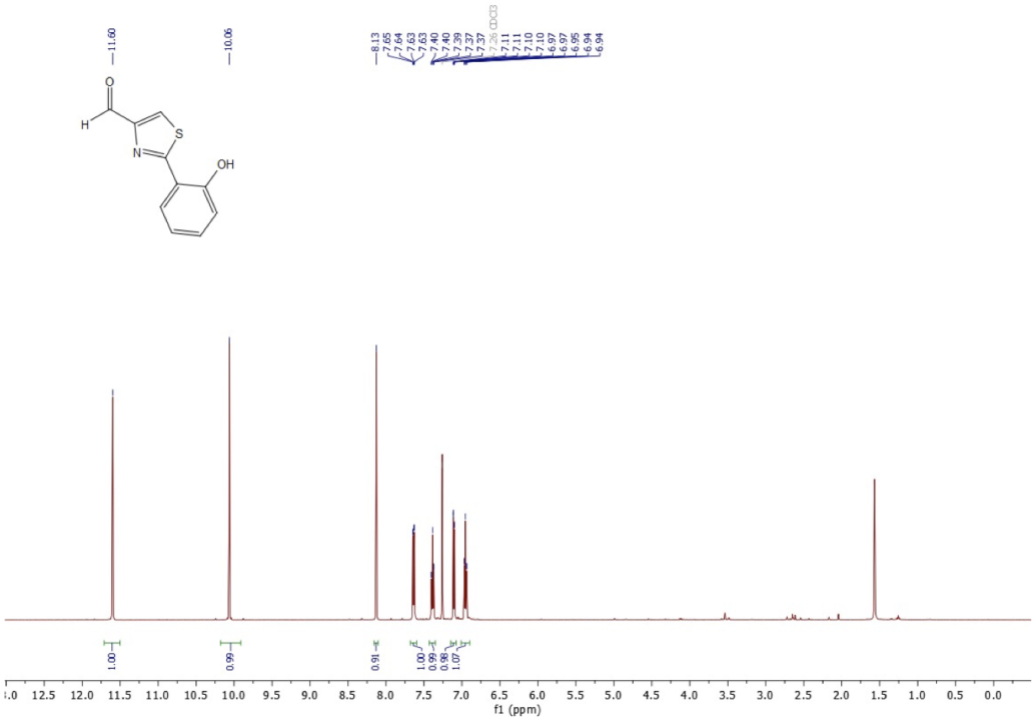

S21

^{13}C NMR spectrum of **7** (125 MHz, $CDCl_3$)

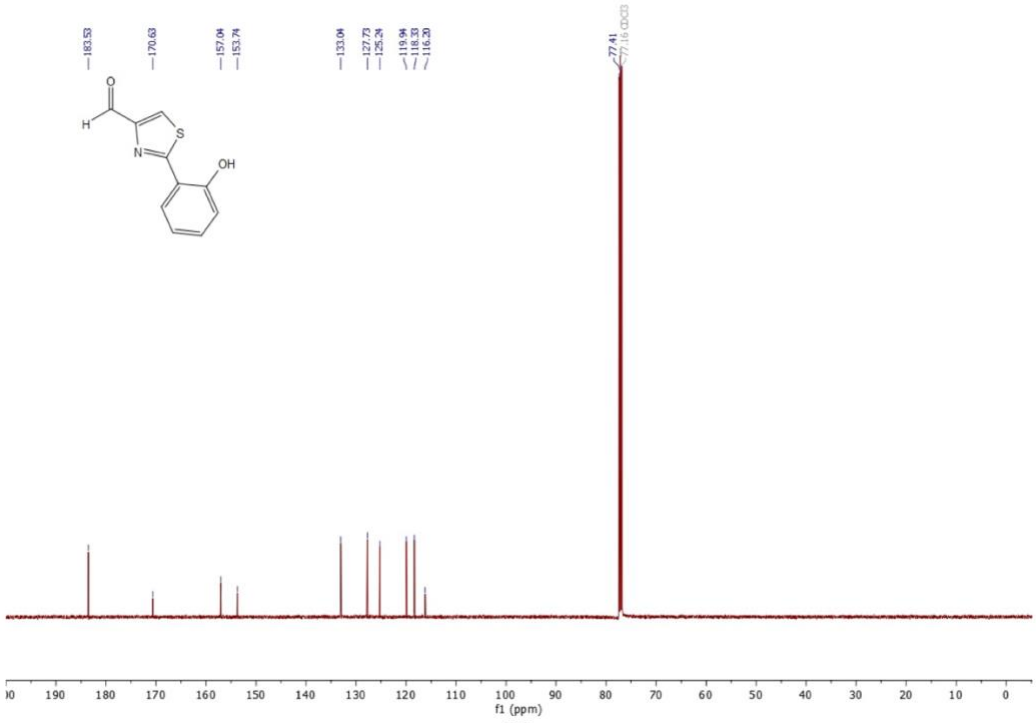

S22

^{1}H NMR spectrum of **18** (500 MHz, $CDCl_3$)

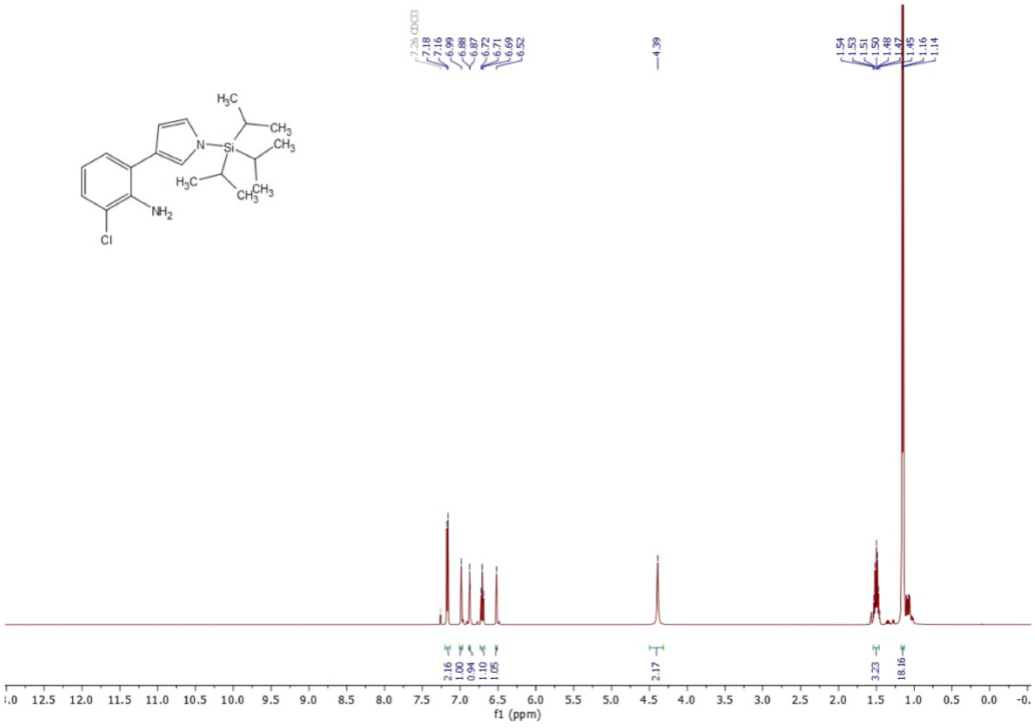

S23

^{13}C NMR spectrum of **18** (125 MHz, $CDCl_3$)

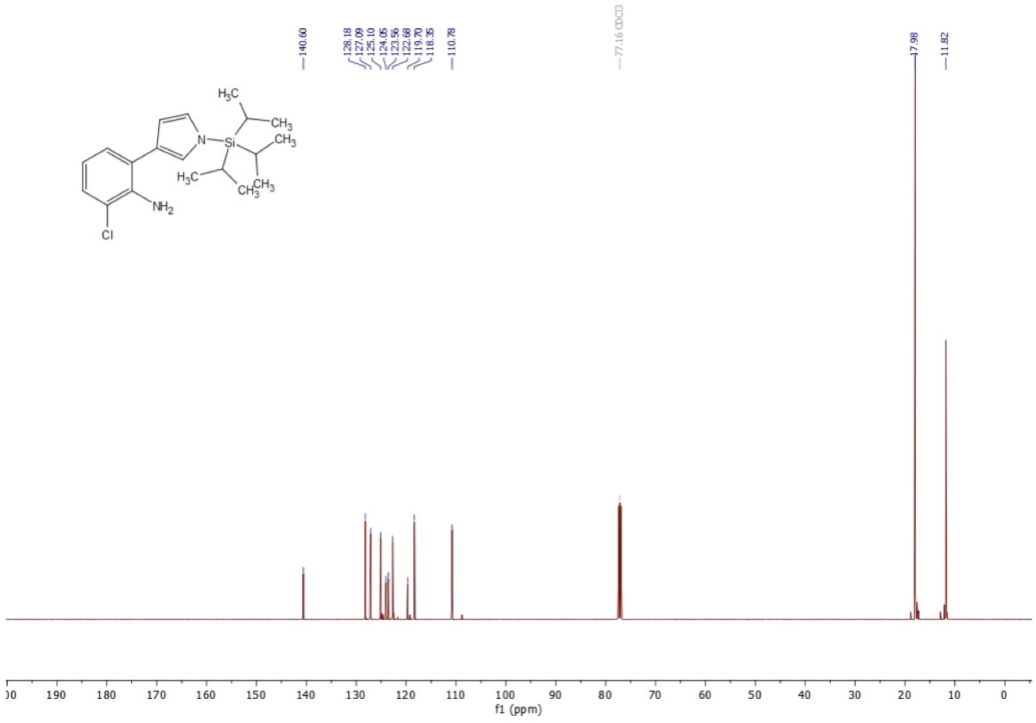

S24

^{1}H NMR spectrum of **22** (500 MHz, $CDCl_3$)

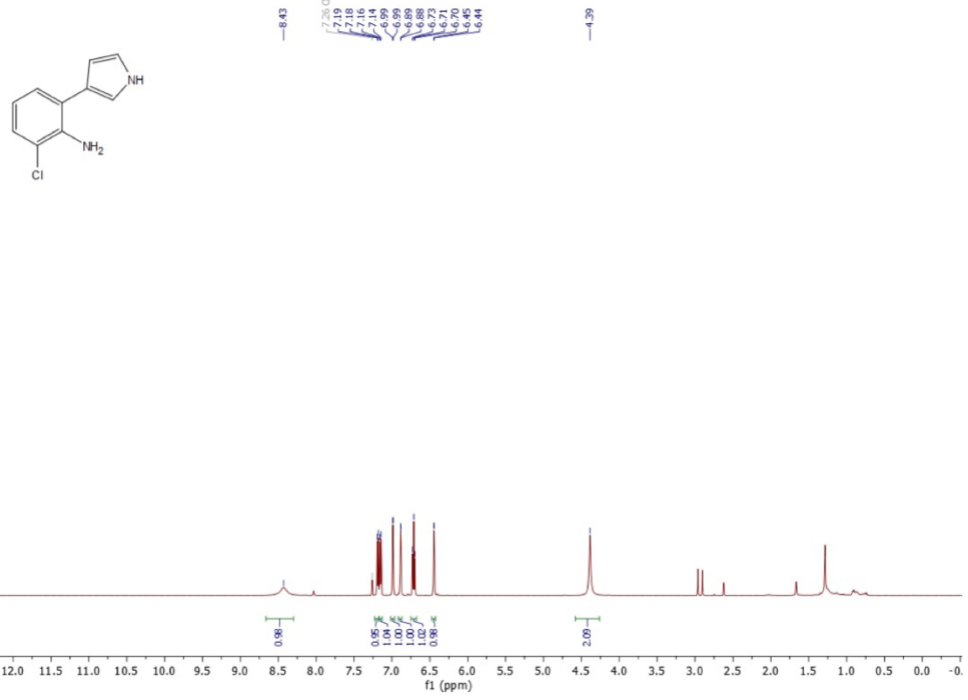

S25

^{13}C NMR spectrum of **22** (125 MHz, $CDCl_3$)

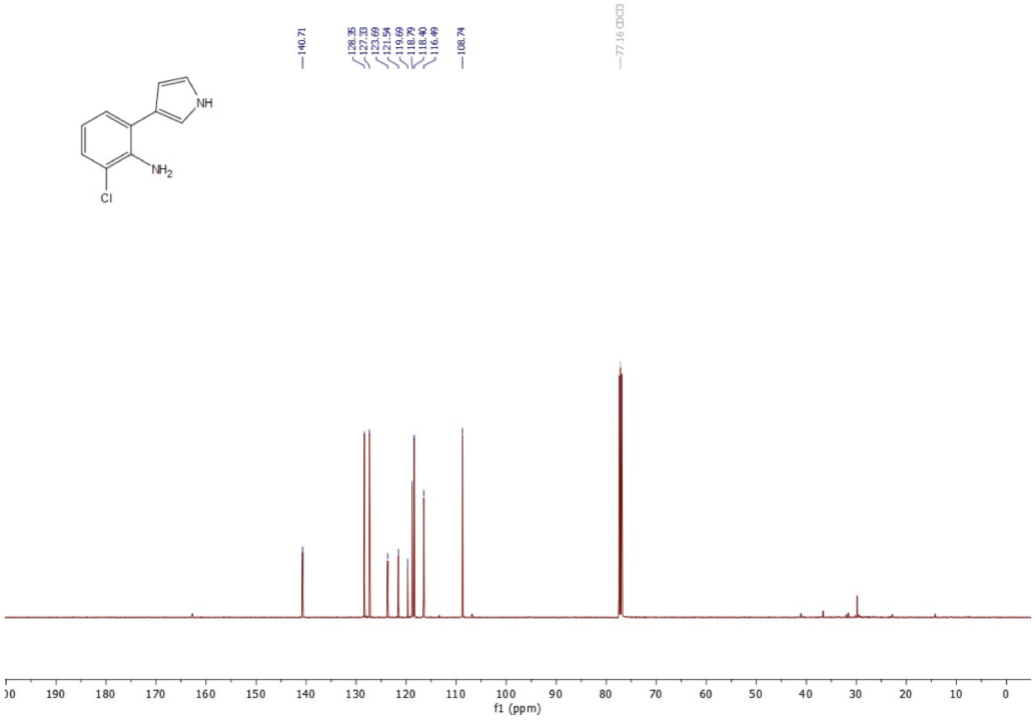

S26

^{1}H NMR spectrum of pyonitrin A **1** (500 MHz, DMSO-d_6)

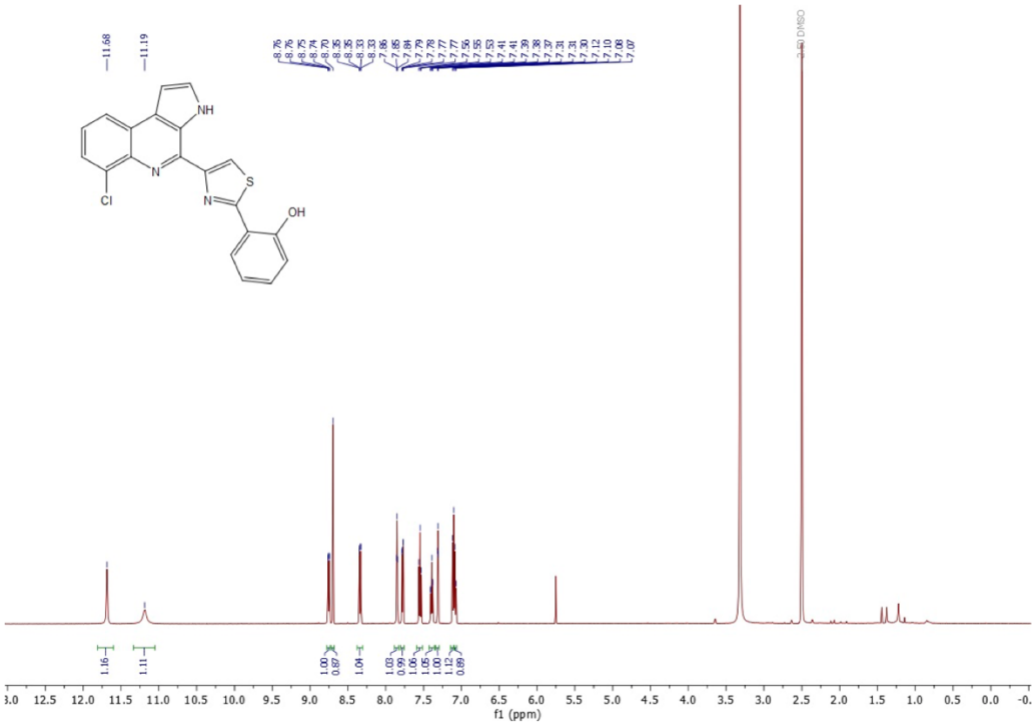

S27

^{13}C NMR spectrum of pyonitrin A **1** (125 MHz, DMSO-d_6)

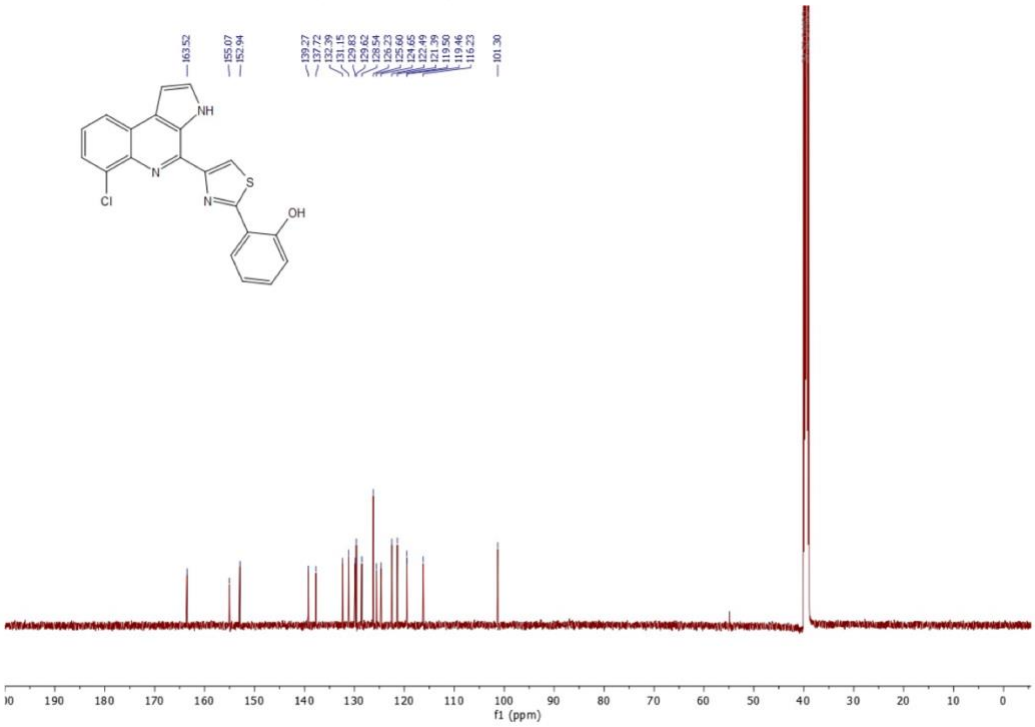

S28

^{1}H NMR spectrum of **19** (500 MHz, $CDCl_3$)

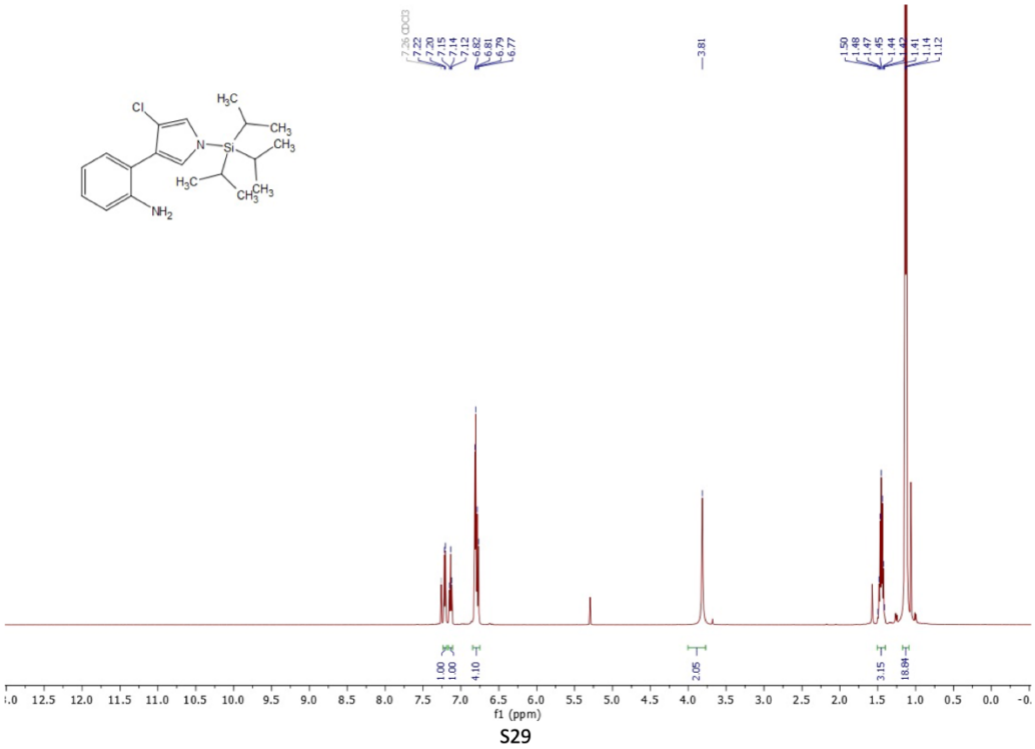

S29

^{13}C NMR spectrum of **19** (125 MHz, $CDCl_3$)

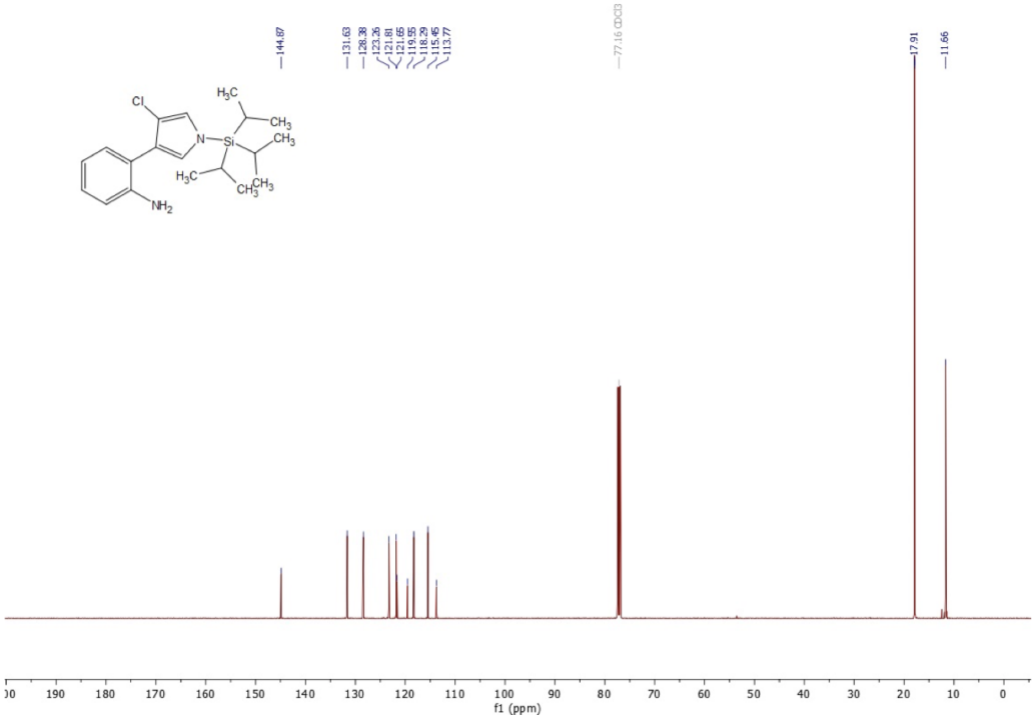

S30

^{1}H NMR spectrum of **23** (500 MHz, $CDCl_3$)

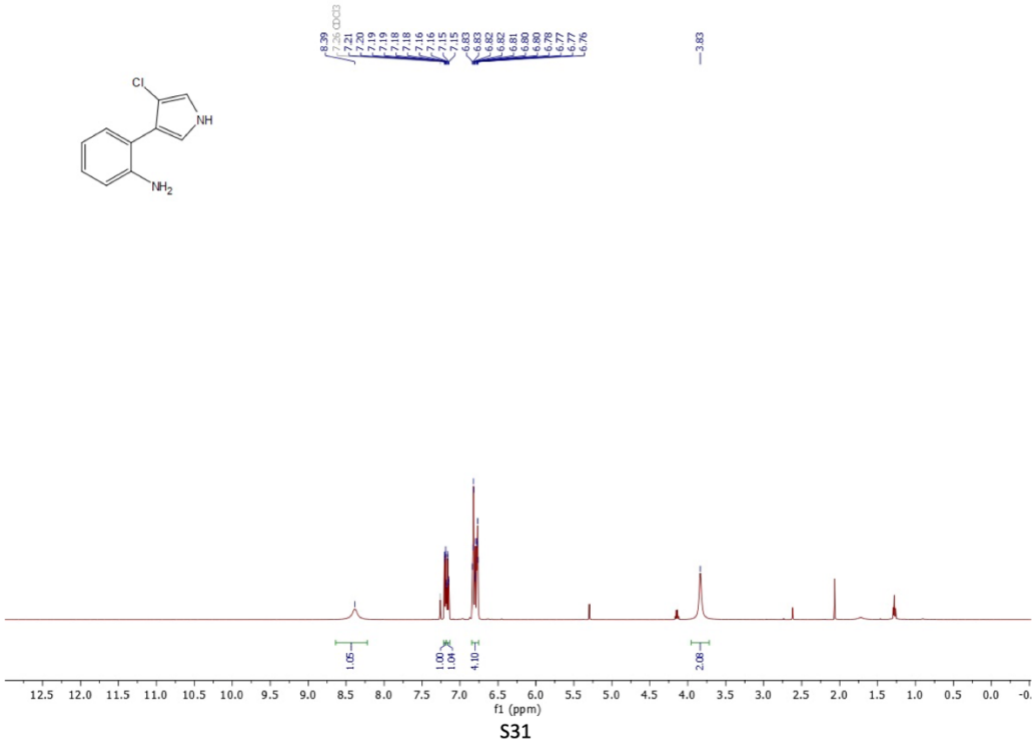

S31

^{13}C NMR spectrum of **23** (125 MHz, $CDCl_3$)

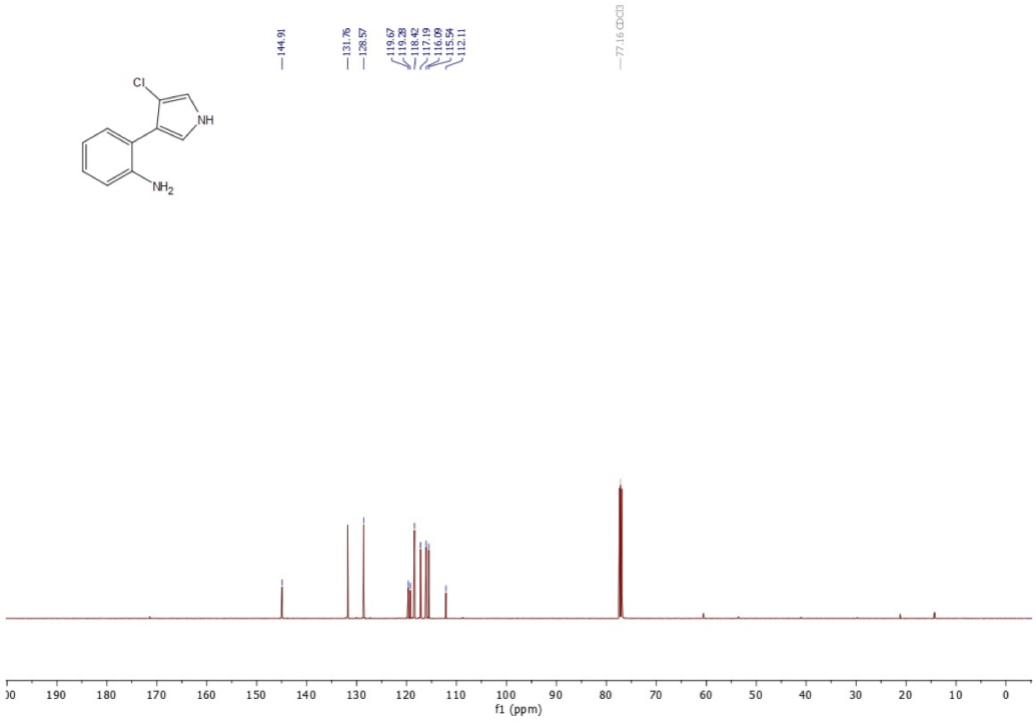

S32

^{1}H NMR spectrum of **pyonitrin B** (800 MHz, DMSO-d_6)

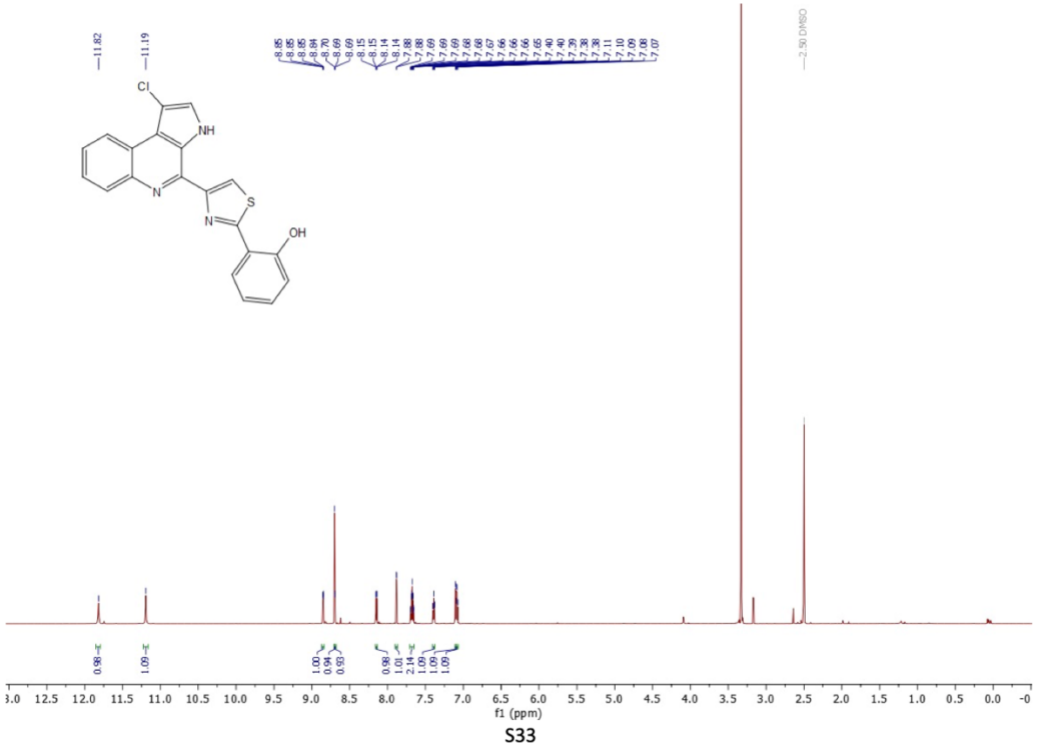

S33

^{13}C NMR spectrum of **pyonitrin B** (200 MHz, DMSO-d_6)

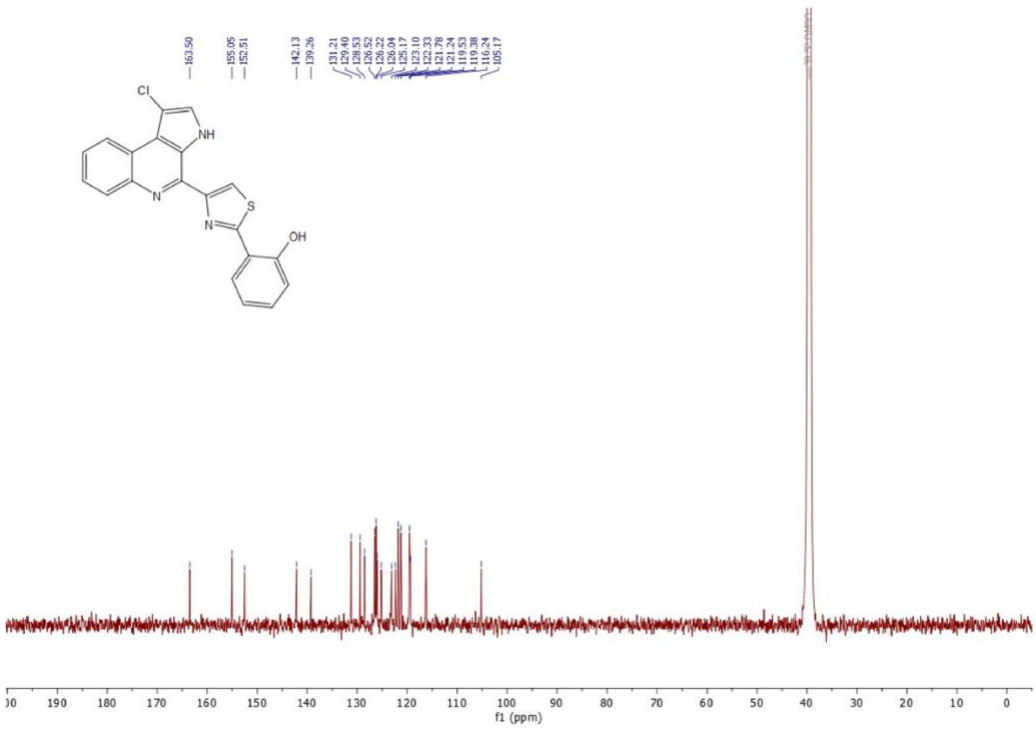

S34

^{1}H NMR spectrum of **20** (500 MHz, $CDCl_3$)

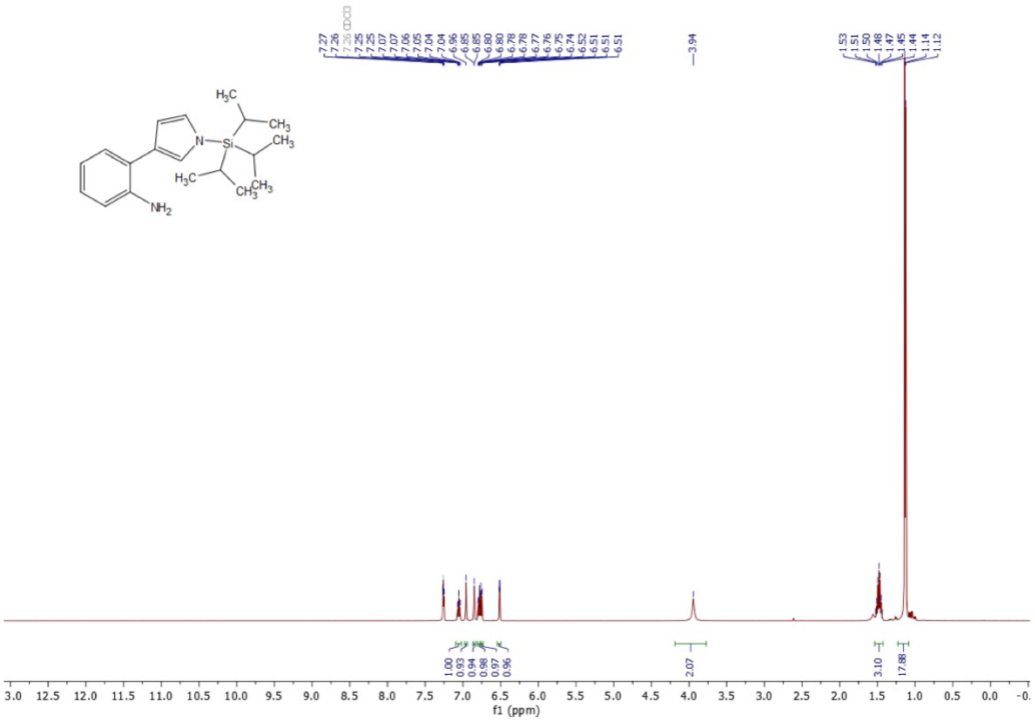

S35

^{13}C NMR spectrum of **20** (125 MHz, $CDCl_3$)

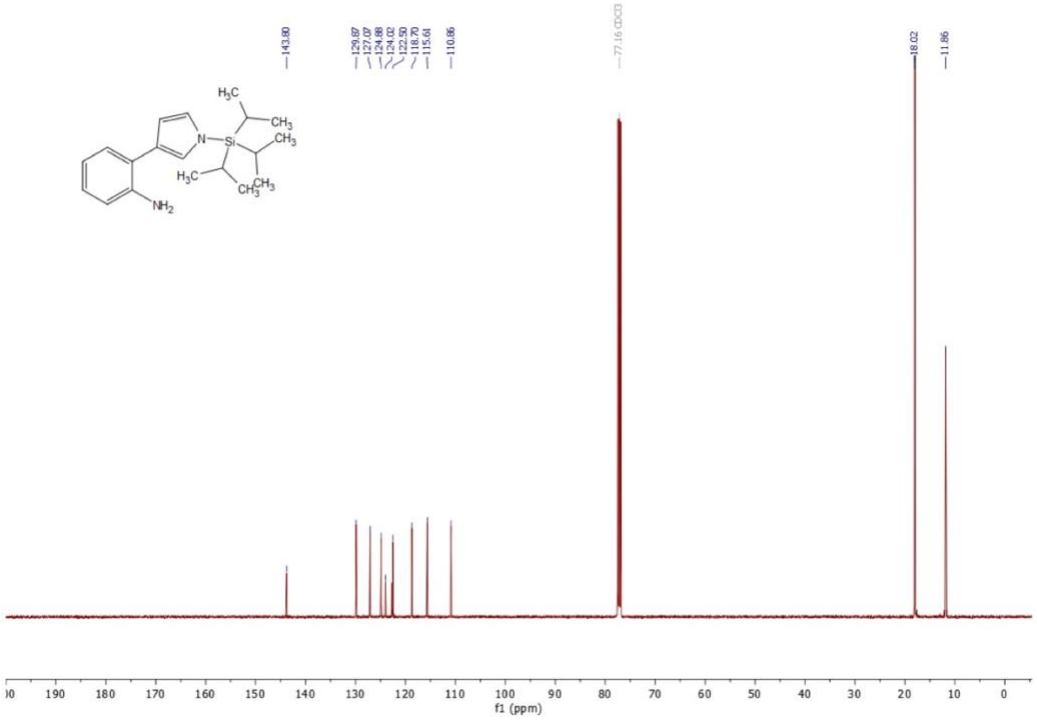

S36

^{1}H NMR spectrum of **24** (500 MHz, $CDCl_3$)

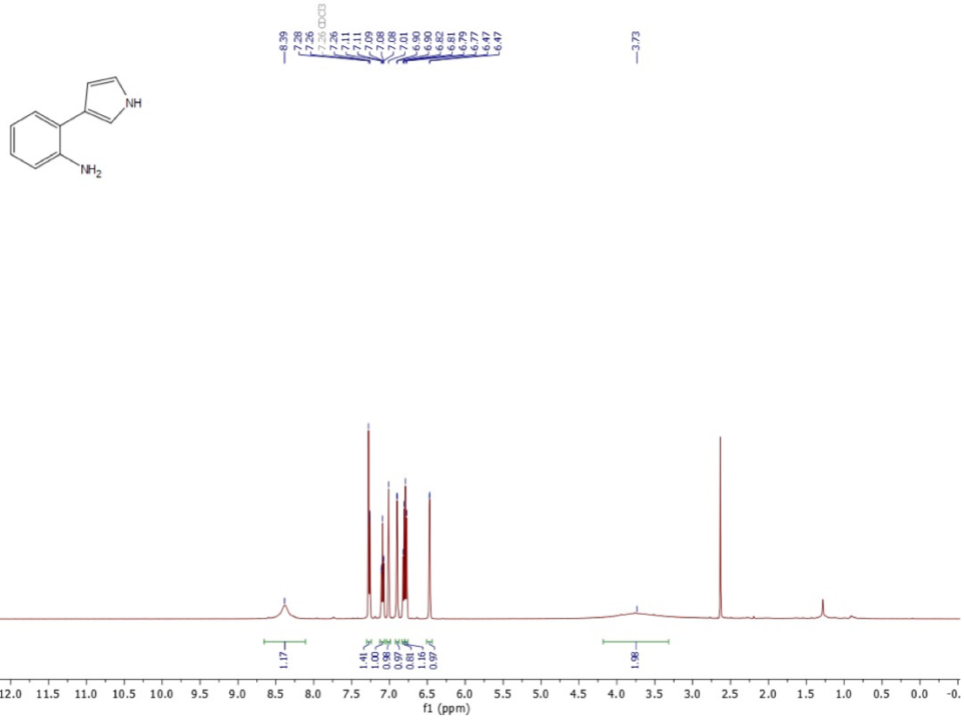

S37

^{13}C NMR spectrum of **24** (125 MHz, $CDCl_3$)

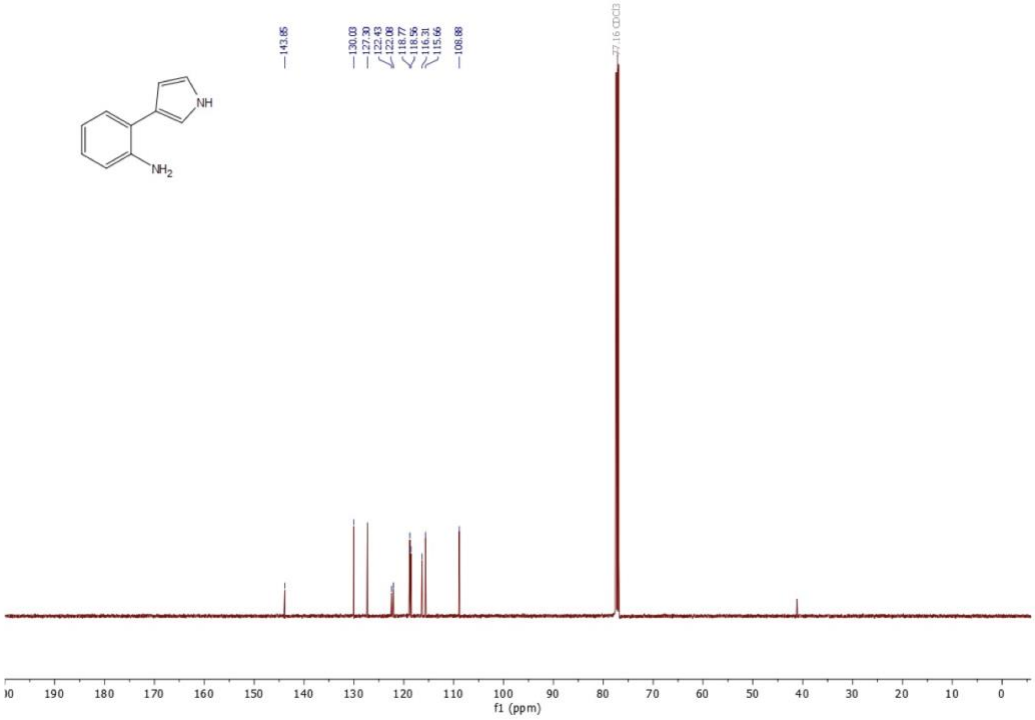

S38

^{1}H NMR spectrum of **pyonitrin C** (800 MHz, DMDO-d_6)

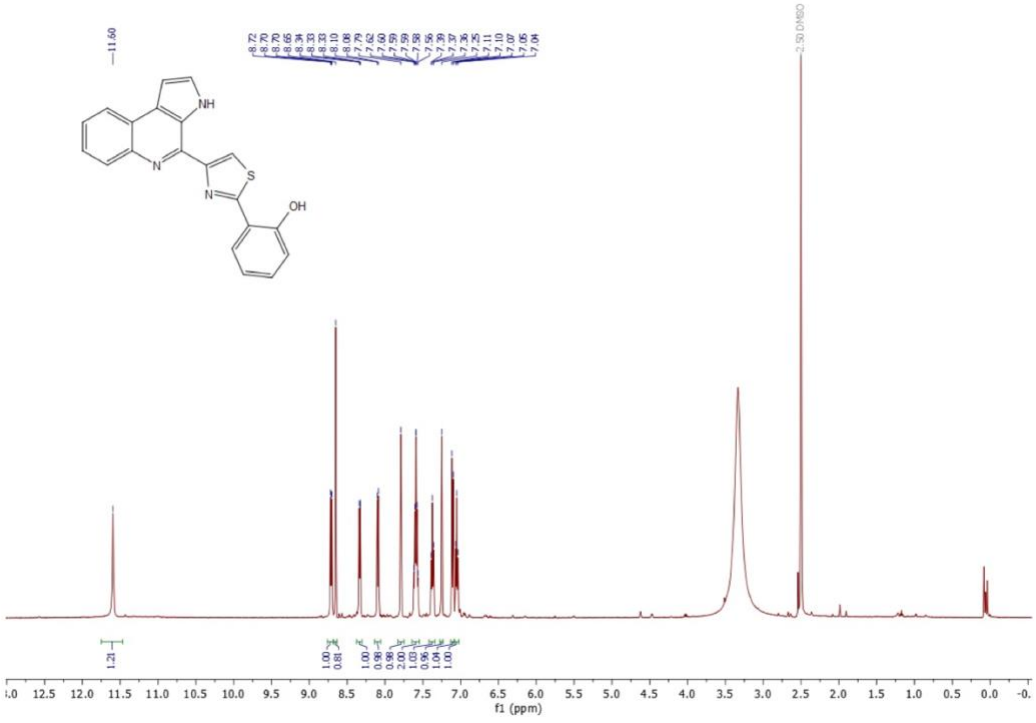

S39

^{13}C NMR spectrum of **pyonitrin C** (200 MHz, DMDO-d_6)

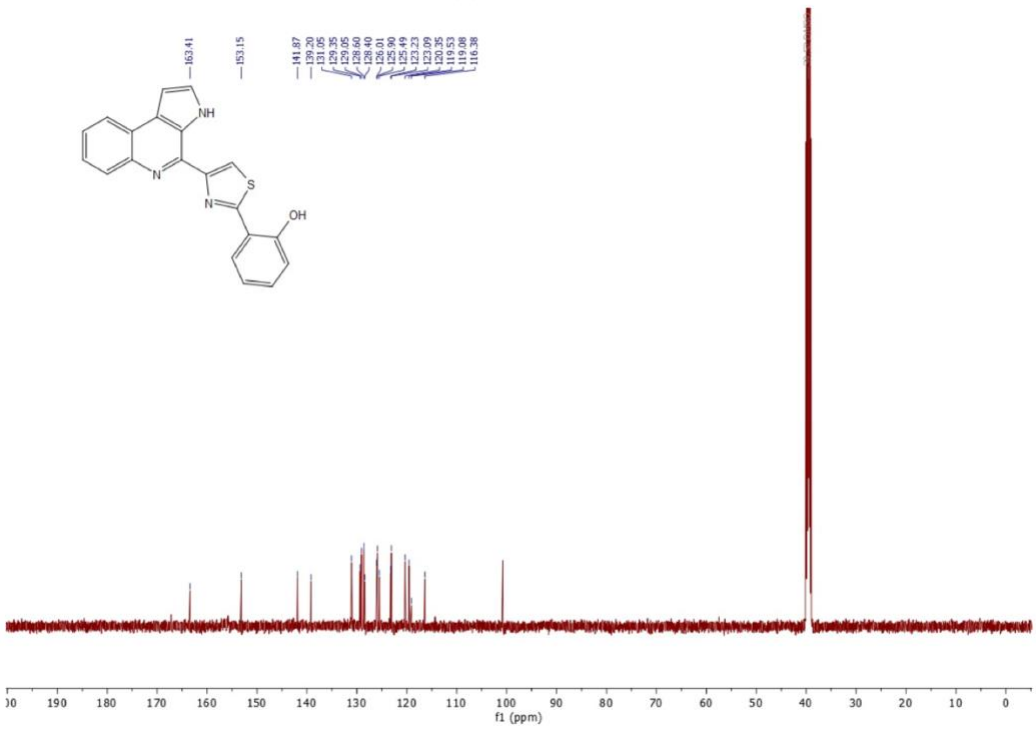

S40

^{1}H NMR spectrum of **21** (500 MHz, $CDCl_3$)

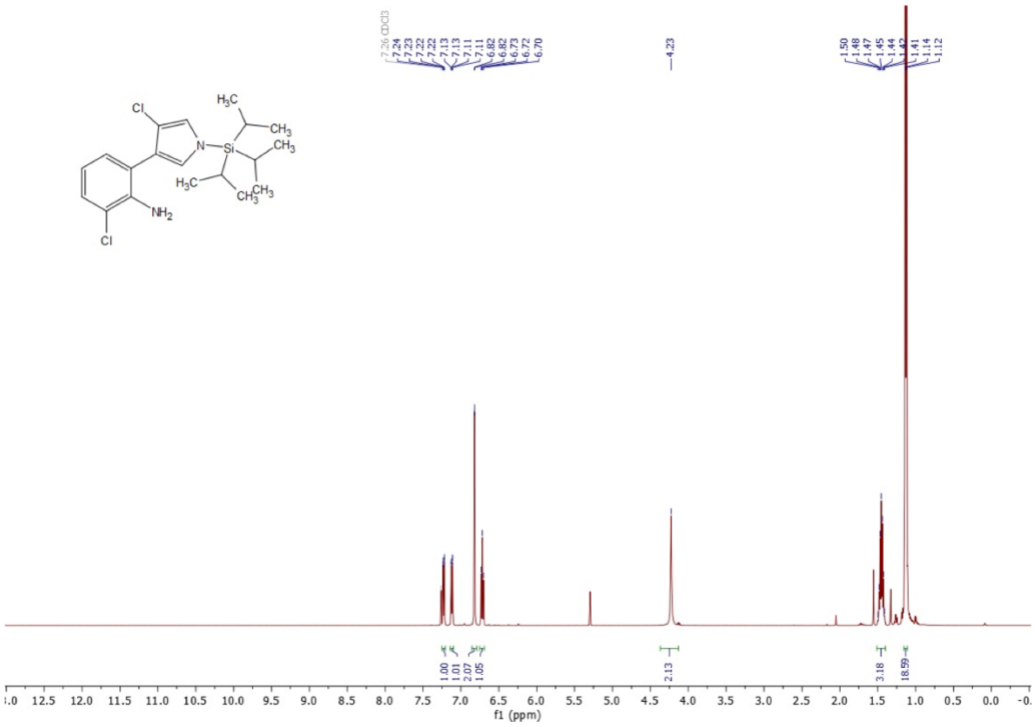

S41

^{13}C NMR spectrum of **21** (125 MHz, $CDCl_3$)

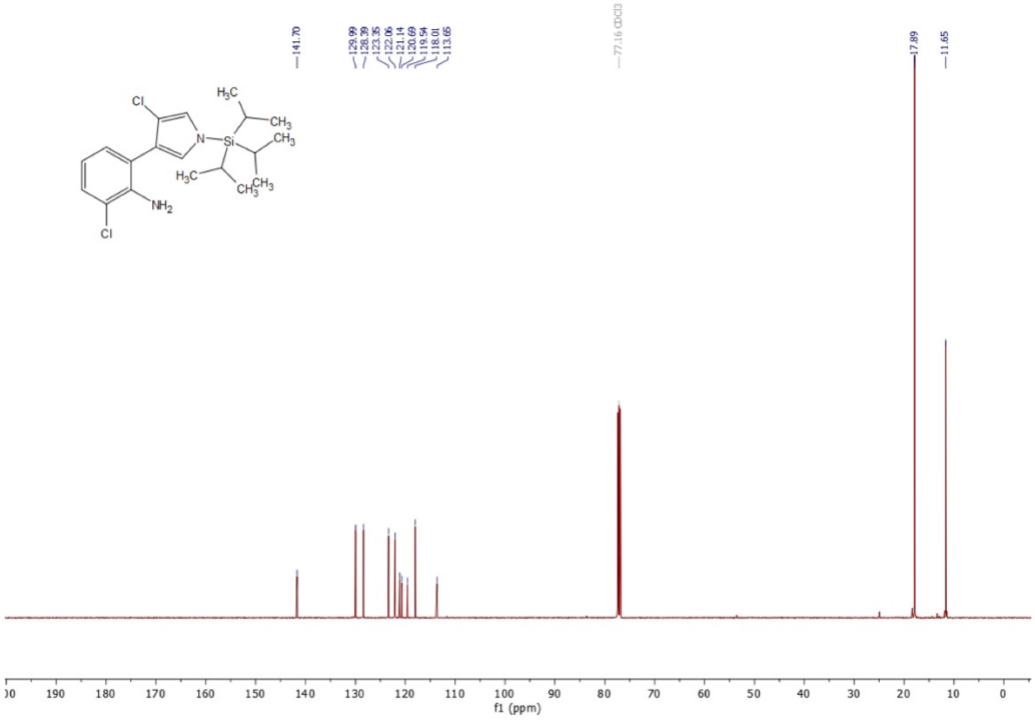

S42

^{1}H NMR spectrum of **25** (500 MHz, $CDCl_3$)

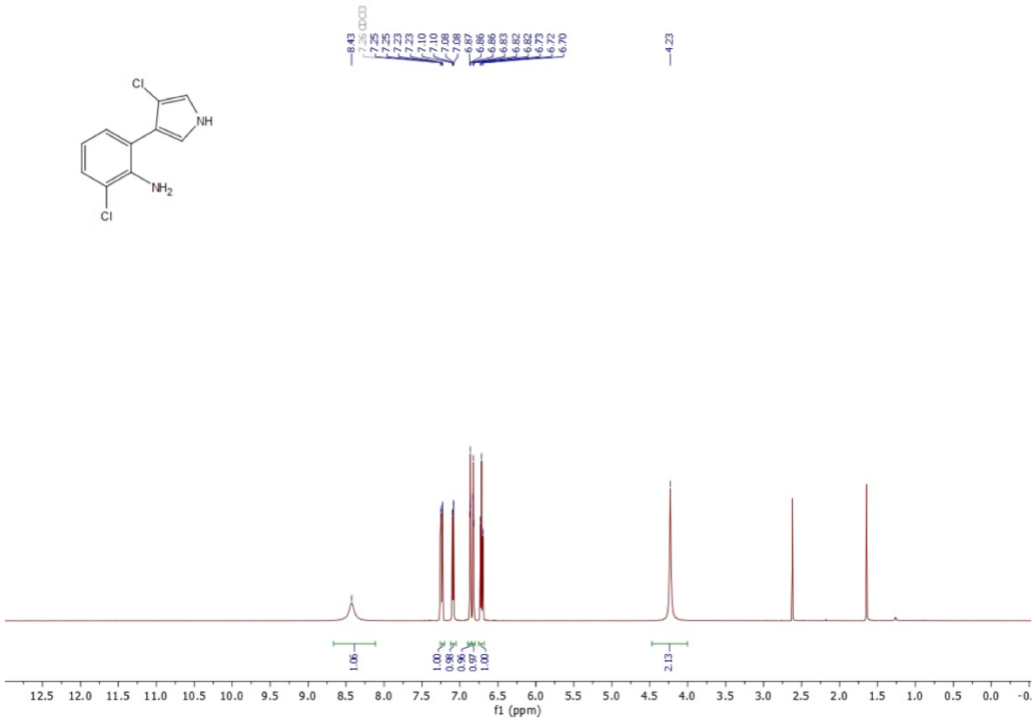

^{13}C NMR spectrum of **25** (125 MHz, $CDCl_3$)

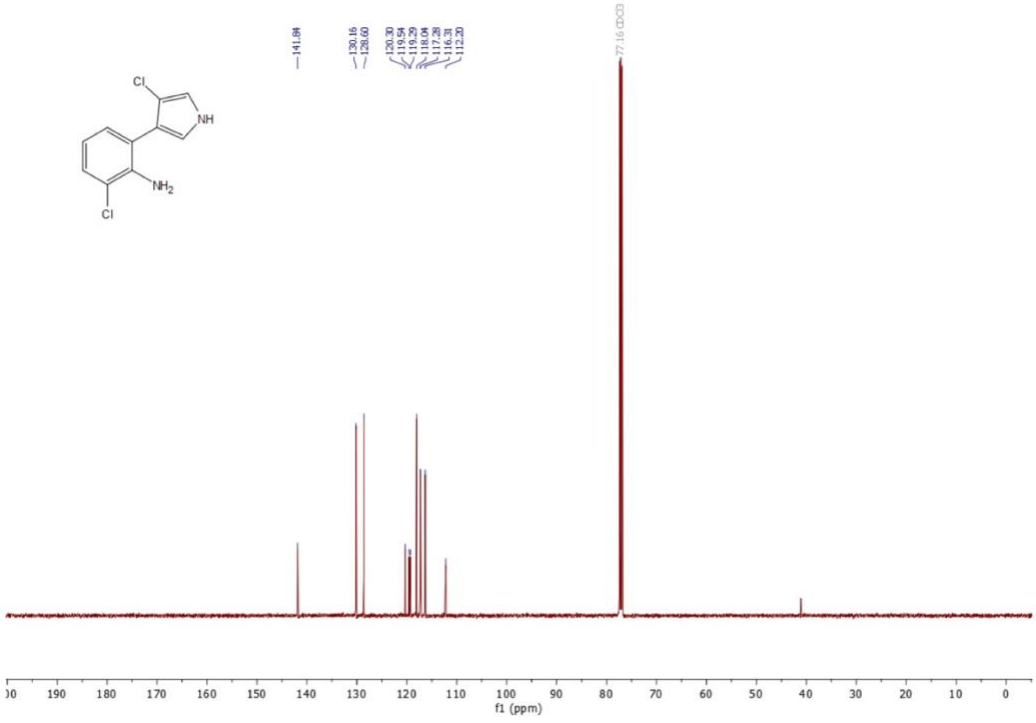

S44

^{1}H NMR spectrum of **pyonitrin D** (500 MHz, DMSO-d_6)

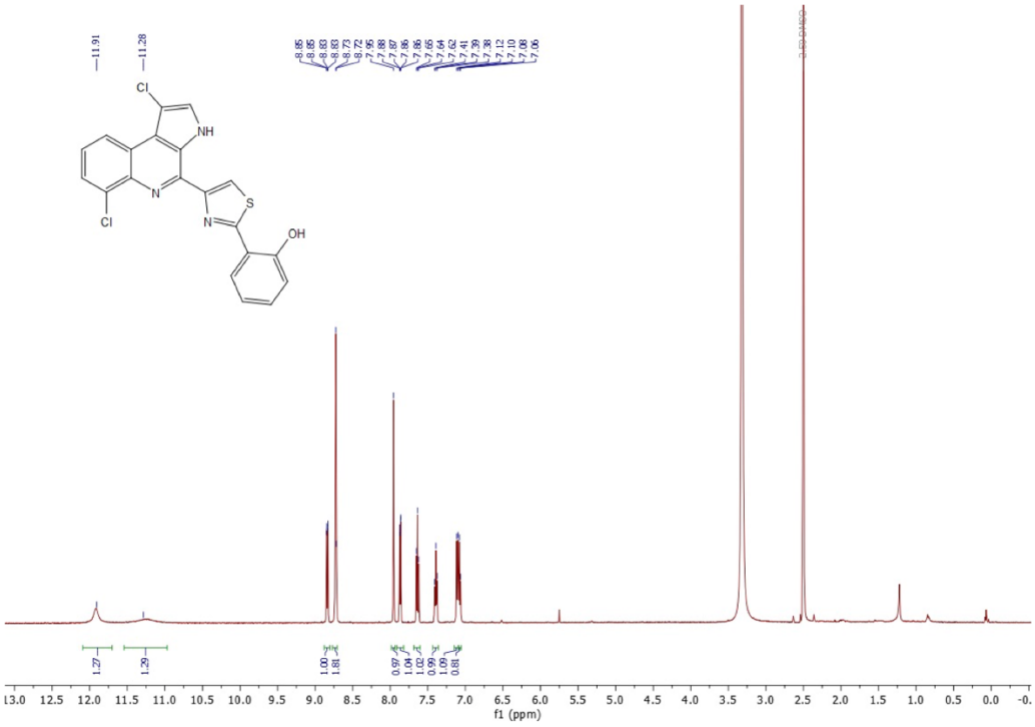

S45

^{13}C NMR spectrum of **pyonitrin D** (200 MHz, DMSO-d_6)

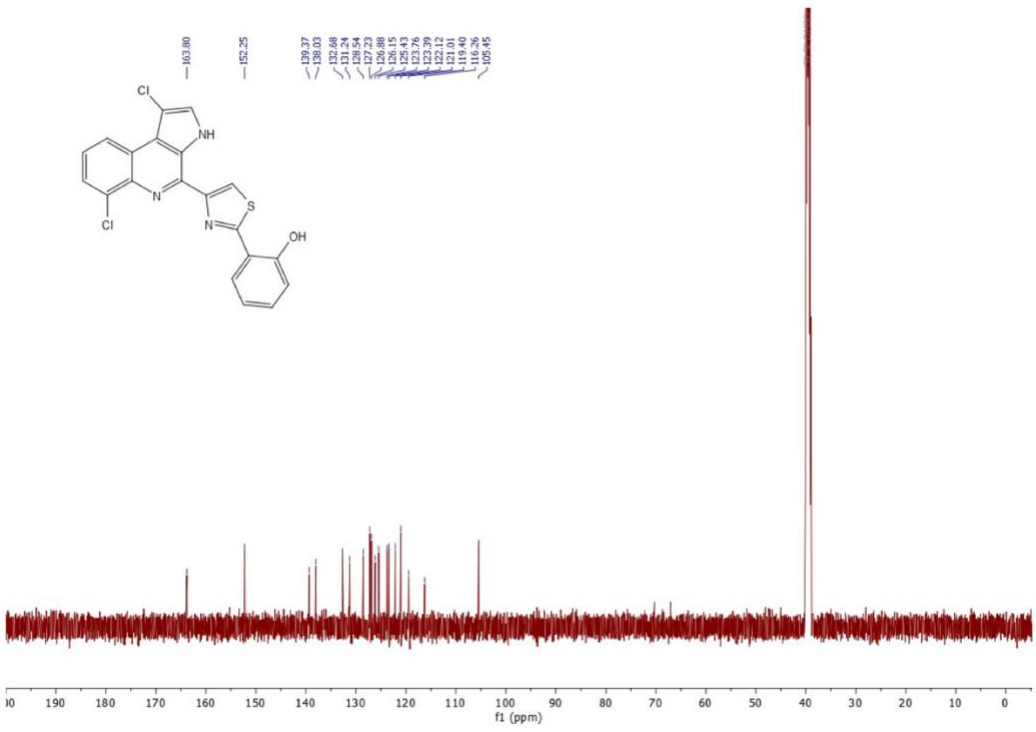

S46

^{1}H NMR spectrum of **26a** (500 MHz, $CDCl_3$)

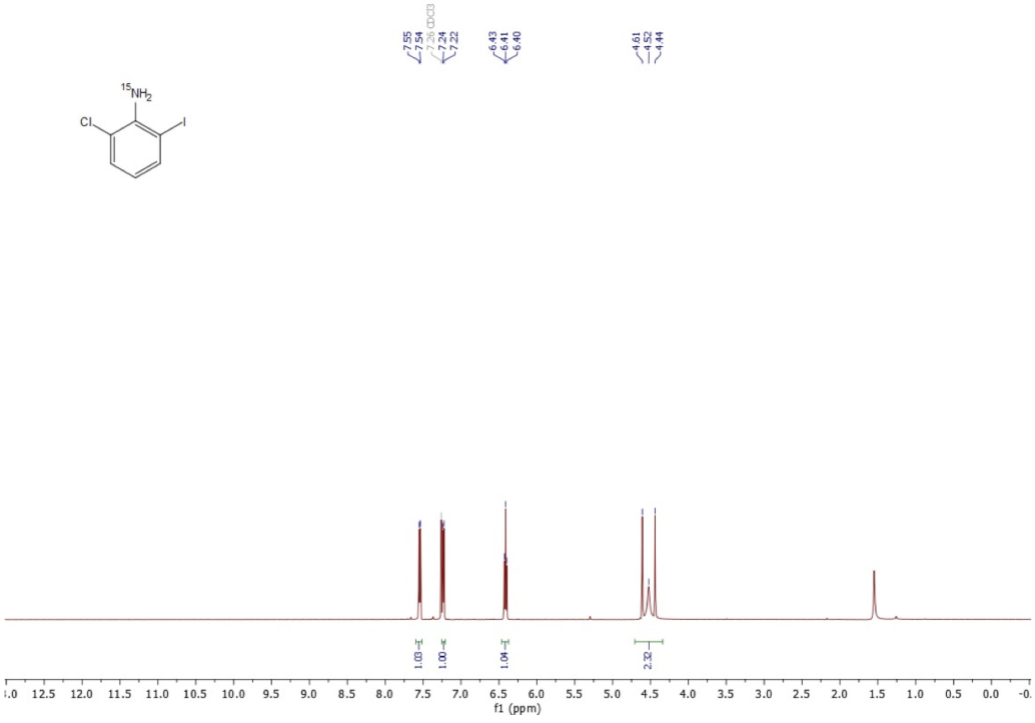

S47

^{13}C NMR spectrum of **26a** (125 MHz, $CDCl_3$)

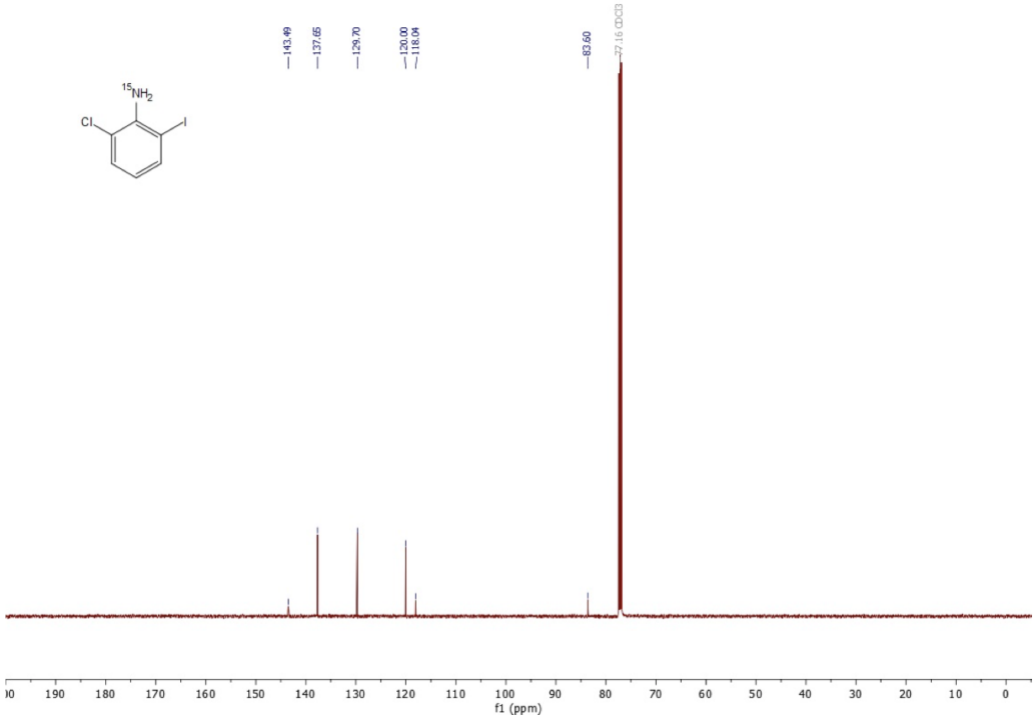

S48

^{1}H NMR spectrum of **26b** (500 MHz, $CDCl_3$)

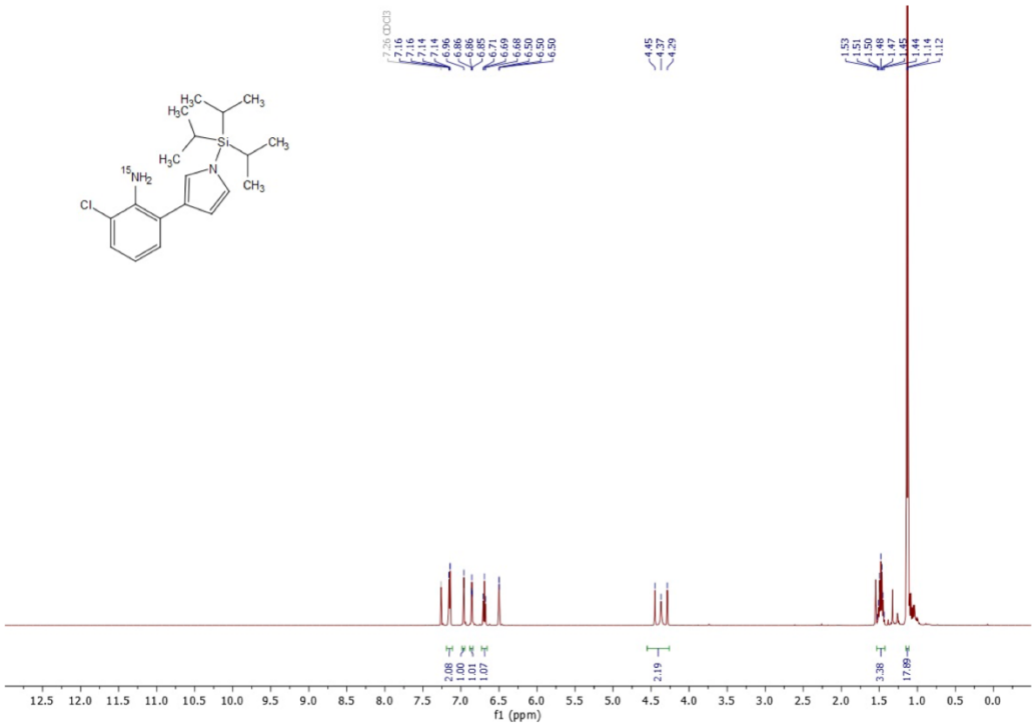

S49

^{13}C NMR spectrum of **26b** (125 MHz, $CDCl_3$)

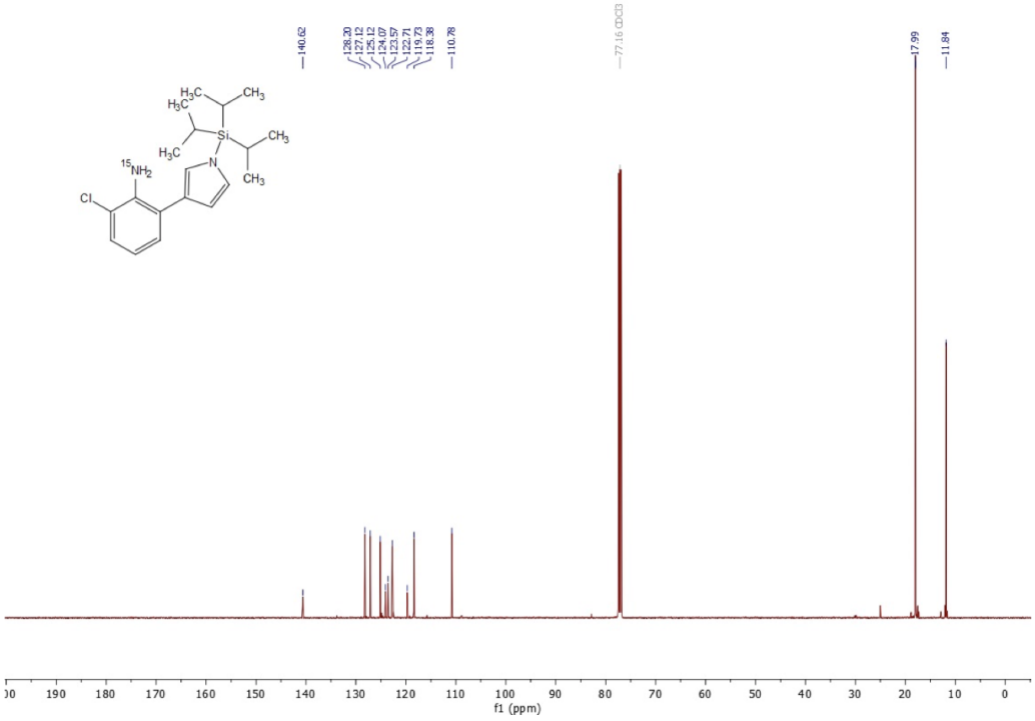

S50

^{1}H NMR spectrum of **26** (800 MHz, DMSO-d_6)

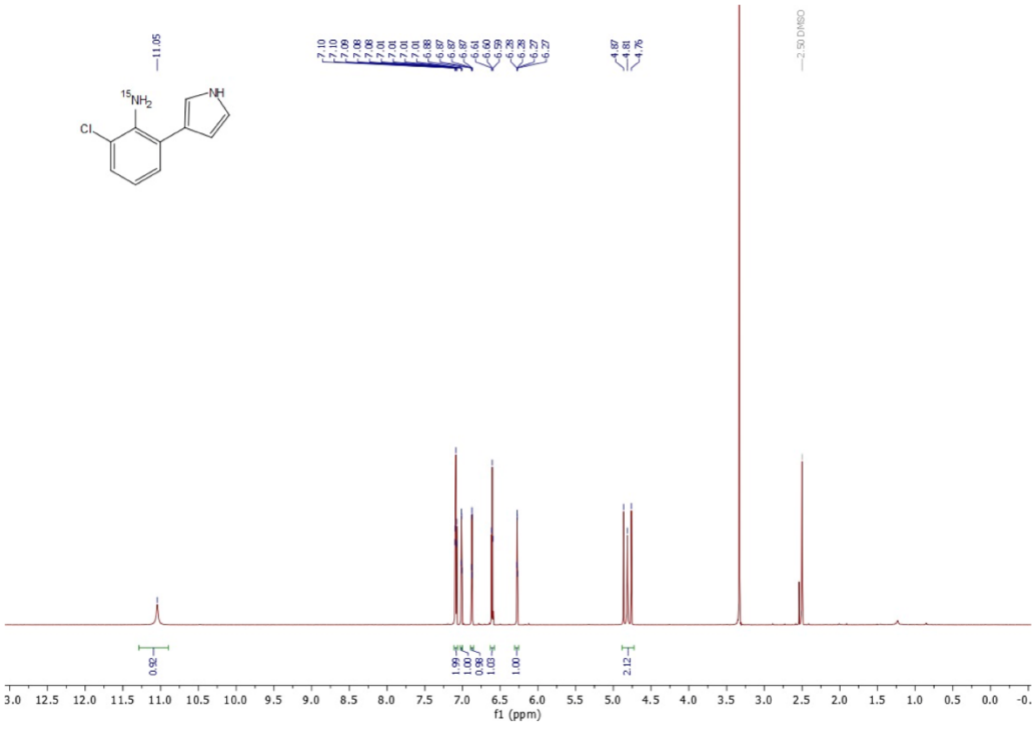

S51

^{13}C NMR spectrum of **26** (200 MHz, DMSO-d_6)

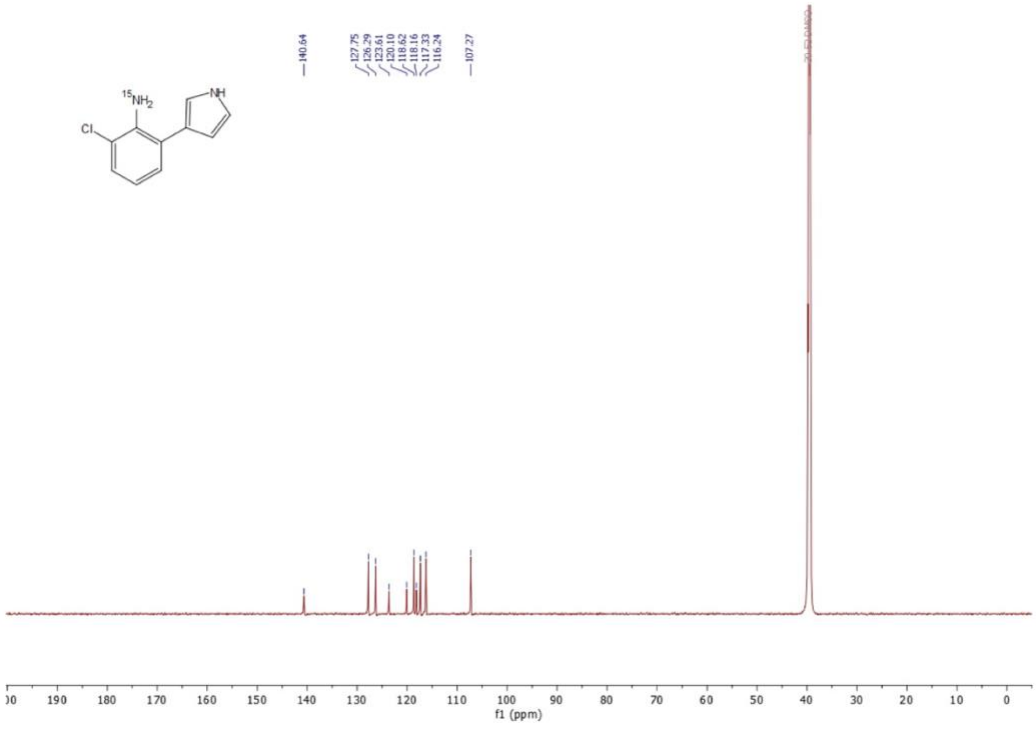

S52

^{1}H NMR spectrum of ^{15}N pyonitrin A **29** (500 MHz, DMSO-d_6)

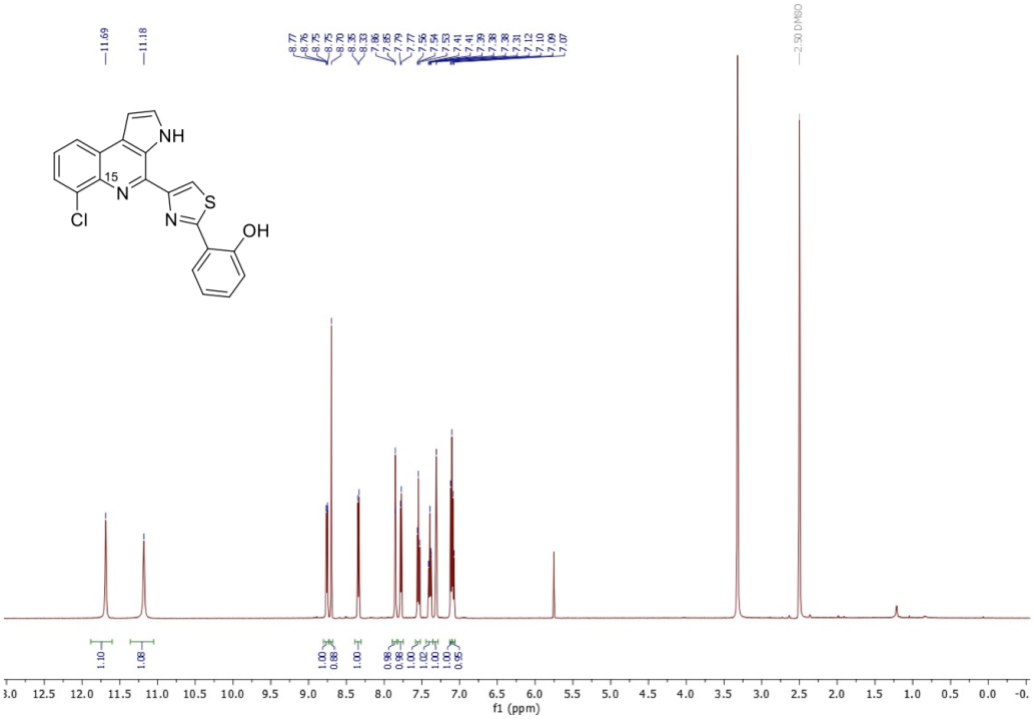

S53

^{13}C NMR spectrum of ^{15}N pyonitrin A **29** (125 MHz, DMSO-d_6)

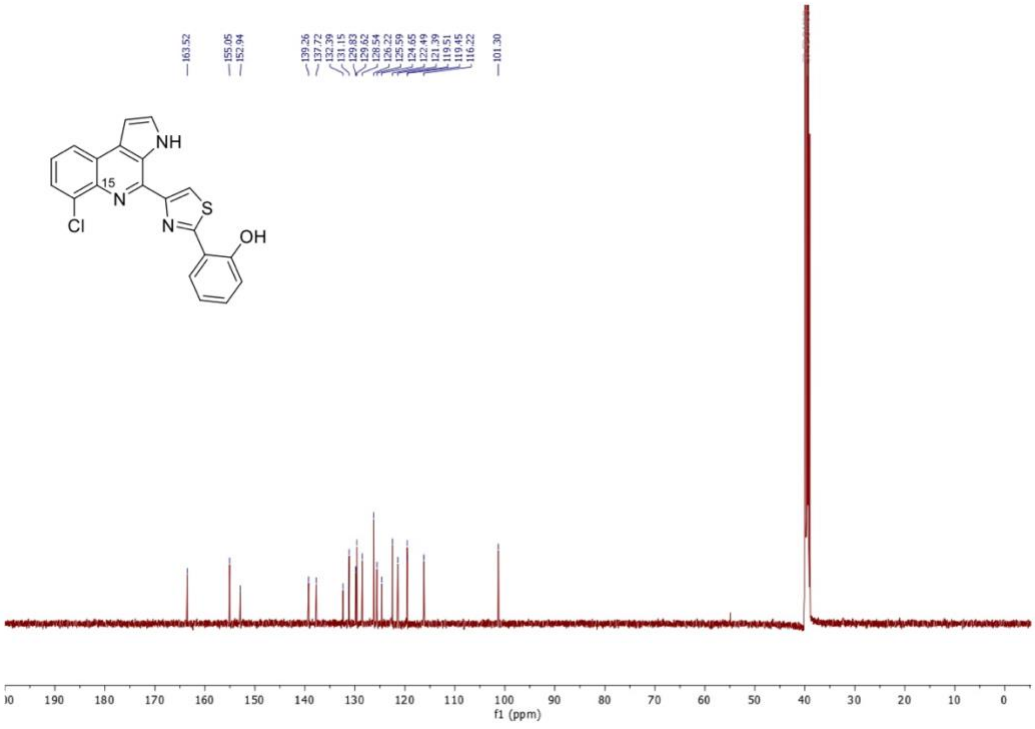

S54

^{1}H NMR spectrum of **28** (500 MHz, DMSO-d_6)

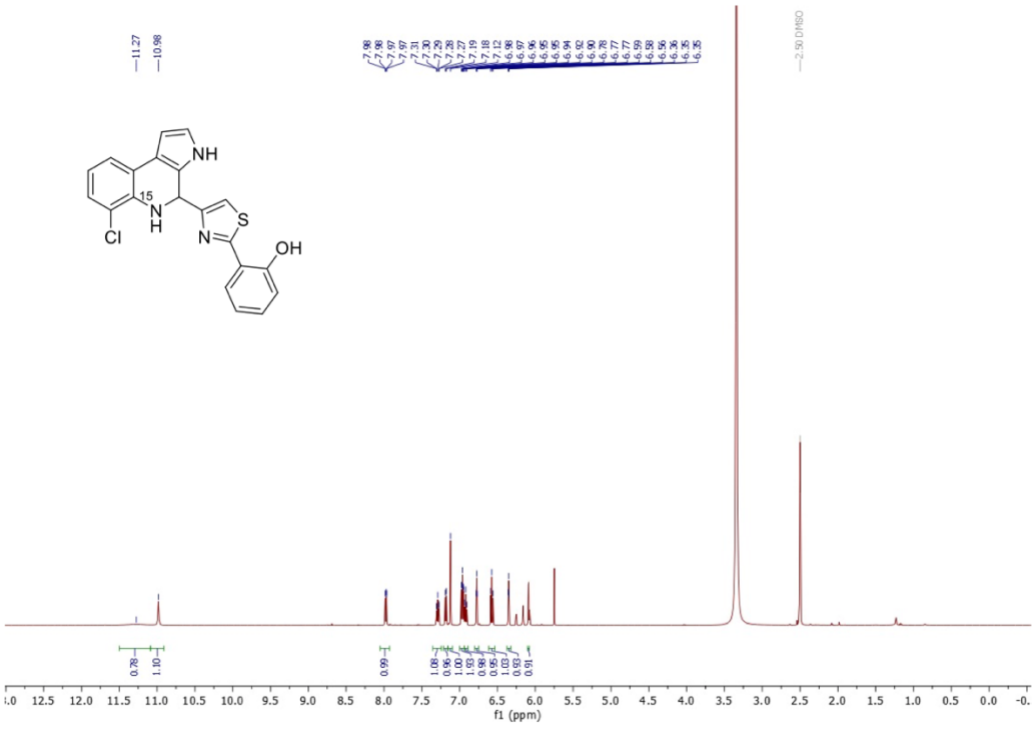

S55

^{13}C NMR spectrum of **28** (125 MHz, DMSO-d_6)

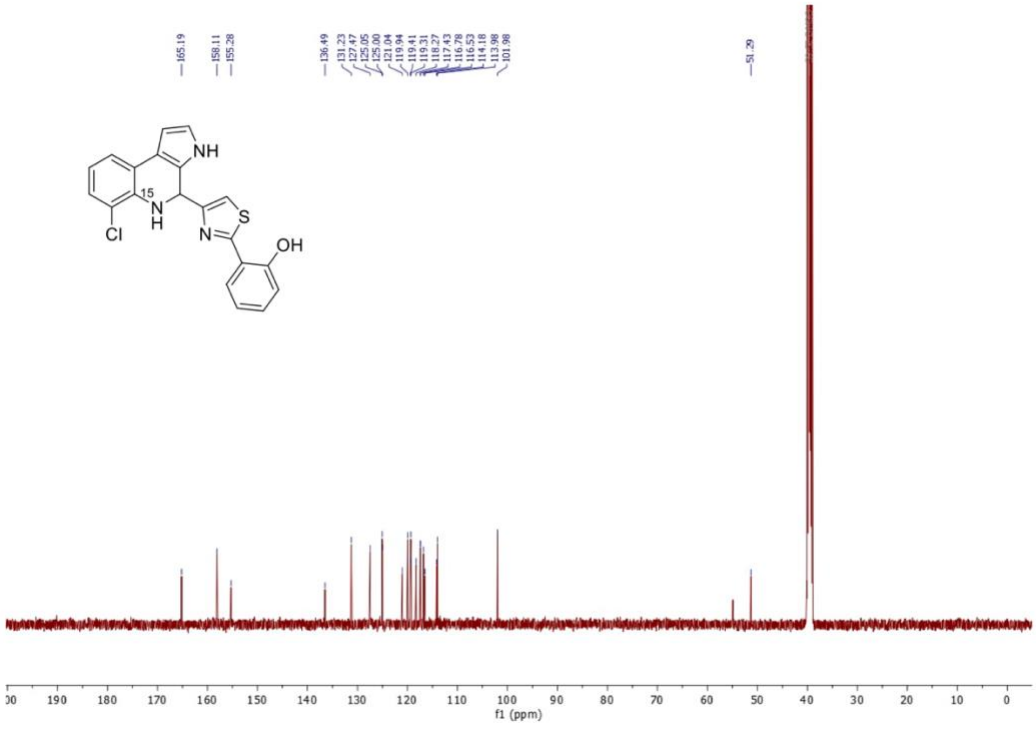

S56

^{1}H-^{15}N HMBC NMR spectrum of **26** (500 MHz, DMSO-d_6)

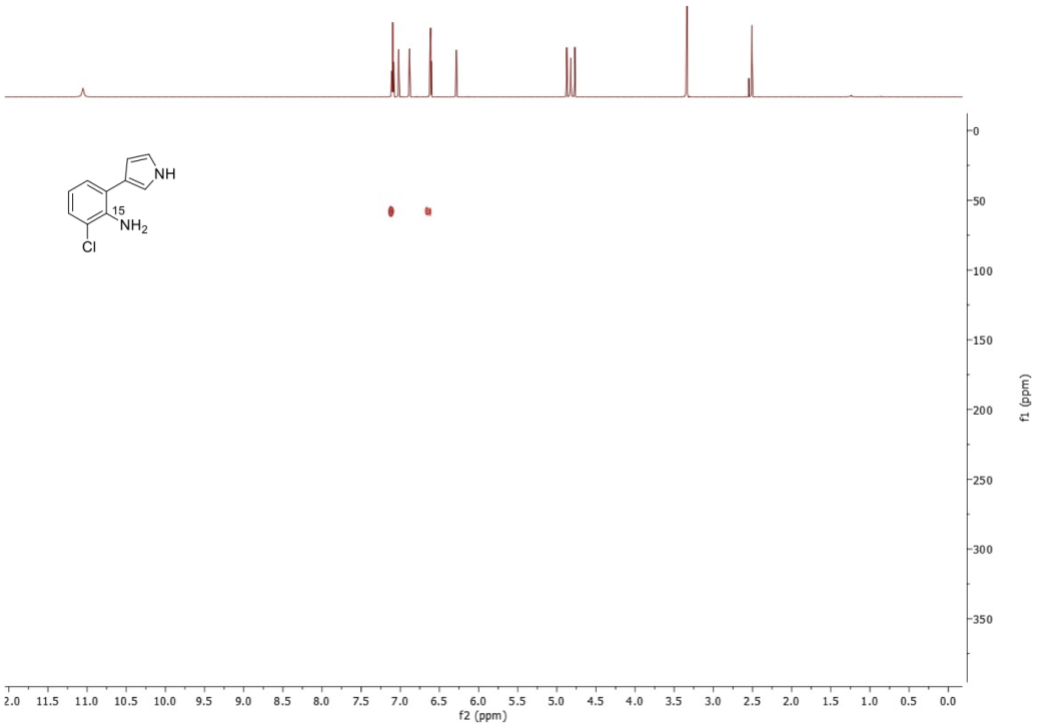

S57

^{1}H-^{15}N HMBC NMR spectrum of **28** (500 MHz, DMSO-d_6)

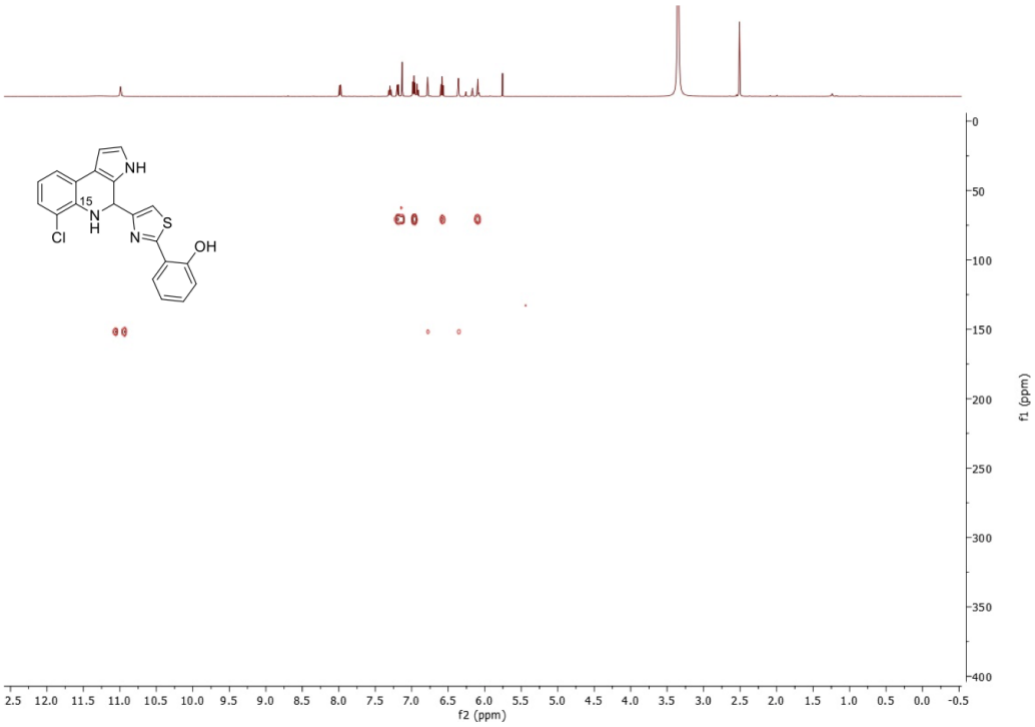

S58

^{1}H-^{15}N HMBC NMR spectrum of **29** (500 MHz, DMSO-d_6)

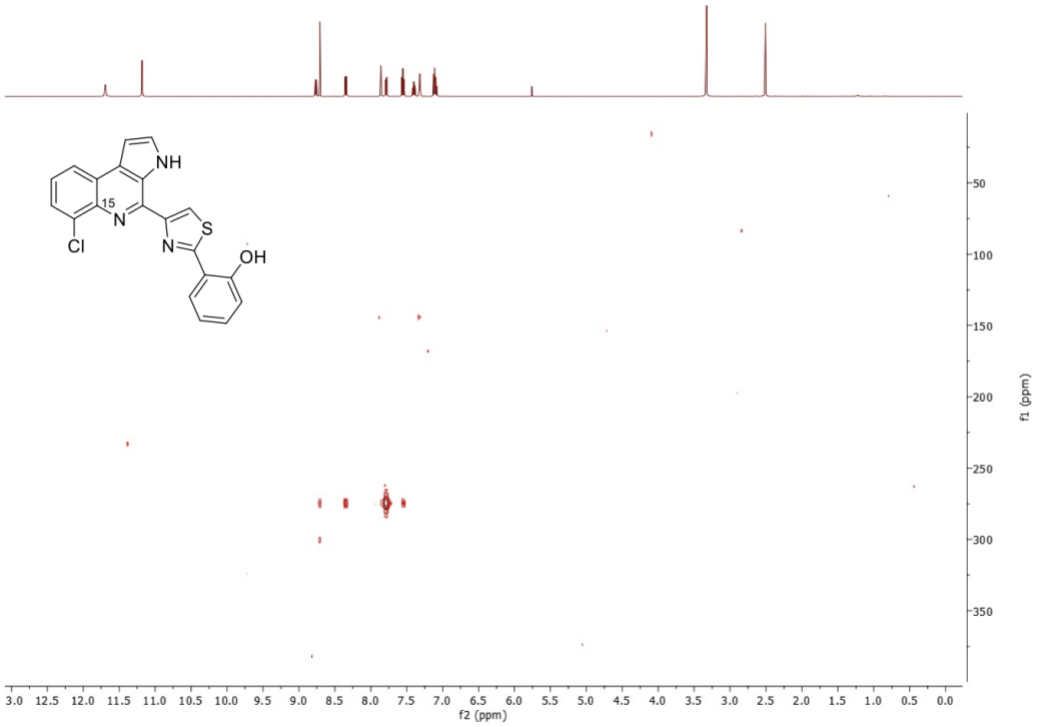

S59

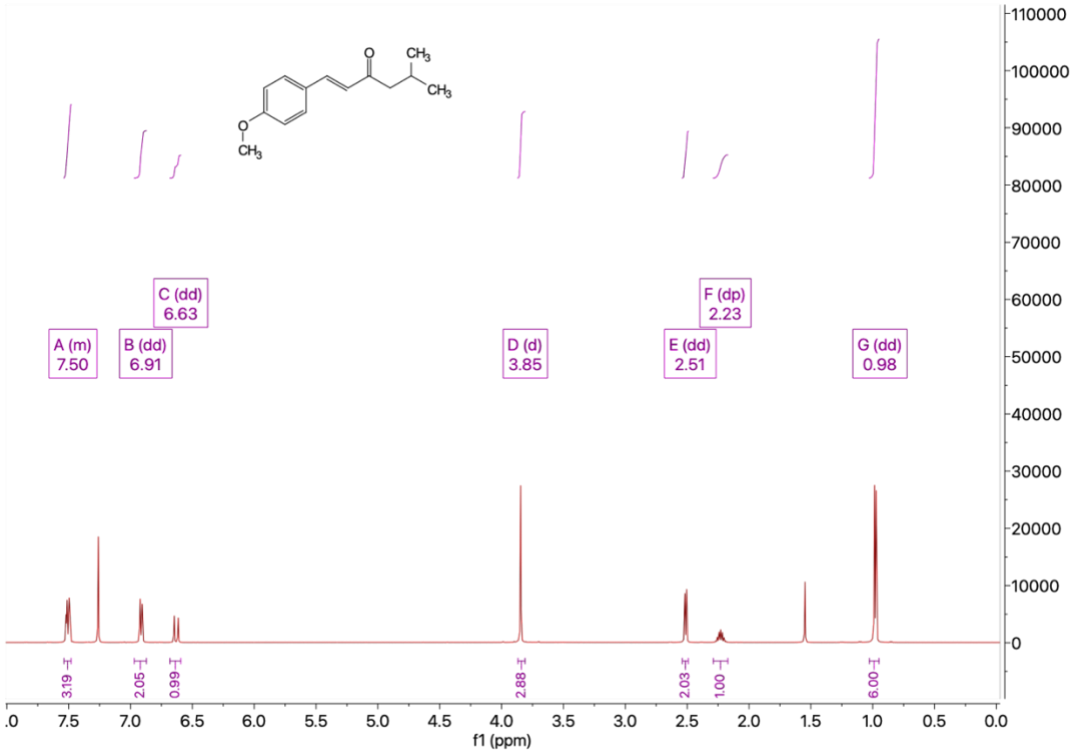
A (m)
7.50
B (dd)
6.91
C (dd)
6.63
D (d)
3.85
E (dd)
2.51
F (dp)
2.23
G (dd)
0.98
3.19
2.05
0.99
2.88
2.03
1.00
6.00
f1 (ppm)

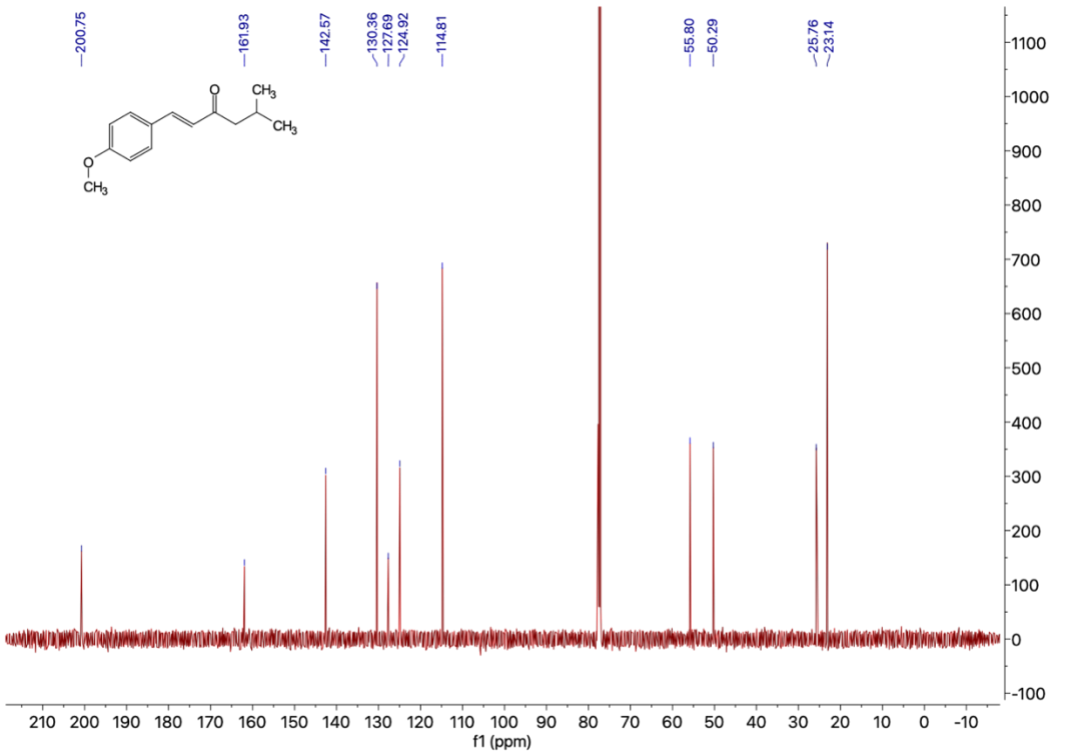
200.75
161.93
142.57
130.36
127.69
124.92
114.81
55.80
50.29
25.76
23.14
f1 (ppm)

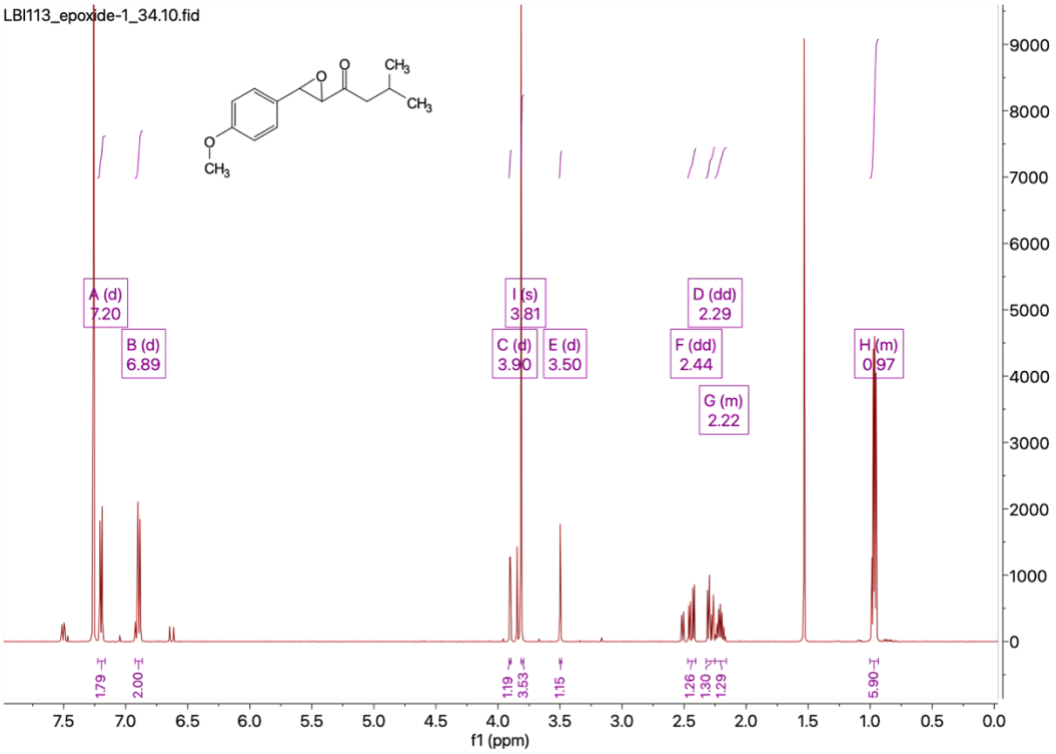
LBI113_epoxide-1_34.10.fid
A (d)
7.20
B (d)
6.89
I (s)
3.81
C (d)
3.90
E (d)
3.50
D (dd)
2.29
F (dd)
2.44
G (m)
2.22
H (m)
0.97
1.79
2.00
1.19
3.53
1.15
1.26
1.30
1.29
5.90
f1 (ppm)

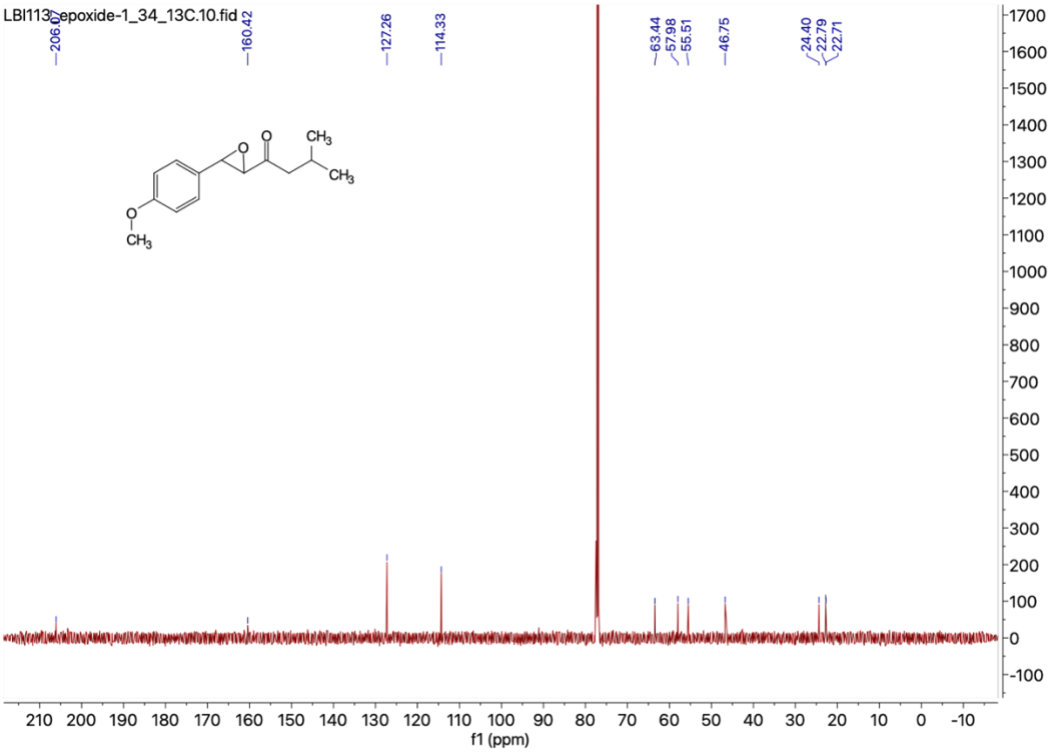
LBI113_epoxide-1_34_13C.10.fid
206.07
160.42
127.26
114.33
63.44
57.98
55.51
46.75
24.40
22.79
22.71
f1 (ppm)

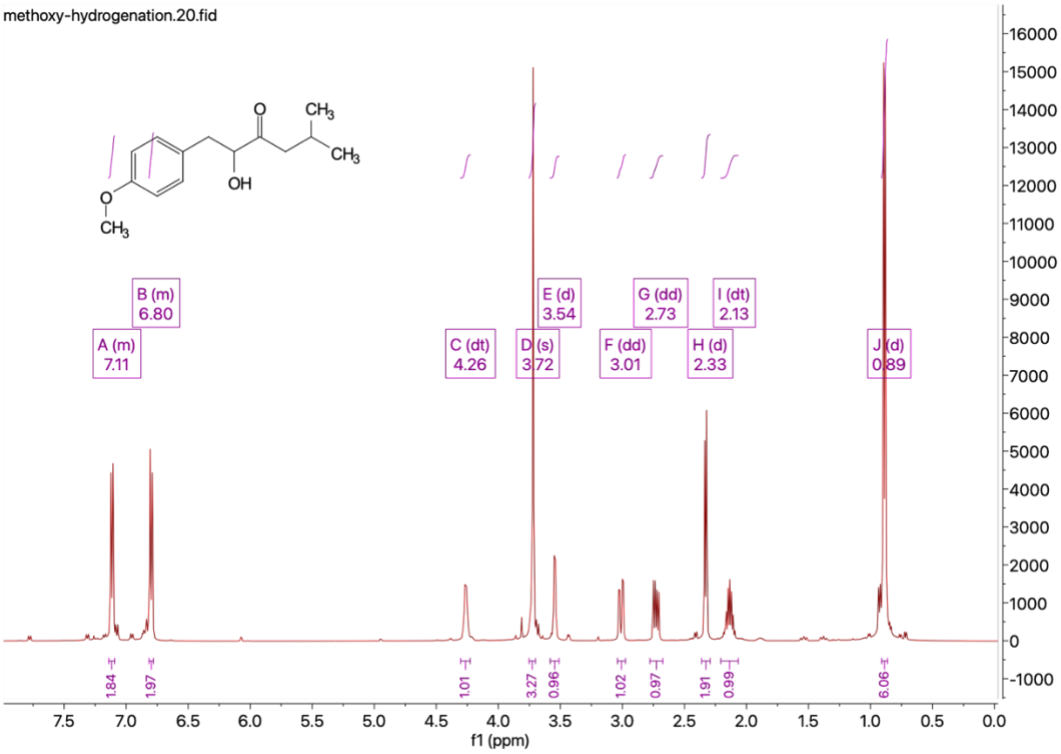
methoxy-hydrogenation.20.fid
A (m) 7.11
B (m) 6.80
C (dt) 4.26
D (s) 3.72
E (d) 3.54
F (dd) 3.01
G (dd) 2.73
H (d) 2.33
I (dt) 2.13
J (d) 0.89
1.84
1.97
1.01
3.27
0.96
1.02
0.97
1.91
0.99
6.06
f1 (ppm)

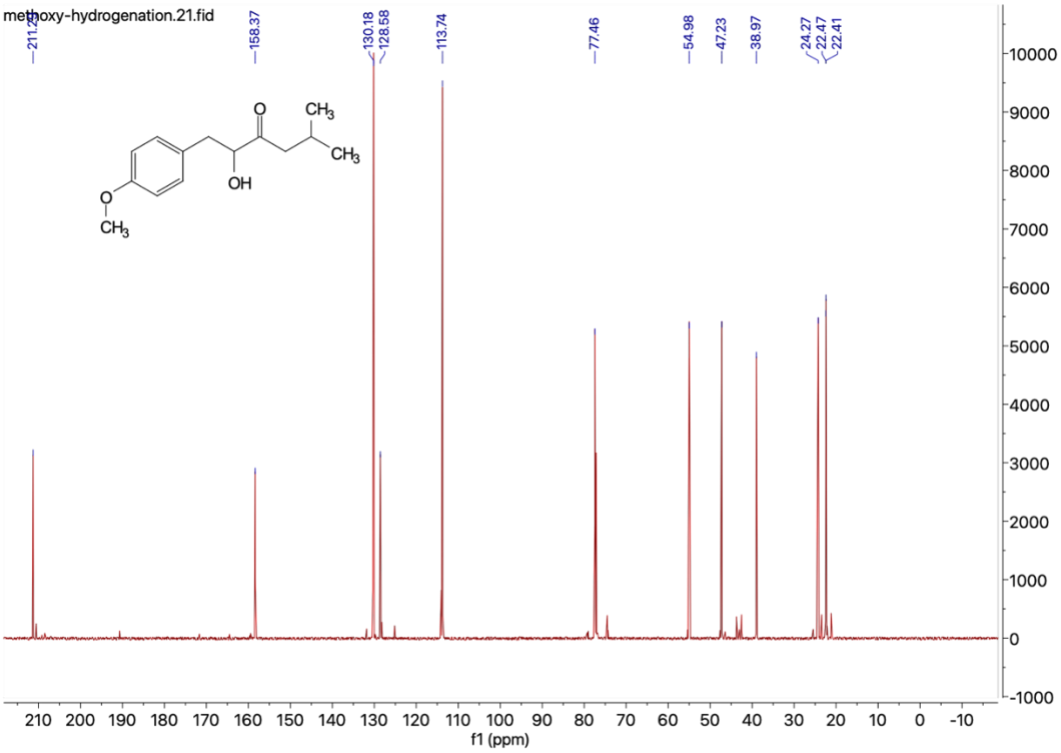
methoxy-hydrogenation.21.fid
211.20
158.37
130.18
128.58
113.74
77.46
54.98
47.23
38.97
24.27
22.47
22.41
f1 (ppm)

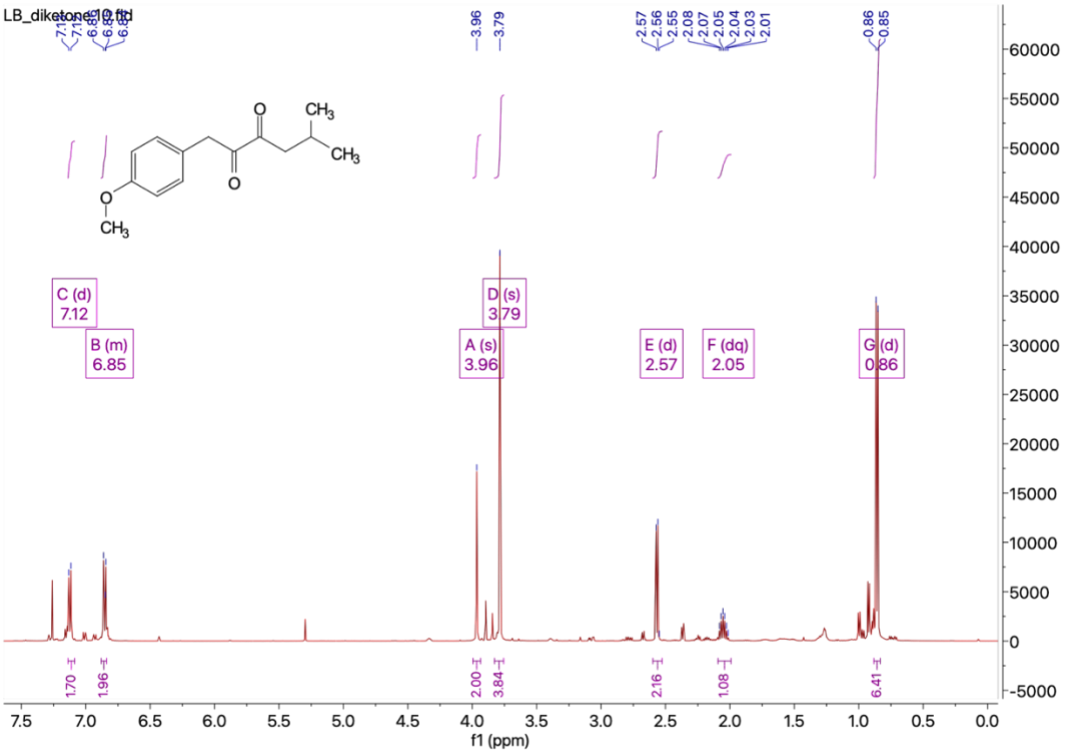
LB_diketone-1H.fid
C (d)
7.12
B (m)
6.85
D (s)
3.79
A (s)
3.96
E (d)
2.57
F (dq)
2.05
G (d)
0.86
f1 (ppm)

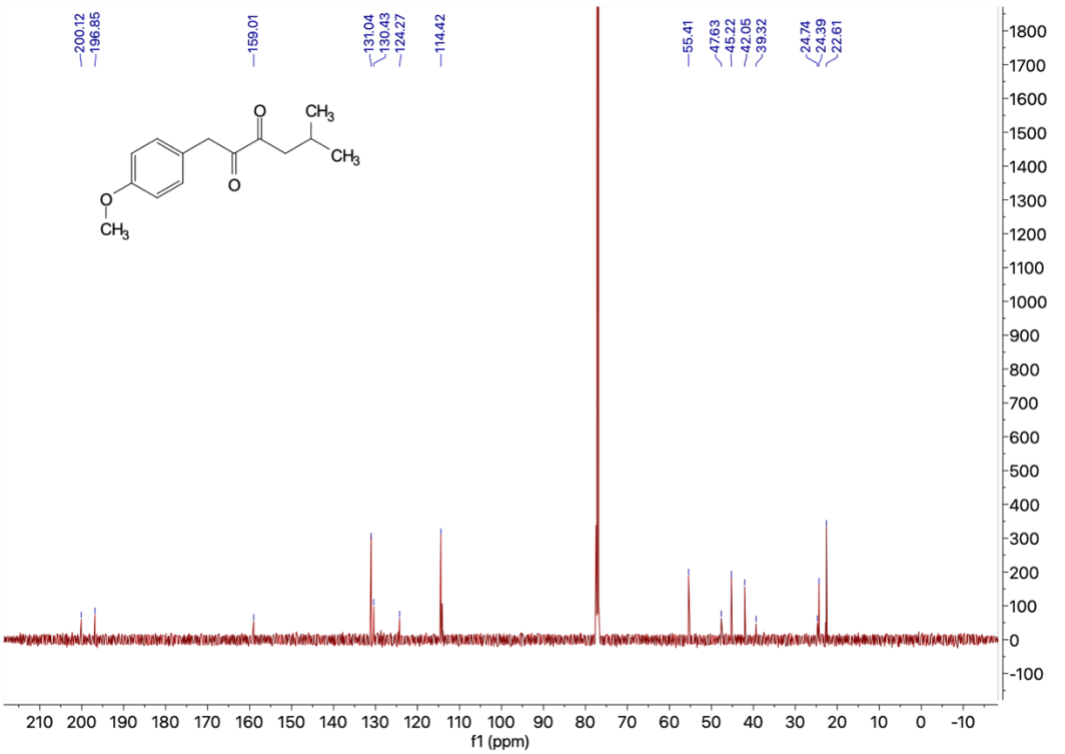
f1 (ppm)

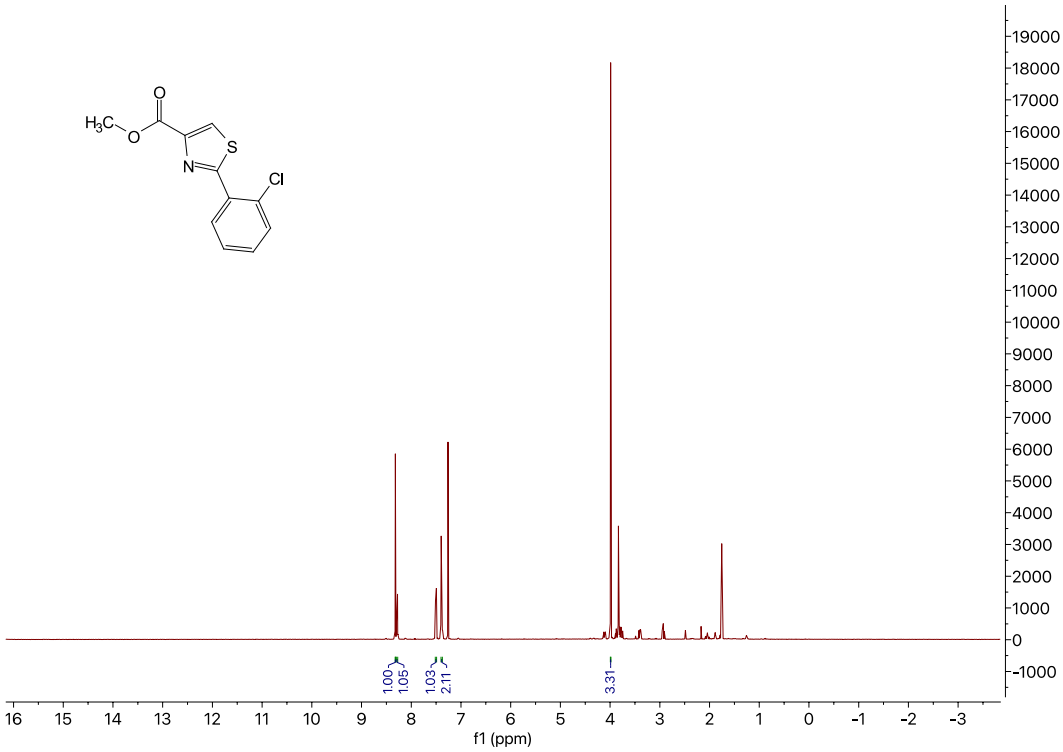
O
H3C
O
S
N
Cl
1.00
1.05
1.03
2.11
3.31
f1 (ppm)

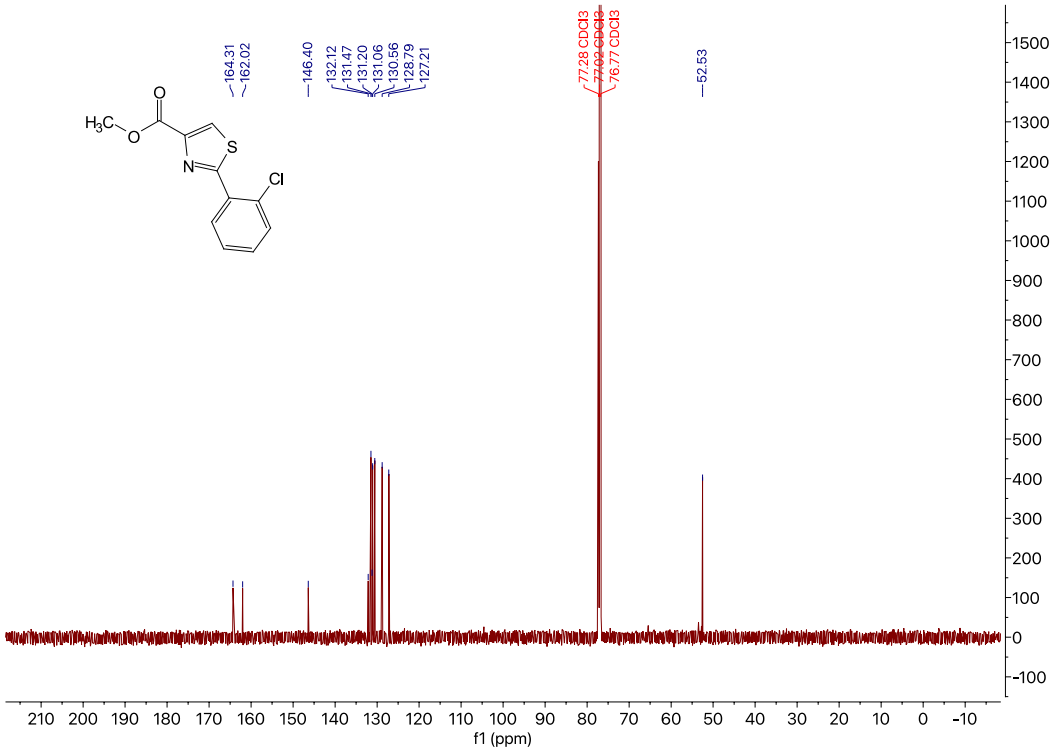
O
H3C
O
S
N
Cl
164.31
162.02
146.40
132.12
131.47
131.20
131.06
130.56
128.79
127.21
77.28 CDCl3
77.03 CDCl3
76.77 CDCl3
52.53
f1 (ppm)

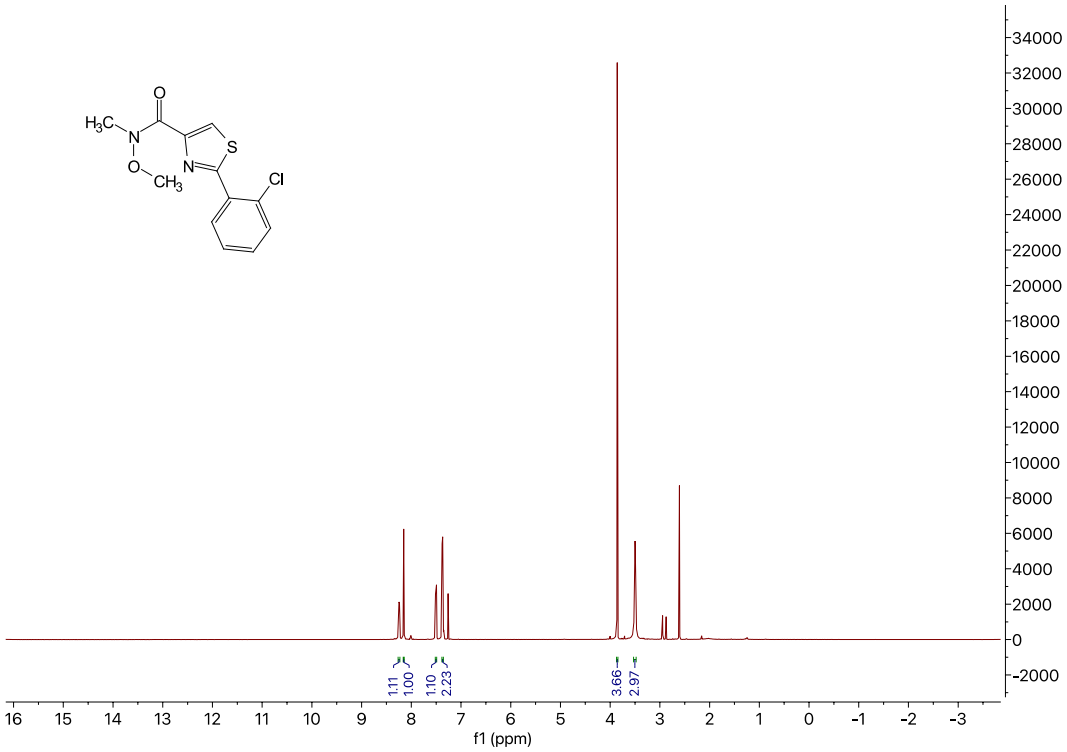
O
H3C
N
O
CH3
S
N
Cl
1.11
1.00
1.10
2.23
3.66
2.97
f1 (ppm)

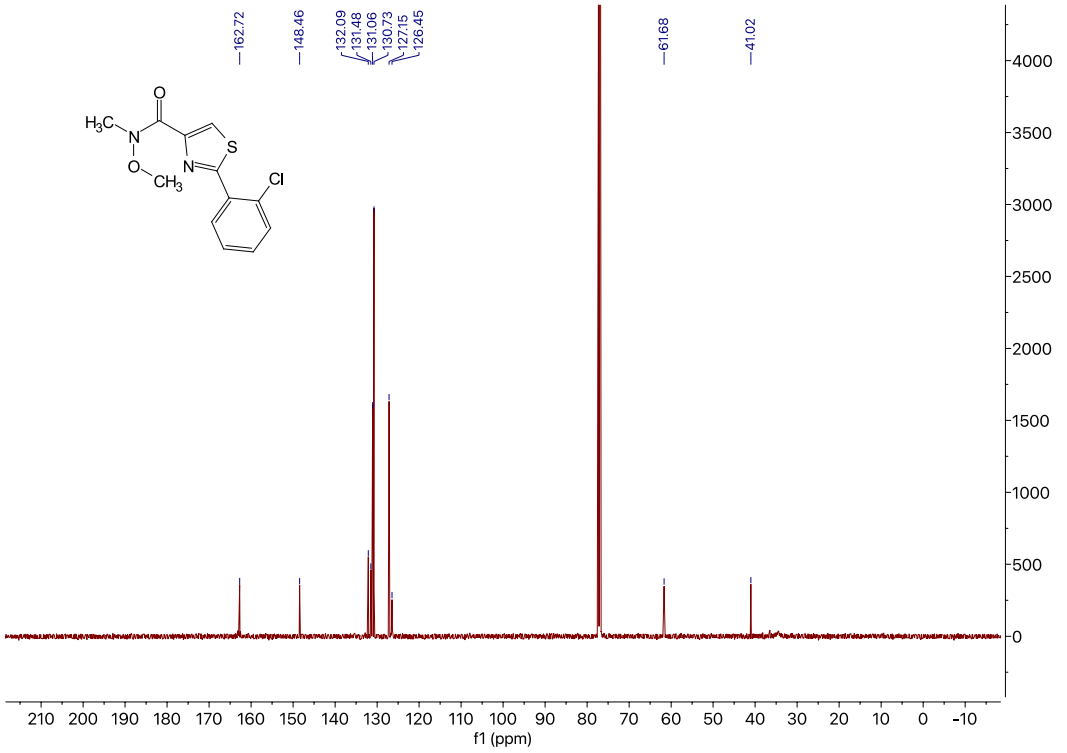
162.72
148.46
132.09
131.48
131.06
130.73
127.15
126.45
61.68
41.02
O
H3C
N
O
CH3
S
N
Cl
f1 (ppm)

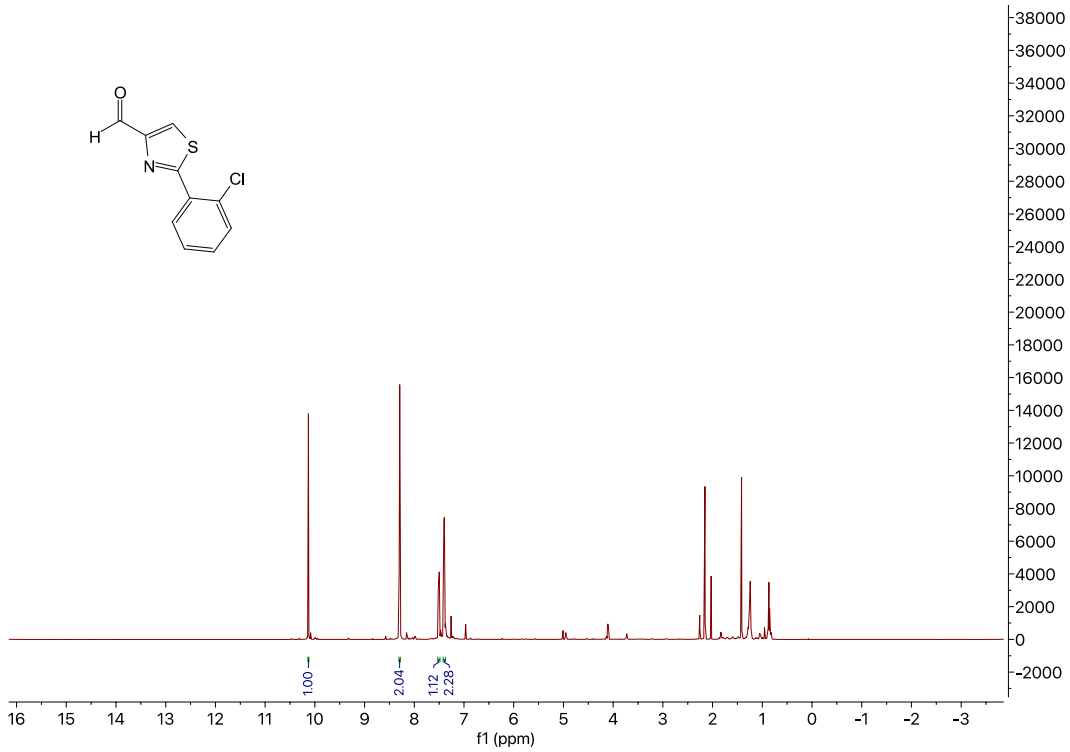
O
H
S
N
Cl
38000
36000
34000
32000
30000
28000
26000
24000
22000
20000
18000
16000
14000
12000
10000
8000
6000
4000
2000
0
-2000
1.00
2.04
1.12
2.28
16 15 14 13 12 11 10 9 8 7 6 5 4 3 2 1 0 -1 -2 -3
f1 (ppm)

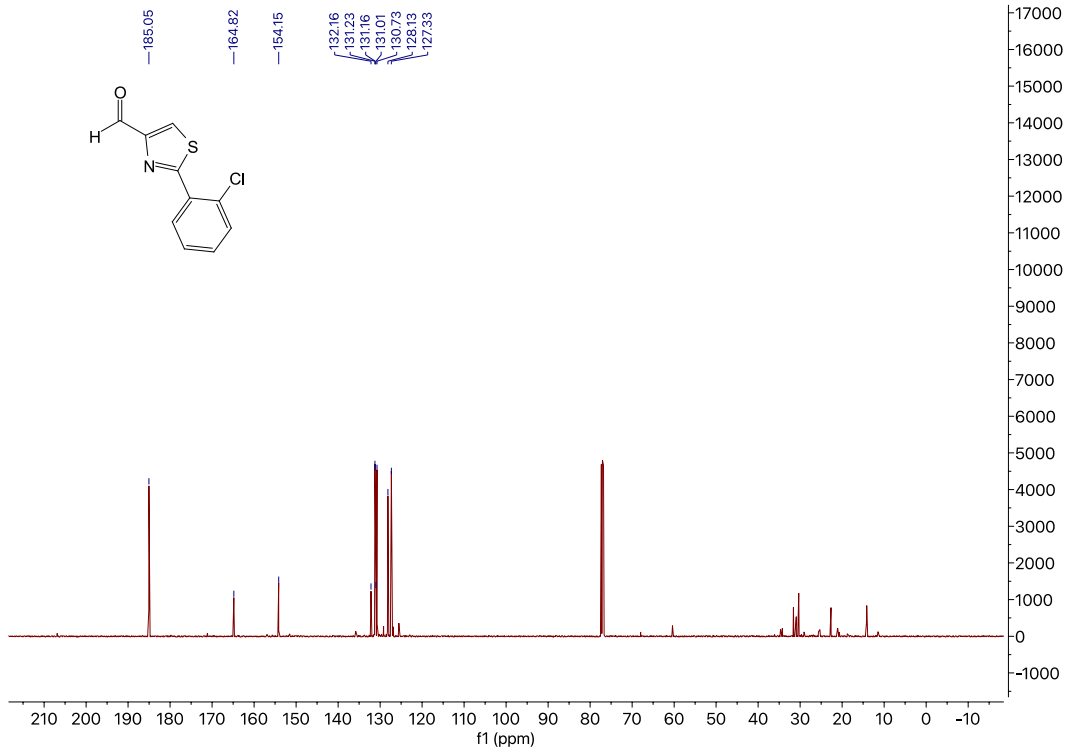
185.05
164.82
154.15
132.16
131.23
131.16
131.01
130.73
128.13
127.33
O
H
S
N
Cl
17000
16000
15000
14000
13000
12000
11000
10000
9000
8000
7000
6000
5000
4000
3000
2000
1000
0
-1000
210 200 190 180 170 160 150 140 130 120 110 100 90 80 70 60 50 40 30 20 10 0 -10
f1 (ppm)

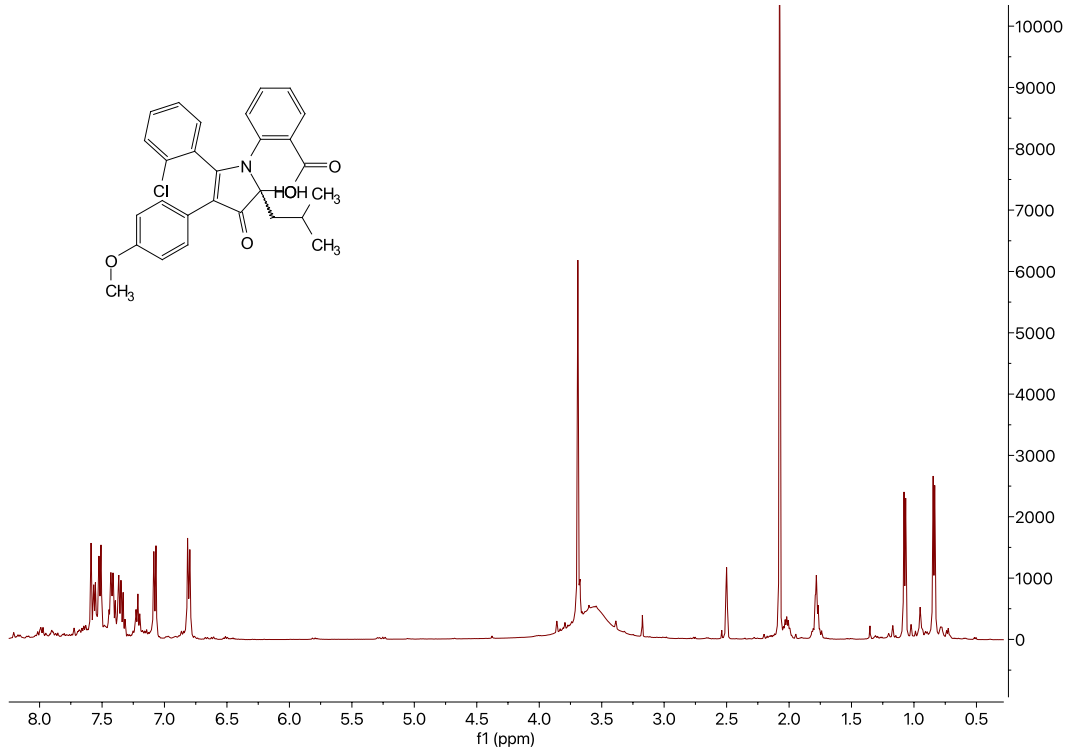
Cl
N
O
HOH
CH3
CH3
O
O
CH3
10000
9000
8000
7000
6000
5000
4000
3000
2000
1000
0
8.0
7.5
7.0
6.5
6.0
5.5
5.0
4.5
4.0
3.5
3.0
2.5
2.0
1.5
1.0
0.5
f1 (ppm)

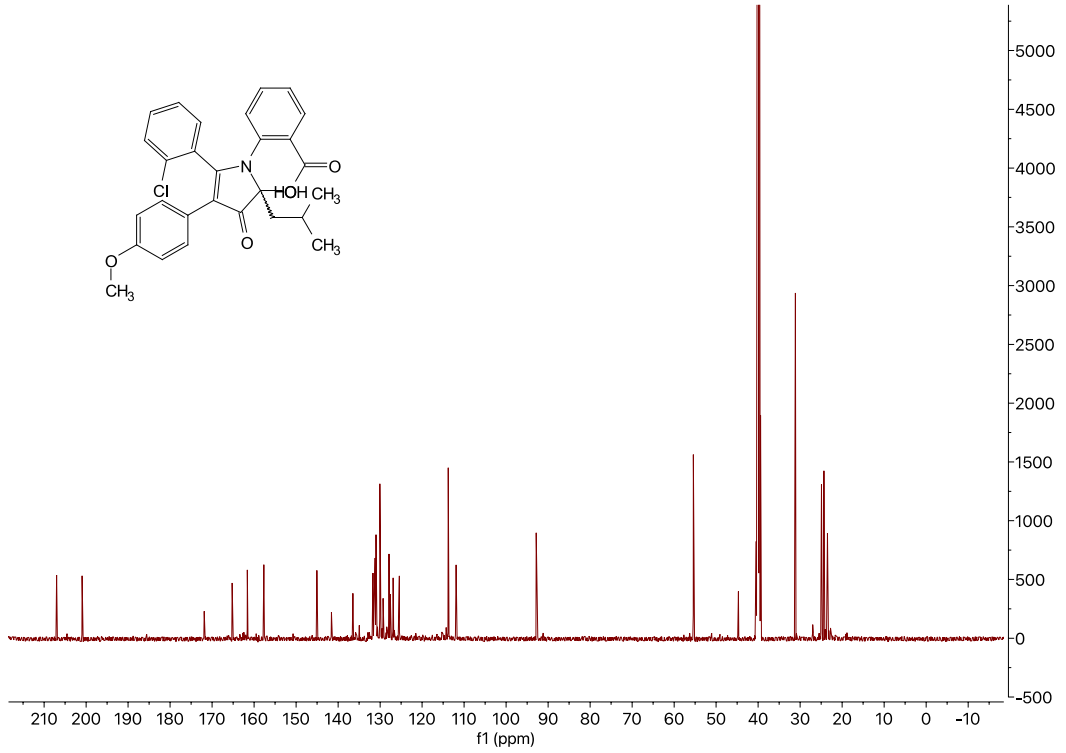
Cl
N
O
HOH
CH3
CH3
O
O
CH3
5000
4500
4000
3500
3000
2500
2000
1500
1000
500
0
-500
210
200
190
180
170
160
150
140
130
120
110
100
90
80
70
60
50
40
30
20
10
0
-10
f1 (ppm)

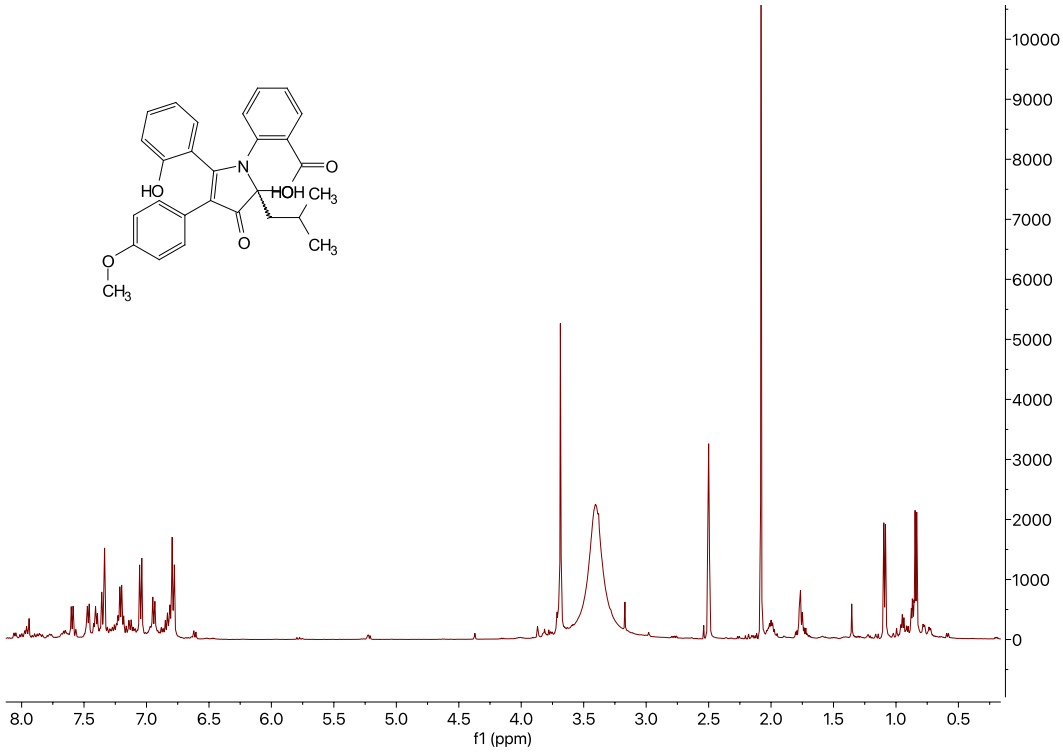
HO
N
O
HO
CH3
O
CH3
O
CH3
10000
9000
8000
7000
6000
5000
4000
3000
2000
1000
0
8.0
7.5
7.0
6.5
6.0
5.5
5.0
4.5
4.0
3.5
3.0
2.5
2.0
1.5
1.0
0.5
f1 (ppm)

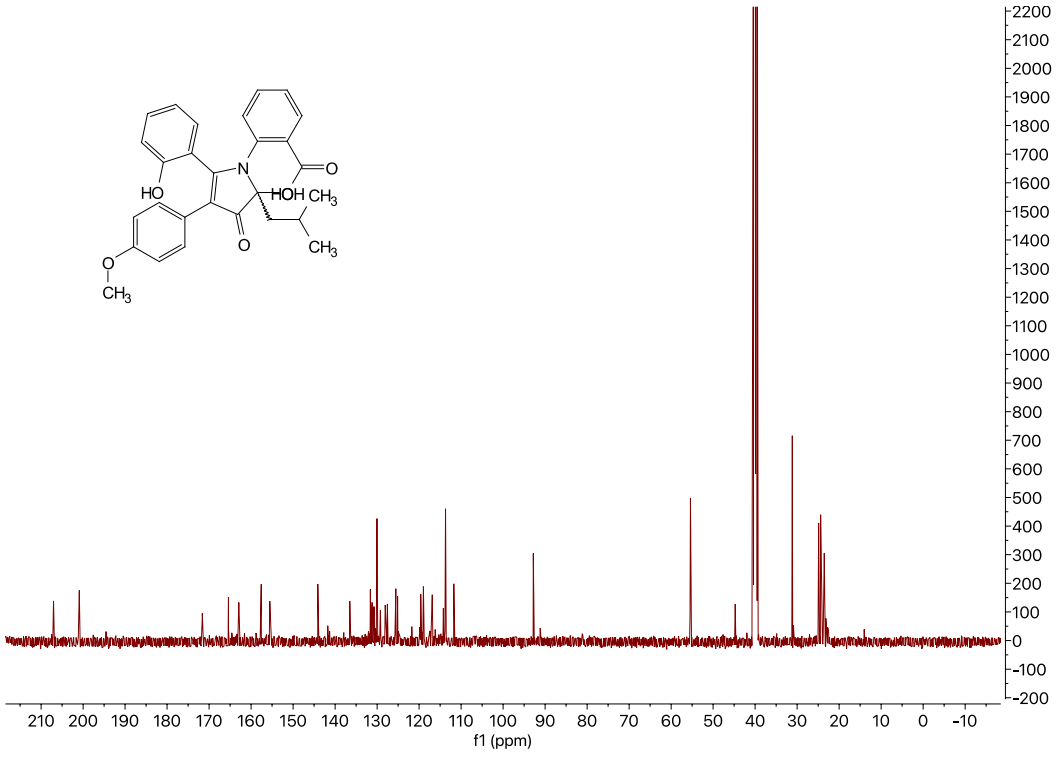
HO
N
O
HO
CH3
O
CH3
O
CH3
2200
2100
2000
1900
1800
1700
1600
1500
1400
1300
1200
1100
1000
900
800
700
600
500
400
300
200
100
0
-100
-200
210
200
190
180
170
160
150
140
130
120
110
100
90
80
70
60
50
40
30
20
10
0
-10
f1 (ppm)

Chapter Four: oxazinin A Mechanistic Elucidation using ^{1}H-^{15}N HMBC

4.1 Introduction

NMR is one of the essential tools for the elucidation and identification of many complex molecules and proteins. In the past, the MacMillan lab has utilized NMR for the elucidation of non-enzymatic mechanisms of the discoipyrroles and the pyonitrins (figure 1,2).[1,2]

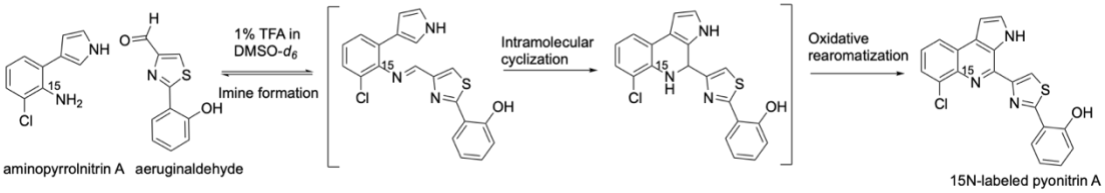

Figure 1. NMR Study of the pyonitrins.

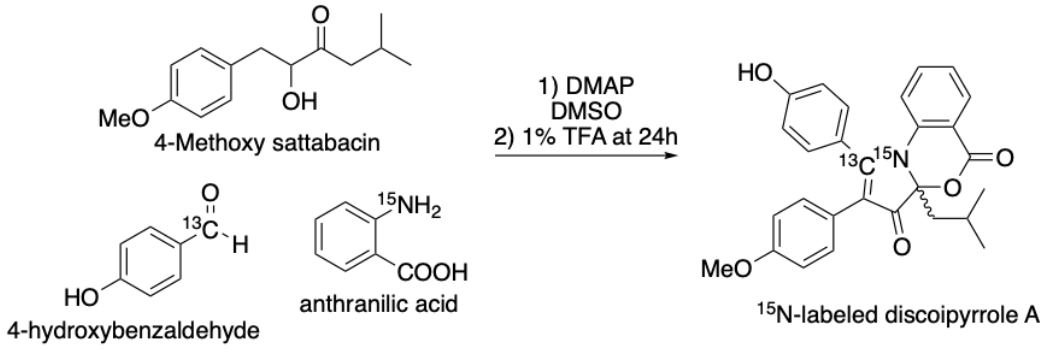

Figure 2. NMR Study of the discoipyrroles.

Since a plethora of non-enzymatic reactions seen in nature occur between reactive aldehydes and amines, we have been able to utilize ^{15}N-labeled amines in both of these non-enzymatic reactions to monitor the formation of these natural products. In a similar manner, we wanted to explore the non-

enzymatic heterodimerization of oxazinin A (**4.1**) from the polyketide aldehyde (**4.3**) and ^{15}N-labeled anthranilic acid (similar to the discoipyrroles; Figure 3).

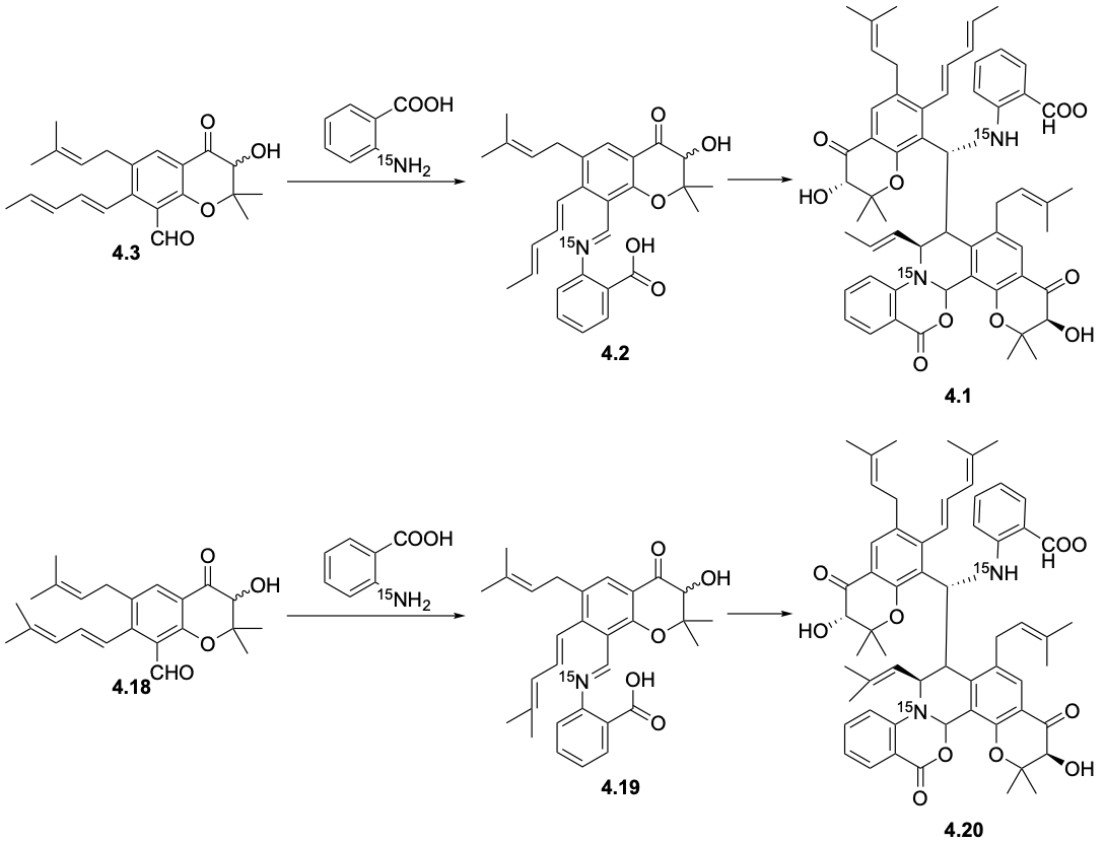

Figure 3. Original (top) and Alternative (bottom) Non-Enzymatic 15N NMR Study of oxazinin A Formation.

4.2 Synthesis of Methyl-Capped Aldehyde

For the NMR mechanistic study of the non-enzymatic formation of oxazinin A, simpler analog of **4.3** was synthesized (**4.18**), where the pentadiene **4.3** is methyl capped to avoid stereochemical mixtures as a result of the Wittig reaction in the original synthesis of oxazinin A. Following the same scheme in

the synthesis of oxazinin A, the DIBAL-H reduced Wittig precursor **4.15** was synthesized (Scheme 1).

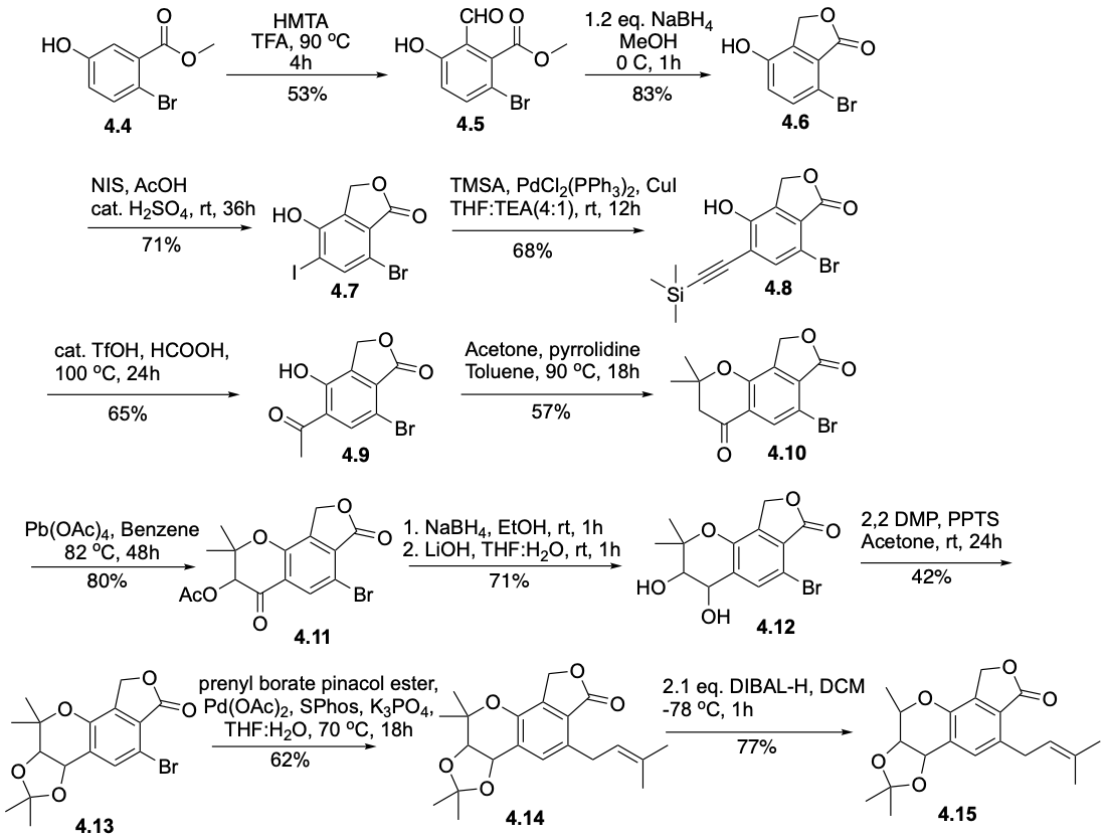

Scheme 1. Synthesis of Intermediate 4.15.

From commercially available starting material **4.4**, a Duff formylation (HMTA in neat TFA) was run to give an aldehyde between the hydroxyl group and the ester (**4.5**, 53% yield). The aldehyde is “protected” as a lactone via reduction with sodium borohydride in MeOH in 83% yield (**4.6**). The lactone is utilized to carry the aldehyde throughout the entire synthesis. **4.6** was halogenated with NIS in Acetic Acid (**4.7**, 71% yield) and coupled with a silyl acetylene via Sonogashira Coupling (**4.8**, 68% yield). This silyl acetylene is

then hydrolyzed to the methyl ketone with catalytic triflic acid in formic acid (**4.9**, 65% yield). Finally, the methyl ketone was cyclized using a modified version of the acetone/pyrrolidine-mediated cyclization (changing the solvent from methanol to toluene improved the yield of the reaction) to give the tricyclic intermediate **4.10** (57% yield). From **4.10**, the alpha position of the ketone was oxidized using $Pb(OAc)_4$ in benzene (**4.11**, 80% yield). The ketone was reduced with $NaBH_4$ and the acetate protecting group was cleaved using LiOH in THF:H_2O (**4.12**, 71% yield). The resulting diol was protected as an acetonide via dimethoxypropane (**4.13**, 42% yield). With the chromanone part of the molecule protected, the Suzuki Coupling was performed to give **4.14** (62% yield). The resulting prenylated lactone is reduced with DIBAL-H to give intermediate **4.15** (77% yield).

With **4.15** in hand, the Wittig Olefination was performed using the methyl capped phosphonium salt (**4.16**, 38% yield). From there the acetonide is removed using aqueous acetic acid at 60 °C (**4.17**). Finally, the benzylic alcohols are selectively oxidized using DMP in DCM to give **4.18** in 63% yield Scheme 2).

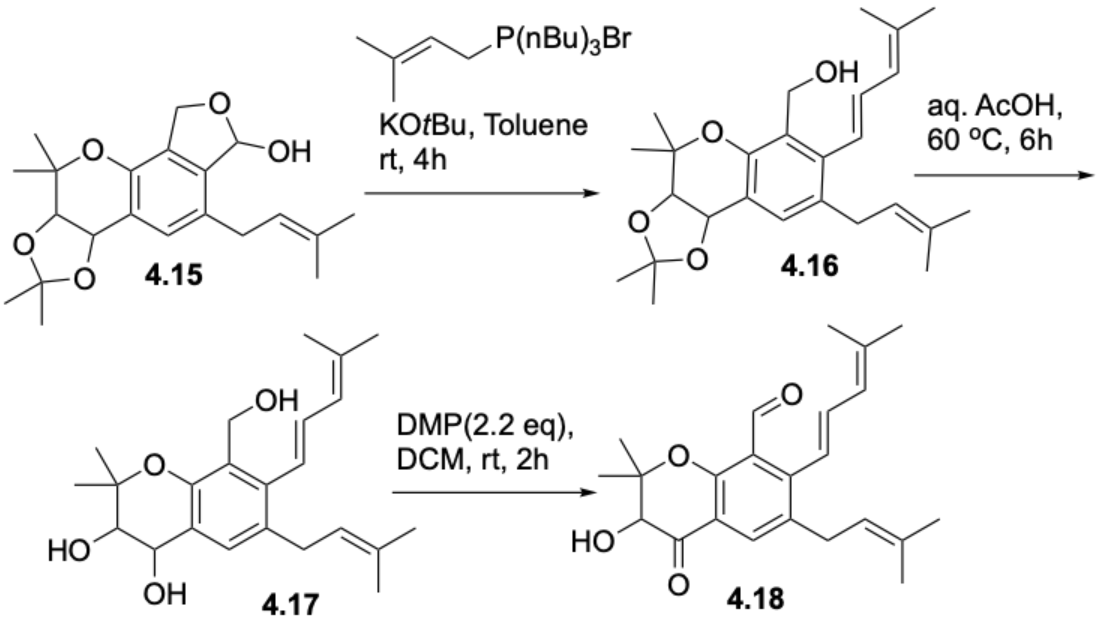

Scheme 2. Synthesis of Methyl-Capped Prenylated Polyketide (4.18) from Intermediate 4.15.

4.3 ^{1}H-^{15}N NMR Study of oxazinin A Formation.

The non-enzymatic reaction with **4.18** and anthranilic acid to form methylated oxazinin A (**4.20**) was explored. ^{15}N-labeled anthranilic acid was synthesized using previously reported methods.[3] Utilizing the same ^{1}H-^{15}N NMR methodology the lab used in the mechanistic elucidation of discoipyrroles and pyonitrins (using liquid NH_3 as a reference), 1 eq of **4.18** and ^{15}N anthranilic acid were mixed in an NMR tube in methanol-d_4 where ^{1}H followed by ^{1}H-^{15}N HMBC were ran every 30 minutes. The disappearance of **4.18** and the formation of methylated oxazinin A and intermediates was monitored over a period of 48 hours. To better view the reaction, a time lapse of the 48 hours

was compiled with each frame representing one hour (Appendix). Figure 4 shows the ^{1}H-^{15}N HMBC of the reaction with only ^{15}N labeled anthranilic acid present in the sample. The ^{15}N signals were referenced to liquid NH_3.

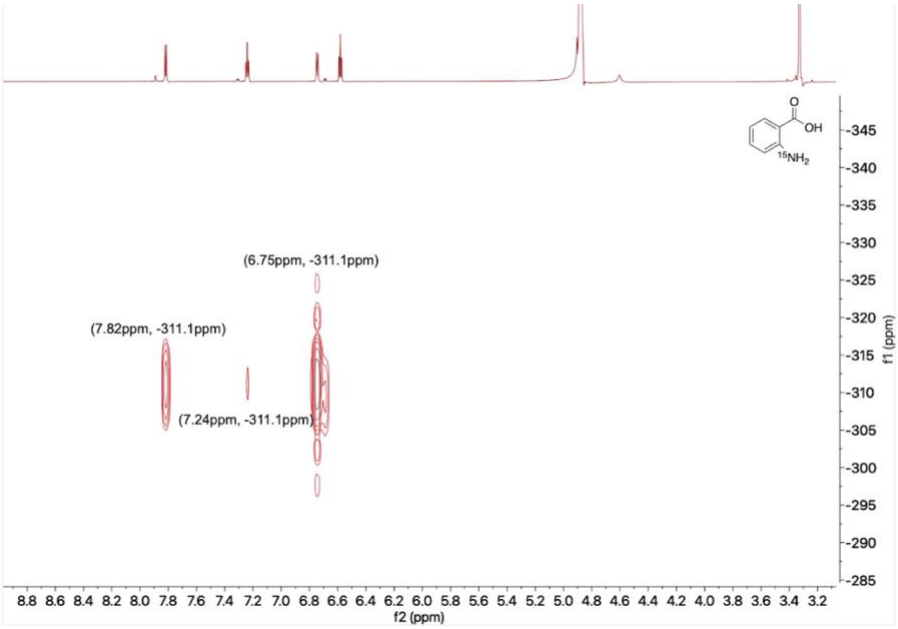

Figure 4. 1H-15N HMBC of Anthranilic Acid.

The spectra show cross peaks at (7.82ppm, -311.1ppm) and (6.75ppm, -311.1ppm) that demonstrate the strong correlation of the ^{15}N labeled anthranilic acid to each of the ortho protons. In addition, there is a weak cross peak at (7.24ppm, -311.1ppm) that corresponds to one of the protons meta to either the carboxylic acid or the labeled aniline (most likely the aniline). For ease of analysis, Figure 5 shows the ^{1}H-^{15}N HMBC data at 30 minutes, 1.5 hours (Figure 6), 9.5 hours (Figure 7), and 47.5 hours (Figure 8) time points as well as atom numbering of key intermediates and methyl-capped oxazinin A analog **4.20**.

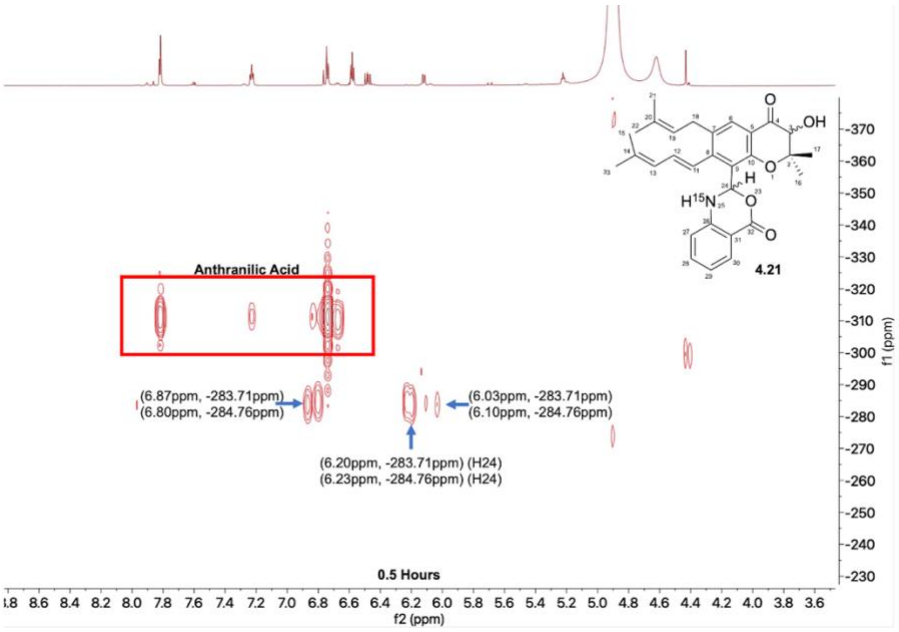

Figure 5. ^{1}H-^{15}N HMBC at 0.5 hours.

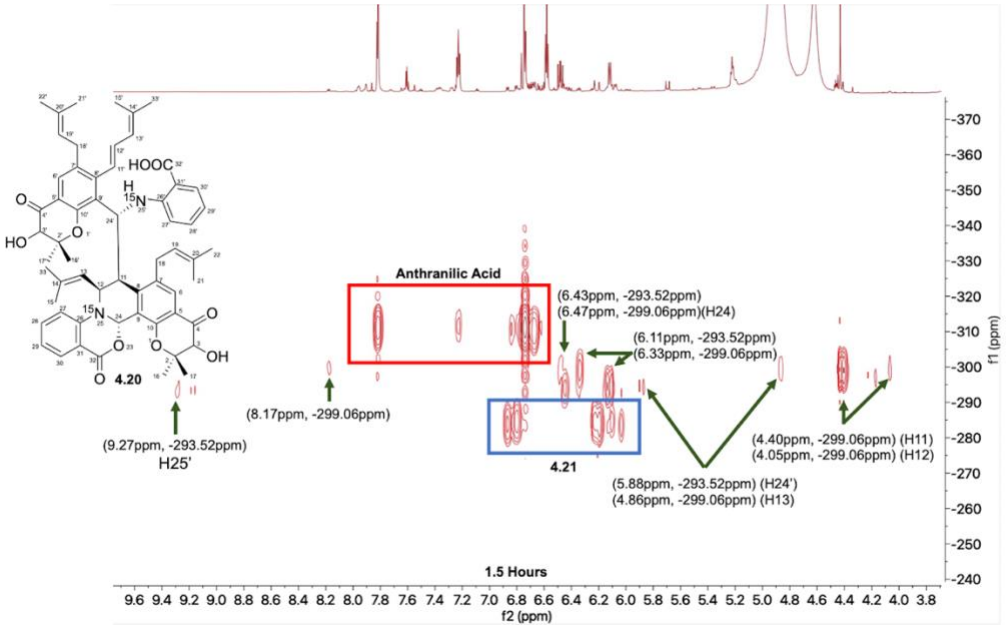

Figure 6. ^{1}H-^{15}N HMBC at 1.5 hours.

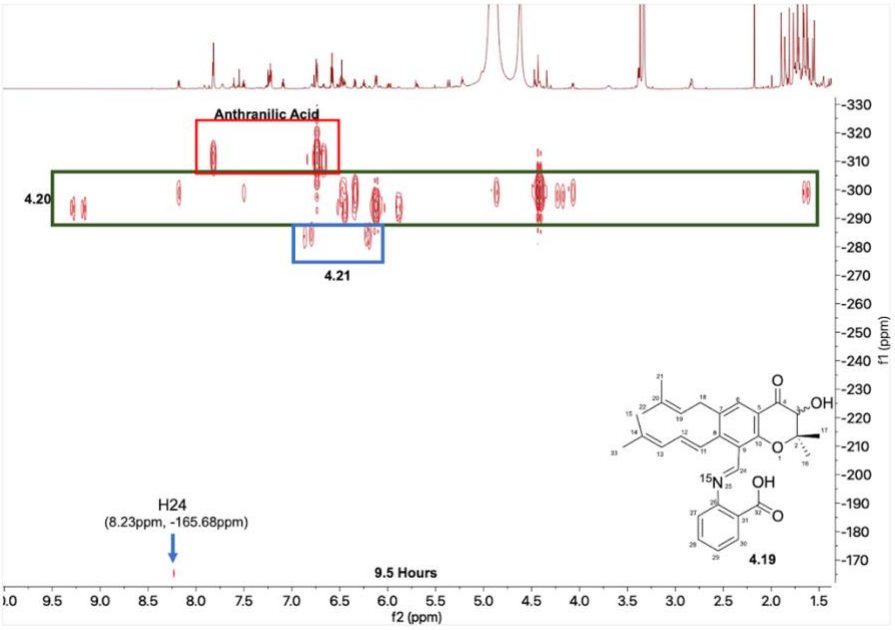

Figure 7. ^{1}H-^{15}N HMBC at 9.5 hours.

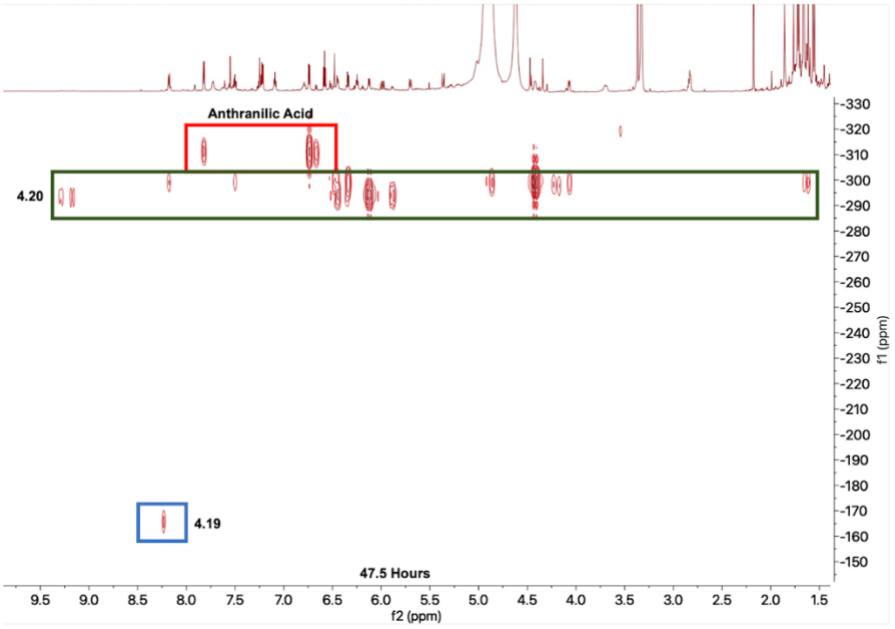

Figure 8. ^{1}H-^{15}N HMBC at 47.5 hours.

30 minutes after the starting materials were added, the formation of **4.21** is noted. The proton NMR showed singlets at 6.20ppm and 6.23ppm that also

correlated to ^{15}N but saw no protons in the 8-9ppm range that would demonstrate an imine. We were also lacking a downfield imine ^{15}N shift in the -50ppm to -200ppm range. A singlet in the 6.00ppm to 6.50ppm range is peculiar since it would not belong to any of our alkene (they are extensively coupled) or our aromatic (they are further downfield) protons. Instead, the peak resembled a tertiary carbon flanked by heteroatoms. The literature has shown that anthranilic acids can react with phenolic aldehydes to form benzoxazinones so this led us to believe that the intermediate we were seeing was an hemiaminal, or an imine that has intramolecularly cyclized with anthranilic acid.[4] We believe that two diastereomers of **4.21** form at 30 minutes with one diastereomer having cross peaks at (6.87ppm, -283.71ppm), (6.20ppm, -283.71ppm), and (6.03ppm, -283.71ppm) while the other has cross peaks at (6.80ppm, -284.76ppm), (6.23ppm, -284.76ppm), and (6.10ppm, -284.76ppm). In the reaction, the cyclization with anthranilic acid to form the hemiaminal forms a new stereocenter, while the alpha-hydroxyl group on the chromanone ring is already present, so there should be two diastereomers present. With those 6 signals that seemingly came in pairs of two, it was assumed that 3 were from each diastereomer rather than 6 signals from the same molecule. For instance, the protons on carbons 27 and 30 typically have about a 1ppm difference in chemical shift. As the two signals that correspond to the anthranilic acid ring (6.87ppm and 6.80ppm) were close together and had a slight difference in ^{15}N shift, we felt more confident in our diastereomer

distinction. This follows what we have seen prior with anthranilic acid ^{1}H-^{15}N HMBC signals: strong signals from the protons para and ortho to the labeled nitrogen. The addition of a new 3rd signal would correspond to a singlet, which corroborated the notion of a hemiaminal group.

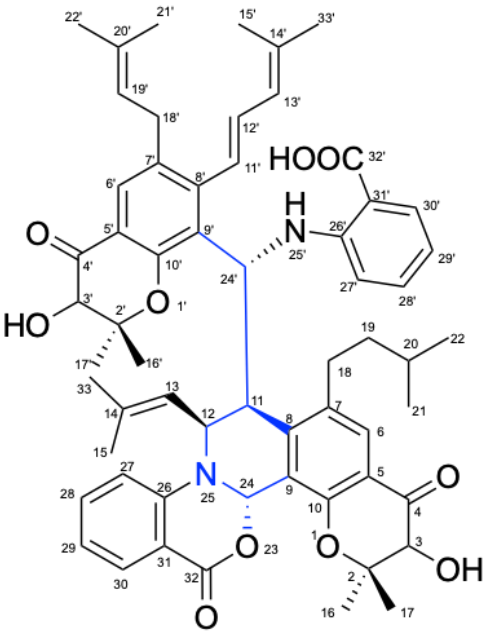

4.20 (in DMSO-d_6)

No	1H NMR
24	6.39 (s, 1H)
11	4.33 (d, *J* = 10.0, 1H)
12	3.98 (d, J = 8.4 Hz, 1H),
13	4.80 (m, 1H)
24’	5.87 – 5.84 (m, 1H)

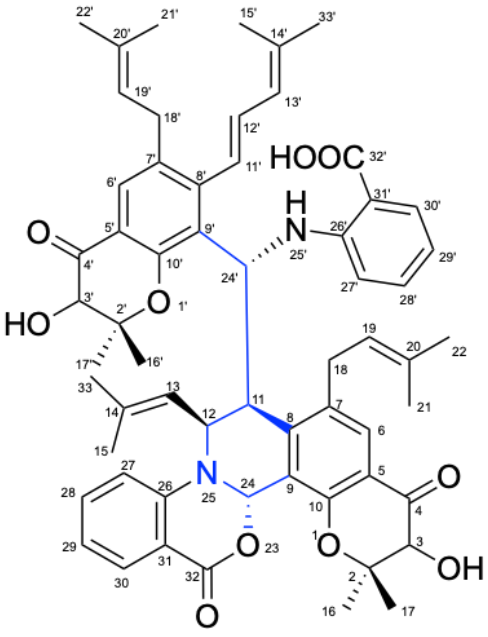

4.20 (in Methanol-d_4)

No	1H NMR
24	6.48 (s, 1H)
11	4.40 (br dd, 1H)
12	4.05 (d, J = 8.4 Hz, 1H),
13	4.86 (under solvent peak, 1H)
24’	5.88 (d, J = 10.1 Hz, 1H)

Figure 9. Chemical Shift Comparison of 4.20 in DMSO-d_6 and Methanol-d_4.

We see the appearance of **4.20** at 1.5 hours. Using the ^{1}H NMR of the product in DMSO-d_6 aided in the assignment of the cross peaks (Figure 9). The rapid appearance of **4.20** is demonstrated by cross peaks: (9.27ppm, -293.52ppm), (9.15ppm, -293.52ppm), (6.43ppm, -293.52ppm), (6.11ppm, -293.52ppm), (5.88ppm, -293.52ppm), (8.17ppm, -299.06ppm), (6.33ppm, -299.06ppm), (6.47ppm, -299.06ppm), (4.86ppm, -299.06ppm), (4.40ppm, -299.06ppm), (4.05ppm, -299.06ppm). The two unique ^{15}N signals corresponded to the labeled nitrogen atoms in each half of the heterodimer. We began our analysis with the ^{15}N signals at -293.52ppm. The protons occurring at 9.27ppm and 9.15ppm were of particular interest. In the original isolation paper, the Schmidt group characterized oxazinin A in both DMSO-d_6 and CD_3CN and in both cases were able to see the proton on nitrogen 25' at 9.01ppm and 9.02ppm, respectively.[5] Normally you would expect the proton attached to an amine to to appear at around 4.00ppm but since that proton can form a 6-membered ring via intramolecular hydrogen bonding with the vicinal carboxylic acid carbonyl, the chemical shift moves far downfield to around 9ppm. Despite the experiment being run in methanol-d_4 and hydrogen-deuterium exchange being prominent, the hydrogen bonding could be sufficient to retain some unexchanged hydrogen atoms and give us a sufficient signal. The ^{15}N peaks are different from anthranilic acid (that also has a ^{15}N-H bond that can interact with the carboxylic acid although we do not see that in the ^{1}H-^{15}N HMBC spectrum). This gave us confidence in our assignment of that

cross peak. As the reaction proceeds and more product is formed, the intensity of the (9.28ppm, -293.52ppm) cross peak increases as well. The peaks at (6.43ppm, -293.52ppm) and (6.11ppm, -293.52ppm) should belong to the anthranilic acid ring. The coupling of the peak at 6.43ppm is 8.7 Hz while the coupling of the proton at 6.11ppm is 9.4 Hz. The ^{15}N at -293.52ppm also sees a doublet at 5.88ppm which we believe correlates to the proton at carbon 24' (compared to 5.84ppm - 5.87ppm on carbon 24' of **4.20** in pure DMSO-d_6), demonstrating the correlation belongs to the secondary amine half of heterodimer **4.20**.

The -299.06ppm labeled nitrogen had peaks at 8.17ppm, 7.50ppm, 6.33ppm, 6.47ppm, 4.86ppm, 4.40ppm, 4.06ppm, 1.64ppm, 1.6ppm. Using the pure sample in DMSO-d_6 as reference, these cross peaks were much simpler to assign. The protons at 8.17ppm and 6.33ppm were from the anthranilic acid ring (carbons 27-30) and had coupling constants of 7.8 and 7.9 Hz respectively. The signal at 6.47ppm correlated with a singlet which corresponds to the hemiaminal proton on carbon 24. The signal at 4.86ppm is underneath the residual solvent peak but corresponds to the alkene proton on carbon 13 (4.86ppm in methanol-d_4 compared to 4.80ppm in DMSO-d_6). The proton on carbon 13 in pure **4.20** in methanol-d_4 appears at 5.22ppm, but the extra methyl at the end of the chain provides extra shielding and moves the chemical shift upfield. 4.40ppm corresponds to the proton on carbon 11, which is close to the DMSO-d_6 value of 4.33ppm. The peak at 4.05ppm corresponds to the proton

on carbon 12 as evidenced by the coupling constant of 8.4 Hz since the analogous proton occurs at 3.98ppm in DMSO-d_6 and has the same coupling constant of 8.4 Hz. With the assignment of these signals, we believed the nitrogen at -299.06ppm corresponded to the bottom half of the heterodimer.

The ^{1}H-^{15}N HMBC cross peaks of intermediate **4.21** begin to disappear after 2 hours while the heterodimer **4.20** continues to form. At 9.5 hours a new peak at (8.23ppm, -165.68ppm) appears, but it was unclear as to what the identity of that orphan ^{1}H-^{15}N HMBC signal belonged to. We suspected it belonged to imine **4.19** but there was not enough evidence to back that claim. We ran an experiment to test this theory. We added ^{15}N labeled anthranilic acid to a simpler version of **4.18** (in an NMR tube) that removed the prenyl group and had a phenolic OH instead of the pentadiene in methanol-d_4 (Figure 10).

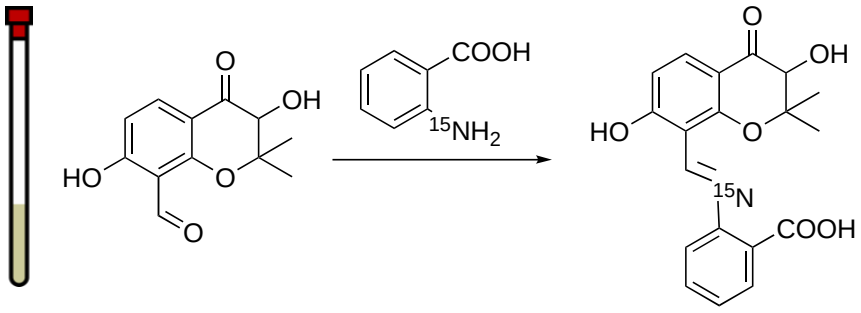

Figure 4.10 Imine Mimic NMR Study.

Without the pentadiene present (i.e., ability to dimerize), we should be able to see imine formation and obtain some clarity on potential ^{1}H and ^{15}N shifts for a similar imine. The reaction was monitored via ^{1}H-^{15}N NMR. The reaction showed the formation of what appeared to be imine after 30 mins

(9.07ppm, -175.41ppm). An ^{1}H-^{13}C HSQC was run on the reaction to further elucidate the identity of the peak at 9.07ppm. The HSQC revealed the proton was attached to a carbon at 154.03ppm. Imines attached to aromatic rings typically appear at around 160ppm which gave further confidence that the peak at 9.07ppm was indeed an imine.[6] Our mimic imine had a ^{1}H-^{15}N signal at (9.07ppm, -175.41ppm), while the peak at 9.5 hours of our NMR study had a cross peak at (8.23ppm, -165.33ppm). This prompted us to believe that the signal we were seeing at (8.23ppm, -165.33ppm) in our study was indeed imine.

The NMR study was stopped after 48 hours and starting material remained, so there was still unreacted imine and starting material present in the sample. We then made a proposal for the dimerization mechanism (Figure 10). When the reaction begins, any imine that forms rapidly converts to the hemiaminal or dimerizes, which is presumably why we do not see any at the beginning time points. As a result, the only products that would be seen at the beginning of the reaction would be the dimer **4.20** and the accumulation of hemiaminal **4.21**. The imine and the hemiaminal should be in an equilibrium as the “open” (imine) and “closed” (hemiaminal) forms, so as the hemiaminal slowly converts to the imine (the hemiaminal is presumably favored in the equilibrium), the imine concentration would increase, and the molecule would dimerize to form **4.20**. This would push the equilibrium toward the production of more imine, via Le Chatelier's Principle, which would explain why hemiaminal

4.21 is relatively absent at approximately 16.5 hours while the concentration of imine **4.19** begins to increase at 9.5 hours.

At around the 17-hour time point, the entirety of **4.21** is gone, and only **4.20**, anthranilic acid, and imine **4.19** remain. With a larger concentration of **4.20**, more signals can be seen in the 1H-15N HMBC spectra: (7.50ppm, -299.06ppm), (1.64ppm, -299.06ppm), and (1.6ppm, -299.06ppm). Figure 8 gives a clear image of reaction milieu from approximately the 17-hour mark onwards. The shift at 7.50ppm comes from anthranilic acid (and has a corresponding coupling constant of 7.8 Hz like the other anthranilic acid peaks at this ^{15}N shift), while the two peaks at 1.64ppm and 1.60ppm come from long range 5-bond coupling from ^{15}N25 to the methyl groups at the end of the pentadiene on carbons 15 and 33. Figure 11 shows the proposed pathway of **4.20**, and analogously oxazinin A, formation.

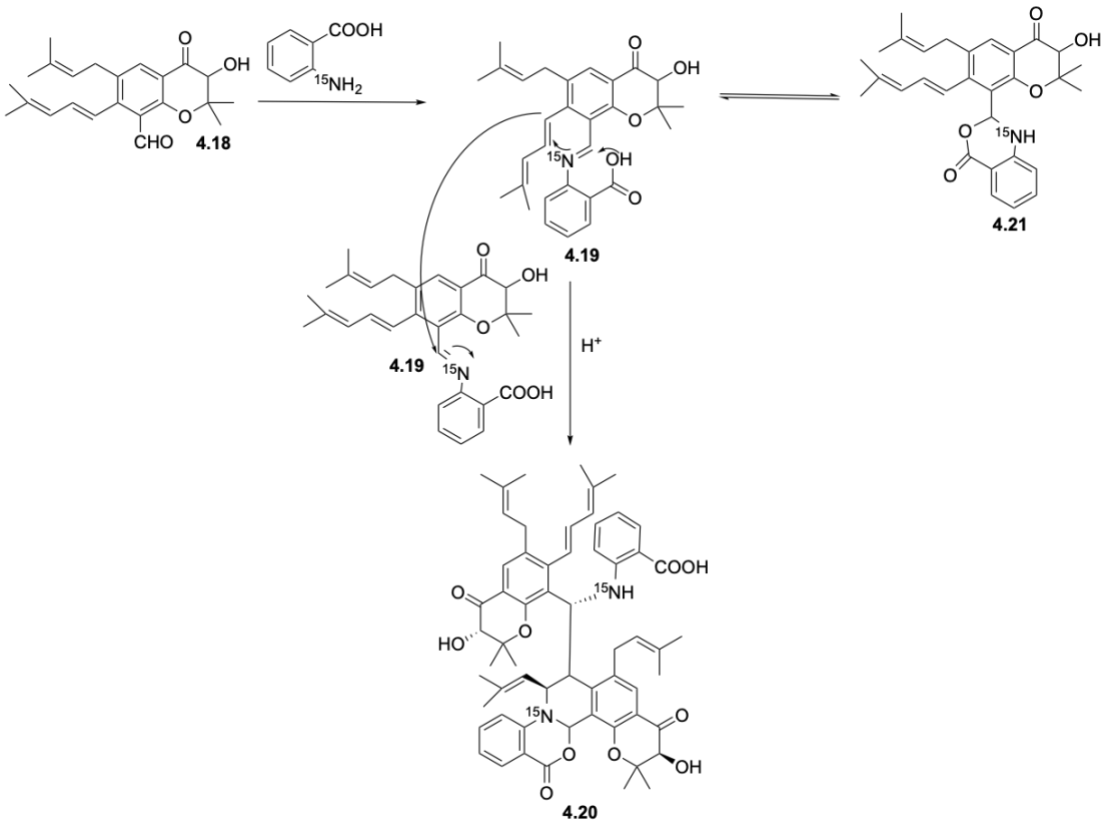

Figure 4.11. Proposed Pathway of 4.20 Formation.

4.4 Conclusion

The non-enzymatic formation of oxazinin A using a methyl-capped analog was explored. Using ^{1}H-^{15}N HMBC correlations, we were able to elucidate and interrogate intermediates relevant to oxazinin A formation. The formation of oxazinin A is controlled by an equilibrium between an imine and a hemiaminal intermediate. As the reaction proceeds, the equilibrium shifts toward the imine, which allows for more heterodimerization of monomeric units. This method can be used for the elucidation of other non-enzymatic natural products and complex compounds.

4.5 Experimental Procedures

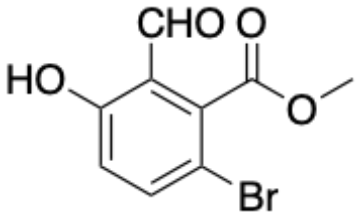

Synthesis of methyl 6-bromo-2-formyl-3-hydroxybenzoate

methyl 2-bromo-5-hydroxybenzoate (12 g, 56.3 mmol) was dissolved in anhydrous TFA (120 mL) under N_2, and hexamethylenetetramine (17.3 g, 123.9 mmol) was added in one portion. The yellow solution was heated in an oil bath until all the starting phenol was converted (TLC control, ca. 6 h); the mixture was then cooled to r.t. The cooled solution was poured into 4 M HCl (200 mL) and stirred for 15 min, the product was extracted with CH_2Cl_2 (2 × 400 mL). The combined organic extracts were washed with water (2 × 200 mL), sat. brine (200 mL), then dried (Na_2SO_4) and the solvent removed in vacuo. The crude residue was purified by column chromatography over silica gel (hexane: ethyl acetate = 8:2), affording 7.2 gm (53 % yield) as a colorless solid.

^{1}H NMR (500 MHz, $CDCl_3$-*d*) δ 12.38 (s, 1H), 9.74 (s, 1H), 8.19 (s, 1H), 4.02 (s, 3H).

^{13}C NMR (125 MHz, $CDCl_3$-*d*) δ 193.78, 165.53, 160.45, 148.91, 138.96, 117.28, 109.92, 88.96, 53.57.

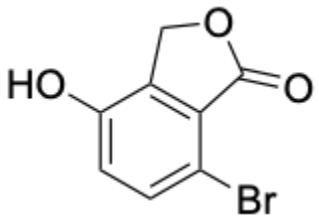

Synthesis of 7-bromo-4-hydroxyisobenzofuran-1(3H)-one

methyl 6-bromo-2-formyl-3-hydroxybenzoate (7 gm, 26.8 mmol) was taken into 100 ml of methanol. To this $NaBH_4$ (1.48 gm, 40.2 mol) was added portion wise at 0 ^oC and the reaction mixture was allowed to warm to room temperature. The reaction mixture was acidified using 1N HCl, with a white precipitate forming. The white solid precipitate was filtered and dried over vacuum to obtain pure product (5.1 gm, 83% yield).

^1H NMR (500 MHz, DMSO-d_6) δ 10.67 (s (broad), 1H), 7.56 (d, J = 8.4 Hz, 1H), 7.04 (d, J = 8.4 Hz, 1H), 5.24 (s, 2H).

^{13}C NMR (125 MHz, DMSO-d_6) δ 168.24, 151.82, 136.46, 134.33, 124.05, 121.66, 106.97, 66.63.

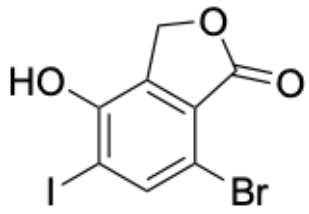

Synthesis of 7-bromo-4-hydroxy-5-iodoisobenzofuran-1(3H)-one

7-bromo-4-hydroxyisobenzofuran-1(3H)-one (5 gm, 22.0 mmol) and N-Iodosuccinimide (10.8 gm, 48.4 mmol) was taken in glacial acetic acid (100

mL). A catalytic amount of H_2SO_4 (0.5 mL) was then added at room temperature and the reaction mixture was stirred for approximately 2 days. The reaction mixture was then poured on crushed ice and stirred for 30 min. The product was then filtered and dried under vacuum. This solid was washed with toluene 3 times to remove any residual water as well as iodine to obtain pure gray solid product (5.6 gm, 71% yield).

^{1}H NMR (500 MHz, DMSO-d_6) δ 11.06 (s, 1H), 8.04 (s, 1H), 5.24 (s, 2H).

^{13}C NMR (125 MHz, DMSO-d_6) δ 167.92, 151.15, 142.30, 135.25, 124.37, 108.16, 94.69, 66.88.

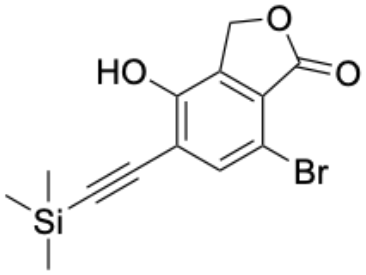

Synthesis of 7-bromo- 4-hydroxy- 5-((trimethylsilyl)ethynyl) isobenzo furan-1(3H)-one

To a solution of 7-bromo-4-hydroxy-5-iodoisobenzofuran-1(3H)-one (5.3 g, 14.9 mmol) in degassed THF (40 mL) and Et_3N (20 mL) were added $PdCl_2(PPh_3)_2$ (0.419 g, 0.598 mmol) and CuI (0.170 g, 0.898 mmol). Then Trimethylsilylacetylene (2.5 mL, 17.9 mmol) was added, and the reaction was stirred overnight at room temperature. The reaction mixture was diluted with

water (100 mL) and acidified (pH 5-6) by adding 1N HCl and extracted with ethyl acetate (2 × 200 mL). The combined organic extracts were washed with water, brine, then dried over sodium sulfate (Na_2SO_4) and the solvent was removed in vacuo. The crude product was purified by silica gel column chromatography (hexanes:ethyl acetate = 7:3) to afford the compound as a light-yellow solid product (3.3 g, 68%).

^{1}H NMR (500 MHz, $CDCl_3$-*d*) δ 7.63 (s, 1H), 6.13 (s, 1H), 5.22 (s, 2H), 0.30 (s, 9H).

^{13}C NMR (125 MHz, $CDCl_3$-*d*) δ 167.99, 150.84, 136.53, 134.52, 125.48, 116.22, 110.00, 107.86, 95.98, 66.22, 0.16.

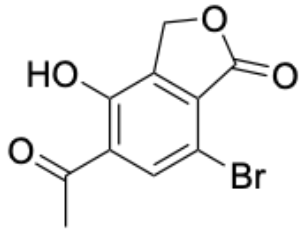

Synthesis of 5-acetyl-7-bromo-4-hydroxyisobenzofuran-1(3H)-one

7-bromo-4-hydroxy-5-((trimethylsilyl)ethynyl)isobenzofuran-1(3H)-one (3.2 gm, 9.90 mmol) was taken in formic acid (50 mL) and cat. TfOH (171 mg, 1.98 mmol) was added. Reaction mixture was then heated in an oil bath at 90 ^{o}C for 18h. The reaction mixture was diluted with water (100 mL) and subsequently extracted with ethyl acetate (150 mL x 2). The combined organic layer was washed with water, brine, dried over sodium sulphate and concentrated in

vacuo. The crude product was purified via silica gel column chromatography (hexanes:ethyl acetate = 8:2) to afford compound as a light brown solid product (2 g, 65%).

^{1}H NMR (500 MHz, $CDCl_3$-*d*) δ 12.28 (s, 1H), 8.00 (s, 1H), 5.27 (s, 2H), 2.73 (s, 3H).

^{13}C NMR (126 MHz, $CDCl_3$-*d*) δ 204.12, 167.52, 156.04, 138.53, 135.61, 130.18, 123.41, 107.85, 66.63, 27.58.

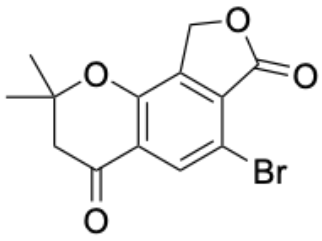

6-bromo-2,2-dimethyl-2,3-dihydro-4H-furo[3,4-h]chromene-4,7(9H)-dione

To a well stirred solution of 5-acetyl- 7-bromo- 4-hydroxy isobenzofuran-1(3H)-one (2 g, 6.47 mmol) and acetone (4.8 mL, 64.7 mmol) in toluene (20 mL), pyrrolidine (0.54 mL, 6.47 mmol) was added at room temperature. After stirring for 10 min AcOH (0.38 mL, 6.47 mmol) was added and the reaction mixture was subsequently heated in an oil bath at 90 ^{o}C for 18h. The reaction mixture was quenched by adding crushed ice then acidified (pH 5-6)with 1N HCl solution. Finally, the aqueous solution was extracted with ethyl acetate (2×100 mL). The organic layer was washed by water, brine and dried over anhydrous

sodium sulfate, and the solvent was removed to obtain the crude product. The crude residue was purified by column chromatography over silica gel (hexane:ethyl acetate = 7:3), affording compound (1.31 gm, 57%) as a yellow solid.

^{1}H NMR (500 MHz, $CDCl_3$-*d*) δ 8.12 (s, 1H), 5.22 (s, 2H), 2.82 (s, 2H), 1.51 (s, 6H).

^{13}C NMR (125 MHz, $CDCl_3$-*d*) δ 190.16, 167.59, 153.55, 138.95, 132.05, 129.98, 124.21, 110.43, 81.65, 66.29, 48.79, 26.70.

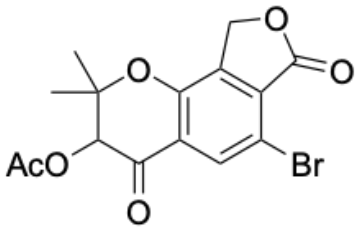

6-bromo-2,2-dimethyl-4,7-dioxo-3,4,7,9-tetrahydro-2H-furo[3,4-h]chromen-3-yl acetate

Lead tetraacetate (4.3 gm, 9.708 mmol) was added in a single portion to a screw-capped vessel containing a solution of the 6-bromo-2,2-dimethyl-2,3-dihydro-4H-furo[3,4-h]chromene-4,7(9H)-dione (1 gm, 3.236) in benzene (30 mL) at room temperatute. The reaction vessel was sealed, and the sealed reaction vessel was placed in an oil bath that had been preheated to 82 °C. The reaction mixture was stirred for 48 h at 82 °C. The product mixture was cooled to 23 °C over 30 min. The cooled product mixture was filtered through a short pad of Celite. The filter cake was rinsed with ethyl acetate (3 × 30 mL).

The filtrates were combined, and the combined filtrates were diluted sequentially with water (40 mL) and saturated aqueous sodium bicarbonate solution (20 mL). The diluted product mixture was transferred to a separatory funnel and the layers that formed were separated. The aqueous layer was extracted with ethyl acetate (2 × 100 mL). The organic layers were combined, and the combined organic layers were washed with brine. The washed organic layer was dried over sodium sulfate. The dried solution was filtered, and the filtrate was concentrated. The residue obtained was purified by flash-column chromatography (hexanes: ethyl acetate = 7:3) to provide the acetate product as a yellow solid (950 mg, 80%).

^{1}H NMR (500 MHz, $CDCl_3$-*d*) δ 8.06 (s, 1H), 5.63 (s, 1H), 5.23 (d, *J* = 5.7 Hz, 2H), 2.25 (s, 3H), 1.59 (s, 3H), 1.39 (s, 3H).

^{13}C NMR (126 MHz, $CDCl_3$-*d*) δ 186.47, 169.42, 167.23, 152.57, 138.68, 132.36, 130.43, 123.85, 111.36, 83.62, 76.61, 66.13, 26.04, 20.61, 19.75.

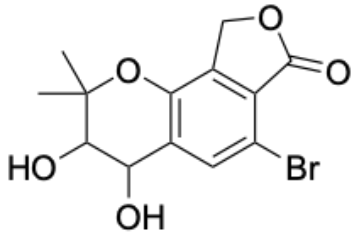

6-bromo-3,4-dihydroxy-2,2-dimethyl-3,4-dihydro-2H-furo[3,4-h]chromen-7(9H)-one

6-bromo-2,2-dimethyl-4,7-dioxo-3,4,7,9-tetrahydro-2H-furo[3,4-h]chromen-3-yl acetate (900 mg, 2.439 mmol) was taken in methanol and $NaBH_4$ (135 mg, 3.658 mmol) was added in portions at 0 ^oC. The reaction was quenched by adding sat. solution of NH_4Cl (10 mL) then extracted with ethyl acetate (20 mL x 3). The reaction mixture was diluted with water and extracted with ethyl acetate (20 mL). The combined organic layers were washed with water, brine and dried over Na_2SO_4. The organic layer was then concentrated in vacuo to obtain crude product (820 mg 90% crude yield). The crude product (820 mg, 2.210 mmol) was then dissolved in 10 mL of THF:H_2O (5:2) and to it LiOH (181 mg, 4.420 mmol) was added and stirred at rt for 1h. Finally, the reaction was acidified with 1N HCl then diluted with water (10 mL) and extracted with ethyl acetate (30 mL x 2). The combined organic layers were washed with water, brine and dried over Na_2SO_4. The concentration of the organic layer in vacuo to obtain crude product (580 mg 79 % crude yield). The crude product was taken forward without further purification

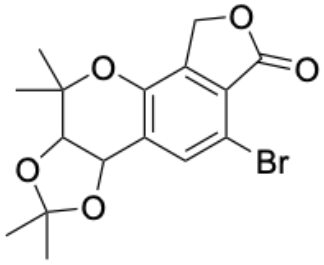

5-bromo-2,2,10,10-tetramethyl-10,10a-dihydro-8H-[1,3]dioxolo[4,5-c]furo[3,4-h]chromen-6(3aH)-one

To a stirred solution of 6-bromo-3,4-dihydroxy-2,2-dimethyl-3,4-dihydro-2H-furo[3,4-h]chromen-7(9H)-one (550 mg, 1.681 mmol) and 2,2-dimethoxypropane (2.05 mL, 16.819 mmol) in acetone (5 mL) was added (Pyridinium p-toluenesulfonate) PPTS (42 mg, 0.168 mmol) at rt. After being stirred at rt for 24 h, the reaction mixture was concentrated under reduced pressure to give the crude residue, which was purified via silica gel column chromatography (30 % ethyl acetate in hexanes) to give pure product (260 mg, 42%).

^{1}H NMR (500 MHz, $CDCl_3$-*d*) δ 7.66 (s, 1H), 5.22 – 5.15 (m, 2H), 5.11 (d, *J* = 5.9 Hz, 1H), 4.18 (d, *J* = 5.7 Hz, 1H), 1.53 (s, 3H), 1.42 (s, 3H), 1.28 (s, 3H), 1.16 (s, 3H).

^{13}C NMR (125 MHz, $CDCl_3$-*d*) δ 168.42, 146.36, 137.46, 135.21, 128.75, 125.03, 111.05, 110.44, 77.71, 77.26, 69.65, 66.49, 27.84, 26.52, 24.91, 23.62.

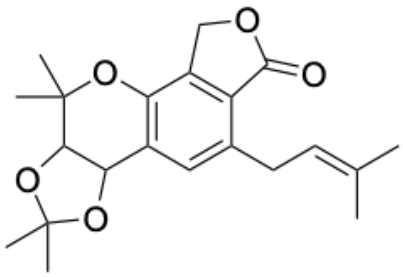

2,2,10,10-tetramethyl-5-(3-methylbut-2-en-1-yl)-10,10a-dihydro-8H-[1,3]dioxolo[4,5-c]furo[3,4-h]chromen-6(3aH)-one:

In an oven-dried round bottom flask, 5-bromo-2,2,10,10-tetramethyl-10,10a-dihydro-8H-[1,3]dioxolo[4,5-c]furo[3,4-h]chromen-6(3aH)-one (160 mg, 0.434 mmol), was taken in degassed THF and degassed deionized water in the ratio of 2.5:1. THF:H_2O (35 mL). Then 4,4,5,5-tetramethyl-2-(3-methylbut-2-en-1-yl)-1,3,2-dioxaborolane (127 mg, 0.652 mmol), palladium acetate (4.8 mg, 0.021 mmol), 2-Dicyclohexyl-phosphino-2′,6′-dimethoxybiphenyl (SPhos, 17 mg, 0.043 mmol), and potassium phosphate (K_3PO_4, 230 mg, 1.086 mmol) was added under inert atmosphere. The resulting mixture was stirred in an oil bath at 70 ^oC for 16 h. The reaction mixture was diluted with water 20 mL and extracted with ethyl acetate (2 x 100 mL). The organic layer was washed with water, brine and dried over Na_2SO_4. The concentration of the organic layer in vacuo followed by silica gel (60–120) column chromatographic purification of the resulting residue using hexane:ethyl acetate (8:2) as an eluent afforded the pure product **10** as white solid (97 mg, 62%).

^{1}H NMR (500 MHz, $CDCl_3$-*d*) δ 7.28 (s, 1H), 5.33 (t, *J* = 7.24 Hz, 1H), 5.23 – 5.15 (m, 2H), 5.15 – 5.11 (m, 2H), 4.17 (d, *J* = 5.8 Hz, 1H), 3.83 (dd, *J* = 15.9, 7.1 Hz, 1H), 3.66 (dd, *J* = 15.9, 7.5 Hz, 1H), 1.74 (s, 3H), 1.72 (s, 3H), 1.50 (s, 3H), 1.43 (s, 3H), 1.26 (s, 3H), 1.16 (s, 3H).

^{13}C NMR (125 MHz, $CDCl_3$-*d*) δ 171.04, 144.98, 135.29, 135.02, 133.43, 130.95, 126.96, 123.99, 122.04, 110.61, 78.16, 76.58, 70.28, 67.23, 28.54, 27.71, 26.56, 25.97, 24.86, 23.77, 18.10.

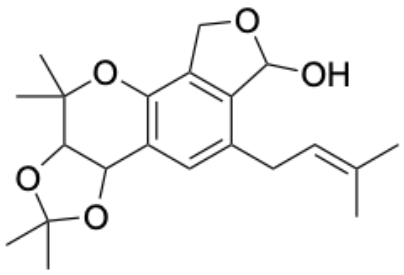

2,2,10,10-tetramethyl-5-(3-methylbut-2-en-1-yl)-3a,6,10,10a-tetrahydro-8H-[1,3]dioxolo[4,5-c]furo[3,4-h]chromen-6-ol

DIBALH (1 M/Hexane; 0.737 mL, 0.737 mmol) was added to a solution of the 2,2,10,10-tetramethyl-5-(3-methylbut-2-en-1-yl)-10,10a-dihydro-8H-[1,3]dioxolo[4,5-c]furo[3,4-h]chromen-6(3aH)-one (110 mg, 0.307 mmol) in anhydrous CH_2Cl_2 (5 mL) at -78 ^oC. After 1h, the quenched by the addition of a saturated aqueous solution of sodium sulfate (0.5 mL) and allowed to warm to room temperature. Then added anhydrous sodium sulfate to remove excess water and filtered and concentrated in vacuo to afford crude (85 mg, 77%) white solid product. The residue used for the next step without further purification.

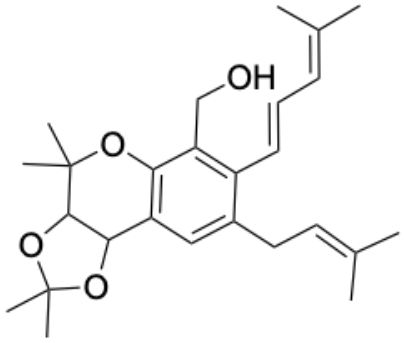

(E)-(2,2,4,4-tetramethyl-8-(3-methylbut-2-en-1-yl)-7-(4-methylpenta-1,3-dien-1-yl)-3a,9b-dihydro-4H-[1,3]dioxolo[4,5-c]chromen-6-yl)methanol

Phosphonium salt bromo(tributyl)(3-methylbut-2-en-1-yl)phosphane (175 mg, 0.500 mmol) and 2,2,10,10-tetramethyl-5-(3-methylbut-2-en-1-yl)-3a,6,10,10a-tetrahydro-8H-[1,3]dioxolo[4,5-c]furo[3,4-h]chromen-6-ol (60 mg, 0.166 mmol) were combined in dry toluene (5 mL). The solution was cooled to 0 °C and *t*-BuOK in 1.0 M in THF (0. 5 mL, 0. 500 mmol) was added slowly dropwise over the period of 10 min. The mixture was allowed to warm to room temperature and stirred for 4 h. Reaction was then quenched by adding saturated solution of NH_4Cl and extracted with ethyl acetate (2 X 10 mL) and washed with water (10 mL) and brine (10 mL). The organic phase was dried (Na_2SO_4), filtered and concentrated. The crude mixture was purified by flash chromatography (hexane:ethyl acetate = 8:2) to afford the coupled product (26 mg, 38%)

^{1}H NMR (800 MHz, $CDCl_3$-*d*) δ 7.12 (s, 1H), 6.53 (dd, *J* = 15.7, 10.8 Hz, 1H), 6.44 (d, *J* = 15.8 Hz, 1H), 6.01 (d, *J* = 10.8 Hz, 1H), 5.20 (dddd, *J* = 7.0, 5.8, 2.7, 1.4 Hz, 1H), 5.11 (d, *J* = 6.3 Hz, 1H), 4.73 (qd, *J* = 11.9, 5.9 Hz, 2H), 4.14 (d, *J* = 6.3 Hz, 1H), 3.26 (t, *J* = 7.3 Hz, 2H), 2.45 (t, *J* = 6.5 Hz, 1H), 1.84 (s, 3H), 1.79 (s, 3H), 1.72 (d, *J* = 0.89 Hz, 3H), 1.67 (s, 3H), 1.47 (s, 3H), 1.44 (s, 3H), 1.29 (s, 3H), 1.24 (s, 3H).

^{13}C NMR (125 MHz, $CDCl_3$-*d*) δ 149.41, 139.01, 136.83, 133.15, 132.89, 131.99, 129.18, 126.89, 125.73, 125.61, 123.58, 120.10, 110.03, 78.45, 76.33, 70.93, 59.02, 32.51, 27.45, 26.42, 26.26, 25.94, 24.54, 24.40, 18.68, 18.10.

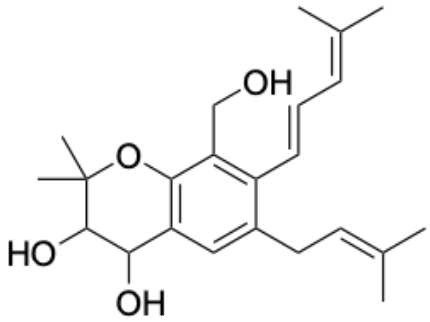

(E)-8-(hydroxymethyl)-2,2-dimethyl-6-(3-methylbut-2-en-1-yl)-7-(4-methylpenta-1,3-dien-1-yl)chromane-3,4-diol

A solution of (E)-(2,2,4,4-tetramethyl-8-(3-methylbut-2-en-1-yl)-7-(4-methylpenta-1,3-dien-1-yl)-3a,9b-dihydro-4H-[1,3] dioxolo[4,5-c]chromen-6-yl)methanol (20 mg, 0.048 mmol) in acetic acid:water (1:1; 1 mL) was stirred for 6 h at 50 °C. The reaction mixture was then concentrated in vacuo and purified by flash chromatography on SiO_2 (ethyl acetate:hexane=6:4) to afford pure product (12 mg, 66 %).

^{1}H NMR (500 MHz, $CDCl_3$-*d*) δ 7.30 (s, 1H), 6.55 (dd, *J* = 15.7, 10.7 Hz, 1H), 6.45 (d, *J* = 15.8 Hz, 1H), 6.03 (d, *J* = 10.6 Hz, 1H), 5.22 (t, *J* = 7.0 Hz, 1H), 4.79 (d, *J* = 3.2 Hz, 1H), 4.77 – 4.68 (m, 2H), 3.71 (d, *J* = 4.3 Hz, 1H), 3.29 (t, *J* = 6.2 Hz, 2H), 1.86 (s, 3H), 1.81 (s, 3H), 1.74 (s, 3H), 1.71 (s, 3H), 1.53 (s, 3H), 1.32 (s, 3H).

^{13}C NMR (125 MHz, $CDCl_3$-*d*) δ 148.91, 139.11, 136.88, 133.09, 132.85, 131.98, 128.30, 126.07, 125.38, 123.32, 120.42, 78.16, 71.50, 65.23, 58.79, 32.36, 26.11, 25.80, 24.85, 23.66, 18.51, 17.95.

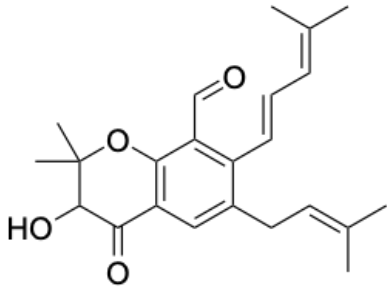

(E)-3-hydroxy-2,2-dimethyl-6-(3-methylbut-2-en-1-yl)-7-(4-methylpenta-1,3-dien-1-yl)-4-oxochromane-8-carbaldehyde

To a solution of (E)-8-(hydroxymethyl)-2,2-dimethyl-6-(3-methylbut-2-en-1-yl)-7-(4-methylpenta-1,3-dien-1-yl)chromane-3,4-diol (8 mg, 0.021 mmol) in dry CH_2Cl_2 (5 mL) at 0 °C was added followed by addition of Dess–Martin periodinane (20 mg, 0.0473 mmol) under nitrogen atmosphere. The resulting mixture was stirred at room temperature for 2 h. After completion of the reaction (TLC analysis), saturated $NaHCO_3$ solution (4 mL) was added, the aqueous phase was separated and extracted with CH_2Cl_2 (2 x 10 mL). The combined organic extracts were dried over Na2SO_4, filtered and concentrated. Purification of the residue by flash chromatography on SiO_2 (ethyl acetate:hexane=2:8) to afford pure product (5 mg, 63 %).

^{1}H NMR (500 MHz, $CDCl_3$-*d*) δ 10.14 (s, 1H), 7.79 (s, 1H), 6.68 (d, *J* = 15.5 Hz, 1H), 6.46 (dd, *J* = 15.5, 10.9 Hz, 1H), 6.08 (d, *J* = 11.1 Hz, 1H), 5.19 (t, *J* = 6.5 Hz, 1H), 4.45 (d, *J* = 2.2 Hz, 1H), 3.71 (d, *J* = 2.3 Hz, 1H), 3.33 (q, *J* = 7.3, 5.8 Hz, 2H), 1.87 (s, 3H), 1.77 (s, 3H), 1.75 (s, 3H), 1.70 (s, 6H), 1.23 (s, 3H).

^{13}C NMR (125 MHz, $CDCl_3$-*d*) δ 193.67, 190.44, 158.50, 149.29, 141.11, 137.26, 133.77, 133.60, 130.81, 125.28, 125.10, 124.15, 122.12, 117.41, 84.76, 31.60, 26.89, 26.47, 25.91, 18.80, 18.15, 17.54.

4.6 Chapter 4 References

(1) Colosimo, D. A.; MacMillan, J. B. Detailed Mechanistic Study of the Non-Enzymatic Formation of the Discoipyrrole Family of Natural Products. *J. Am. Chem. Soc.* **2016**, *138* (7), 2383–2388.

(2) Shingare, R. D.; Aniebok, V.; Lee, H.-W.; MacMillan, J. B. Synthesis and Investigation of the Abiotic Formation of Pyonitrins A-D. *Org. Lett.* **2020**, *22* (4), 1516–1519.

(3) Schörghuber, J.; Geist, L.; Bisaccia, M.; Weber, F.; Konrat, R.; Lichtenecker, R. J. Anthranilic Acid, the New Player in the Ensemble of Aromatic Residue Labeling Precursor Compounds. *J. Biomol. NMR* **2017**, *69* (1), 13–22.

(4) Patel, K.; Deshmukh, S. S.; Bodkhe, D.; Mane, M.; Vanka, K.; Shinde, D.; Rajamohanan, P. R.; Nandi, S.; Vaidhyanathan, R.; Chikkali, S. H. Secondary Interactions Arrest the Hemiaminal Intermediate To Invert the Modus Operandi of Schiff Base Reaction: A Route to Benzoxazinones. *J. Org. Chem.* **2017**, *82* (8), 4342–4351.

(5) Lin, Z.; Koch, M.; Abdel Aziz, M. H.; Galindo-Murillo, R.; Tianero, M. D.; Cheatham, T. E.; Barrows, L. R.; Reilly, C. A.; Schmidt, E. W. Oxazinin A, a

Pseudodimeric Natural Product of Mixed Biosynthetic Origin from a Filamentous Fungus. *Org. Lett.* **2014**, *16* (18), 4774–4777.

(6)NMRSpectroscopy https://organicchemistrydata.org/hansreich/resources/nmr/?index=nmr_index%2F13C_shift#cdata174 (accessed 2022 -02 -23).

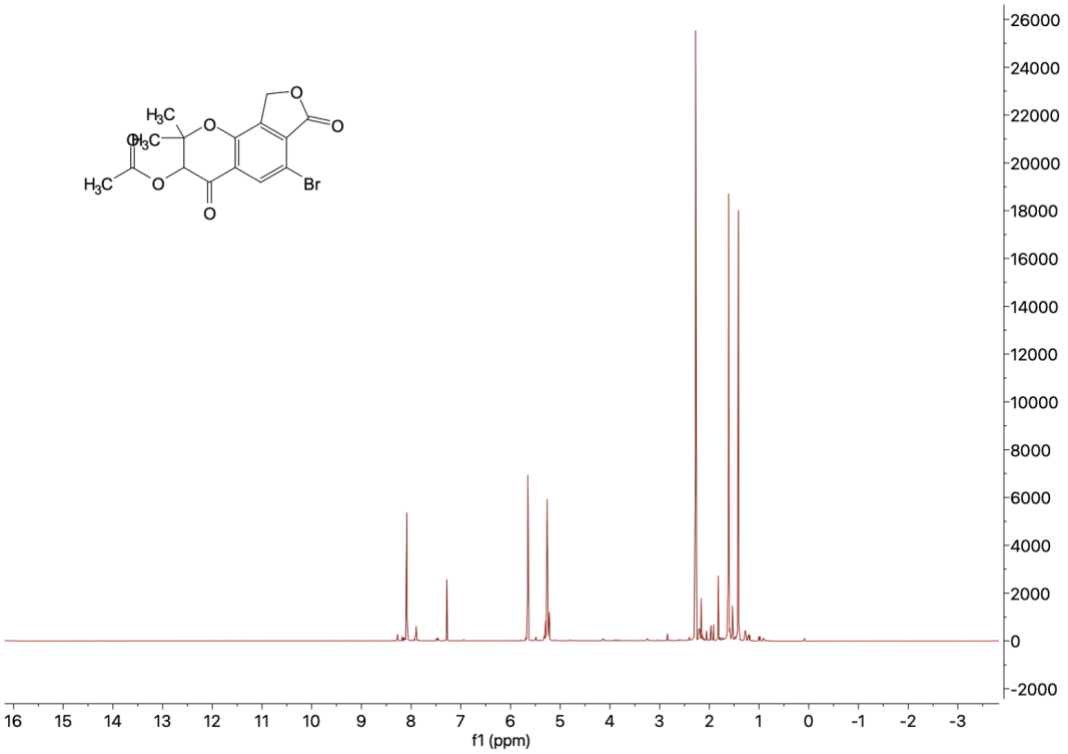
H3C
CH3
H3C
O
O
O
O
O
Br
26000
24000
22000
20000
18000
16000
14000
12000
10000
8000
6000
4000
2000
0
-2000
16 15 14 13 12 11 10 9 8 7 6 5 4 3 2 1 0 -1 -2 -3
f1 (ppm)

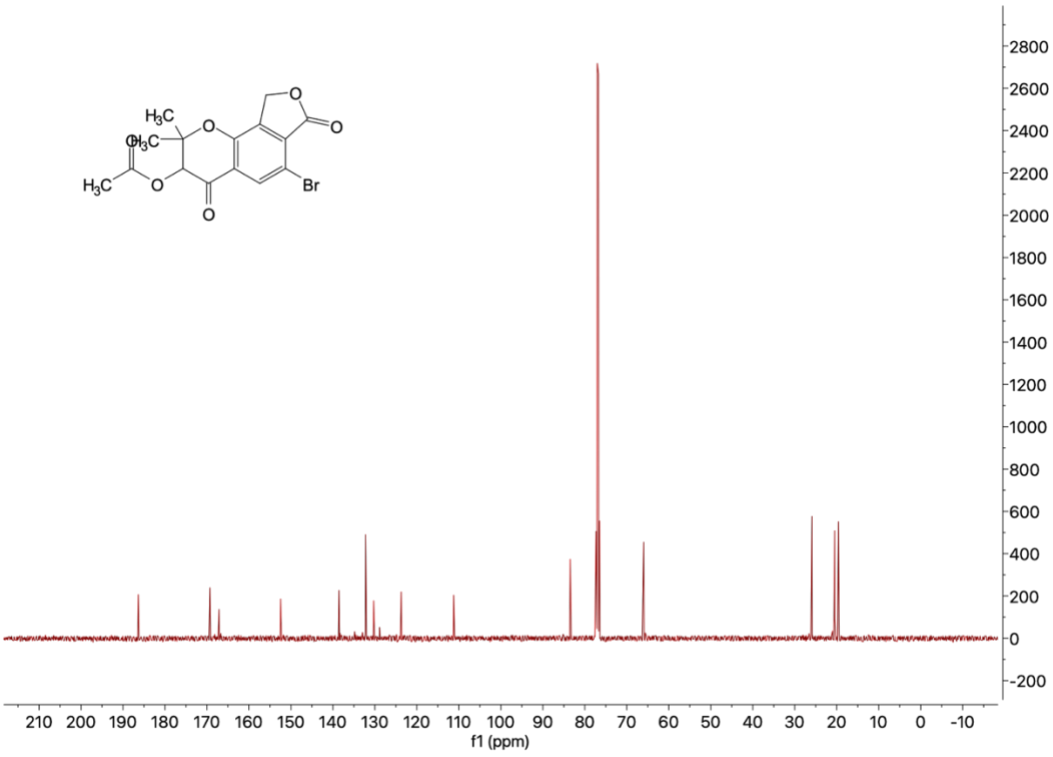
H3C
CH3
H3C
O
O
O
O
O
Br
2800
2600
2400
2200
2000
1800
1600
1400
1200
1000
800
600
400
200
0
-200
210 200 190 180 170 160 150 140 130 120 110 100 90 80 70 60 50 40 30 20 10 0 -10
f1 (ppm)

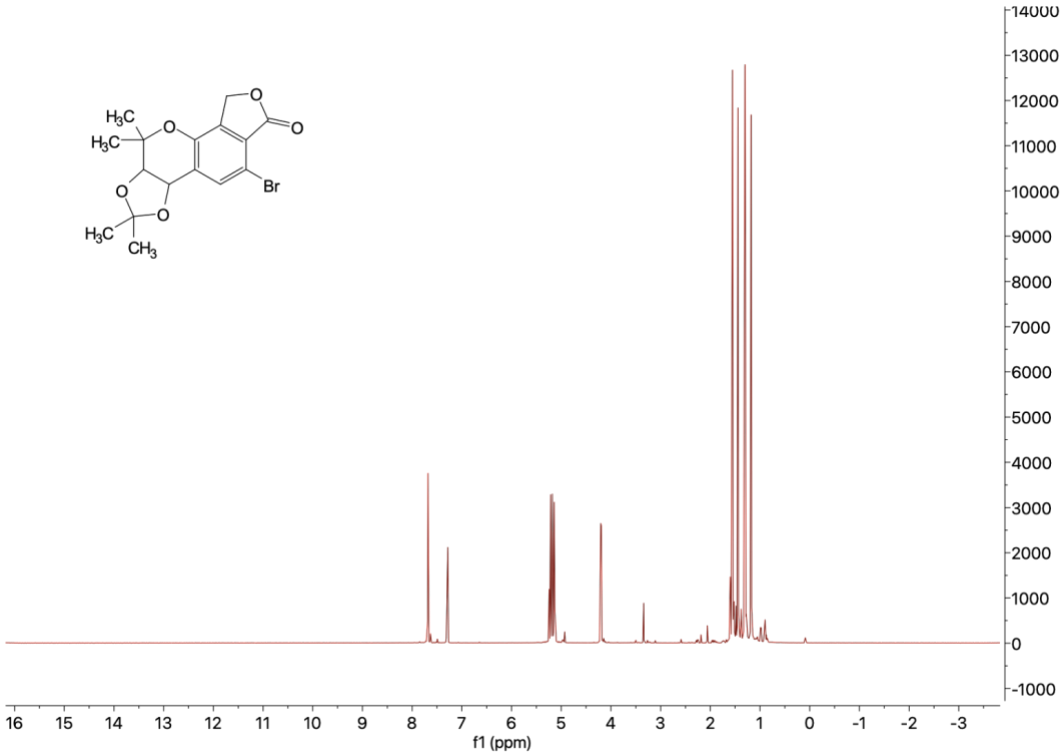
H3C
H3C
O
O
O
Br
O
O
H3C
CH3
14000
13000
12000
11000
10000
9000
8000
7000
6000
5000
4000
3000
2000
1000
0
-1000
16 15 14 13 12 11 10 9 8 7 6 5 4 3 2 1 0 -1 -2 -3
f1 (ppm)

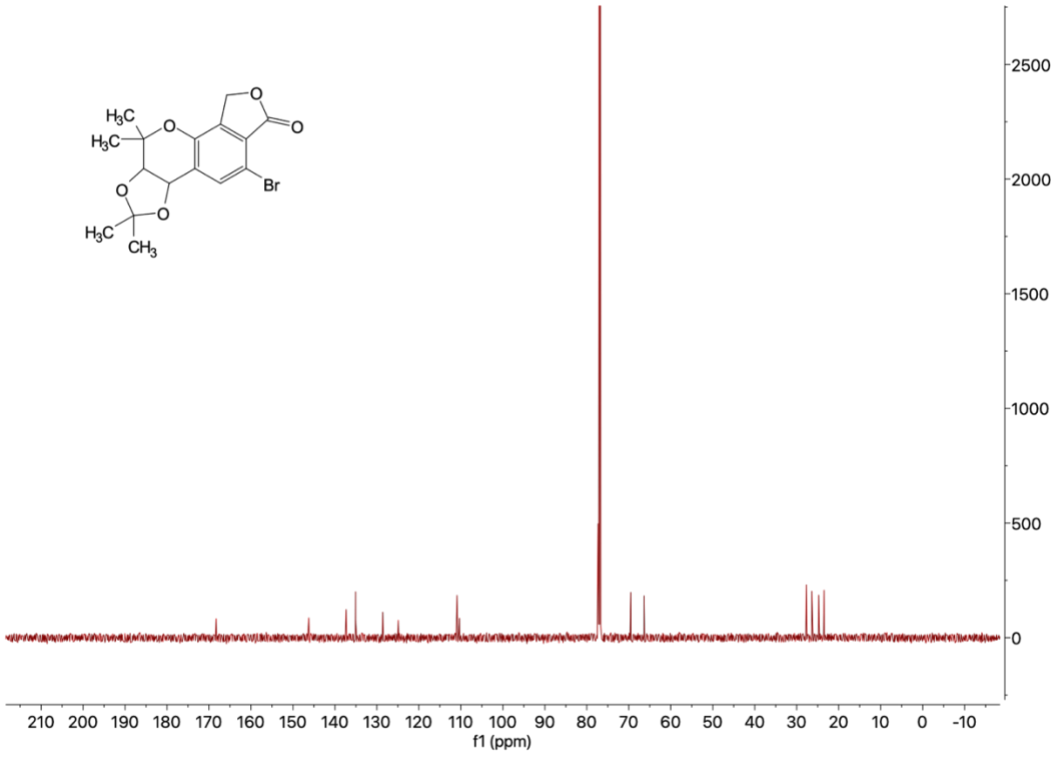
H3C
H3C
O
O
O
Br
O
O
H3C
CH3
2500
2000
1500
1000
500
0
210 200 190 180 170 160 150 140 130 120 110 100 90 80 70 60 50 40 30 20 10 0 -10
f1 (ppm)

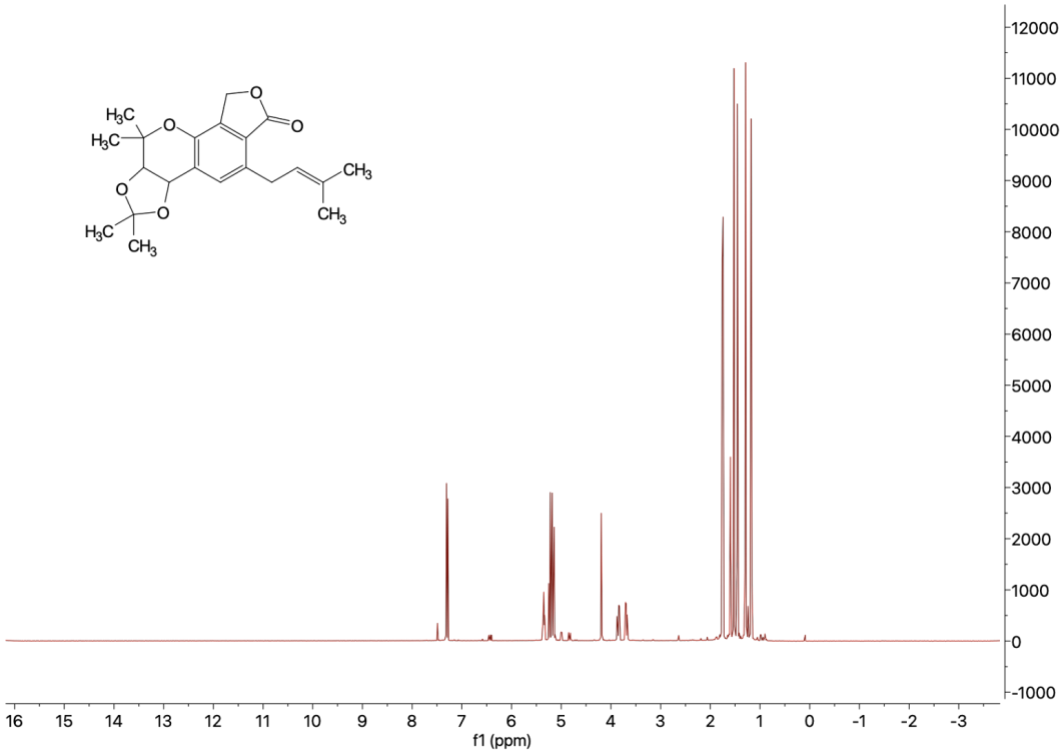
H3C
H3C
O
O
O
O
H3C
CH3
CH3
CH3
12000
11000
10000
9000
8000
7000
6000
5000
4000
3000
2000
1000
0
-1000
16 15 14 13 12 11 10 9 8 7 6 5 4 3 2 1 0 -1 -2 -3
f1 (ppm)

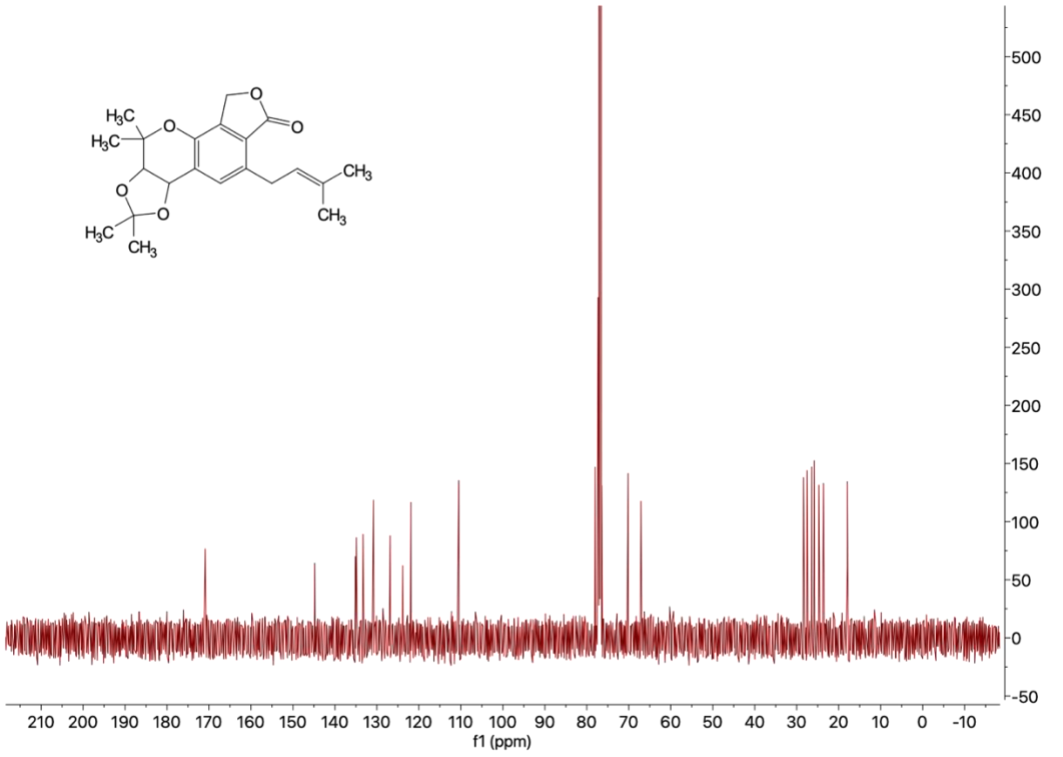
H3C
H3C
O
O
O
O
H3C
CH3
CH3
CH3
500
450
400
350
300
250
200
150
100
50
0
-50
210 200 190 180 170 160 150 140 130 120 110 100 90 80 70 60 50 40 30 20 10 0 -10
f1 (ppm)

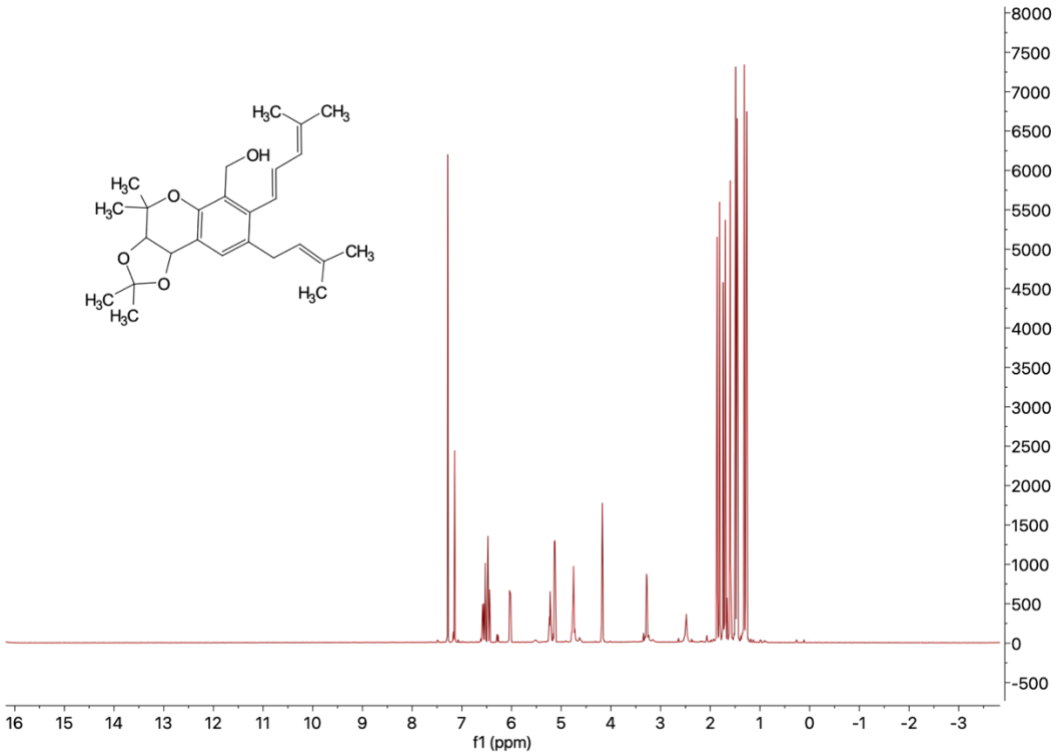
OH
CH3
CH3
f1 (ppm)

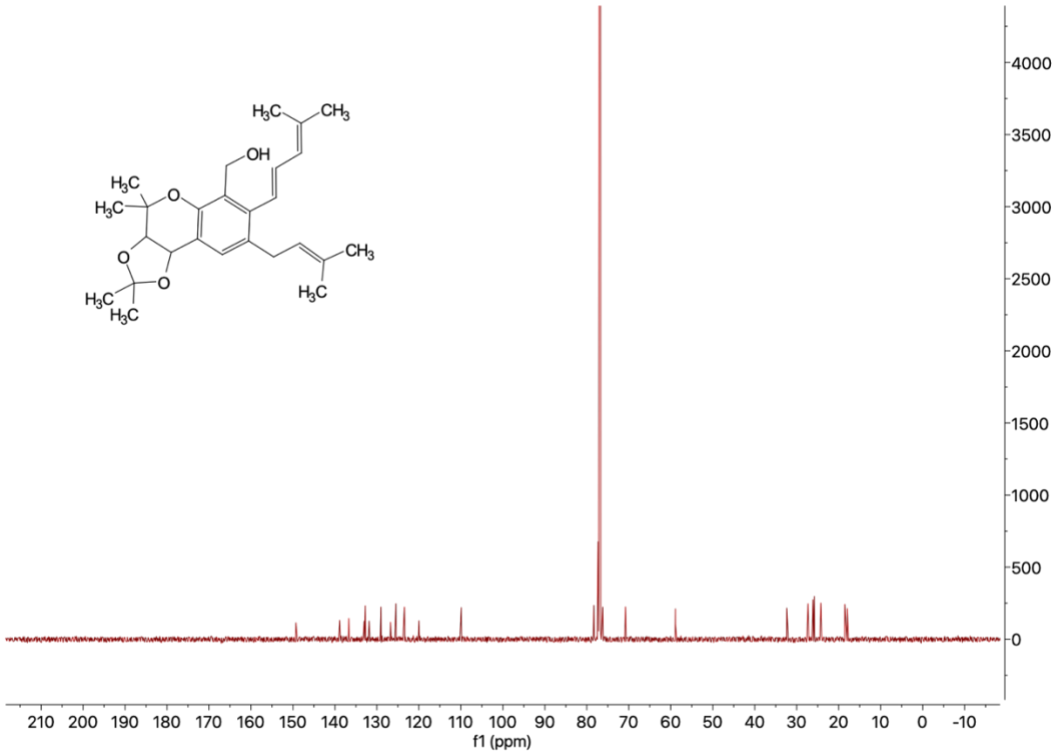
OH
CH3
CH3
f1 (ppm)

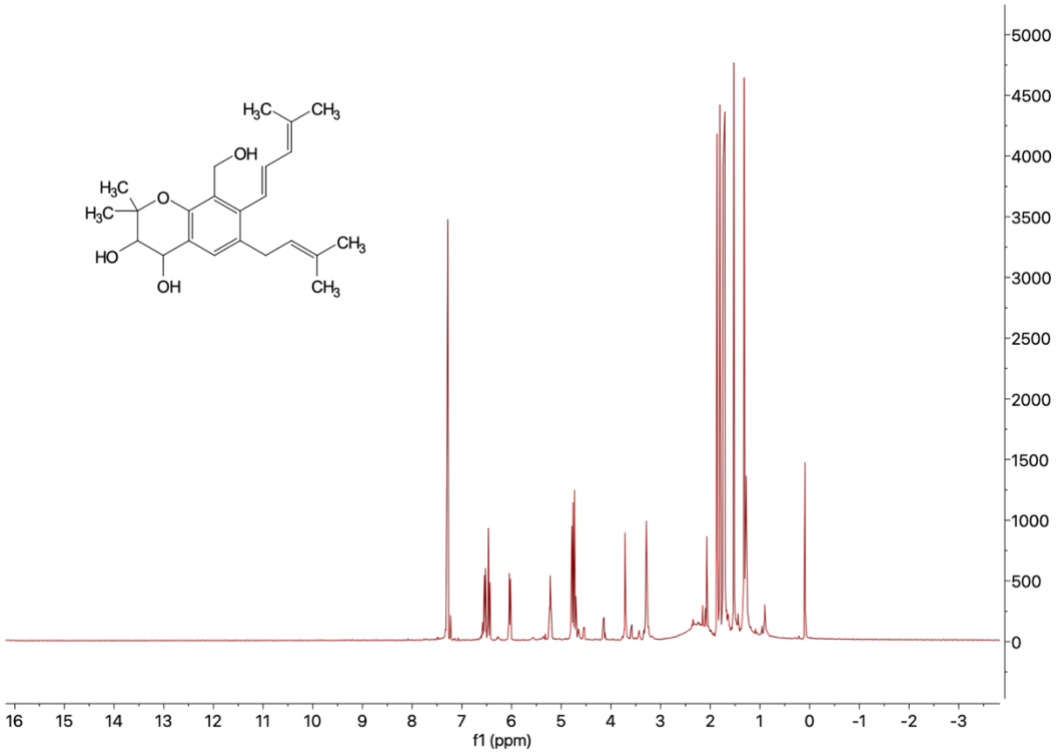
H3C
CH3
OH
H3C
O
H3C
HO
OH
CH3
CH3
5000
4500
4000
3500
3000
2500
2000
1500
1000
500
0
16 15 14 13 12 11 10 9 8 7 6 5 4 3 2 1 0 -1 -2 -3
f1 (ppm)

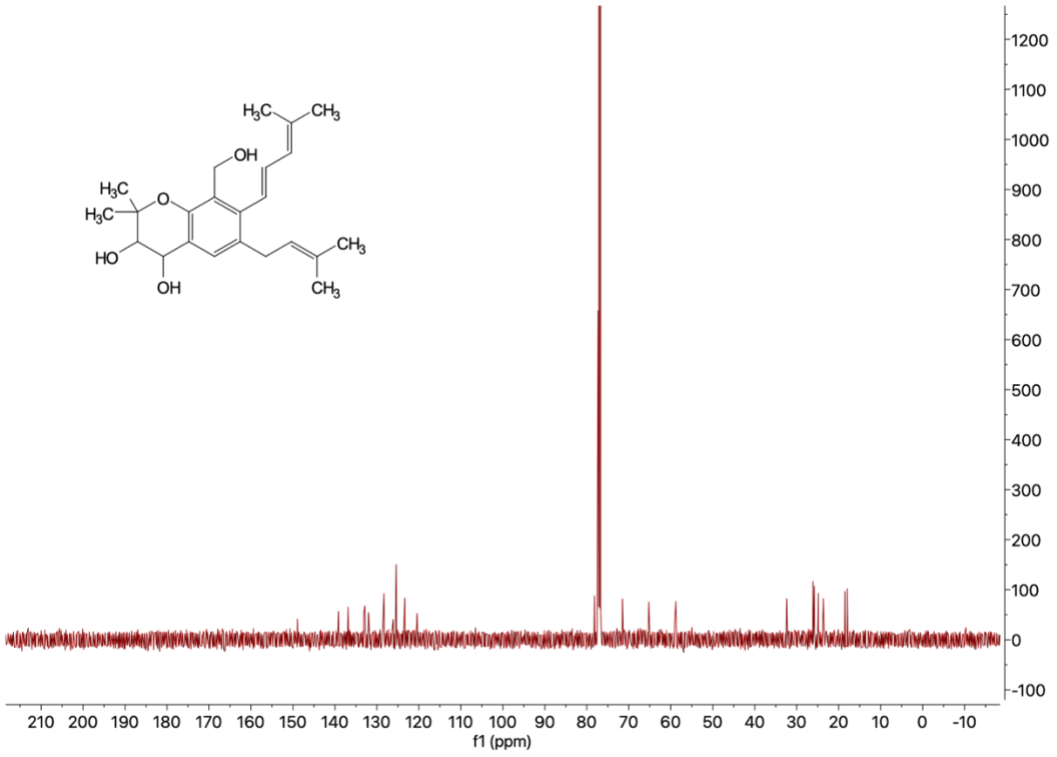
H3C
CH3
OH
H3C
O
H3C
HO
OH
CH3
CH3
1200
1100
1000
900
800
700
600
500
400
300
200
100
0
-100
210 200 190 180 170 160 150 140 130 120 110 100 90 80 70 60 50 40 30 20 10 0 -10
f1 (ppm)

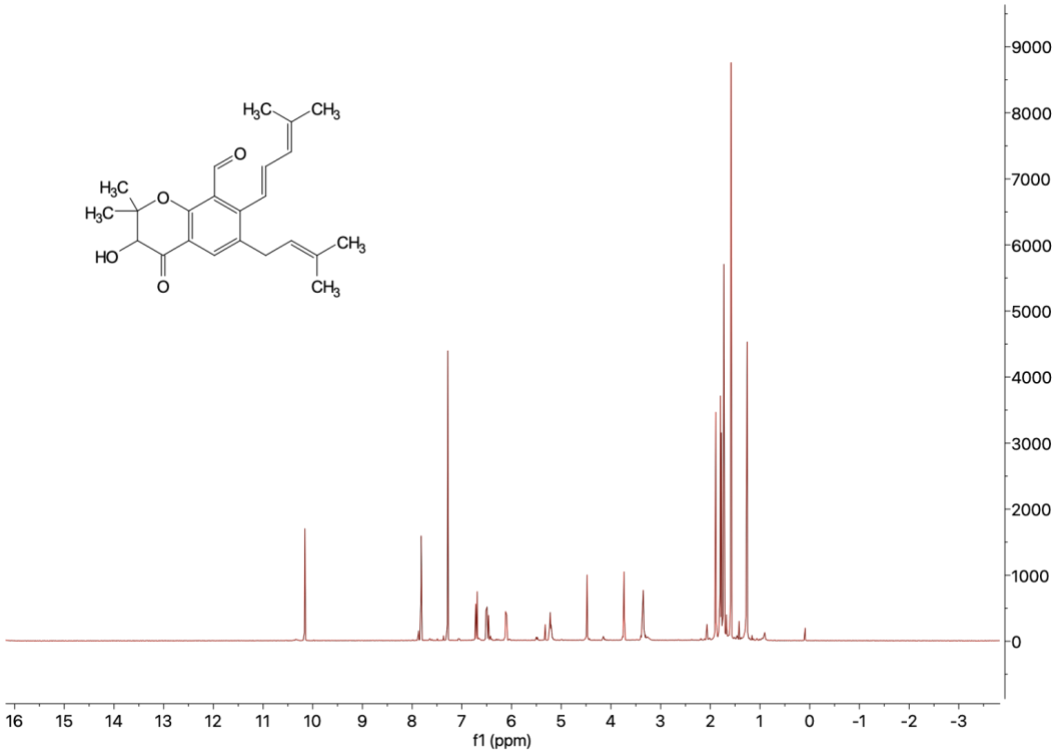
H3C
CH3
O
H3C
H3C
O
HO
O
CH3
CH3
9000
8000
7000
6000
5000
4000
3000
2000
1000
0
16 15 14 13 12 11 10 9 8 7 6 5 4 3 2 1 0 -1 -2 -3
f1 (ppm)

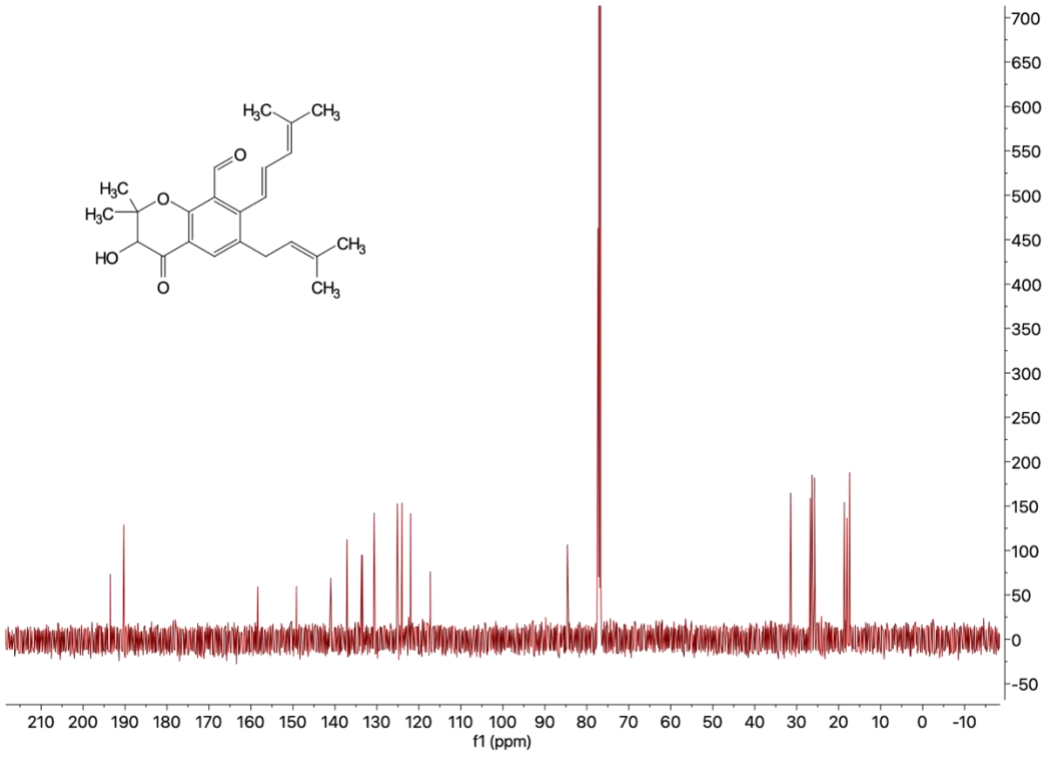
H3C
CH3
O
H3C
H3C
O
HO
O
CH3
CH3
700
650
600
550
500
450
400
350
300
250
200
150
100
50
0
-50
210 200 190 180 170 160 150 140 130 120 110 100 90 80 70 60 50 40 30 20 10 0 -10
f1 (ppm)

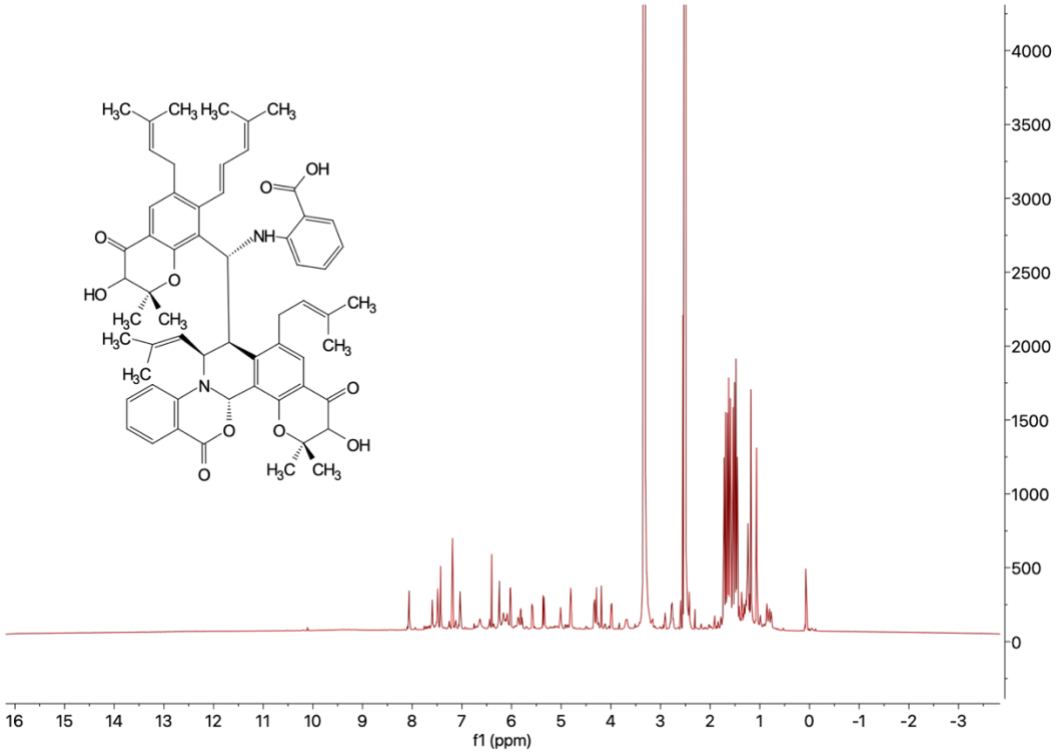
4000
3500
3000
2500
2000
1500
1000
500
0
16 15 14 13 12 11 10 9 8 7 6 5 4 3 2 1 0 -1 -2 -3
f1 (ppm)

Bibliography

[No title] https://cs.uwaterloo.ca/~cdimarco/pdf/cogsci600/7_Greenberg.pdf (accessed 2022 -01 -01).

[No title] https://iopscience.iop.org/article/10.1086/381182/pdf (accessed 2022 -01 -01).

Amils, R.; Quintanilla, J. C.; Cleaves, H. J.; Irvine, W. M.; Pinti, D.; Viso, M. *Encyclopedia of Astrobiology*; Springer, 2011.

Antifungal Resistance in Candida https://www.cdc.gov/fungal/diseases/candidiasis/antifungal-resistant.html#:~:text=About%207%25%20of%20all%20Candida,Candida%20glabrata%2C%20and%20Candida%20parapsilosis. (accessed 2022 -02 -08).

Barron, L. D. True and False Chirality and Absolute Asymmetric Synthesis. *Journal of the American Chemical Society*. 1986, pp 5539–5542. https://doi.org/10.1021/ja00278a029.

Bernstein, M. P.; Dworkin, J. P.; Sandford, S. A.; Cooper, G. W.; Allamandola, L. J. Racemic Amino Acids from the Ultraviolet Photolysis of Interstellar Ice Analogues. *Nature* **2002**, *416* (6879), 401–403.

Bouza, E.; Garcia-Garrote, F.; Cercenado, E.; Marin, M.; Diaz, M. S. Pseudomonas Aeruginosa: A Survey of Resistance in 136 Hospitals in Spain. The Spanish Pseudomonas Aeruginosa Study Group. *Antimicrob. Agents Chemother.* **1999**, *43* (4), 981–982.

CDCTB. Drug-Resistant TB https://www.cdc.gov/tb/topic/drtb/default.htm (accessed 2022 -01 -27).

Chakraborty, S.; Rhee, K. Y. Tuberculosis Drug Development: History and Evolution of the Mechanism-Based Paradigm. *Cold Spring Harb. Perspect. Med.* **2015**, *5* (8), a021147.

Colosimo, D. A.; MacMillan, J. B. Detailed Mechanistic Study of the Non-Enzymatic Formation of the Discoipyrrole Family of Natural Products. *J. Am. Chem. Soc.* **2016**, *138* (7), 2383–2388.

Cooper, G.; Rios, A. C. Enantiomer Excesses of Rare and Common Sugar Derivatives in Carbonaceous Meteorites. *Proc. Natl. Acad. Sci. U. S. A.* **2016**, *113* (24), E3322–E3331.

Cowen, L. E.; Sanglard, D.; Howard, S. J.; Rogers, P. D.; Perlin, D. S. Mechanisms of Antifungal Drug Resistance. *Cold Spring Harb. Perspect. Med.* **2014**, *5* (7), a019752.

Cronin, J. R.; Pizzarello, S. Amino Acid Enantiomer Excesses in Meteorites: Origin and Significance. *Advances in Space Research*. 1999, pp 293–299. https://doi.org/10.1016/s0273-1177(99)00050-2.

Cronin, J. R.; Pizzarello, S. Enantiomeric Excesses in Meteoritic Amino Acids. *Science* **1997**, *275* (5302), 951–955.

Delogu, G.; Sali, M.; Fadda, G. The Biology of Mycobacterium Tuberculosis Infection. *Mediterr. J. Hematol. Infect. Dis.* **2013**, *5* (1). https://doi.org/10.4084/MJHID.2013.070.

Doyle, T. W.; Nettleton, D. E.; Balitz, D. M.; Moseley, J. E.; Grulich, R. E.; Mccabe, T.; Clardy, J. ChemInform Abstract: ISOLATION AND STRUCTURE OF BOHEMAMINE (1Aβ,2α,6Aβ,6Bβ)-3-METHYL-N-(1A,6,6A,6B-TETRAHYDRO-2,6A-DI# METHYL-6-OXO-2H-OXIRENO(A)PYRROLIZIN-4-YL)-2-BUTENAMIDE. *Chemischer Informationsdienst*. 1980. https://doi.org/10.1002/chin.198029340.

Dragotakes, Q.; Stouffer, K. M.; Fu, M. S.; Sella, Y.; Youn, C.; Yoon, O. I.; De Leon-Rodriguez, C. M.; Freij, J. B.; Bergman, A.; Casadevall, A. Macrophages Use a Bet-Hedging Strategy for Antimicrobial Activity in Phagolysosomal Acidification. *J. Clin. Invest.* **2020**, *130* (7), 3805–3819.

Fu, P.; Legako, A.; La, S.; MacMillan, J. B. Discovery, Characterization, and Analogue Synthesis of Bohemamine Dimers Generated by Non-Enzymatic Biosynthesis. *Chemistry - A European Journal*. 2016, pp 3491–3495. https://doi.org/10.1002/chem.201600024.

Garcia, A. D.; Meinert, C.; Sugahara, H.; Jones, N. C.; Hoffmann, S. V.; Meierhenrich, U. J. The Astrophysical Formation of Asymmetric Molecules and the Emergence of a Chiral Bias. *Life* **2019**, *9* (1). https://doi.org/10.3390/life9010029.

Gargaud, M.; Irvine, W. M.; Amils, R.; Quintanilla, J. C.; Cleaves, H. J.; Pinti, D.; Rouan, D.; Spohn, T.; Tirard, S.; Viso, M. *Encyclopedia of Astrobiology*; Springer, 2015.

Gaynes, R. The Discovery of Penicillin—New Insights After More Than 75 Years of Clinical Use. *Emerging Infectious Diseases*. 2017, pp 849–853. https://doi.org/10.3201/eid2305.161556.

Havlickova, B.; Czaika, V. A.; Friedrich, M. Epidemiological Trends in Skin Mycoses Worldwide. *Mycoses* **2008**, *51 Suppl 4*, 2–15.

Heifets, L. B. Antimycobacterial Drugs. *Semin. Respir. Infect.* **1994**, *9* (2), 84–103.

Helfrich, E. J. N.; Lin, G.-M.; Voigt, C. A.; Clardy, J. Bacterial Terpene Biosynthesis: Challenges and Opportunities for Pathway Engineering. *Beilstein J. Org. Chem.* **2019**, *15*, 2889–2906.

Hertweck, C.; Luzhetskyy, A.; Rebets, Y.; Bechthold, A. Type II Polyketide Synthases: Gaining a Deeper Insight into Enzymatic Teamwork. *Nat. Prod. Rep.* **2007**, *24* (1), 162–190.

Hooper, D. C. Mechanisms of Action of Antimicrobials: Focus on Fluoroquinolones. *Clin. Infect. Dis.* **2001**, *32 Suppl 1*, S9–S15.

Hu, Y.; Potts, M. B.; Colosimo, D.; Herrera-Herrera, M. L.; Legako, A. G.; Yousufuddin, M.; White, M. A.; MacMillan, J. B. ChemInform Abstract: Discoipyrroles A-D: Isolation, Structure Determination, and Synthesis of Potent Migration Inhibitors from Bacillus Hunanensis. *ChemInform*. 2014, p no – no. https://doi.org/10.1002/chin.201408219.

Hughes, C. C.; MacMillan, J. B.; Gaudêncio, S. P.; Jensen, P. R.; Fenical, W. The Ammosamides: Structures of Cell Cycle Modulators from a Marine-Derived Streptomyces Species. *Angew. Chem. Int. Ed Engl.* **2009**, *48* (4), 725–727.

Kathiravan, M. K.; Salake, A. B.; Chothe, A. S.; Dudhe, P. B.; Watode, R. P.; Mukta, M. S.; Gadhwe, S. The Biology and Chemistry of Antifungal Agents: A Review. *Bioorg. Med. Chem.* **2012**, *20* (19), 5678–5698.

Keller, M. A.; Turchyn, A. V.; Ralser, M. Non-enzymatic Glycolysis and Pentose Phosphate Pathway-like Reactions in a Plausible A Rchean Ocean. *Molecular Systems Biology*. 2014, p 725. https://doi.org/10.1002/msb.20145228.

Keller, M. A.; Zylstra, A.; Castro, C.; Turchyn, A. V.; Griffin, J. L.; Ralser, M. Conditional Iron and pH-Dependent Activity of a Non-Enzymatic Glycolysis and Pentose Phosphate Pathway. *Science Advances*. 2016. https://doi.org/10.1126/sciadv.1501235.

Khoshnood, S.; Taki, E.; Sadeghifard, N.; Kaviar, V. H.; Haddadi, M. H.; Farshadzadeh, Z.; Kouhsari, E.; Goudarzi, M.; Heidary, M. Mechanism of Action, Resistance, Synergism, and Clinical Implications of Delamanid Against Multidrug-Resistant Mycobacterium Tuberculosis. *Frontiers in Microbiology*. 2021. https://doi.org/10.3389/fmicb.2021.717045.

Kieser, K. J. *Spatiotemporal Control of Mycobacterium Tuberculosis Cell Wall Biogenesis by the Peptidoglycan Synthase PonA1*; 2015.

Kotra, L. P.; Haddad, J.; Mobashery, S. Aminoglycosides: Perspectives on Mechanisms of Action and Resistance and Strategies to Counter Resistance. *Antimicrob. Agents Chemother.* **2000**, *44* (12), 3249–3256.

Kvenvolden, K.; Lawless, J.; Pering, K.; Peterson, E.; Flores, J.; Ponnamperuma, C.; Kaplan, I. R.; Moore, C. Evidence for Extraterrestrial Amino-Acids and Hydrocarbons in the Murchison Meteorite. *Nature* **1970**, *228* (5275), 923–926.

Lin, Z.; Koch, M.; Abdel Aziz, M. H.; Galindo-Murillo, R.; Tianero, M. D.; Cheatham, T. E.; Barrows, L. R.; Reilly, C. A.; Schmidt, E. W. Oxazinin A, a Pseudodimeric Natural Product of Mixed Biosynthetic Origin from a Filamentous Fungus. *Org. Lett.* **2014**, *16* (18), 4774–4777.

Maitra, A.; Munshi, T.; Healy, J.; Martin, L. T.; Vollmer, W.; Keep, N. H.; Bhakta, S. Cell Wall Peptidoglycan in Mycobacterium Tuberculosis: An Achilles' Heel for the TB-Causing Pathogen. *FEMS Microbiology Reviews*. 2019, pp 548–575. https://doi.org/10.1093/femsre/fuz016.

Marek, R.; Lycka, A.; Kolehmainen, E.; Sievanen, E.; Tousek, J. 15N NMR Spectroscopy in Structural Analysis: An Update (2001 - 2005). *Curr. Org. Chem. 11* (13), 1154–1205.

Martínez-Núñez, M. A.; López y López, V. E. Nonribosomal Peptides Synthetases and Their Applications in Industry. *Sustainable Chemical Processes*. 2016. https://doi.org/10.1186/s40508-016-0057-6.

Meinert, C.; Myrgorodska, I.; de Marcellus, P.; Buhse, T.; Nahon, L.; Hoffmann, S. V.; d'Hendecourt, L. L. S.; Meierhenrich, U. J. Ribose and Related Sugars from Ultraviolet Irradiation of Interstellar Ice Analogs. *Science* **2016**, *352* (6282), 208–212.

Messner, C. B.; Driscoll, P. C.; Piedrafita, G.; De Volder, M. F. L.; Ralser, M. Nonenzymatic Gluconeogenesis-like Formation of Fructose 1,6-Bisphosphate in Ice. *Proc. Natl. Acad. Sci. U. S. A.* **2017**, *114* (28), 7403–7407.

Metabolites https://byjus.com/biology/metabolites/ (accessed 2022 -02 -11).

Mevers, E.; Saurí, J.; Helfrich, E. J. N.; Henke, M.; Barns, K. J.; Bugni, T. S.; Andes, D.; Currie, C. R.; Clardy, J. Pyonitrins A–D: Chimeric Natural Products Produced by Pseudomonas Protegens. *Journal of the American Chemical Society*. 2019, pp 17098–17101. https://doi.org/10.1021/jacs.9b09739.

Miyanaga, A. Structure and Function of Polyketide Biosynthetic Enzymes: Various Strategies for Production of Structurally Diverse Polyketides. *Biosci. Biotechnol. Biochem.* **2017**, *81* (12), 2227–2236.

Morrison, M. D.; Hanthorn, J. J.; Pratt, D. A. Synthesis of Pyrrolnitrin and Related Halogenated Phenylpyrroles. *Org. Lett.* **2009**, *11* (5), 1051–1054.

Muñoz Caro, G. M.; Meierhenrich, U. J.; Schutte, W. A.; Barbier, B.; Arcones Segovia, A.; Rosenbauer, H.; Thiemann, W. H.-P.; Brack, A.; Greenberg, J. M. Amino Acids from Ultraviolet Irradiation of Interstellar Ice Analogues. *Nature* **2002**, *416* (6879), 403–406.

Newman, D. J.; Cragg, G. M. Natural Products as Sources of New Drugs from 1981 to 2014. *J. Nat. Prod.* **2016**, *79* (3), 629–661.

NMR Spectroscopy https://organicchemistrydata.org/hansreich/resources/nmr/?index=nmr_index%2F13C_shift#cdata174 (accessed 2022 -02 -23).

Nuevo, M.; Cooper, G.; Sandford, S. A. Deoxyribose and Deoxysugar Derivatives from Photoprocessed Astrophysical Ice Analogues and Comparison to Meteorites. *Nat. Commun.* **2018**, *9* (1), 5276.

Patel, K.; Deshmukh, S. S.; Bodkhe, D.; Mane, M.; Vanka, K.; Shinde, D.; Rajamohanan, P. R.; Nandi, S.; Vaidhyanathan, R.; Chikkali, S. H. Secondary Interactions Arrest the Hemiaminal Intermediate To Invert the Modus Operandi of Schiff Base Reaction: A Route to Benzoxazinones. *J. Org. Chem.* **2017**, *82* (8), 4342–4351.

Pizzarello, S.; Cronin, J. R. Non-Racemic Amino Acids in the Murray and Murchison Meteorites. *Geochim. Cosmochim. Acta* **2000**, *64* (2), 329–338.

Pye, C. R.; Bertin, M. J.; Lokey, R. S.; Gerwick, W. H.; Linington, R. G. Retrospective Analysis of Natural Products Provides Insights for Future Discovery Trends. *Proc. Natl. Acad. Sci. U. S. A.* **2017**, *114* (22), 5601–5606.

Reddy, P. V. N.; Jensen, K. C.; Mesecar, A. D.; Fanwick, P. E.; Cushman, M. Design, Synthesis, and Biological Evaluation of Potent Quinoline and Pyrroloquinoline Ammosamide Analogues as Inhibitors of Quinone Reductase 2. *J. Med. Chem.* **2012**, *55* (1), 367–377.

Riddelliine N-Oxide Is a Phytochemical and Mammalian Metabolite with Genotoxic Activity That Is Comparable to the Parent Pyrrolizidine Alkaloid Riddelliine. *Toxicol. Lett.* **2003**, *145* (3), 239–247.

Saha, B.; Sharma, S.; Sawant, D.; Kundu, B. Water as an Efficient Medium for the Synthesis of Tetrahydro-β-Carbolines via Pictet—Spengler Reactions. *ChemInform*. 2007. https://doi.org/10.1002/chin.200722147.

Sapkota, A. Primary vs Secondary Metabolites- Definition, 12 Differences, Examples https://microbenotes.com/primary-vs-secondary-metabolites/ (accessed 2022 -02 -11).

Sarathy, J. P.; Gruber, G.; Dick, T. Re-Understanding the Mechanisms of Action of the Anti-Mycobacterial Drug Bedaquiline. *Antibiotics (Basel)* **2019**, *8* (4). https://doi.org/10.3390/antibiotics8040261.

Schiebler, M.; Brown, K.; Hegyi, K.; Newton, S. M.; Renna, M.; Hepburn, L.; Klapholz, C.; Coulter, S.; Obregón-Henao, A.; Henao Tamayo, M.; Basaraba, R.; Kampmann, B.; Henry, K. M.; Burgon, J.; Renshaw, S. A.; Fleming, A.; Kay, R. R.; Anderson, K. E.; Hawkins, P. T.; Ordway, D. J.; Rubinsztein, D. C.; Floto, R. A. Functional Drug Screening Reveals Anticonvulsants as Enhancers of mTOR-Independent Autophagic Killing of Mycobacterium Tuberculosis through Inositol Depletion. *EMBO Mol. Med.* **2015**, *7* (2), 127–139.

Schörghuber, J.; Geist, L.; Bisaccia, M.; Weber, F.; Konrat, R.; Lichtenecker, R. J. Anthranilic Acid, the New Player in the Ensemble of Aromatic Residue Labeling Precursor Compounds. *J. Biomol. NMR* **2017**, *69* (1), 13–22.

Sensi, P. History of the Development of Rifampin. *Rev. Infect. Dis.* **1983**, *5 Suppl 3*, S402–S406.

Shen, B. Polyketide Biosynthesis beyond the Type I, II and III Polyketide Synthase Paradigms. *Curr. Opin. Chem. Biol.* **2003**, *7* (2), 285–295.

Shih, J.-L.; Nguyen, T. S.; May, J. A. Organocatalyzed Asymmetric Conjugate Addition of Heteroaryl and Aryl Trifluoroborates: A Synthetic Strategy for Discoipyrrole D. *Angew. Chem. Int. Ed Engl.* **2015**, *54* (34), 9931–9935.

Shinabarger, D. Mechanism of Action of the Oxazolidinone Antibacterial Agents. *Expert Opinion on Investigational Drugs*. 1999, pp 1195–1202. https://doi.org/10.1517/13543784.8.8.1195.

Shingare, R. D.; Aniebok, V.; Lee, H.-W.; MacMillan, J. B. Synthesis and Investigation of the Abiotic Formation of Pyonitrins A-D. *Org. Lett.* **2020**, *22* (4), 1516–1519.

Takiff, H. E.; Salazar, L.; Guerrero, C.; Philipp, W.; Huang, W. M.; Kreiswirth, B.; Cole, S. T.; Jacobs, W. R., Jr; Telenti, A. Cloning and Nucleotide Sequence of Mycobacterium Tuberculosis gyrA and gyrB Genes and Detection of Quinolone Resistance Mutations. *Antimicrob. Agents Chemother.* **1994**, *38* (4), 773–780.

Takiff, H.; Guerrero, E. Current Prospects for the Fluoroquinolones as First-Line Tuberculosis Therapy. *Antimicrob. Agents Chemother.* **2011**, *55* (12), 5421–5429.

Tan, F.; Shi, B.; Li, J.; Wu, W.; Zhang, J. Design and Synthesis of New 2-Aryl-4,5-Dihydro-Thiazole Analogues: In Vitro Antibacterial Activities and Preliminary Mechanism of Action. *Molecules* **2015**, *20* (11), 20118–20130.
The Classes of Natural Product and Their Isolation. *Tutorial Chemistry Texts*. 2003, pp 1–34. https://doi.org/10.1039/9781847551535-00001.

Tia, M.; Cunha de Miranda, B.; Daly, S.; Gaie-Levrel, F.; Garcia, G. A.; Nahon, L.; Powis, I. VUV Photodynamics and Chiral Asymmetry in the Photoionization of Gas Phase Alanine Enantiomers. *J. Phys. Chem. A* **2014**, *118* (15), 2765–2779.

Treating and Managing Tuberculosis https://www.lung.org/lung-health-diseases/lung-disease-lookup/tuberculosis/treating-and-managing#:~:text=If%20you%20have%20an%20active,%E2%80%94rifampin%2C%20pyrazinamide%20and%20ethambutol. (accessed 2022 -01 -25).

Tuberculosis https://www.who.int/news-room/fact-sheets/detail/tuberculosis (accessed 2022 -01 -18).

Unissa, A. N.; Subbian, S.; Hanna, L. E.; Selvakumar, N. Overview on Mechanisms of Isoniazid Action and Resistance in Mycobacterium Tuberculosis. *Infect. Genet. Evol.* **2016**, *45*, 474–492.

Website https://arxiv.org/abs/1902.04575.

Wehrli, W. Rifampin: Mechanisms of Action and Resistance. *Clinical Infectious Diseases*. 1983, pp S407–S411. https://doi.org/10.1093/clinids/5.supplement_3.s407.

Williams, D. R.; Lowder, P. D.; Gu, Y.-G.; Brooks, D. A. Studies of Mild Dehydrogenations in Heterocyclic Systems. *Tetrahedron Letters*. 1997, pp 331–334. https://doi.org/10.1016/s0040-4039(96)02344-1.